Measurements of $b \to s\ell\ell$ decays at LHCb

Renato Quagliani (EPFL)

on behalf of the LHCb collaboration

15 May 2023

Introduction

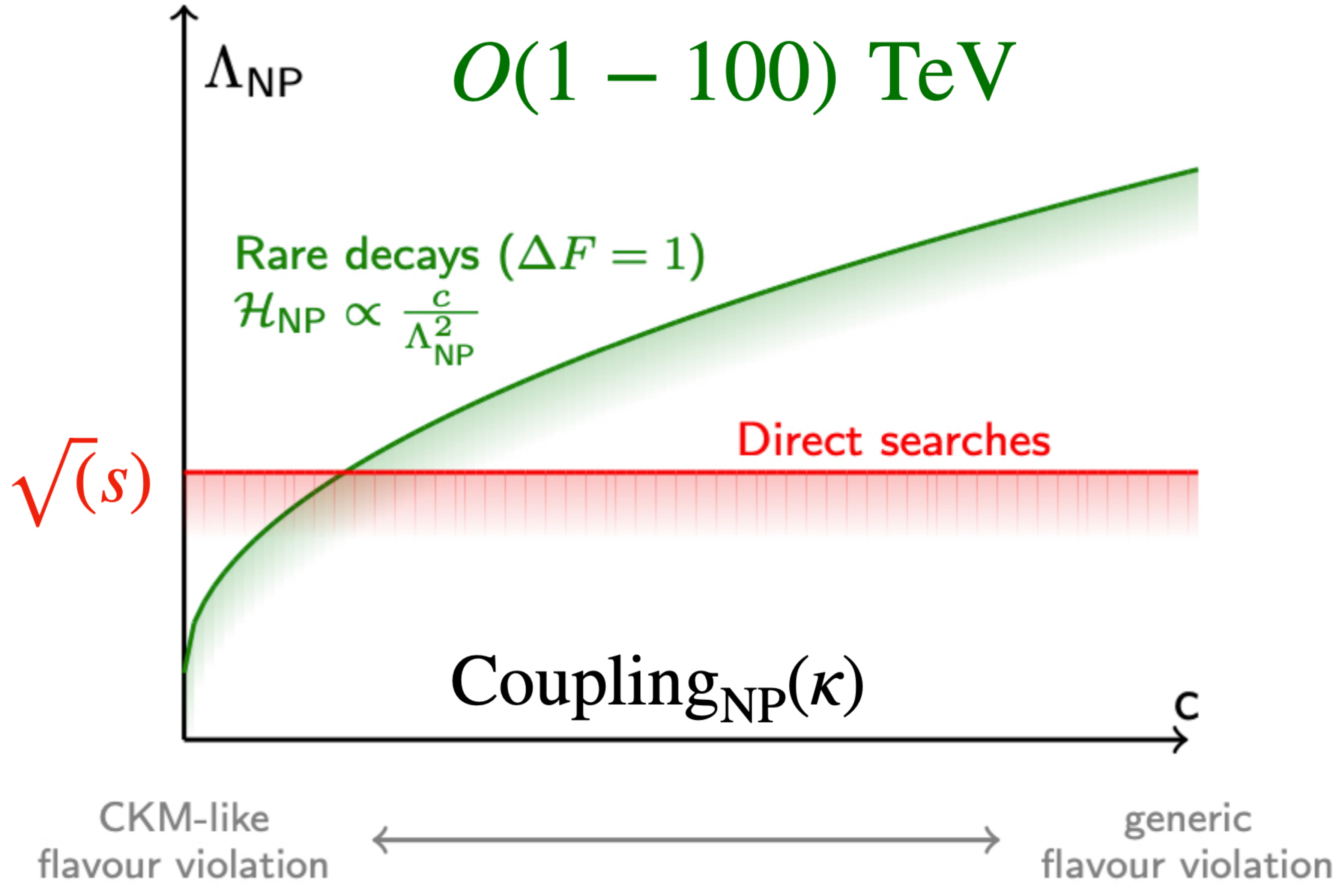

- **No direct evidence of New Physics (NP) so far**
  - Indirect searches/exclusion of generic NP models in rare b-decays very powerful beyond current direct searches reach
- $b \to s\ell\ell$ ($B \to M\ell\ell$): a powerful laboratory to hunt NP
  - $\mathcal{B} \sim 10^{-6}$ in the Standard Model (SM)
  - NP can affect modify
    1. Decay rates
    2. Angular distributions
    3. Rate asymmetries (CP, lepton flavour asymmetries)

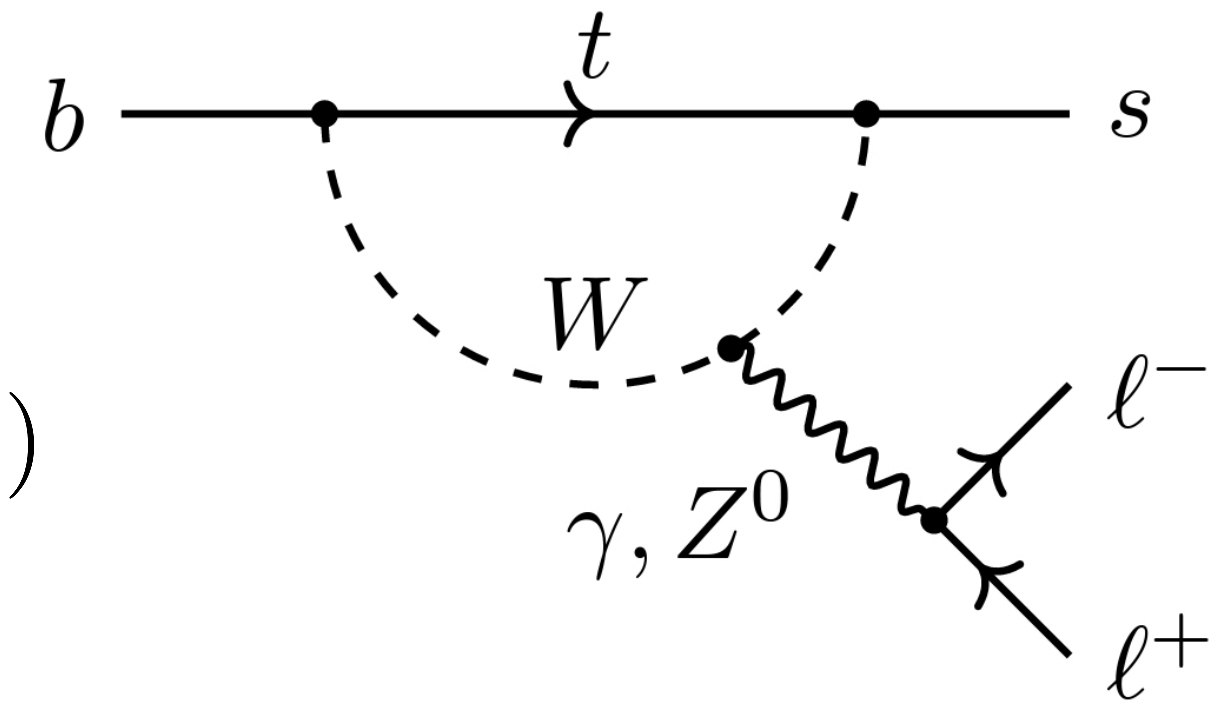

- Experimental measurement interpreted through an effective field theory
- Related measurements for interpretation: ($b \to s\gamma, B \to \ell\ell$). NP Model building constraints (Diego's talk)

$b \to s\ell^+\ell^-$ as a probe for NP in a nutshell

$$H_{eff} = -\frac{G_F}{\sqrt{2}} V_{tb} V_{ts}^* \sum_i (C_i^{SM} + \Delta_i^{NP}) O_i$$

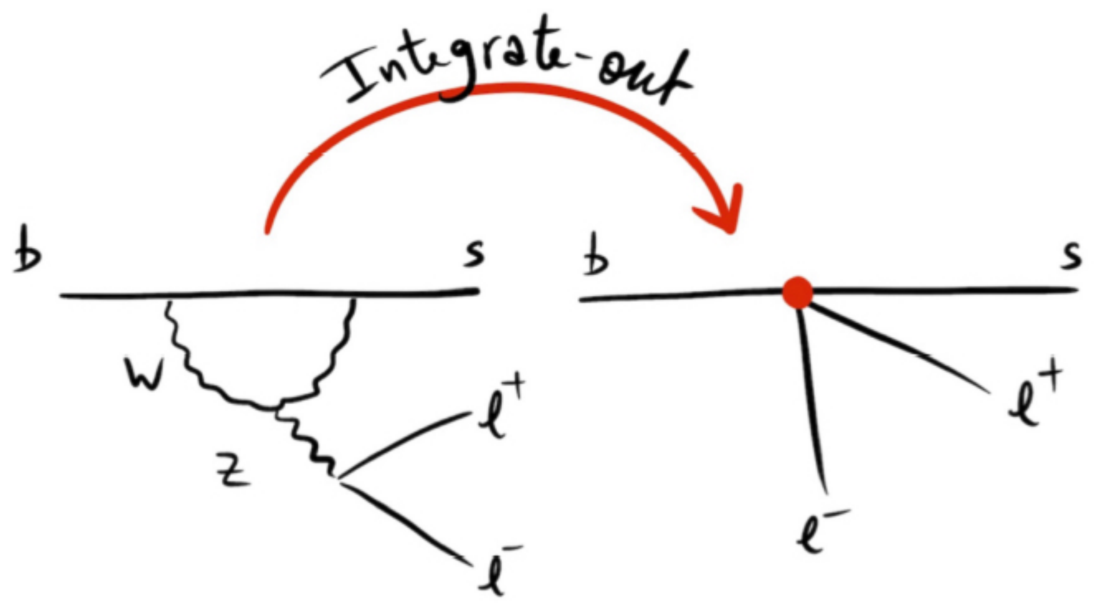

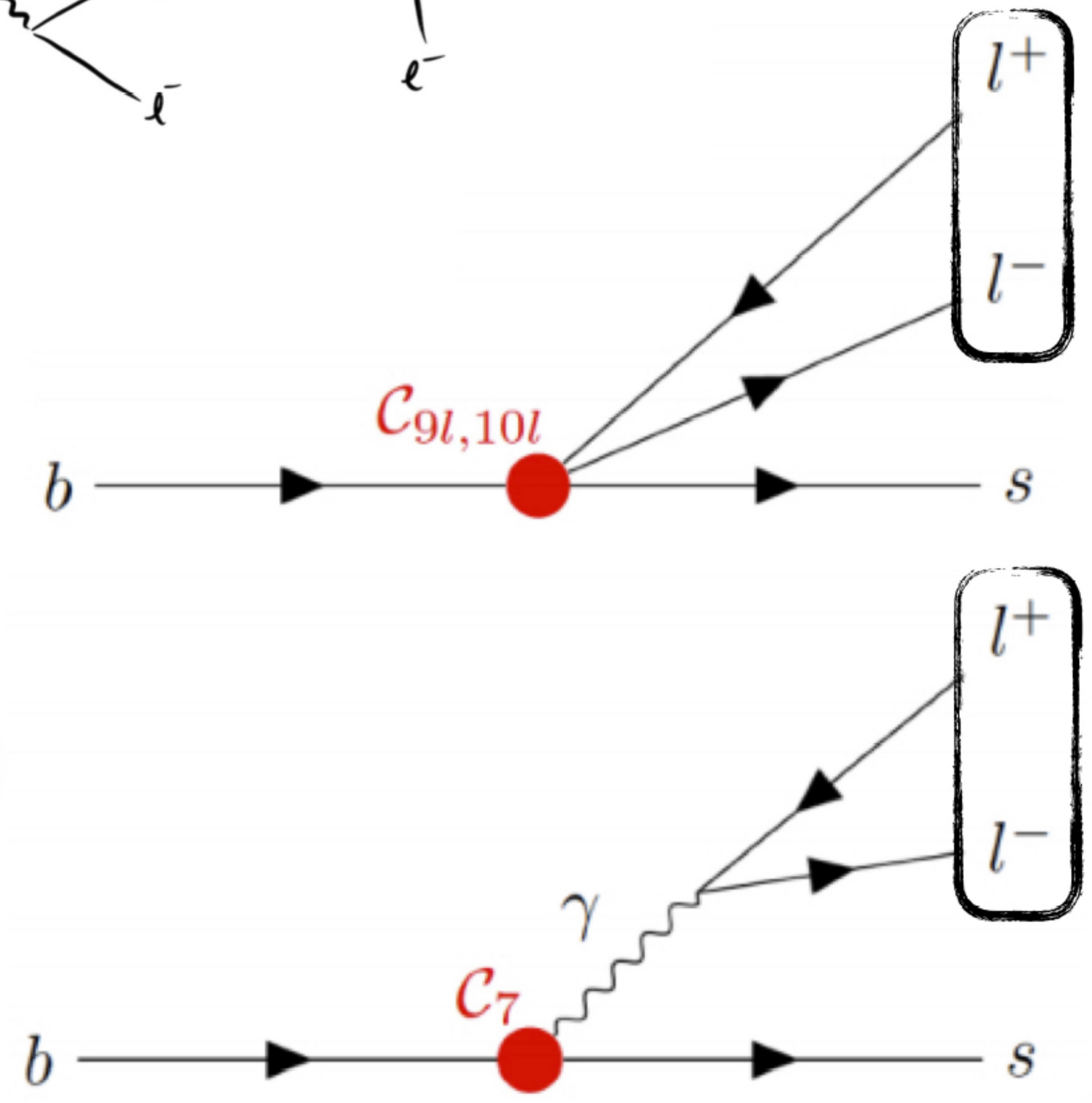

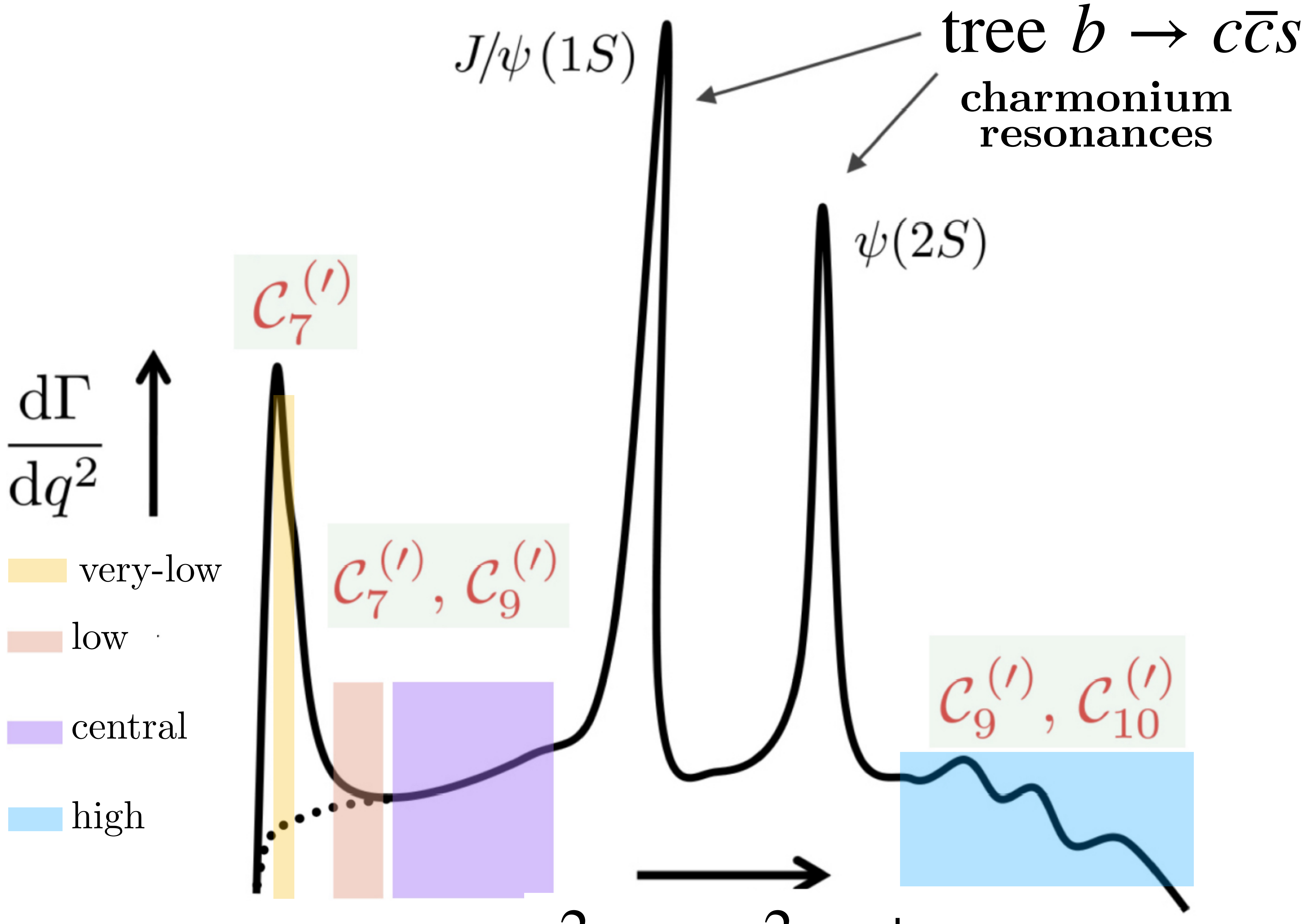

$$q^2 = m^2(\ell^+\ell^-)$$

···· : with PseudoScalar H_s in final state, K_s^0, K^+

— : with Vector H_s in final state, $K^{*0}, K^{*+}, \phi, \ldots$

Rare b-decays and $b \to s\ell^+\ell^-$

	Radiative $b \to s\gamma$	**Leptonic** $bs(d) \to \ell\ell$	**Semileptonic** $b \to s\ell\ell$
$\mathcal{C}_7^{(\prime)}$	✓		✓
$\mathcal{C}_9^{(\prime)}$			✓
$\mathcal{C}_{10}^{(\prime)}$		✓	✓
$\mathcal{C}_S^{(\prime)}$		✓	
$\mathcal{C}_P^{(\prime)}$		✓	

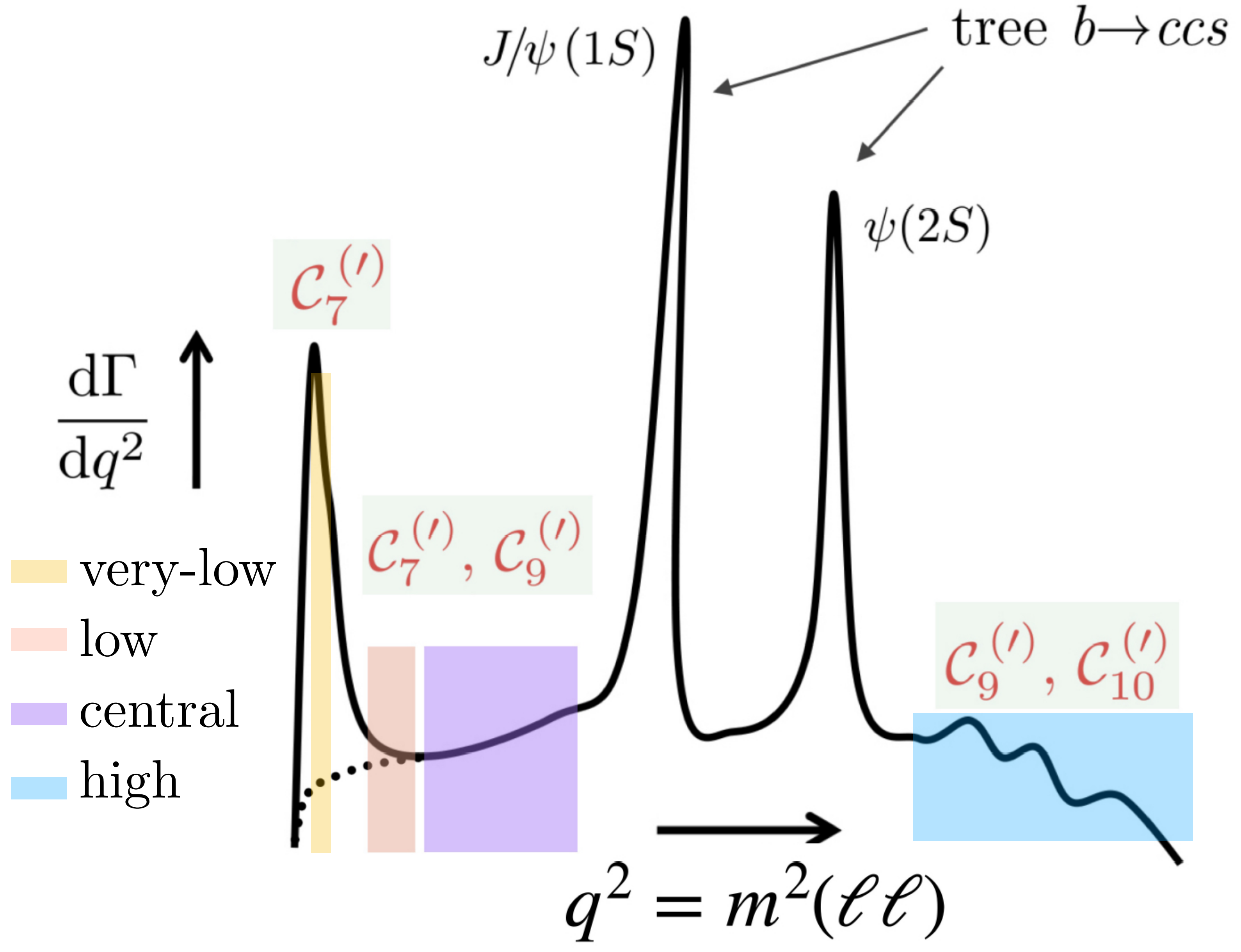

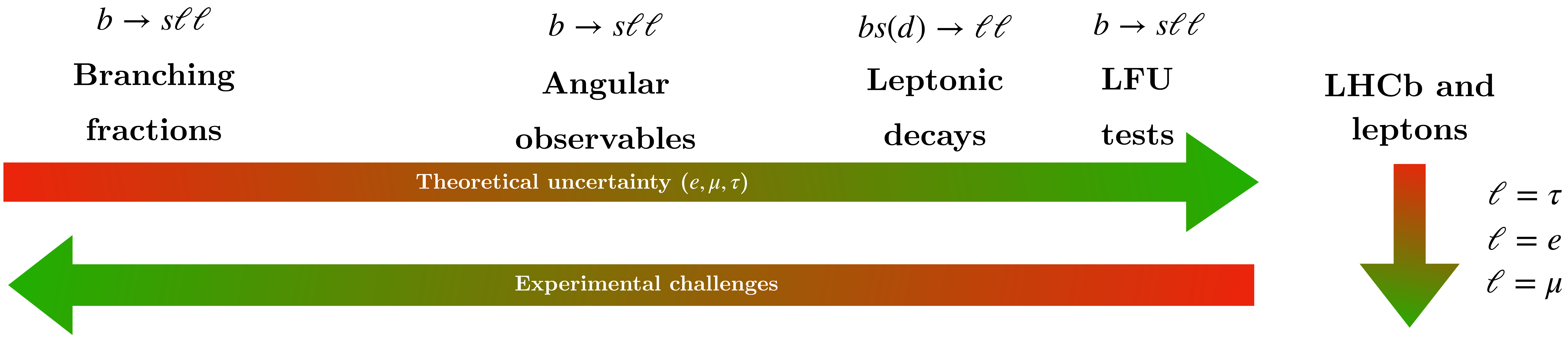

$b \to s\ell\ell$

Branching fractions

$b \to s\ell\ell$

Angular observables

$bs(d) \to \ell\ell$

Leptonic decays

$b \to s\ell\ell$

LFU tests

LHCb and leptons

Theoretical uncertainty (e, μ, τ)

$\ell = \tau$
$\ell = e$
$\ell = \mu$

Experimental challenges

LHCb detector

Exploit large $\sigma_{pp\to b\bar{b},c\bar{c}}$

in $\eta \in [2,5]$ at LHC

Run1 :

$$\int_{2011}^{2012} \mathscr{L} = 3\text{fb}^{-1}, \ \sqrt{s} = 7 - 8\text{TeV}$$

Run2 :

$$\int_{2015}^{2018} \mathscr{L} = 6\text{fb}^{-1}, \ \sqrt{s} = 13\text{TeV}$$

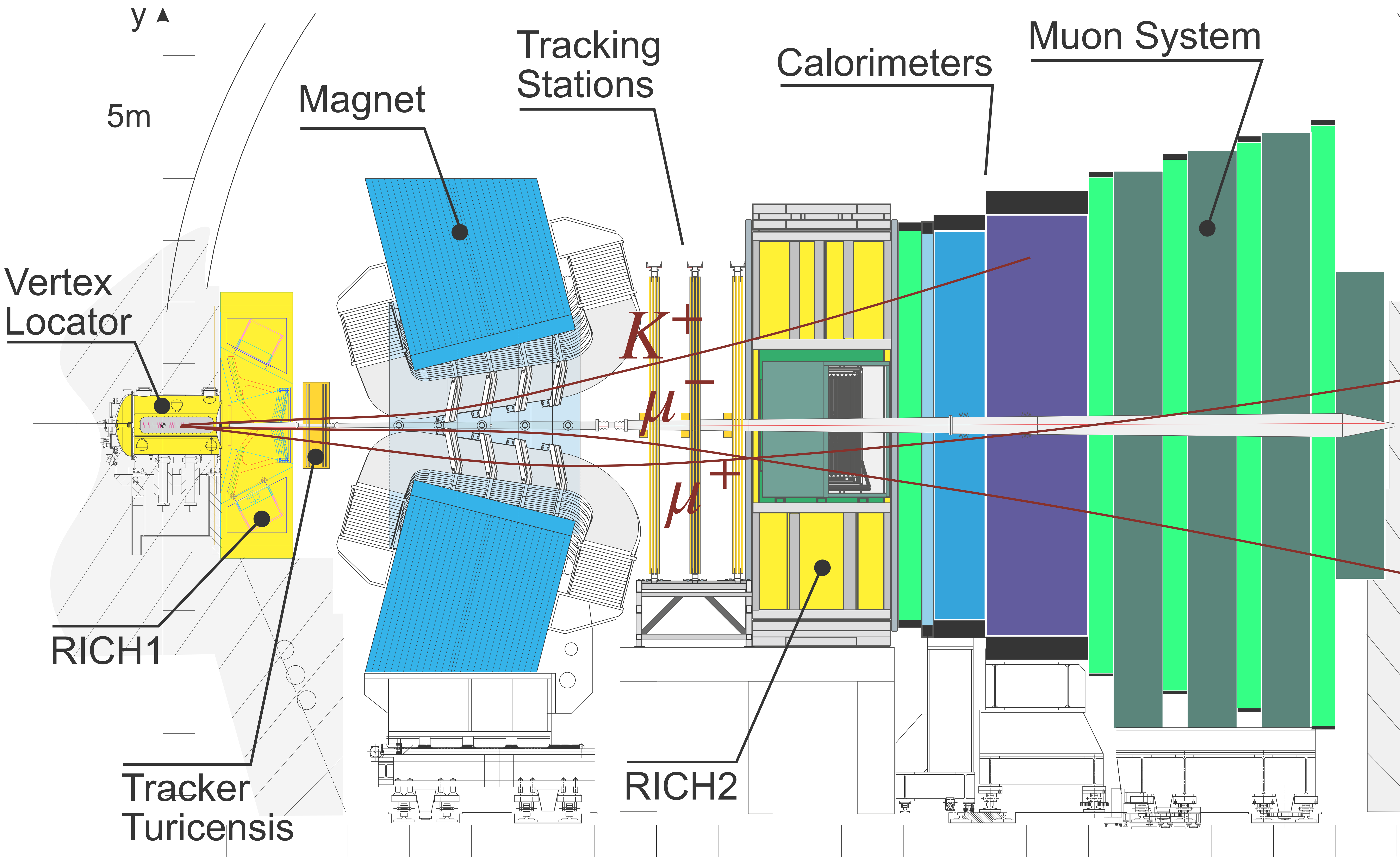

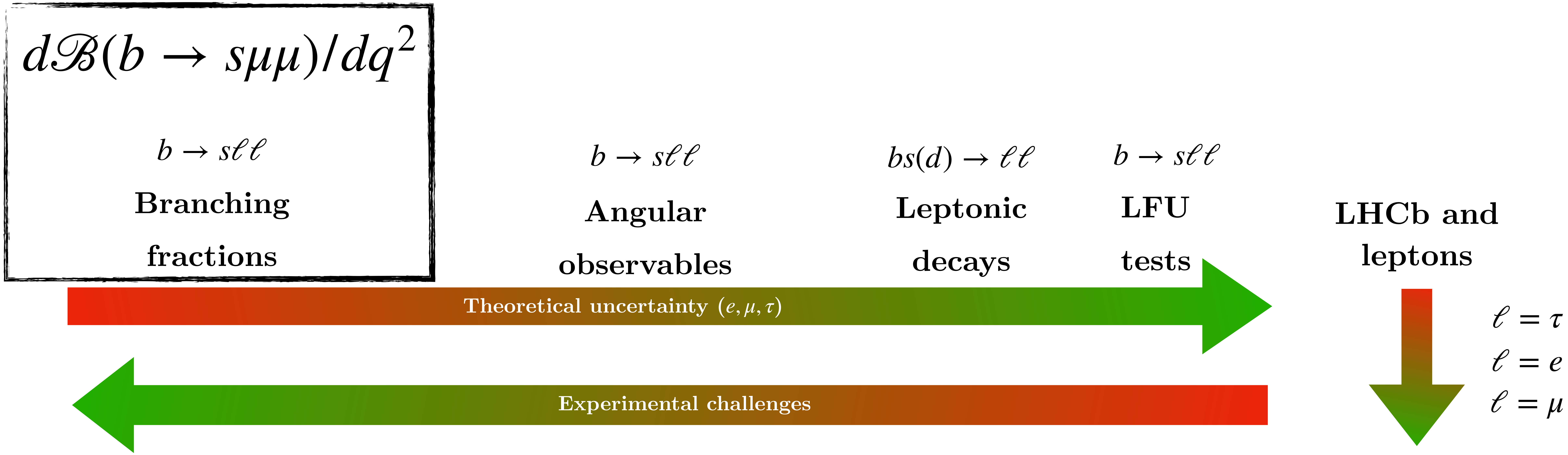

Latest $b \to s\mu\mu$ differential decay rates at LHCb

$\langle M|(\dots)|B\rangle$ in decay amplitude parameterised by 3(7) form factors for spin 0(1) final state

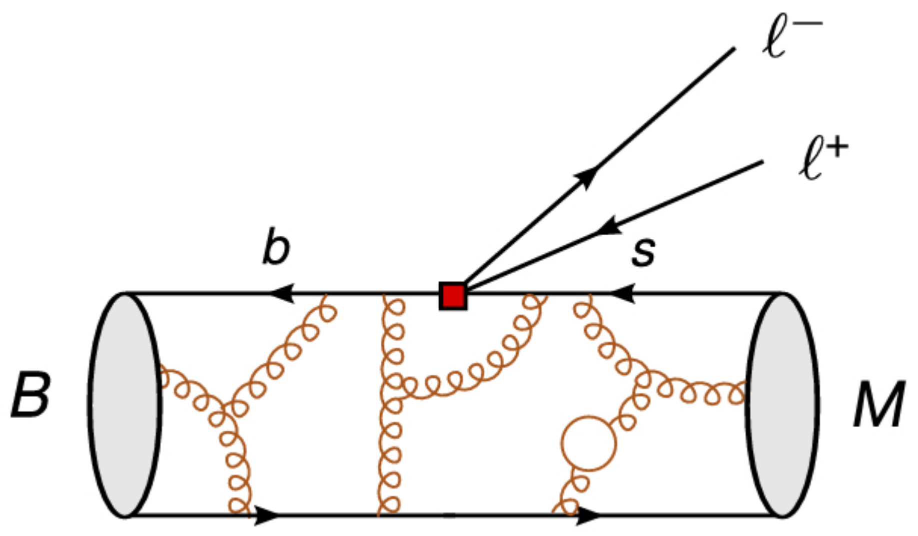

Form factors predictions

$C_i \times FF(q^2)$

@high q^2 *LQCD*

[0] HPQCD,arXiv:1306.2384,2207.12468
[1] Fermilab,MILC,arXiv:1509.06235
[2] Horgan,Liu,Meinel,Wingate,arXiv:1310.3722,arXiv:1501.00367

@low q^2 *Continuum methods (LCSR)*

[0] Ball,Zwicky,arXiv:hep-ph/0406232
[1] Khodjamirian,Mannel,Pivovarov,Wang,arXiv:1006.4945
[2] Bharucha,Straub,Zwicky,arXiv:1503.05534
[3] Gubernari,Kokulu,vanDyk,arXiv:1811.00983

@low+high q^2 *Combined fit continuum + LQCD/LQCD*

[0] Altmannshofer,Straub,arXiv:1411.3161
[1] Bharucha,Straub,Zwicky,arXiv:1503.05534
[2] Gubernari,Kokulu,vanDyk,arXiv:1811.

Most recent LHCb results

$B_s^0 \to \phi\mu^+\mu^-$ (Run1 + Run2)

[PRL 127 (2021) 151801]

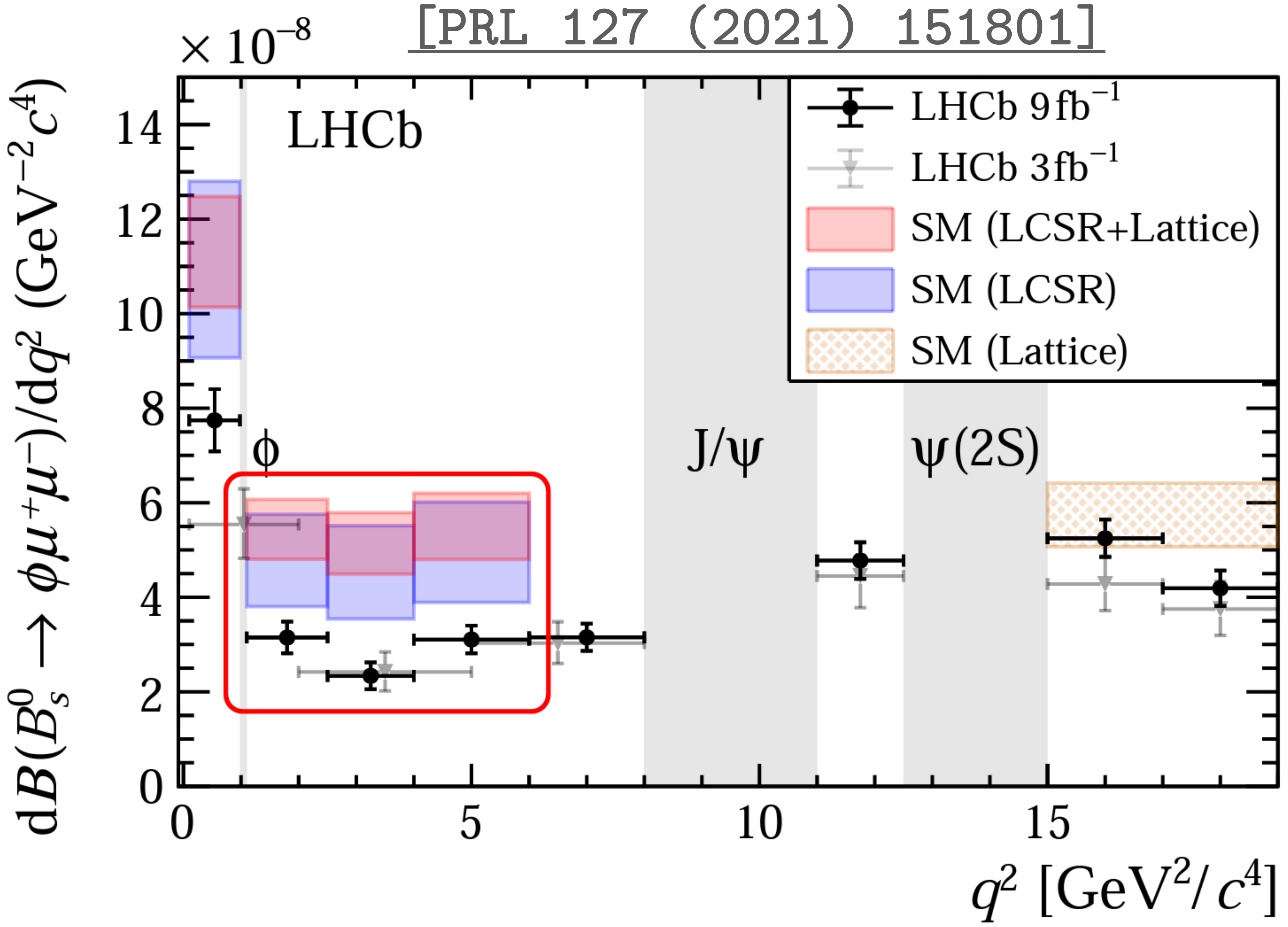

$\Lambda_b^0 \to \Lambda(1520)\mu^+\mu^-$ (Run1 + Run2)

[arXiv:2302.08262]

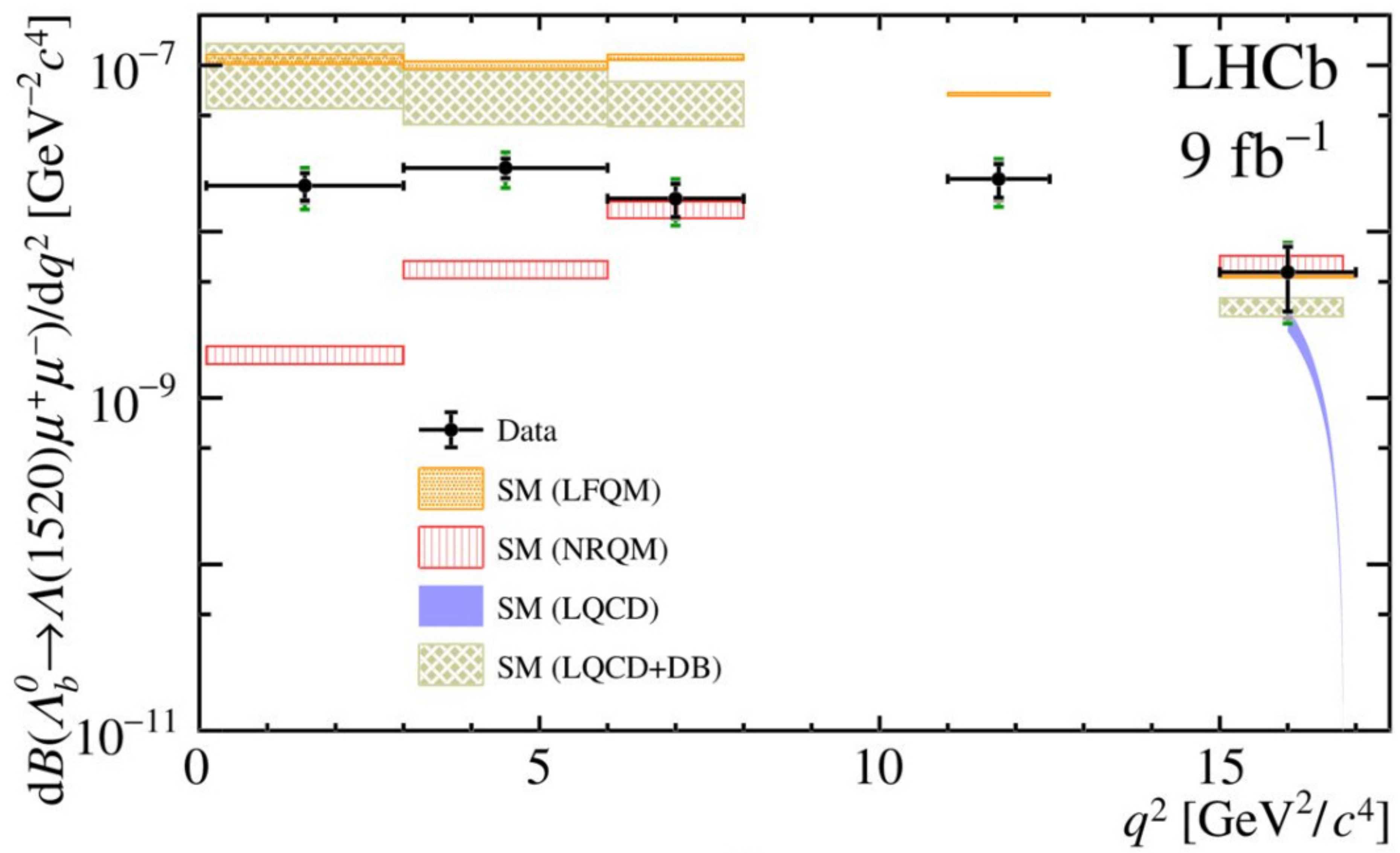

(*) with baryons, spin-structure: substantial improvements on theory side needed

Other $b \to s\mu\mu$ differential decay rates at LHCb

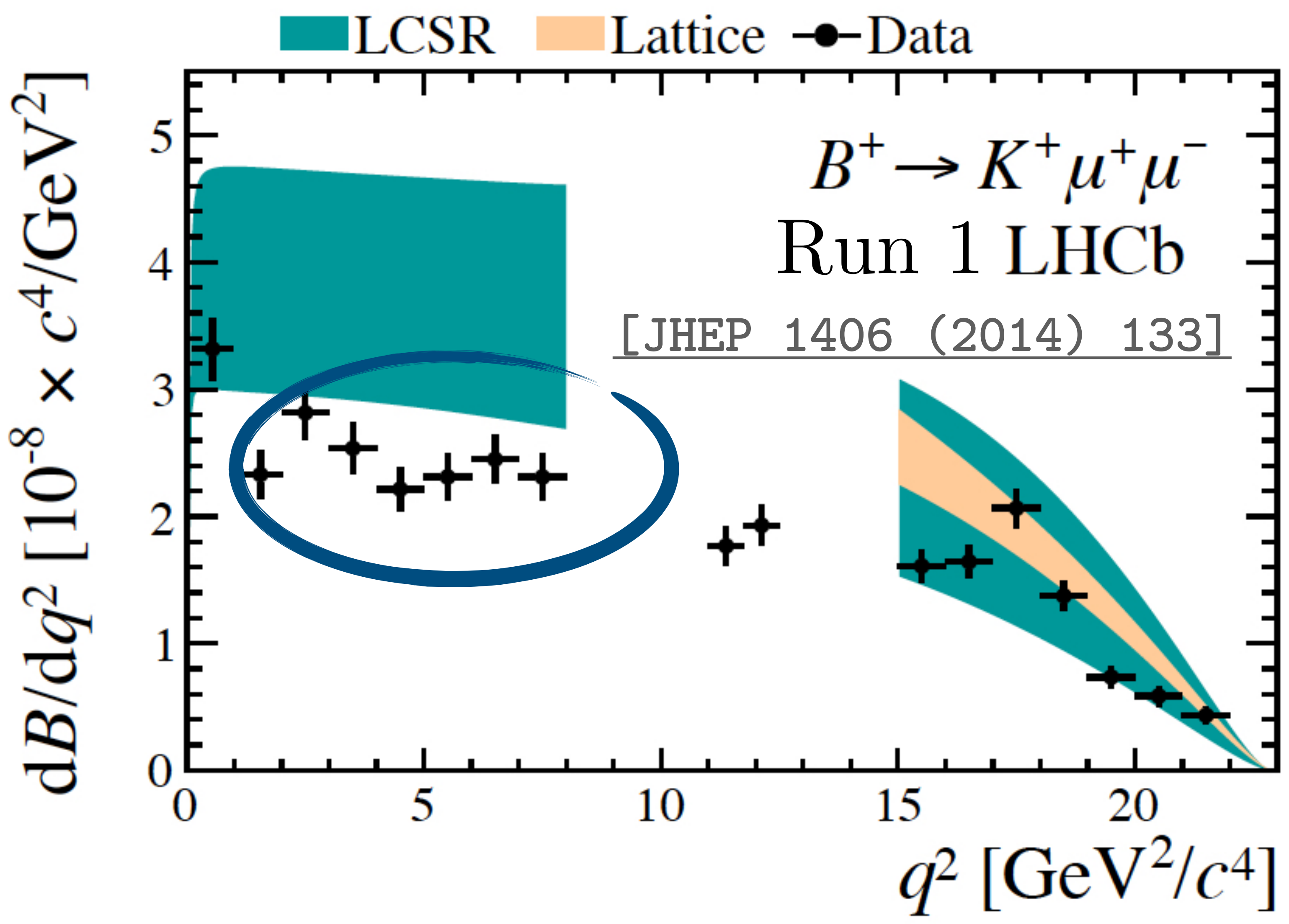

[JHEP 1406 (2014) 133]

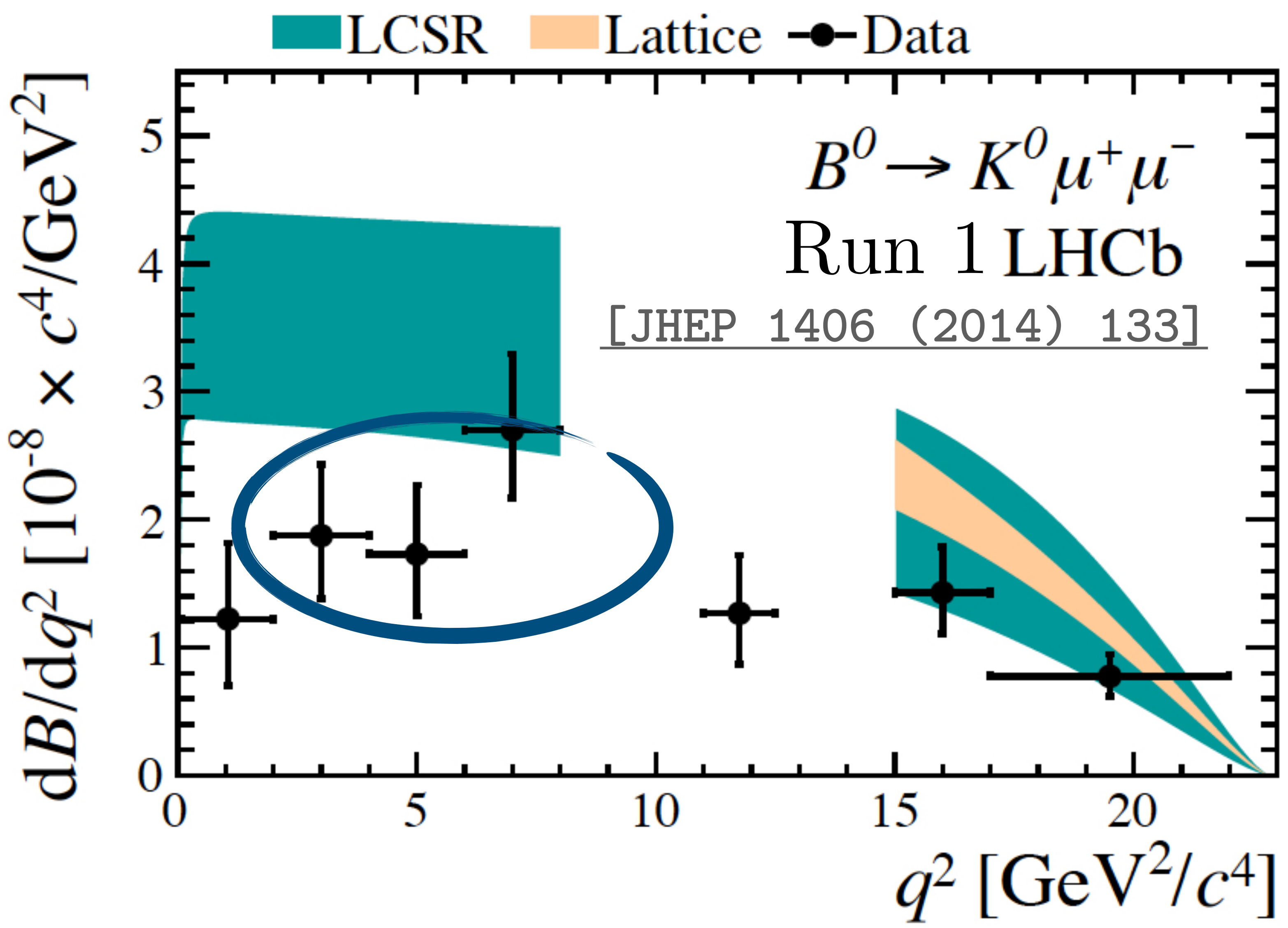

[JHEP 1406 (2014) 133]

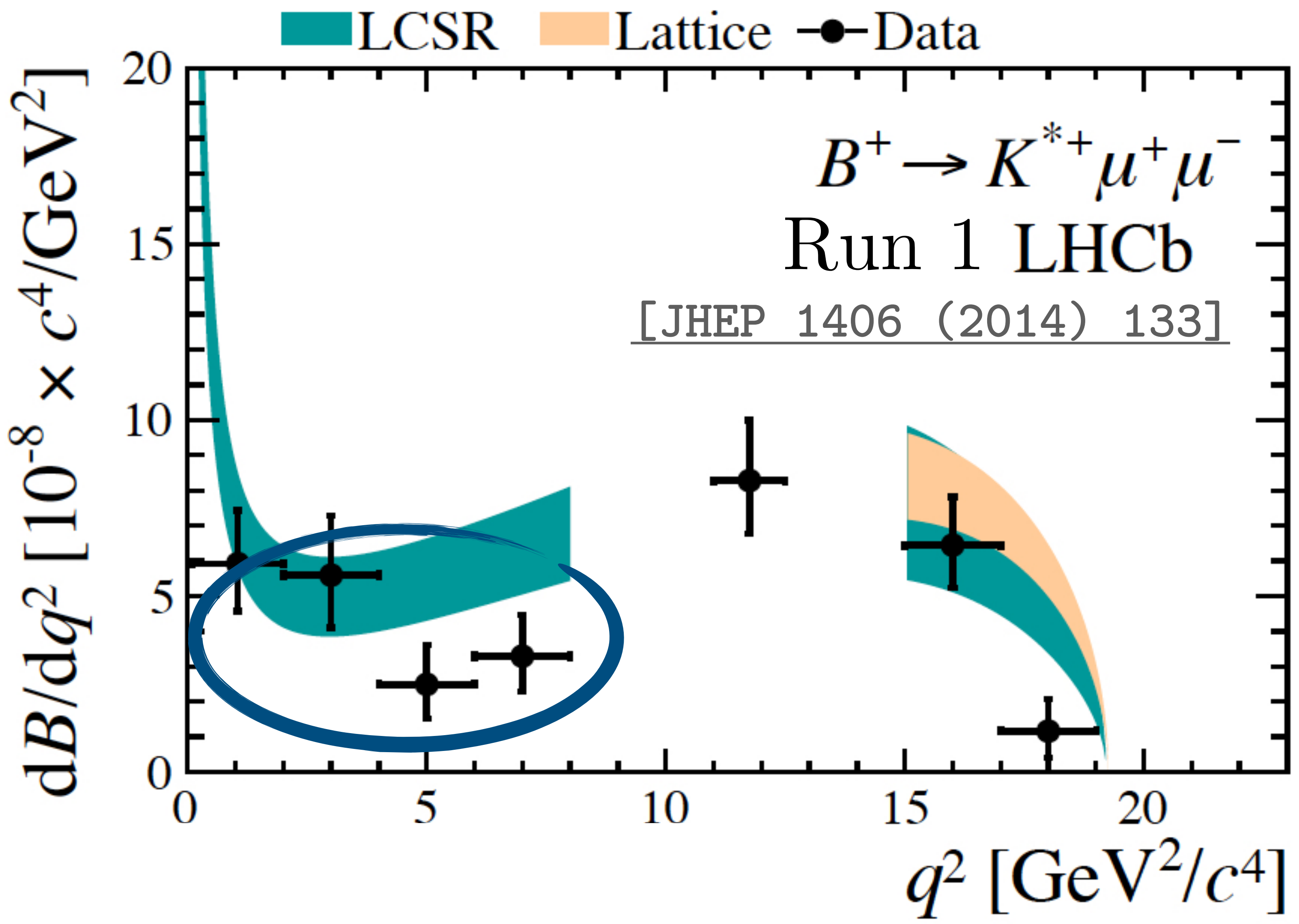

[JHEP 1406 (2014) 133]

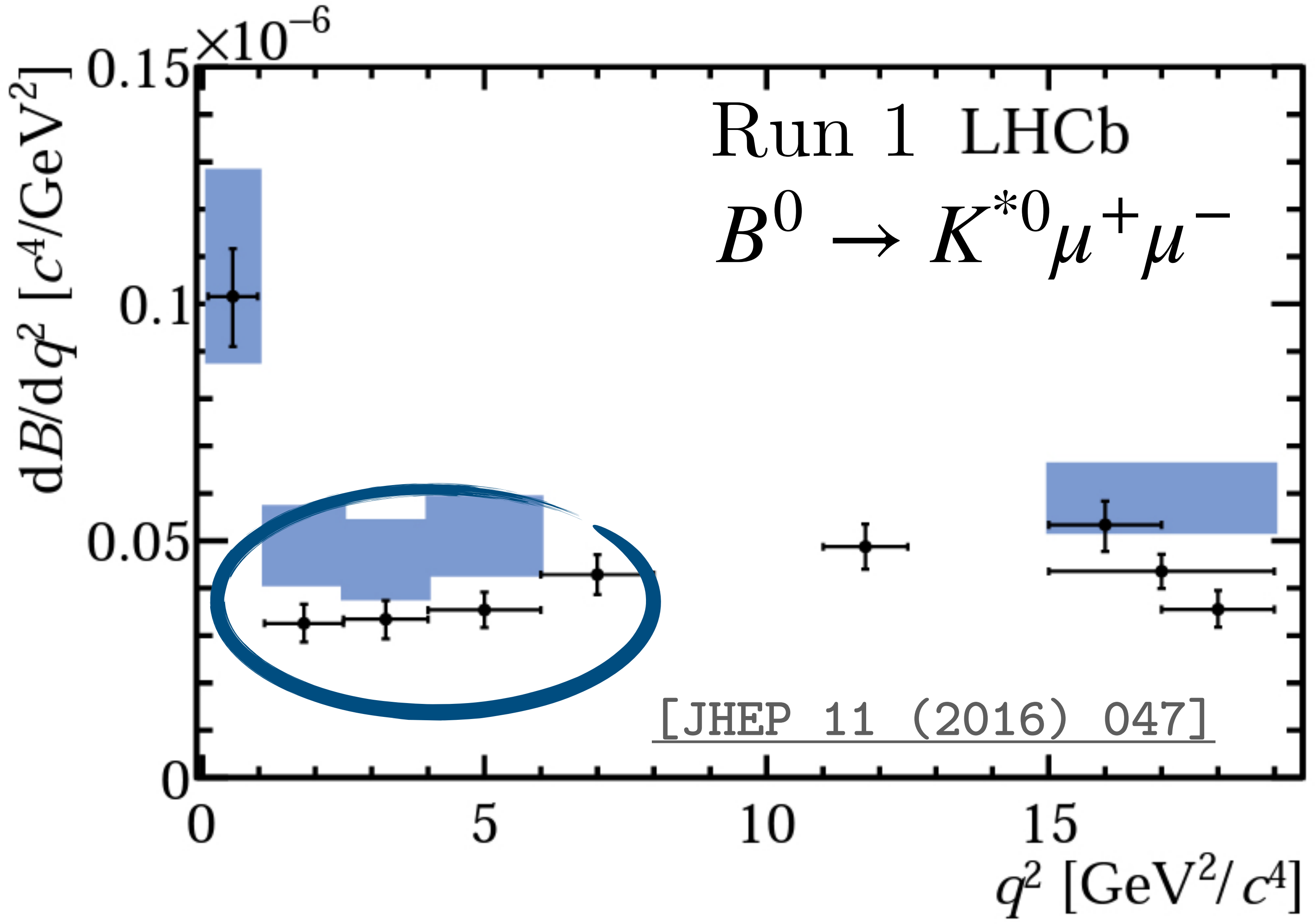

[JHEP 11 (2016) 047]

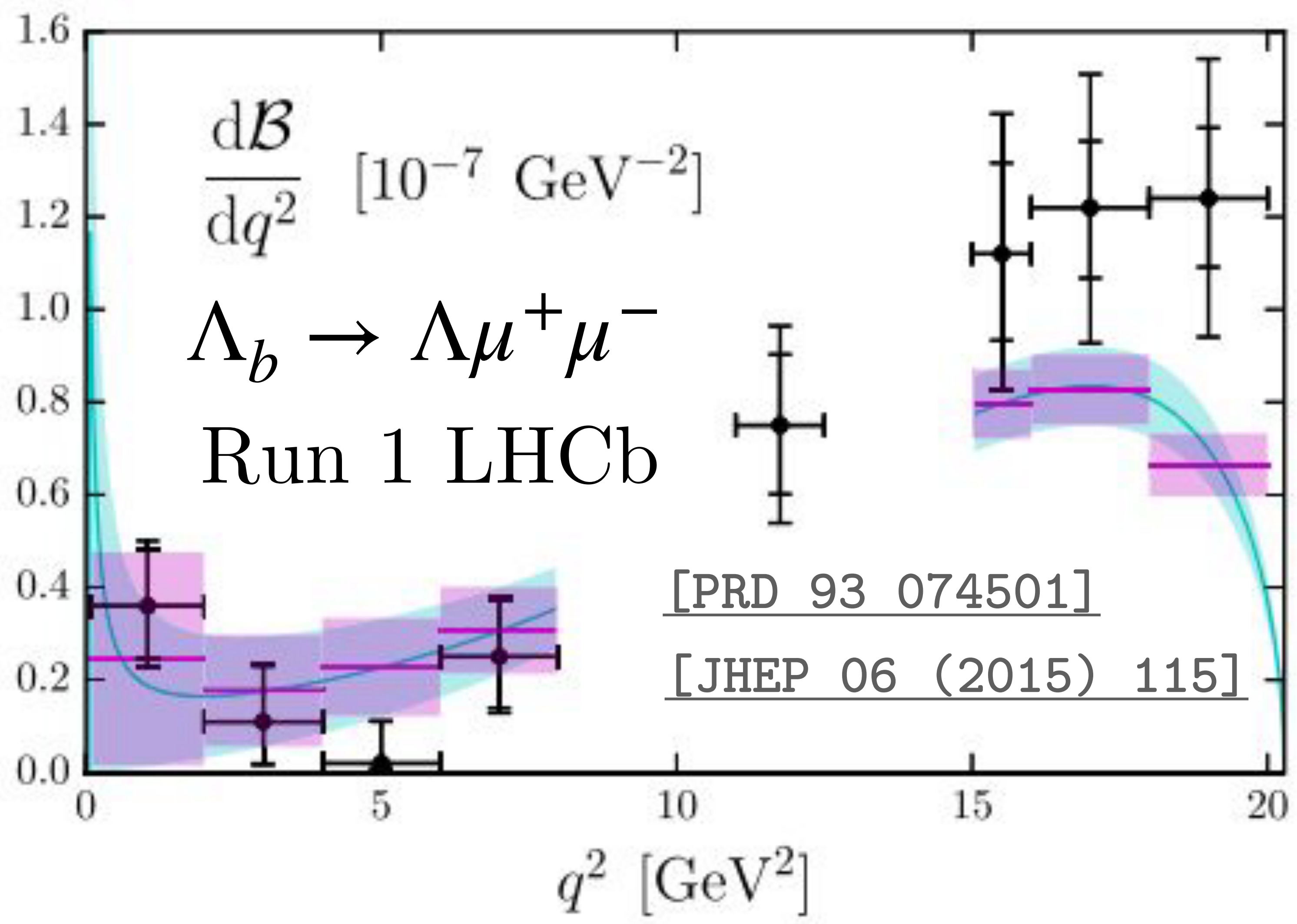

[PRD 93 074501]

[JHEP 06 (2015) 115]

- dB/dq^2 in exclusive $b \to s\mu\mu$ seems to undershoot SM in several exclusive modes
- A sign of weaker muon coupling or a common issue with form factors from SM?

Other $b \to s\mu\mu$ differential decay rates at LHCb

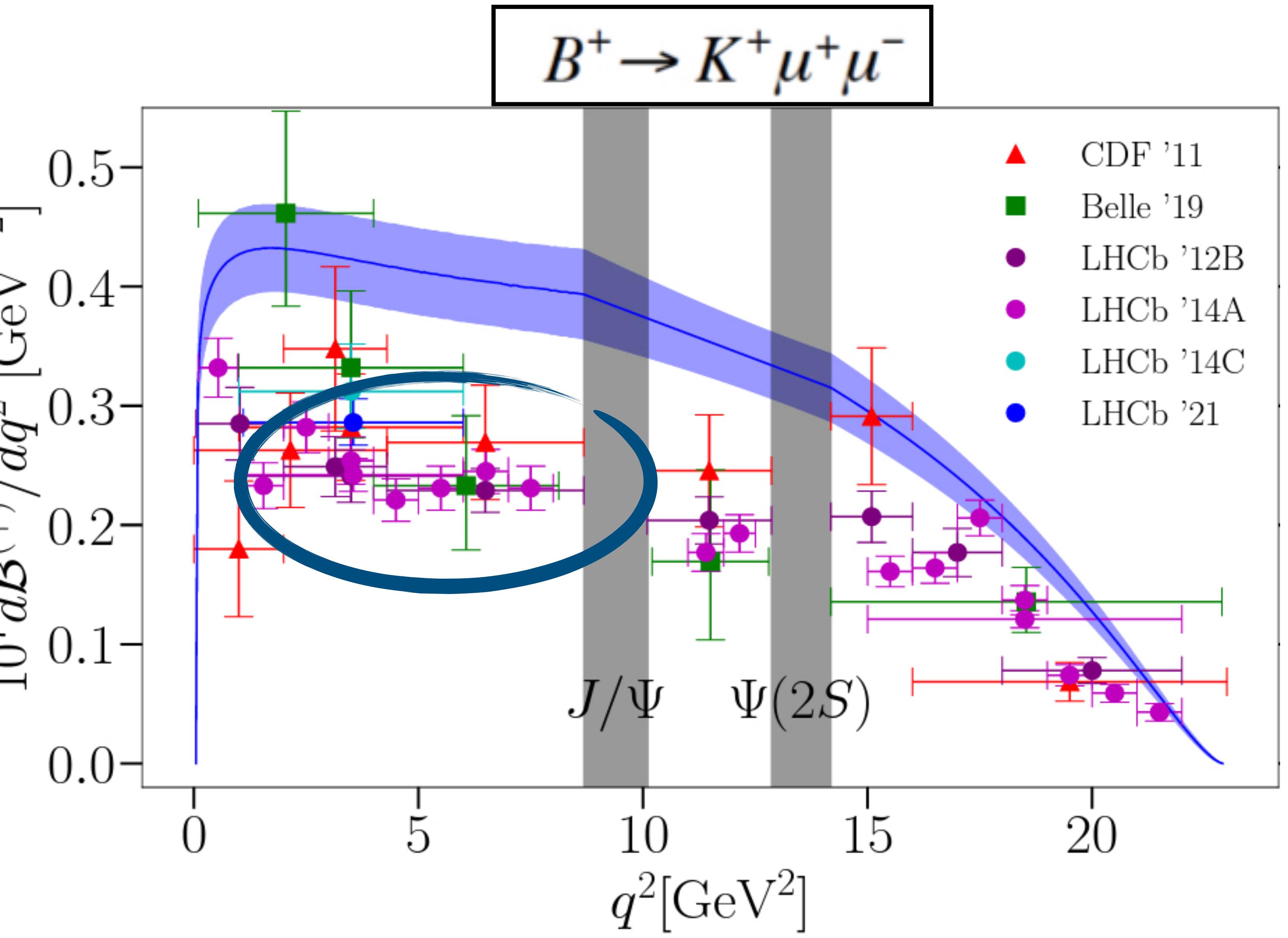

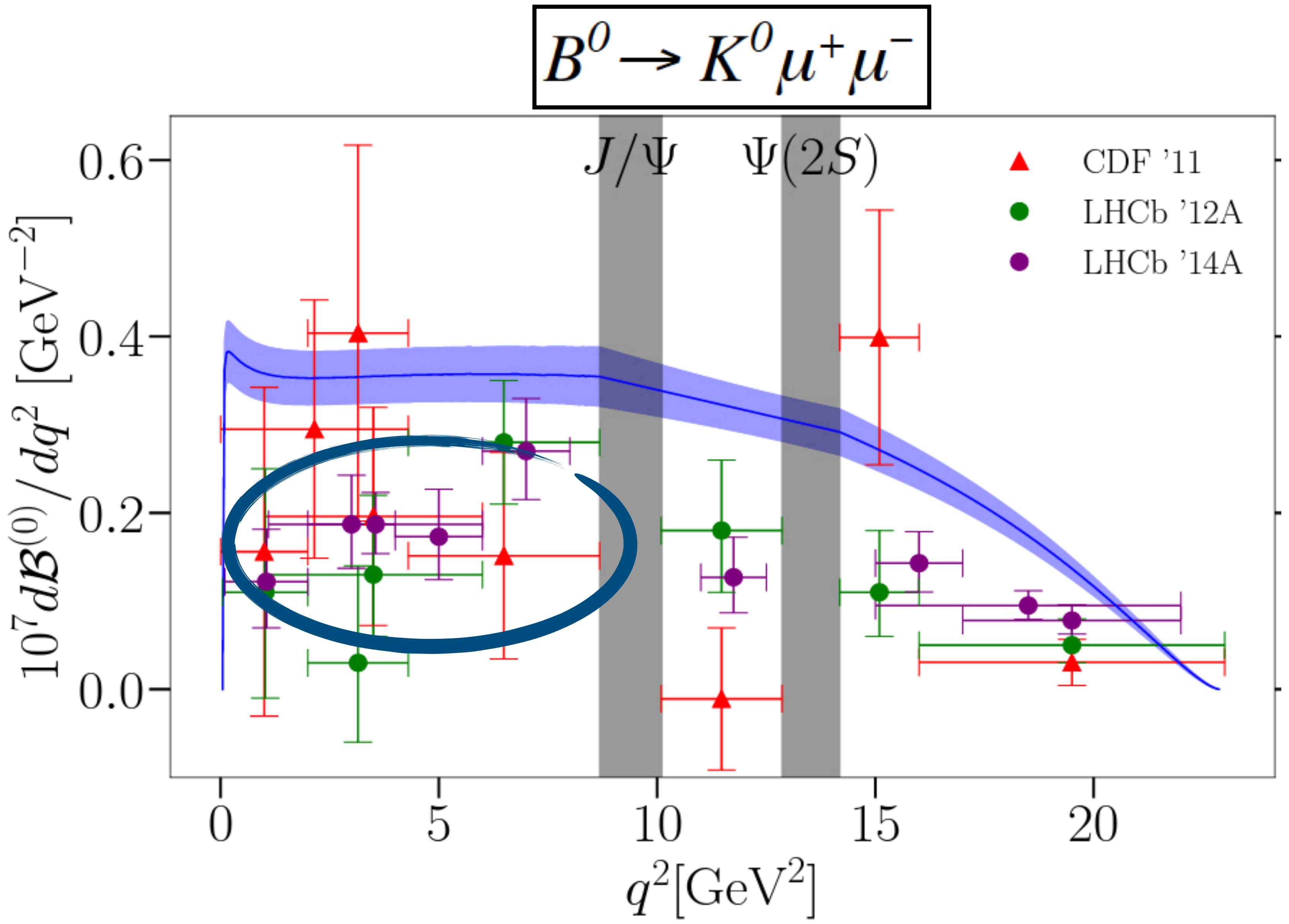

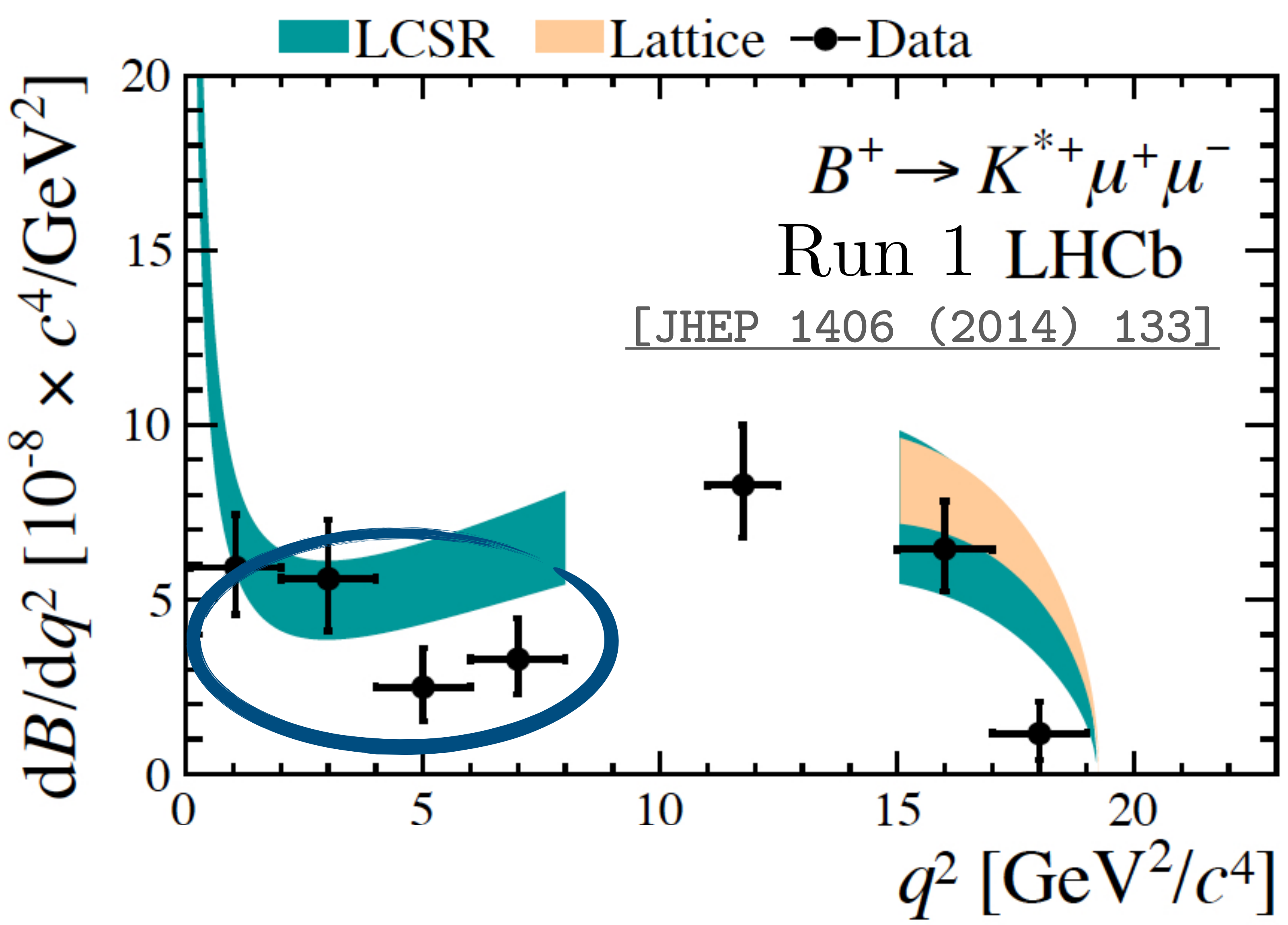

[JHEP 1406 (2014) 133]

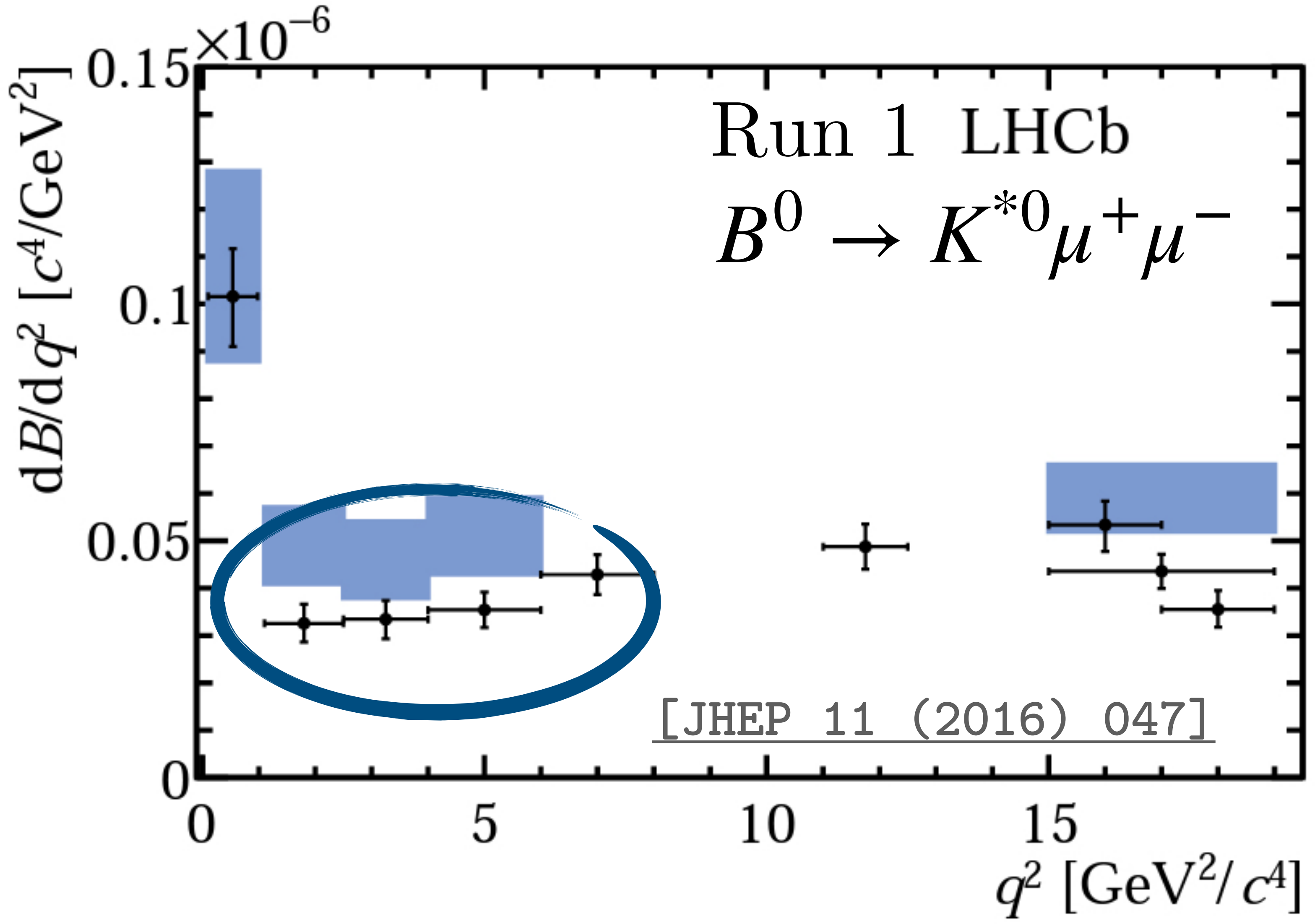

[JHEP 11 (2016) 047]

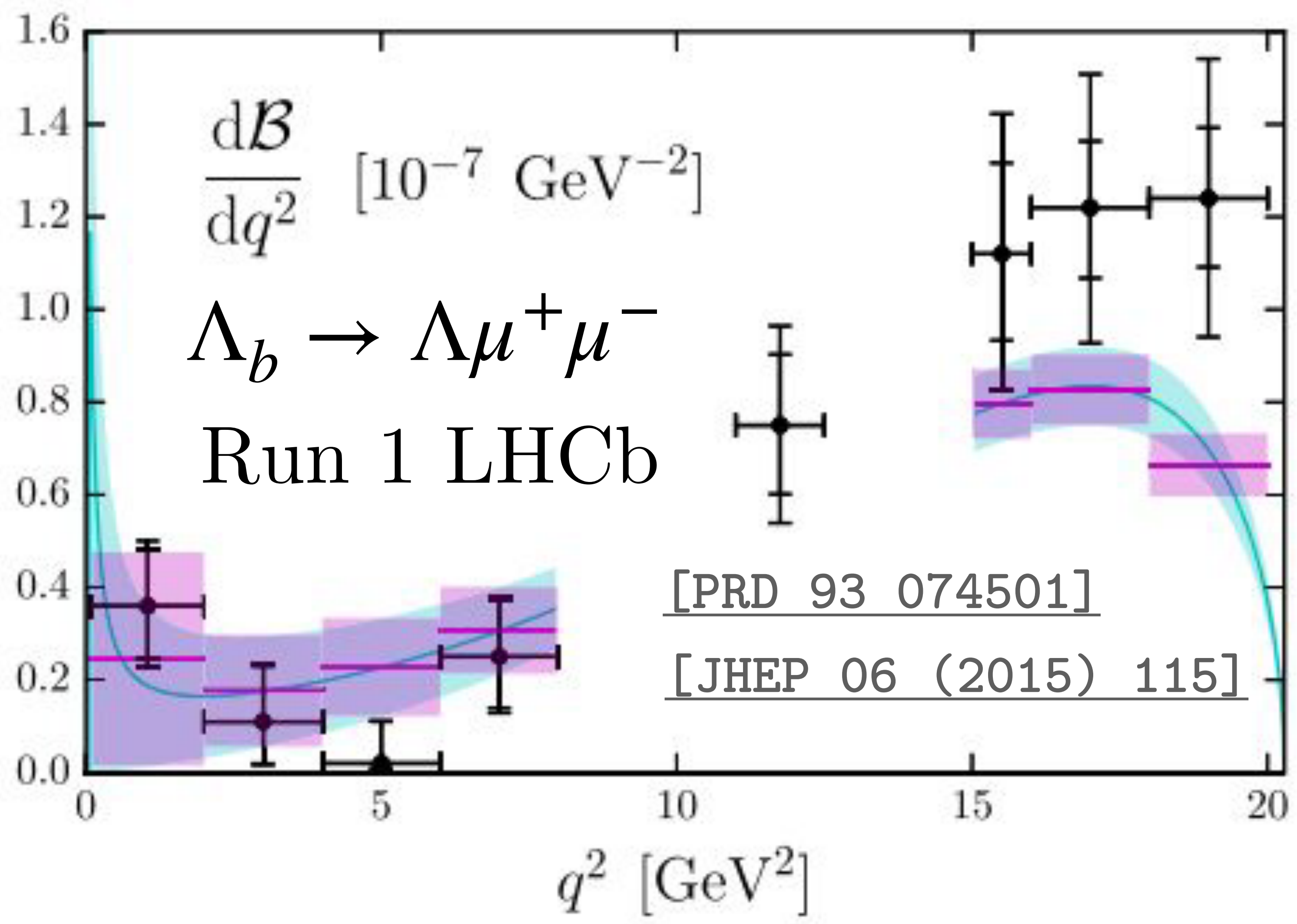

[PRD 93 074501]

[JHEP 06 (2015) 115]

- Nice progresses recently in computing the FF in $B \to K$ from LQCD [arXiv:2207.13371] and non-local corrections [JHEP 09 (2022) 133]

$b \to s\ell\ell$ measurements: angular analyses

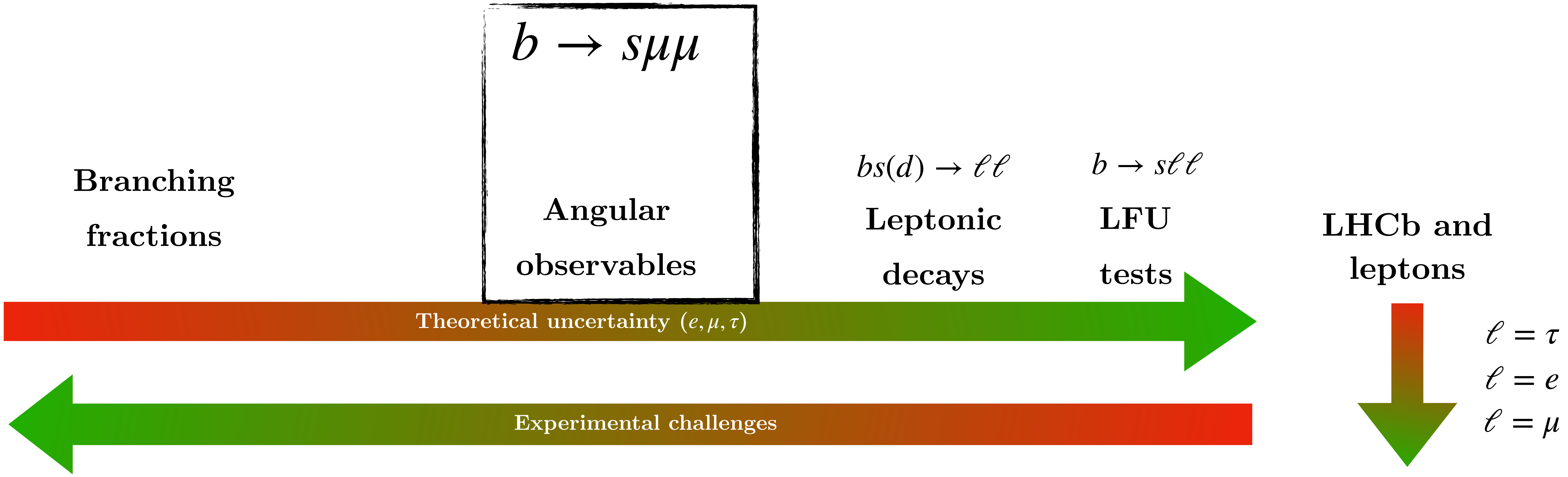

Branching fractions

$b \to s\mu\mu$

Angular observables

$bs(d) \to \ell\ell$

Leptonic decays

$b \to s\ell\ell$

LFU tests

LHCb and leptons

Theoretical uncertainty (e, μ, τ)

Experimental challenges

$\ell = \tau$

$\ell = e$

$\ell = \mu$

Angular $b \to s\mu\mu$ analyses

- **$B \to V\mu^+\mu^-$: vector in final state has rich kinematic structure → characterise NP**
- Described by 3 angles and q^2

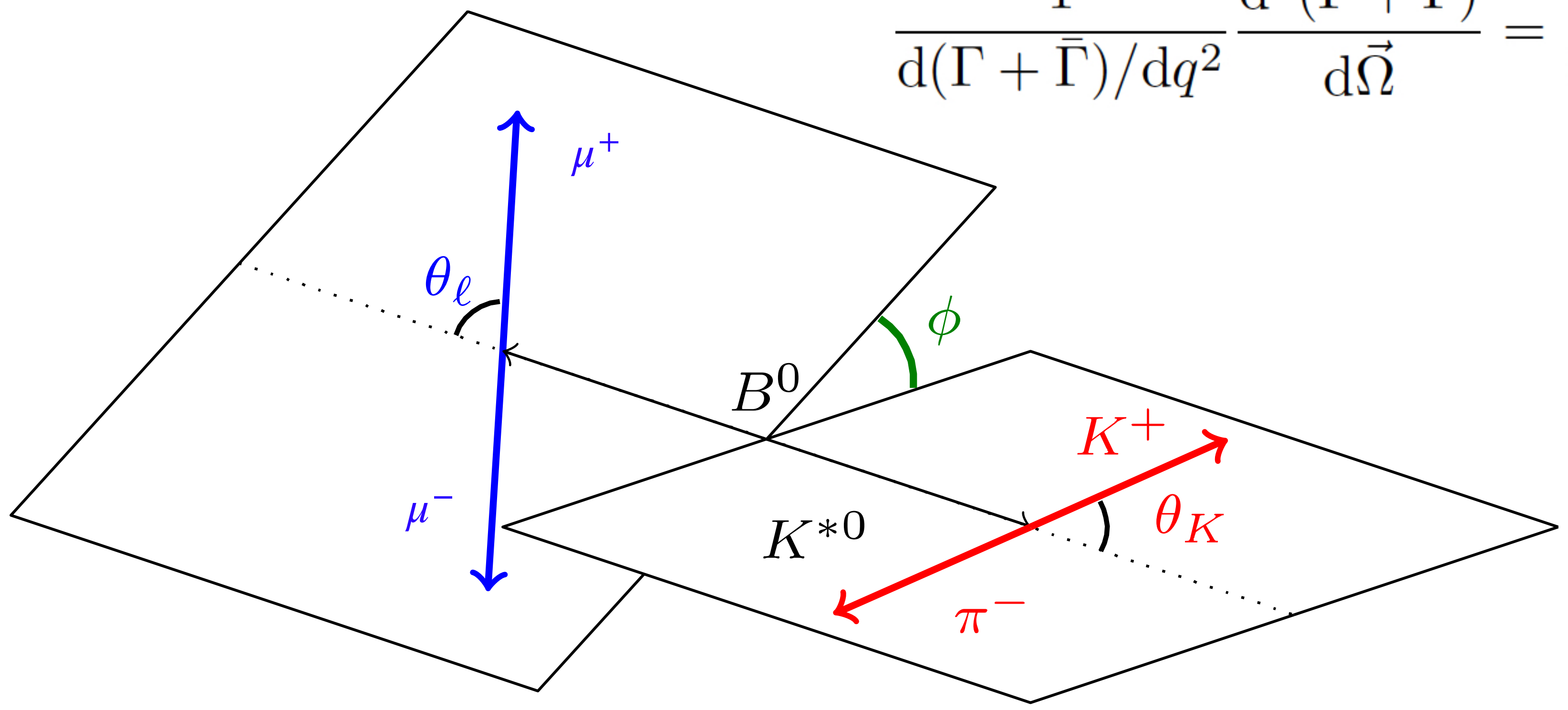

$$\frac{1}{\mathrm{d}(\Gamma+\bar{\Gamma})/\mathrm{d}q^2}\frac{\mathrm{d}^3(\Gamma+\bar{\Gamma})}{\mathrm{d}\vec{\Omega}} = \frac{9}{32\pi}\Big[\tfrac{3}{4}(1-F_{\mathrm{L}})\sin^2\theta_K + F_{\mathrm{L}}\cos^2\theta_K + \tfrac{1}{4}(1-F_{\mathrm{L}})\sin^2\theta_K\cos 2\theta_\ell$$
$$- F_{\mathrm{L}}\cos^2\theta_K\cos 2\theta_\ell + S_3\sin^2\theta_K\sin^2\theta_\ell\cos 2\phi$$
$$+ S_4\sin 2\theta_K\sin 2\theta_\ell\cos\phi + S_5\sin 2\theta_K\sin\theta_\ell\cos\phi$$
$$+ \tfrac{4}{3}A_{\mathrm{FB}}\sin^2\theta_K\cos\theta_\ell + S_7\sin 2\theta_K\sin\theta_\ell\sin\phi$$
$$+ S_8\sin 2\theta_K\sin 2\theta_\ell\sin\phi + S_9\sin^2\theta_K\sin^2\theta_\ell\sin 2\phi\Big]$$

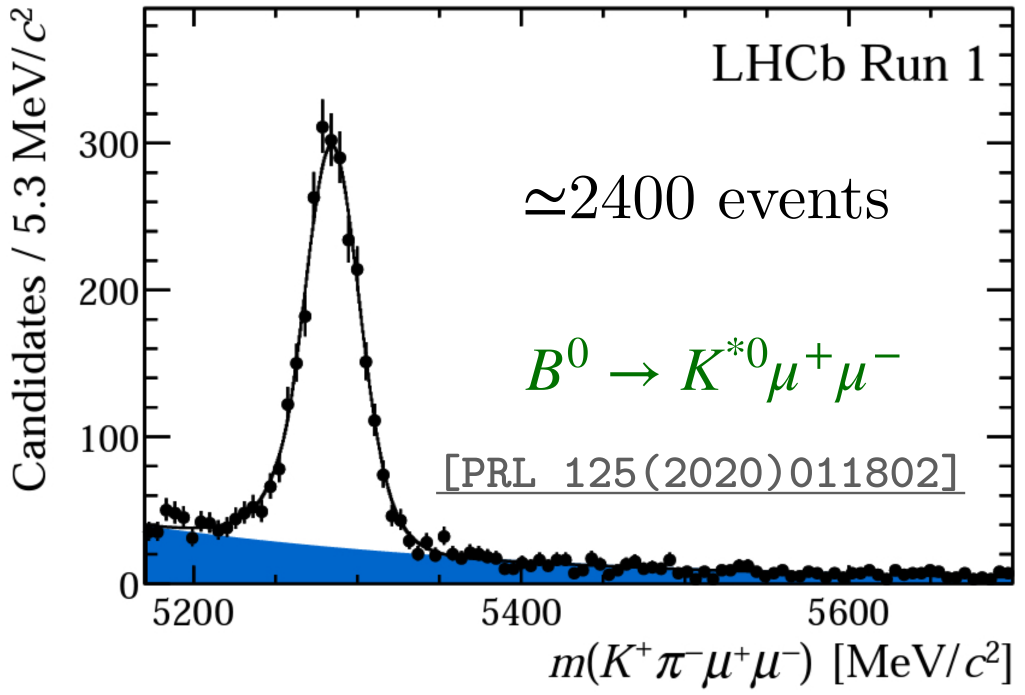

[PRL 125(2020)011802]

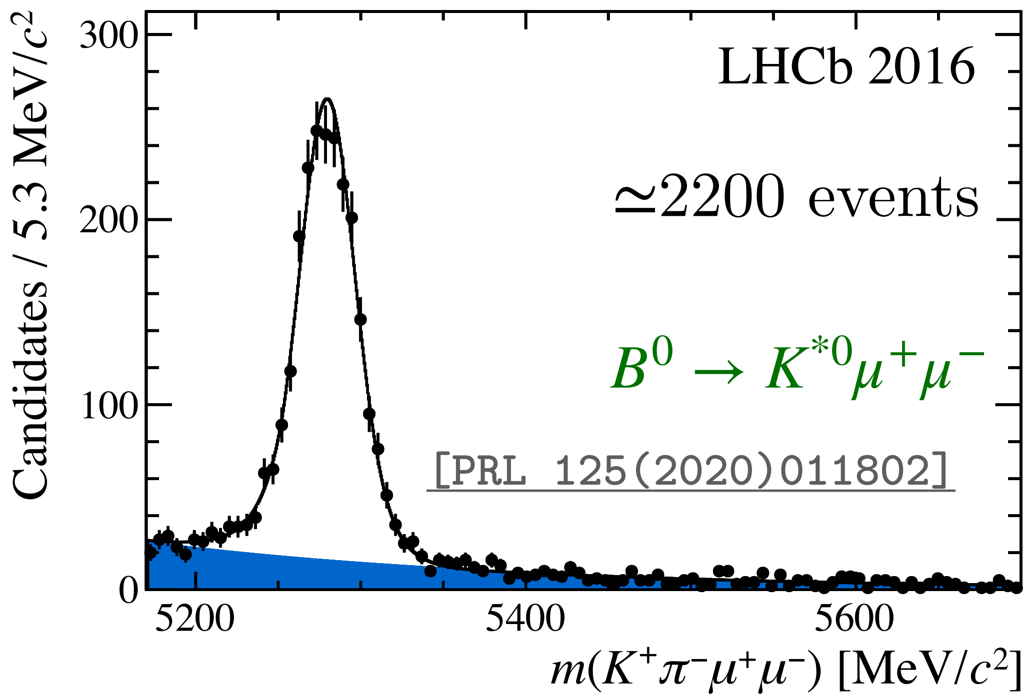

[PRL 125(2020)011802]

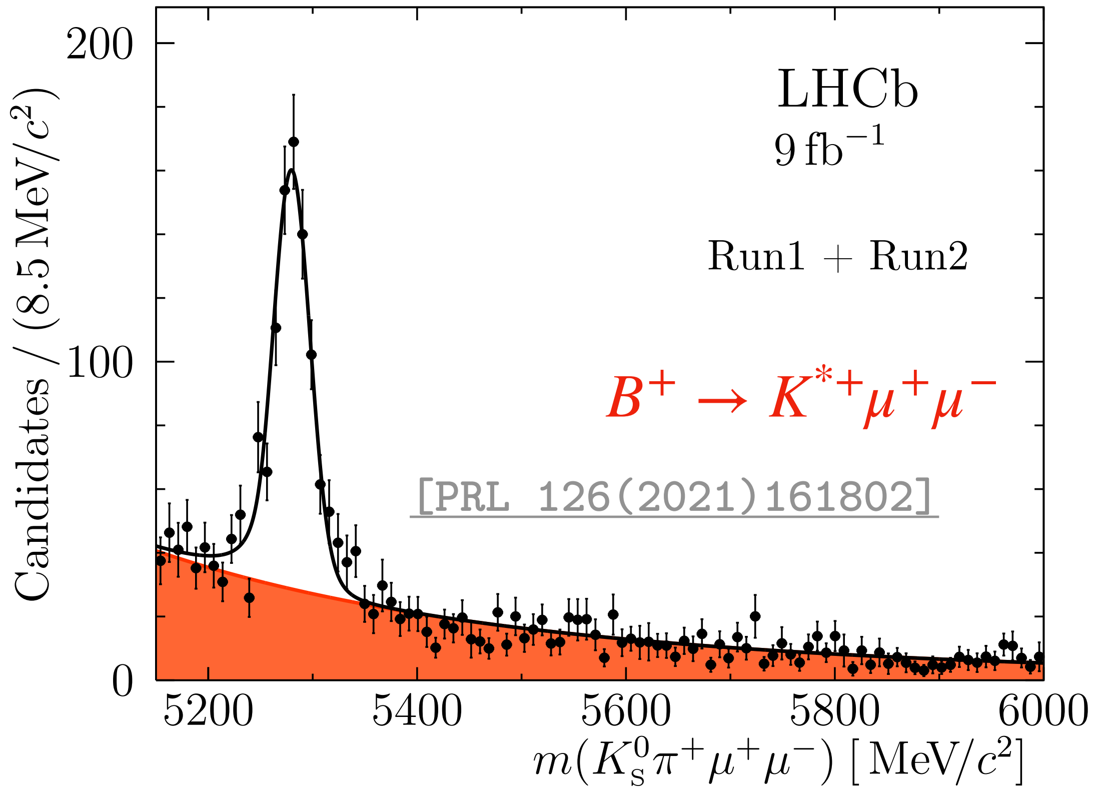

[PRL 126(2021)161802]

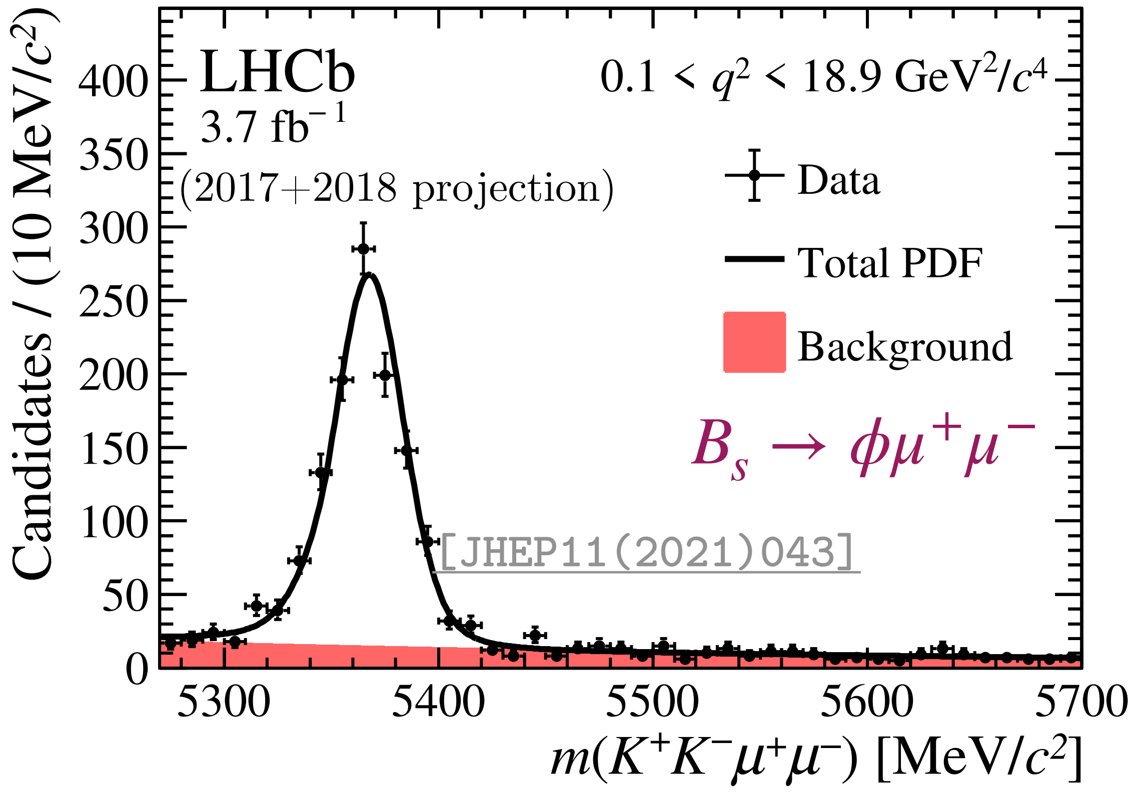

[JHEP11(2021)043]

- **Recent results from LHCb:**
  - $B^0 \to K^{*0}\mu^+\mu^-$with 6 fb-1 (~4600 events)
  - $B^+ \to K^{*+}\mu^+\mu^-$ with 9 fb-1 (~700 events)
  - $B_s \to \phi\mu^+\mu^-$ with 9 fb-1 (~1900 events)

Angular $b \to s\mu\mu$ analyses

- **$B \to V\mu^+\mu^-$: vector in final state has rich kinematic structure → characterise NP**
- Described by 3 angles and q^2

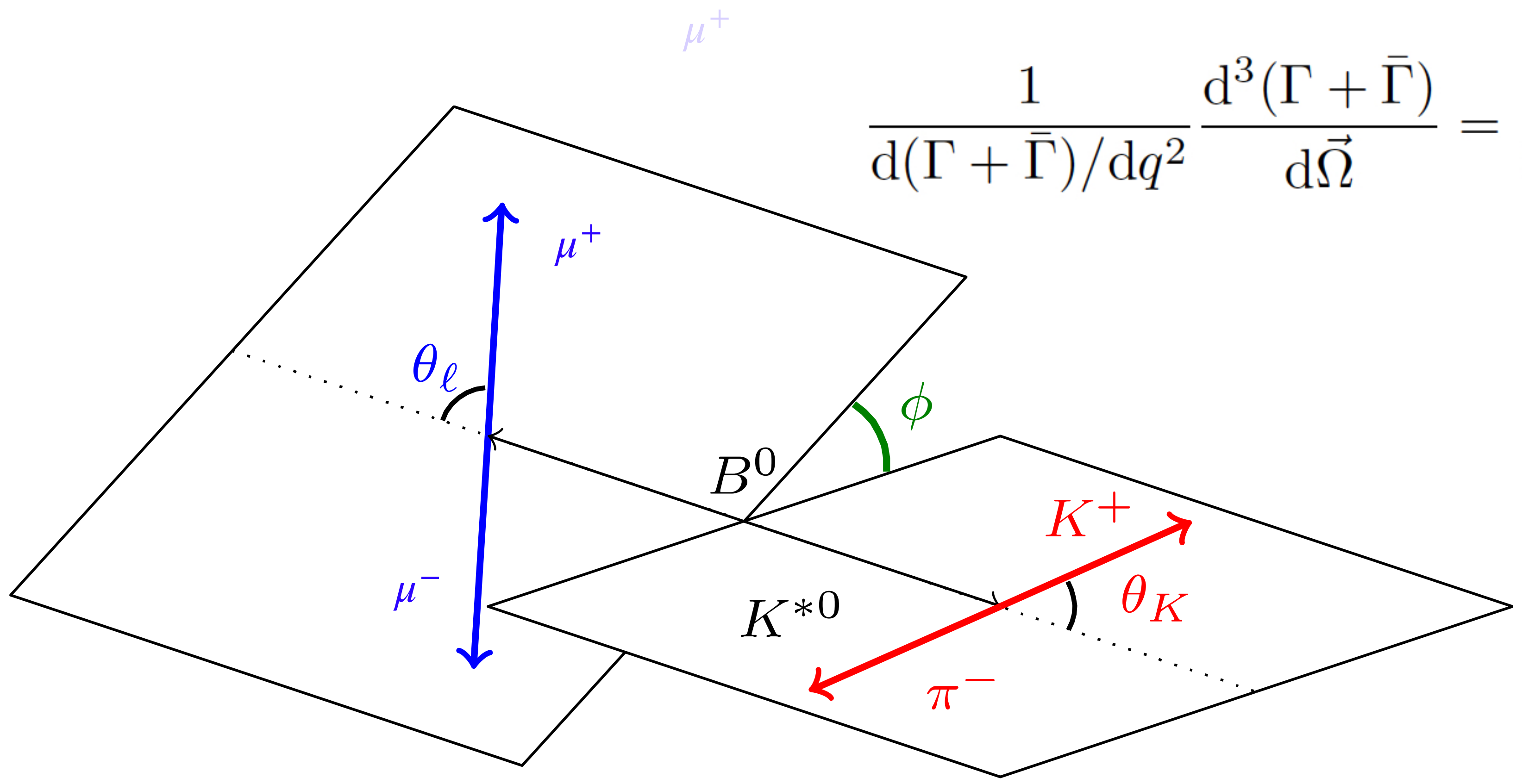

$$\frac{1}{\mathrm{d}(\Gamma+\bar{\Gamma})/\mathrm{d}q^2}\frac{\mathrm{d}^3(\Gamma+\bar{\Gamma})}{\mathrm{d}\vec{\Omega}} = \frac{9}{32\pi}\Big[\tfrac{3}{4}(1-F_\mathrm{L})\sin^2\theta_K + F_\mathrm{L}\cos^2\theta_K + \tfrac{1}{4}(1-F_\mathrm{L})\sin^2\theta_K\cos 2\theta_\ell$$
$$- F_\mathrm{L}\cos^2\theta_K\cos 2\theta_\ell + S_3\sin^2\theta_K\sin^2\theta_\ell\cos 2\phi$$
$$+ S_4\sin 2\theta_K\sin 2\theta_\ell\cos\phi + S_5\sin 2\theta_K\sin\theta_\ell\cos\phi$$
$$+ \tfrac{4}{3}A_\mathrm{FB}\sin^2\theta_K\cos\theta_\ell + S_7\sin 2\theta_K\sin\theta_\ell\sin\phi$$
$$+ S_8\sin 2\theta_K\sin 2\theta_\ell\sin\phi + S_9\sin^2\theta_K\sin^2\theta_\ell\sin 2\phi\Big]$$

- **Fit angular spectrum in different q^2 bins**
- **8 angular coefficients sensitive to NP**
  - F_L fraction of longitudinal polarisation
  - A_{FB} forward backward asymmetry
  - S_i : 6-independent angular coefficients

$B^0 \to K^{*0}\mu^+\mu^-$

[PRL 125(2020)011802]

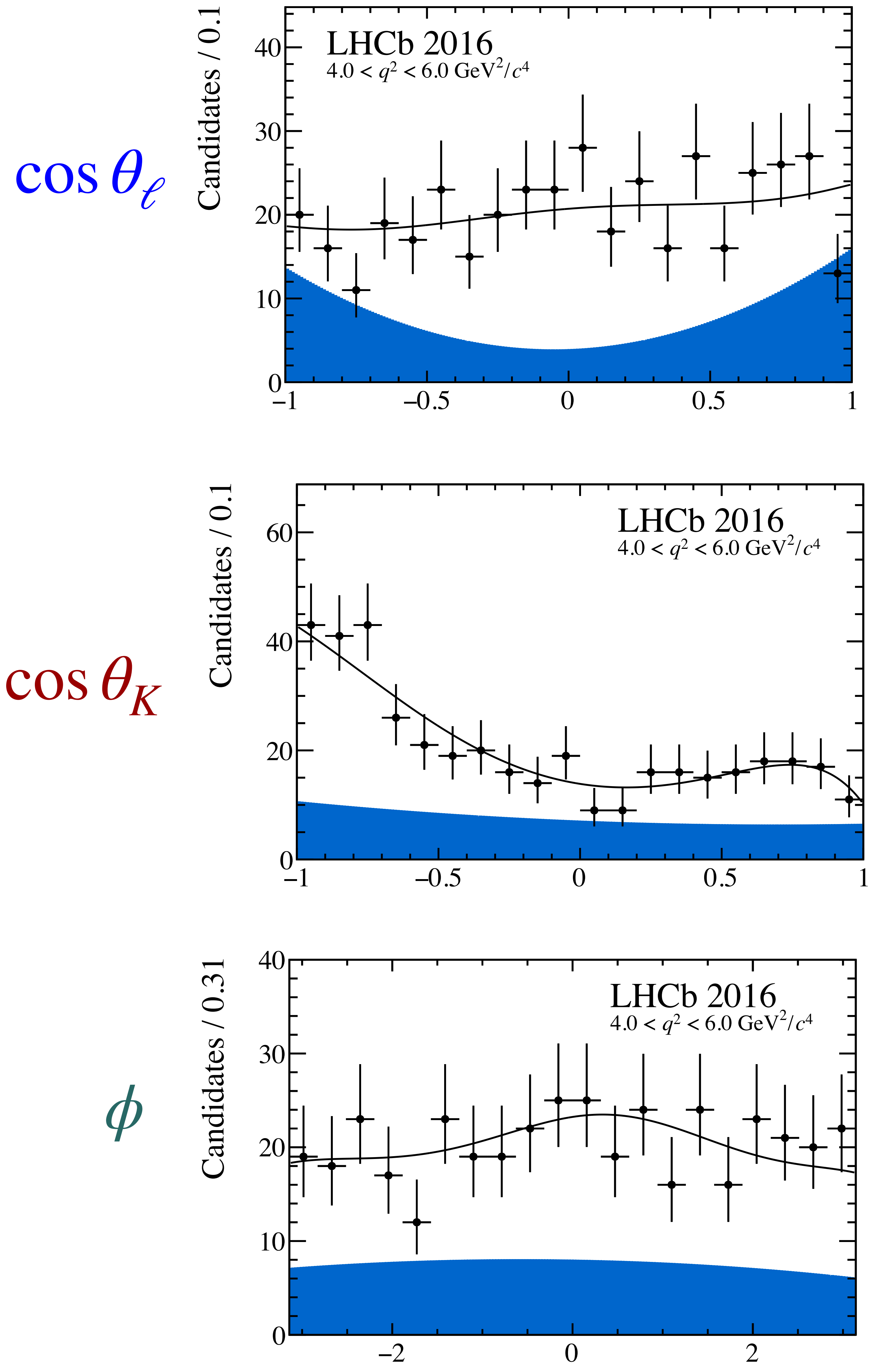

Angular $b \to s\mu\mu$ analyses

- **Optimised variables to reduce form factors uncertainties** $P_5' = \frac{S_5}{\sqrt{F_L(1-F_L)}}$

[JHEP, 05 (2013) 137]

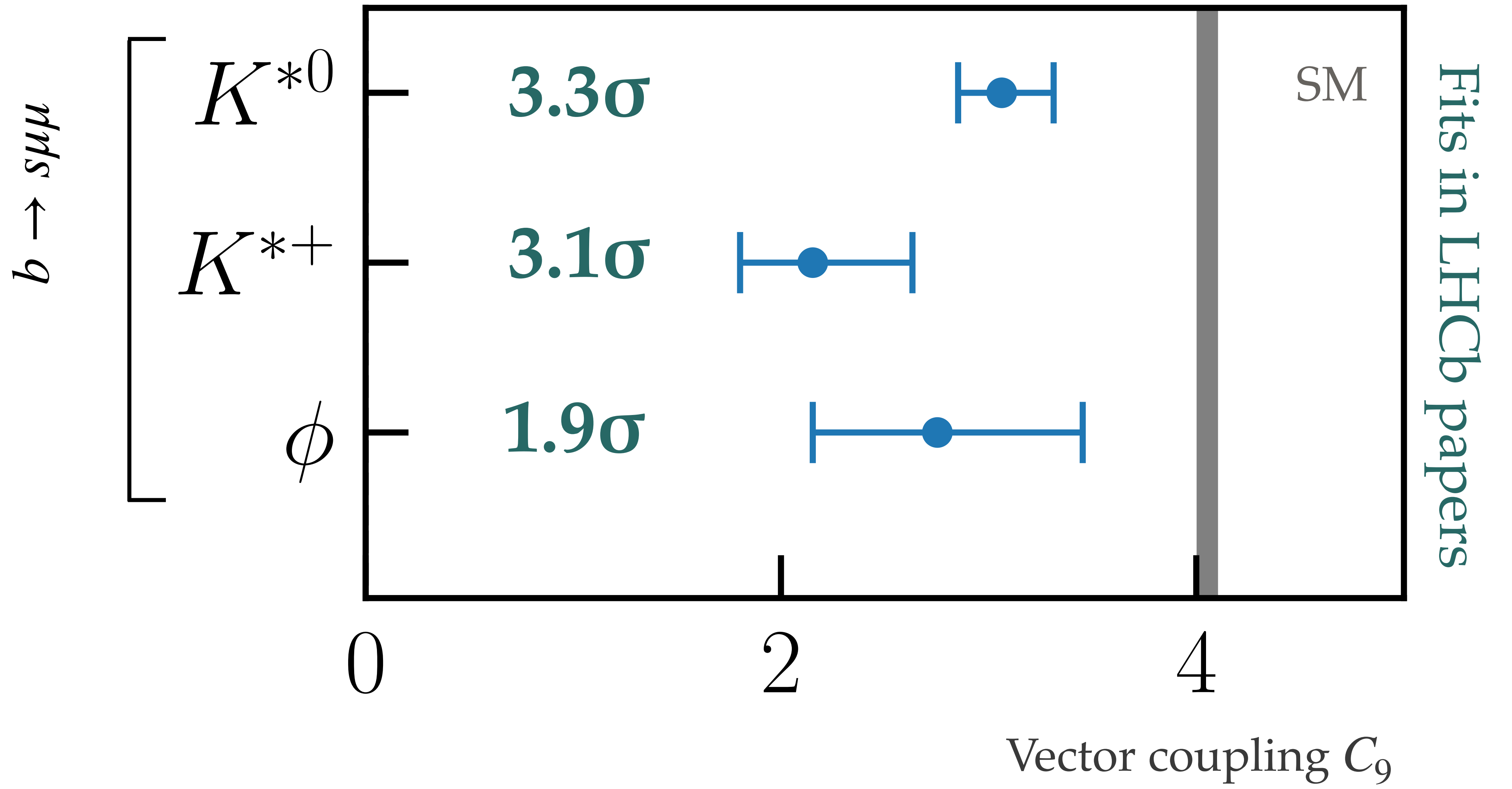

[PRL 125(2020)011802]

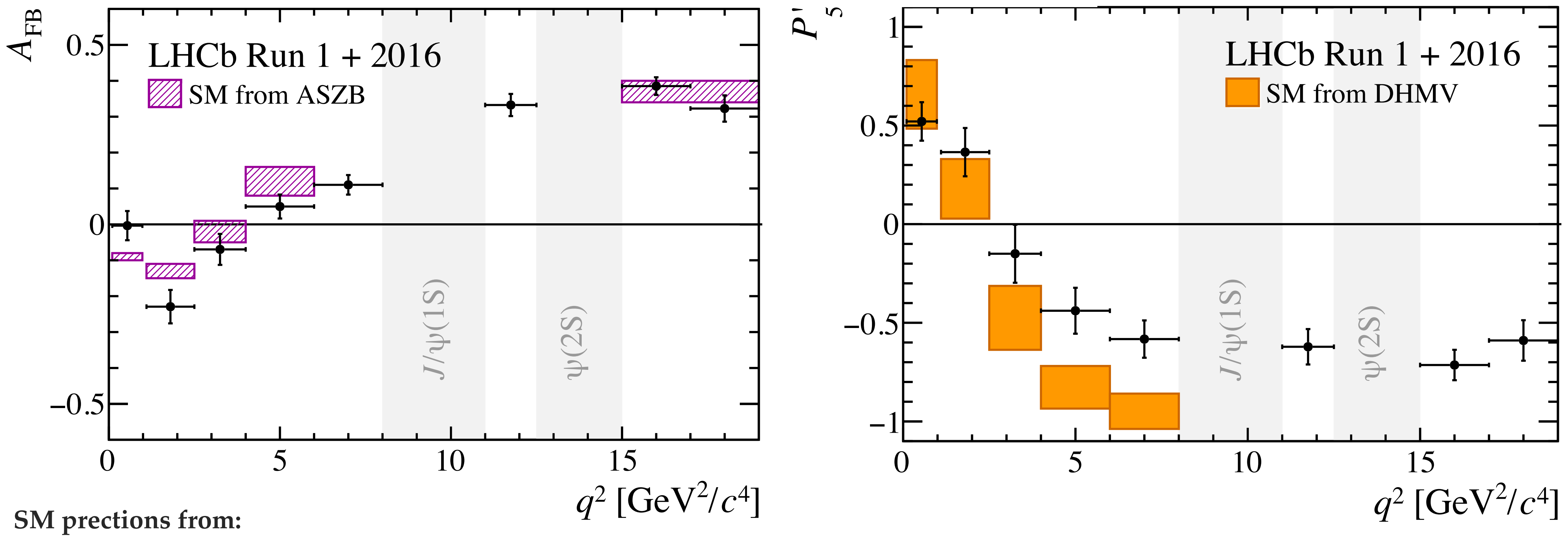

SM prections from:

▨ Bharucha et al arXiv:1503.05534
Altmannshofer et al arXiv:1411.3161

🟧 Descotes-Genon et al arXiv:1407.8526
Khodjamirian et al arXiv:1006.4945

- Deviations are coherent and significant when interpreted as modified vector coupling C_9
  - σ_{th} **under scrutiny (charm loops)**
- **Full Run2 still to exploit at LHCb in K^{*0} mode**

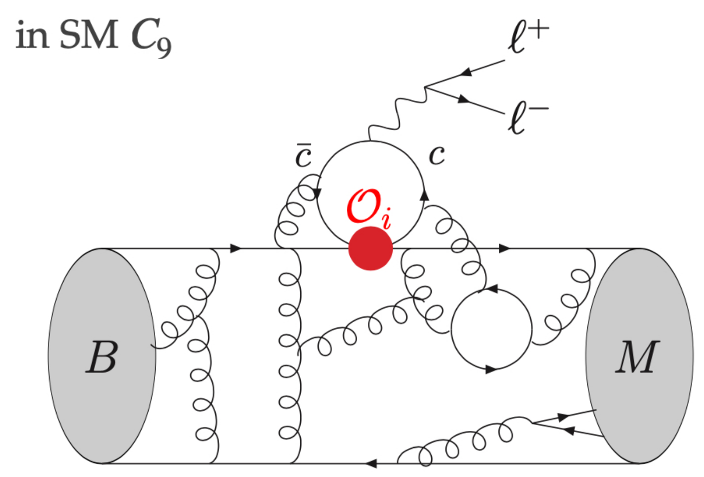

Angular $b \to s\mu\mu$ analyses

- Optimised variables to reduce form factors uncertainties $P'_5 = \frac{S_5}{\sqrt{F_L(1-F_L)}}$

[JHEP, 05 (2013) 137]

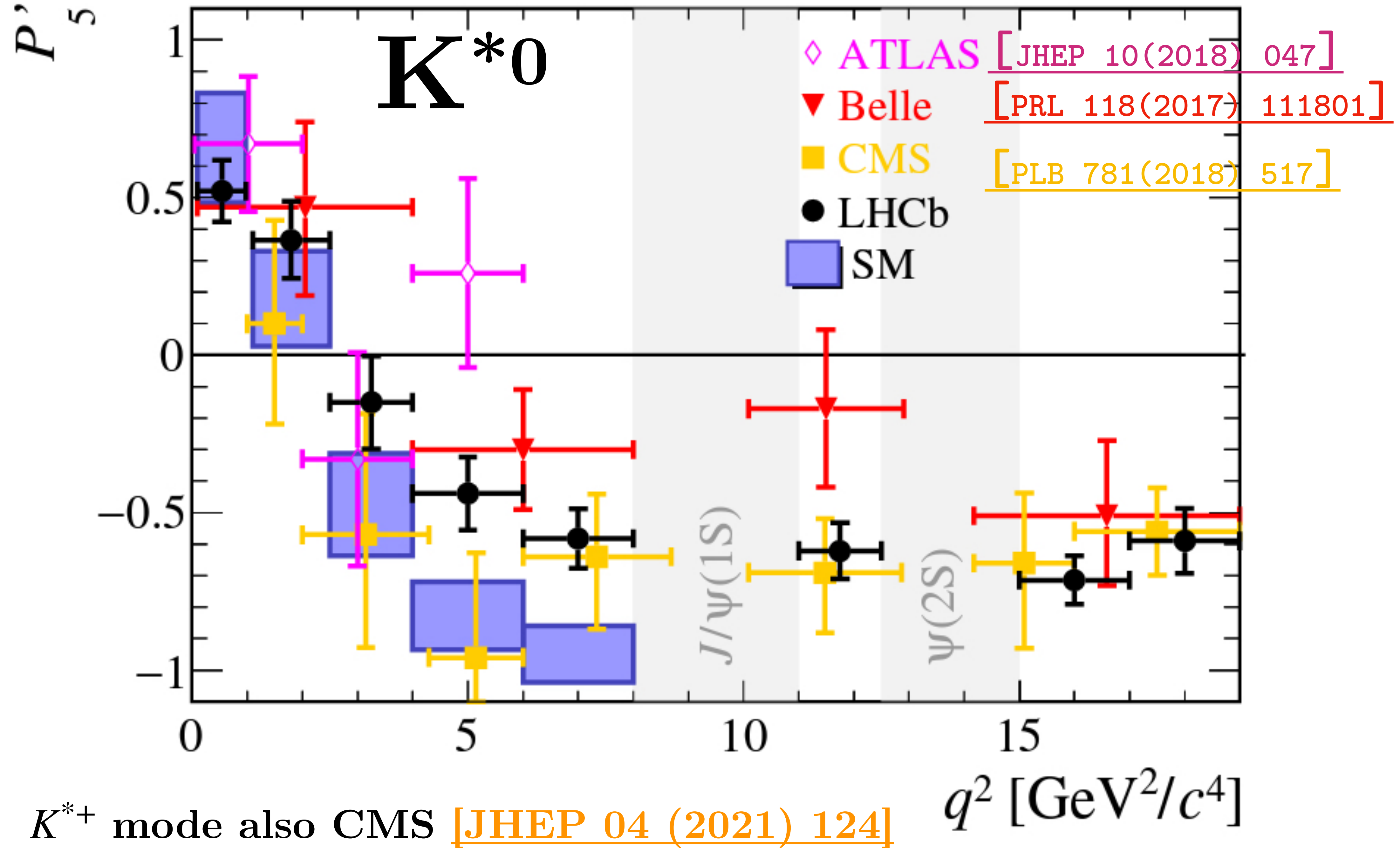

K^{*+} mode also CMS [JHEP 04 (2021) 124]

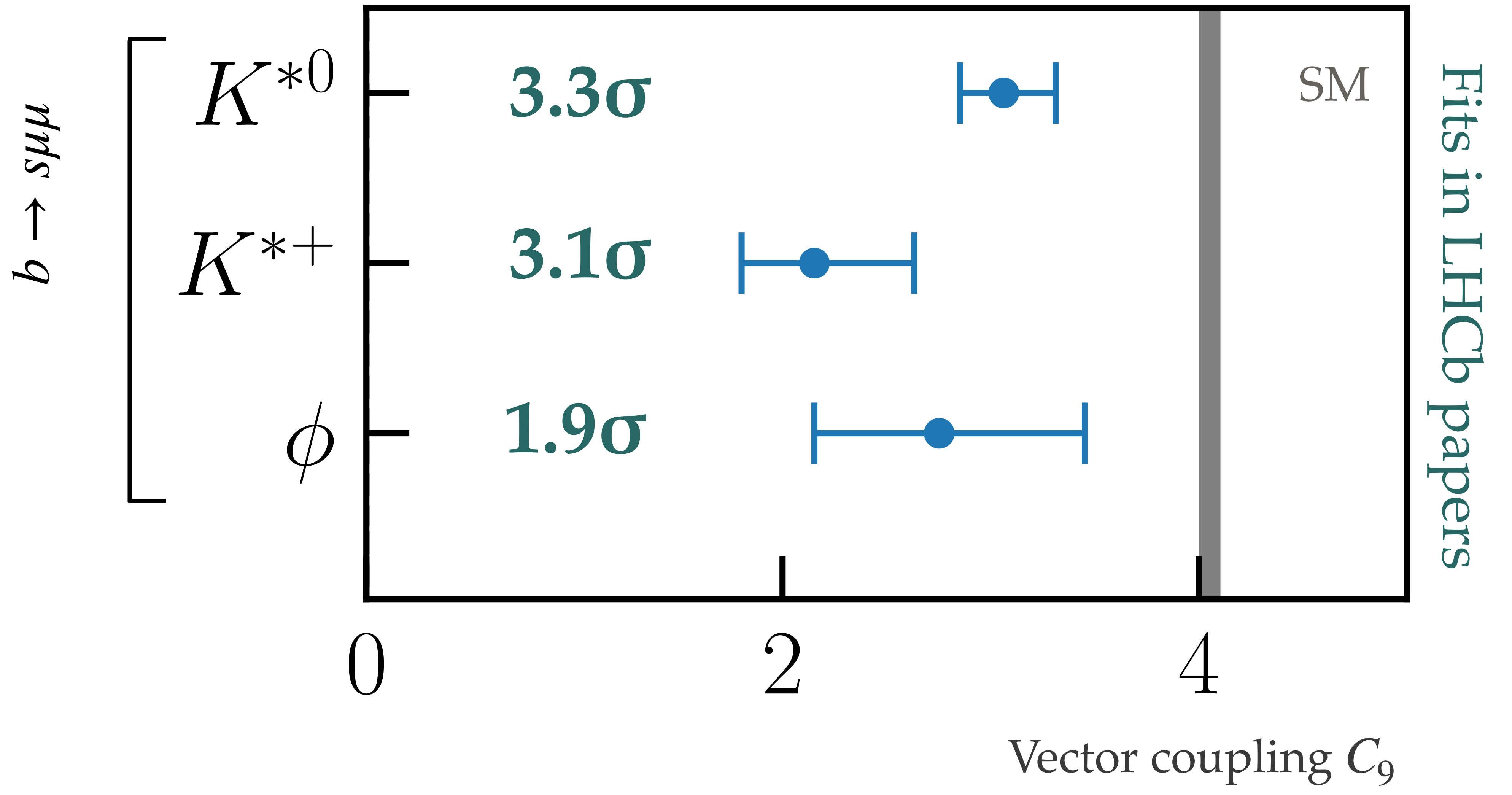

- Deviations are coherent and significant when interpreted as modified vector coupling C_9
  - σ_{th} under scrutiny (charm loops)

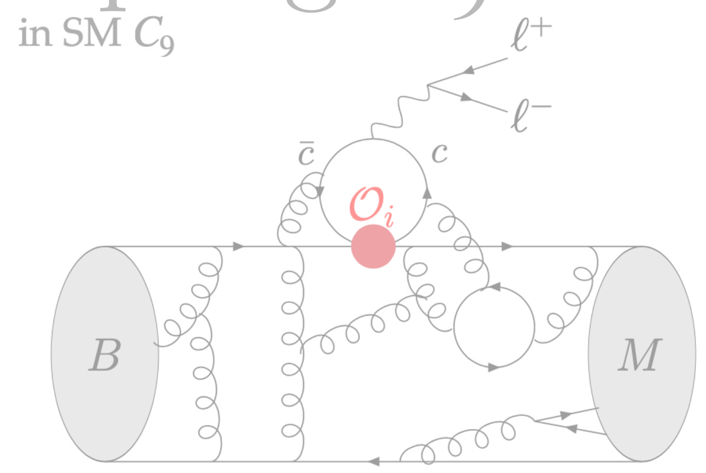

- **Full Run2 still to exploit at LHCb in K^{*0} mode**

- **Towards a Run1+2 results across LHC collaborations, waiting for BelleII**

$bs(d) \to \ell\ell$ measurements: pure leptonic

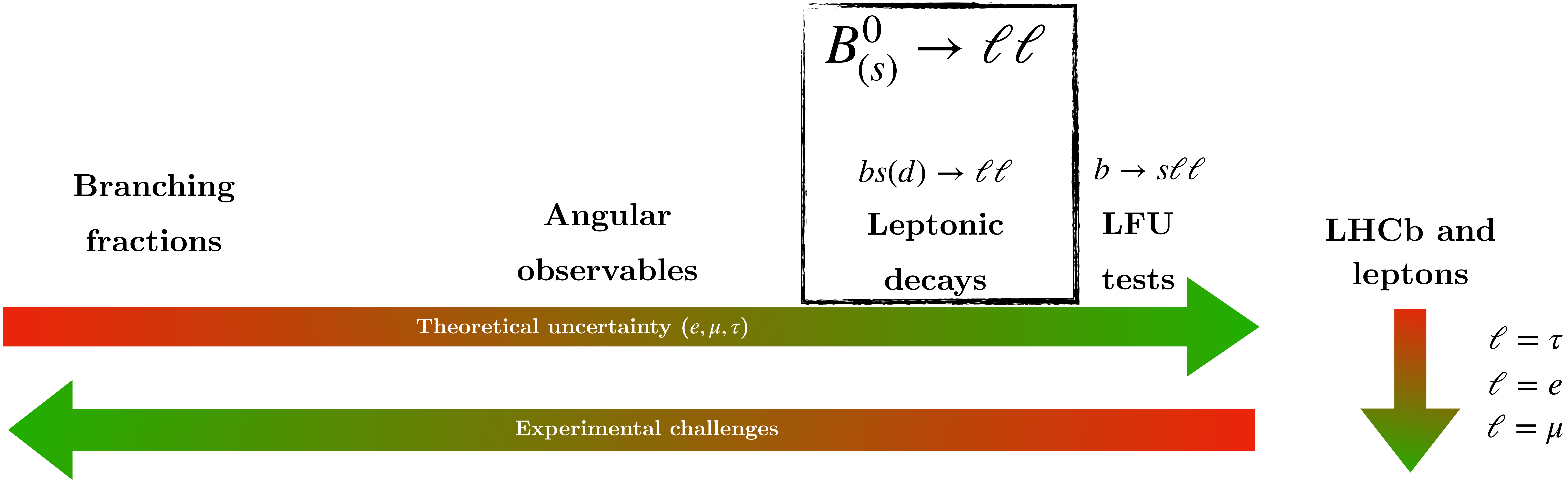

$B^0_{(s)} \to \ell\ell$

Branching fractions

Angular observables

$bs(d) \to \ell\ell$

Leptonic decays

$b \to s\ell\ell$

LFU tests

LHCb and leptons

Theoretical uncertainty (e, μ, τ)

Experimental challenges

$\ell = \tau$

$\ell = e$

$\ell = \mu$

The golden $B \to \mu\mu$ decay

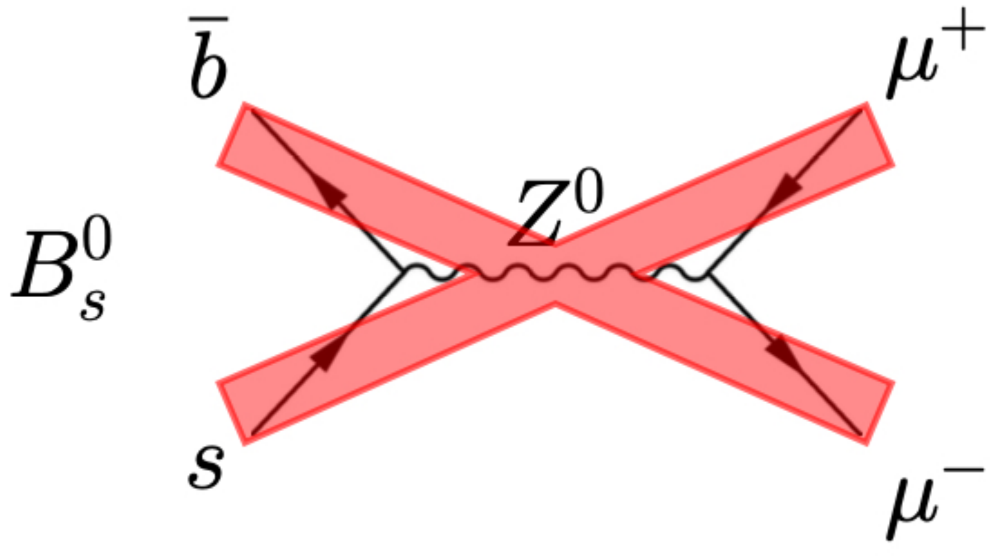

(tree)

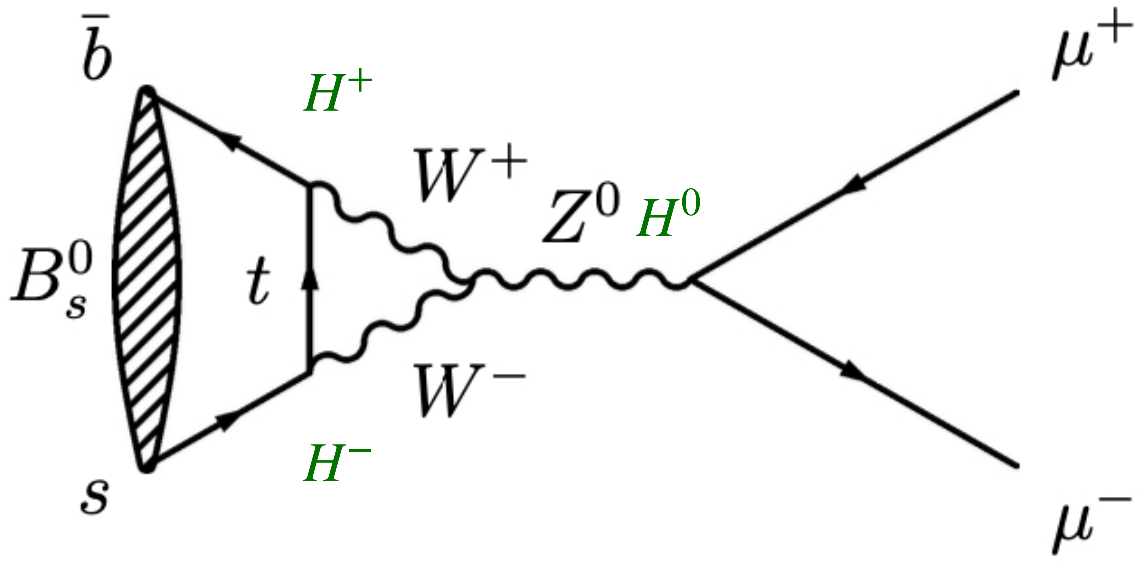

(penguin)

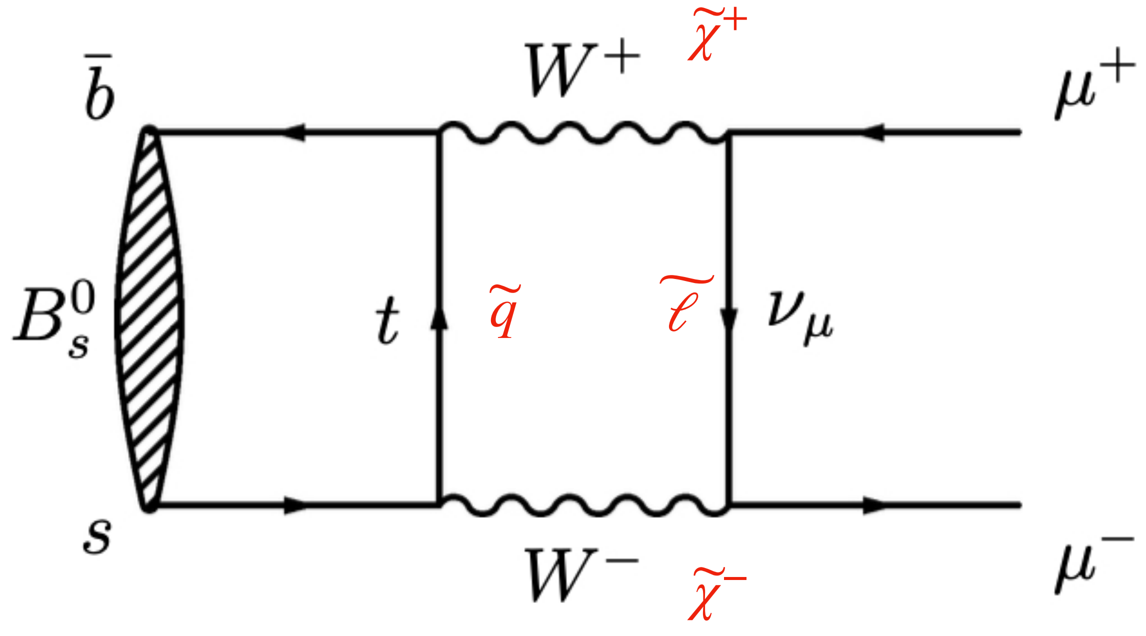

(box)

- **FCNC process + helicity suppressed :** $\mathscr{B}(B_s \to \mu\mu) \sim 10^{-9}$

$$\mathscr{B}(B_q^0 \to \mu^+\mu^-)_{\text{SM}} = \frac{\tau_{B_q} G_F^4 M_W^4 \sin^4\theta_W}{8\pi^5} |C_{10}^{\text{SM}} V_{tb} V_{tq}^*|^2 f_{B_q}^2 m_{B_q} m_\mu^2 \sqrt{1 - \frac{4m_\mu^2}{m_{B_q}^2}} \frac{1}{1-y_q} \qquad q = d, s$$

Single Wilson

f_{B_q} known at 0.5% [PRD 98 (2019) 074512]

- **Clean predictions in SM (largest source from $\left|V_{cb}\right|$ inclusive $^{(*)}$)**

$$\mathscr{B}(B_s^0 \to \mu^+\mu^-)_{\text{SM}} = (3.66 \pm 0.14) \times 10^{-9}$$
$$\mathscr{B}(B^0 \to \mu^+\mu^-)_{\text{SM}} = (1.03 \pm 0.05) \times 10^{-10}$$

[JHEP 10 (2019) 232]

$(*)$ $\mathscr{B}(B_s^0 \to \mu^+\mu^-)_{V_{cb}-\text{independent estimate}} : (3.78^{+0.15}_{-0.10}) \times 10^{-9}$

- Sensitive to scalar/pseudo-scalar couplings
- Extended Higgs boson sectors

A golden channel for all LHC experiments (ATLAS/CMS/LHCb)

The golden $B \to \mu\mu$ decay status

- **CMS compatible with SM, better/equal sensitivity than LHCb contrary to $b \to s\ell\ell$**

- First observation on $B^0 \to \mu\mu$ still to do, also $b \to \mu\mu\gamma$ in full $m(\mu\mu)$ range

CMS UL

$\mathcal{B}(B^0 \to \mu^+\mu^-) < 1.9 \times 10^{-10}$ at 95% CL,

LHCb UL

$\mathcal{B}(B^0 \to \mu^+\mu^-) < 2.6 \times 10^{-10}$ at 95% CL,

- More data, challenges from $B \to hh$ backgrounds

$\mathcal{B}(B^0_s \to \mu^+\mu^-\gamma) < 2.0 \times 10^{-9}$ at 95% CL,
for $m(\mu\mu) > 4.9$GeV

- Direct search on-going

- ***Waiting for LHC combination***

[PRL 128 (2022) 041801]
[PRD 105 (2022) 012010]

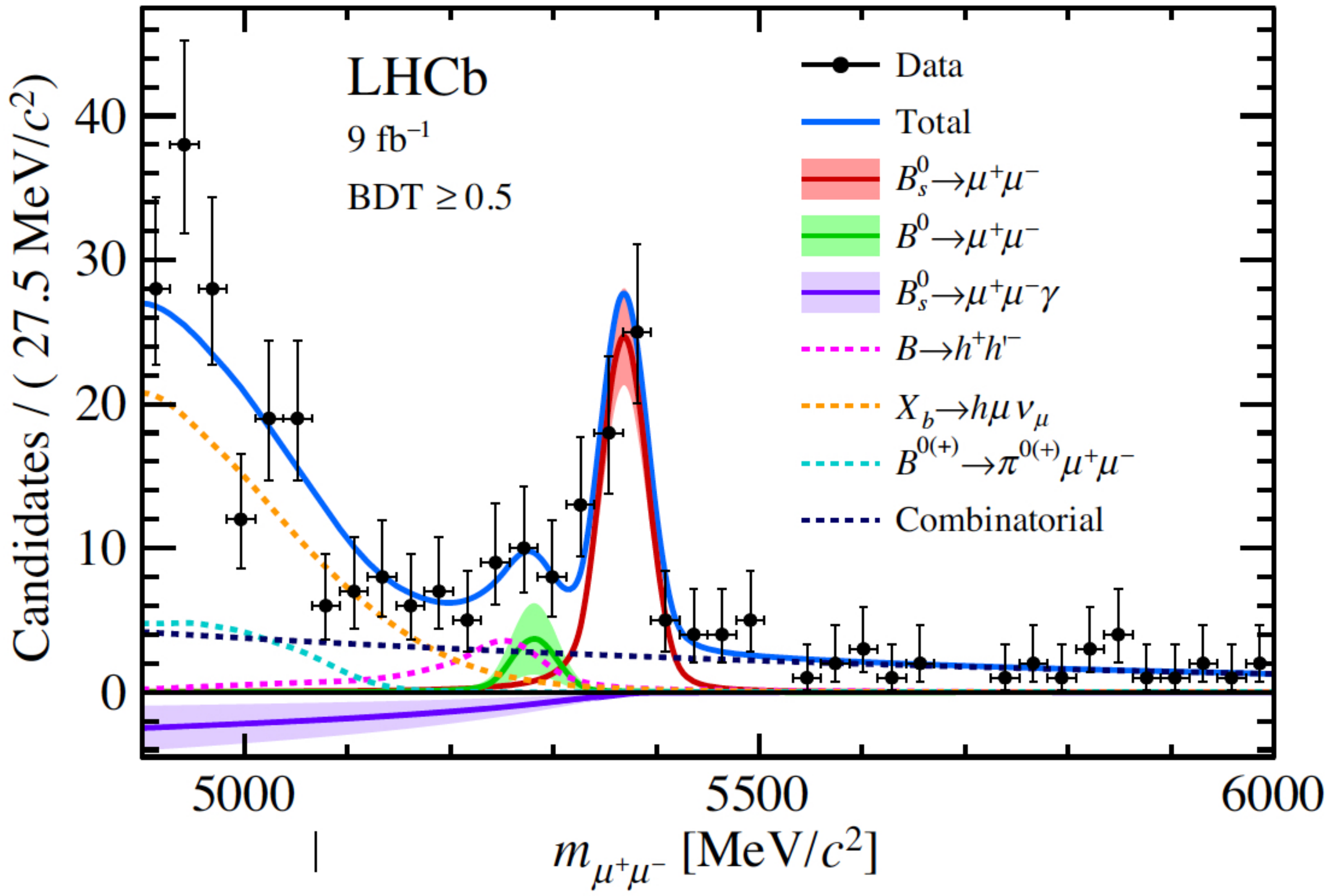

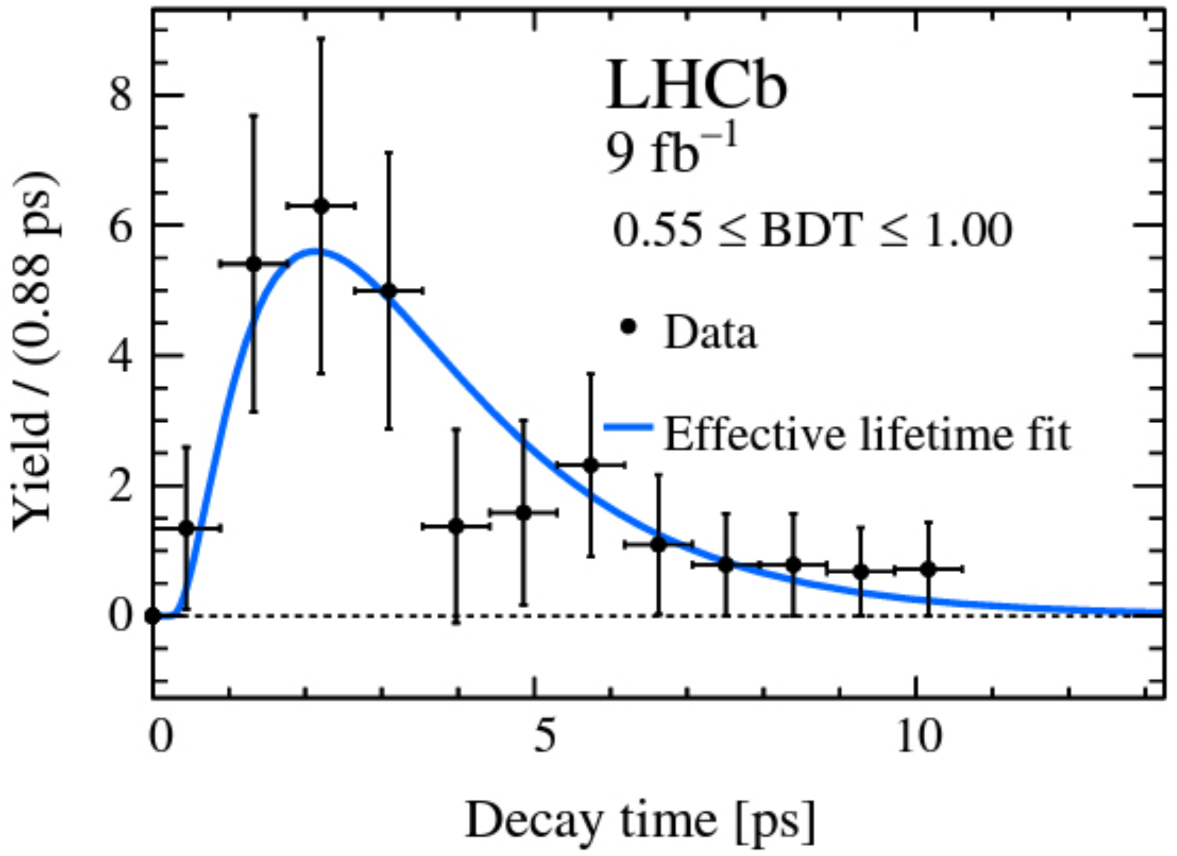

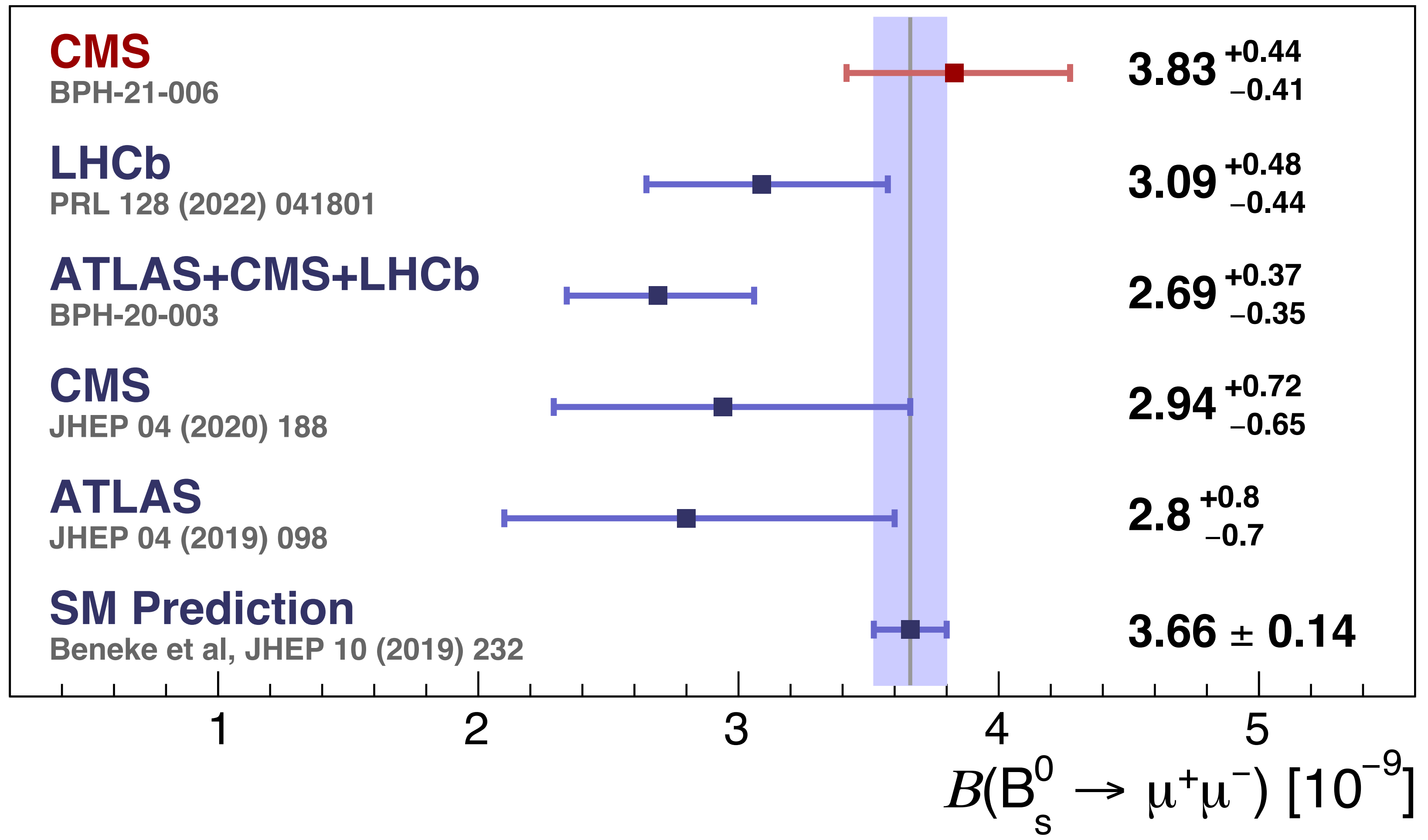

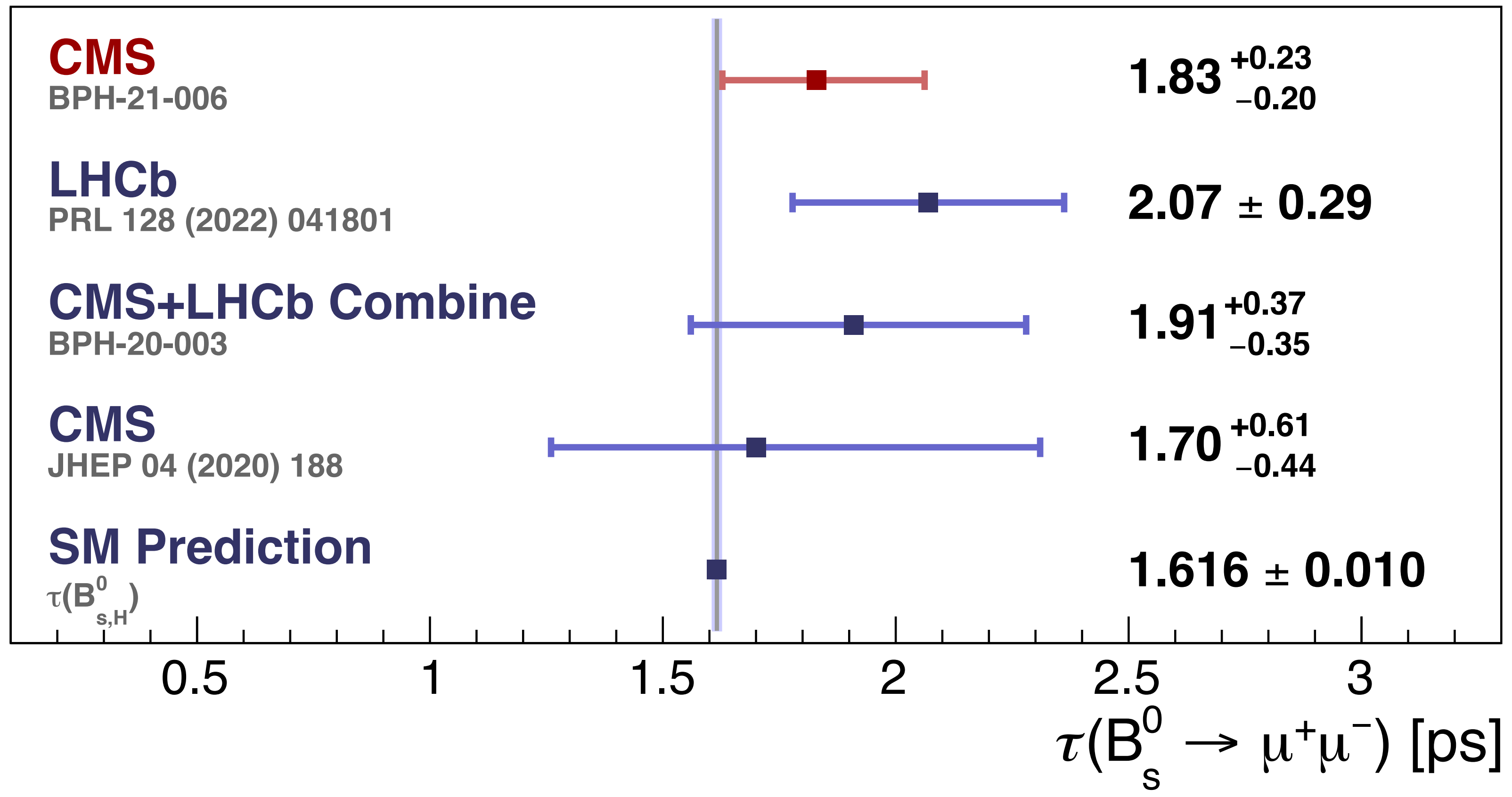

Beyond $b \to \mu\mu$, other fully leptonic decays at LHCb

- $B_{s,d} \to ee$ limits PRL 124 (2020) 211802

  $\mathcal{B}(B_s^0 \to e^+e^-) < 9.4 \times 10^{-9}$ (90 % CL)

  $\mathcal{B}(B^0 \to e^+e^-) < 2.5 \times 10^{-9}$ (90 % CL)

- $B_{s,d} \to \tau\tau$ limits PRL 118 (2017) 251802

  $\mathcal{B}(B_s^0 \to \tau^+\tau^-) < 6.8 \times 10^{-3}$ (90 % CL)

  $\mathcal{B}(B^0 \to \tau^+\tau^-) < 2.1 \times 10^{-3}$ (90 % CL)

- $B_{s,d} \to 4\mu$ limits [JHEP 3 (2022) 109]

  $\mathcal{B}(B_s^0 \to \mu^+\mu^-\mu^+\mu^-) < 8.6 \times 10^{-10}$

  $\mathcal{B}(B^0 \to \mu^+\mu^-\mu^+\mu^-) < 1.8 \times 10^{-10}$

  - Also limits on intermediate $a(\mu\mu)$ resonances at $10^{-9} - 10^{-10}$ with $m(a) = 1\text{GeV}$

- **Complementary but more experimentally challenging**

$B^0_{(s)} \to ee$

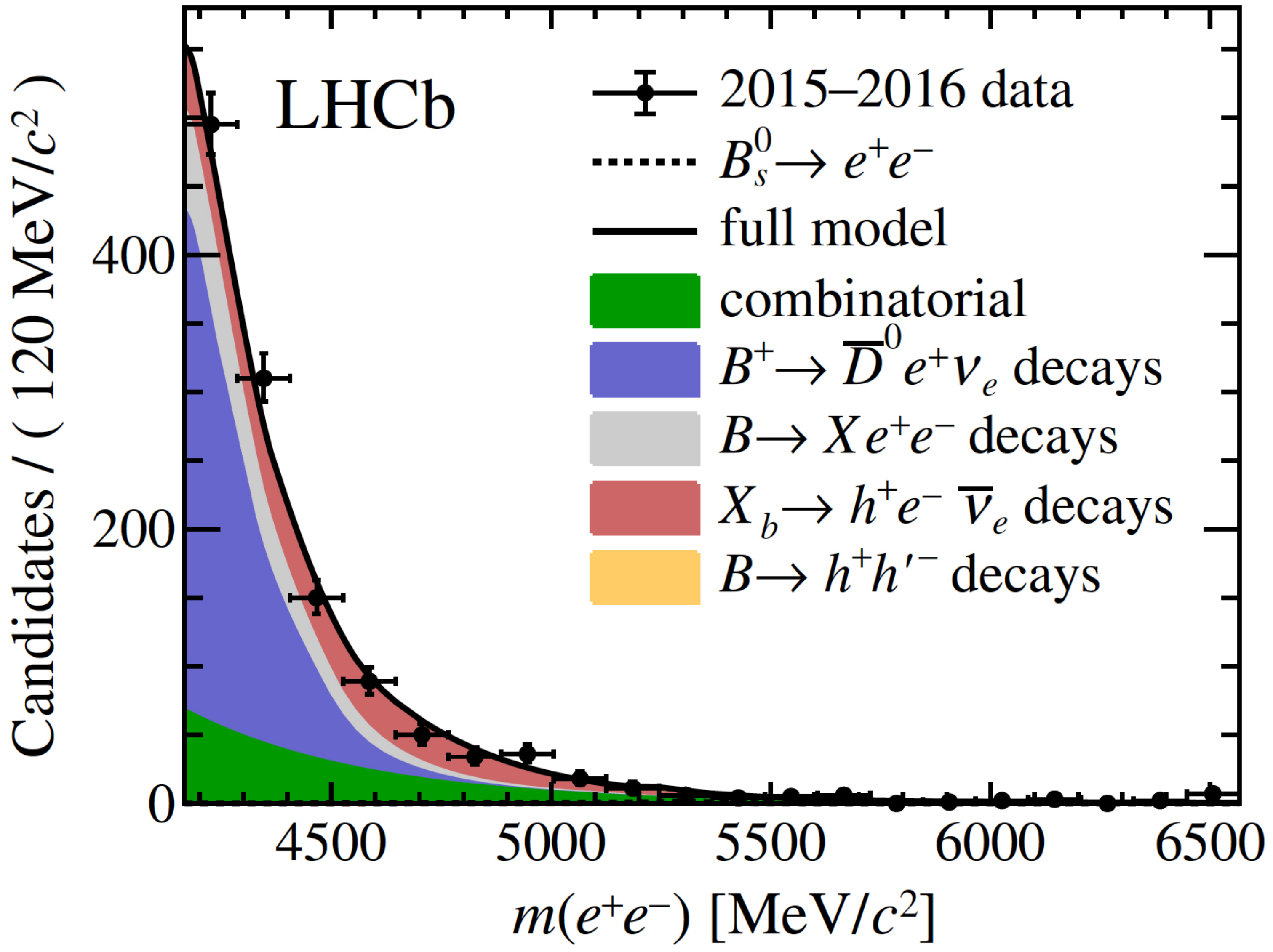

$B^0_{(s)} \to \tau\tau$

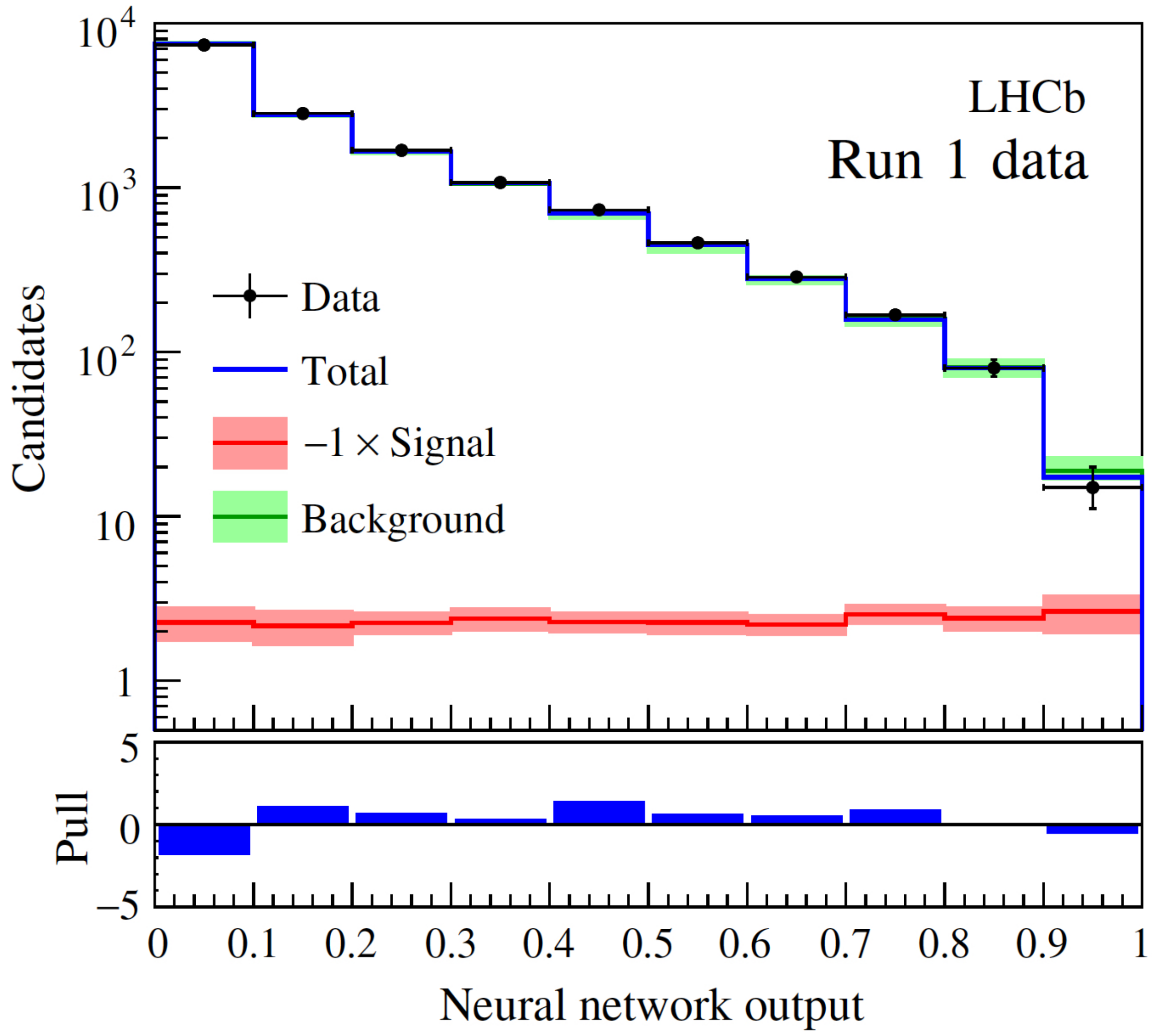

$B^0_{(s)} \to 4\mu$

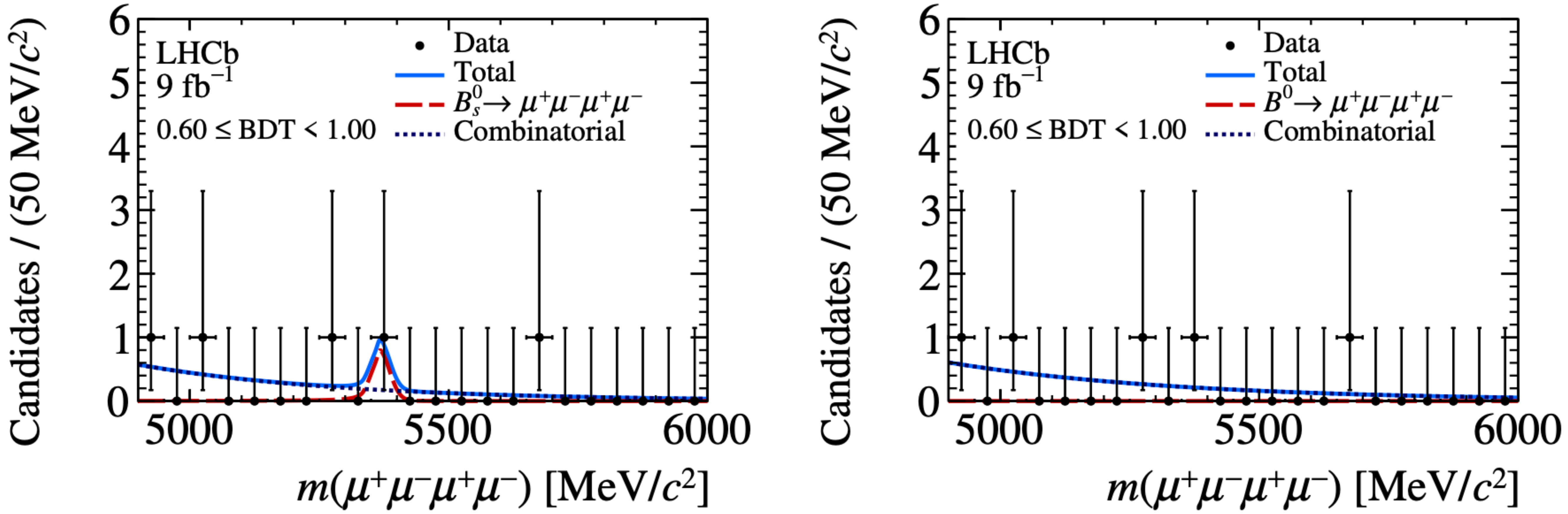

$b \to s\ell\ell$ measurements: LFU tests

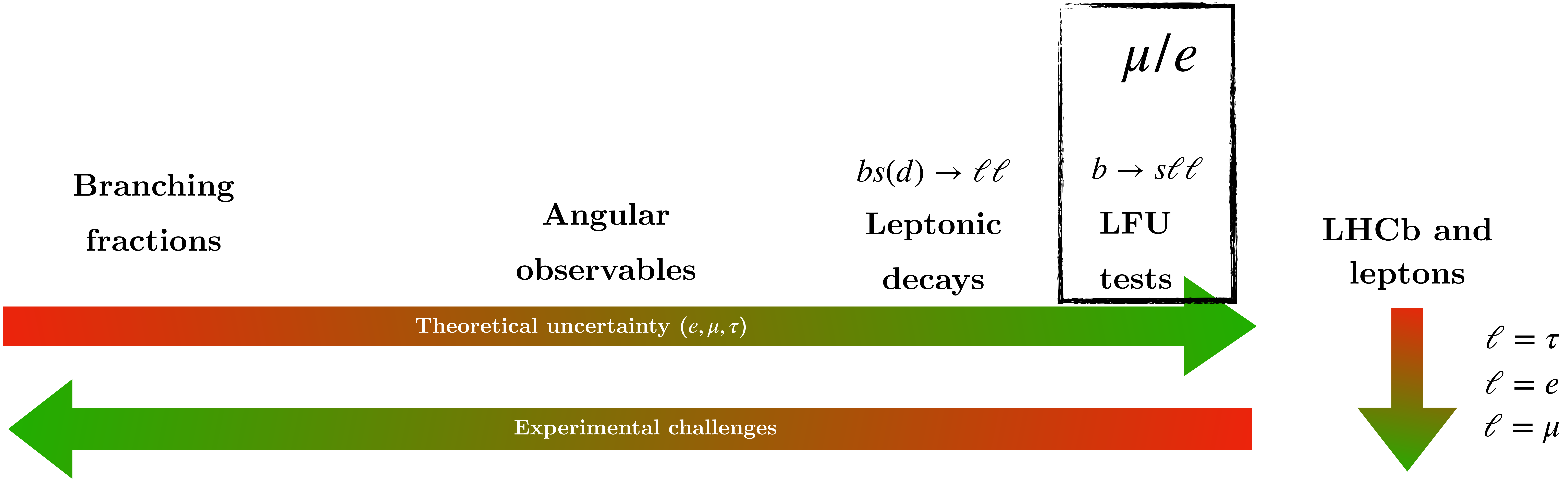

Branching fractions

Angular observables

$bs(d) \to \ell\ell$

Leptonic decays

μ/e

$b \to s\ell\ell$

LFU tests

LHCb and leptons

Theoretical uncertainty (e, μ, τ)

Experimental challenges

$\ell = \tau$

$\ell = e$

$\ell = \mu$

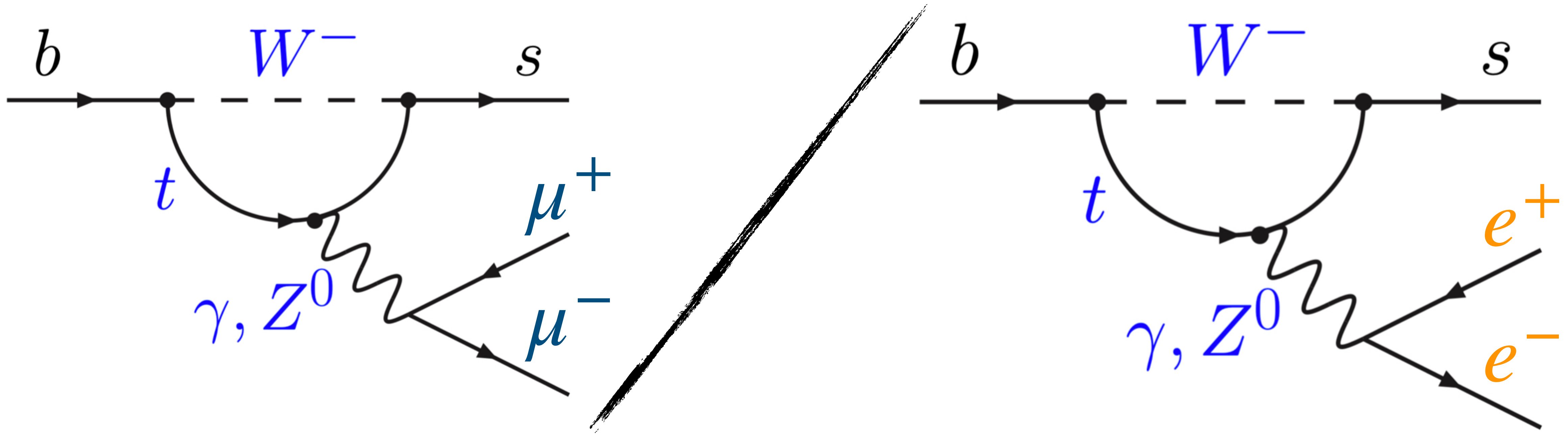

Lepton Flavour Universality (LFU) tests in $b \to s\ell^+\ell^-$ (late 2022)

- Status late 2022 showed an intriguing pattern of tension to SM

- R_X ratio extremely well predicted in SM
  - Cancellation of hadronic uncertainties at 10^{-4}
  - $\mathcal{O}(1\%)$ QED correction [Eur.Phys.J.C 76 (2016) 8]
  - Statistically limited

- **Any departure from unity is a clear sign of New Physics**

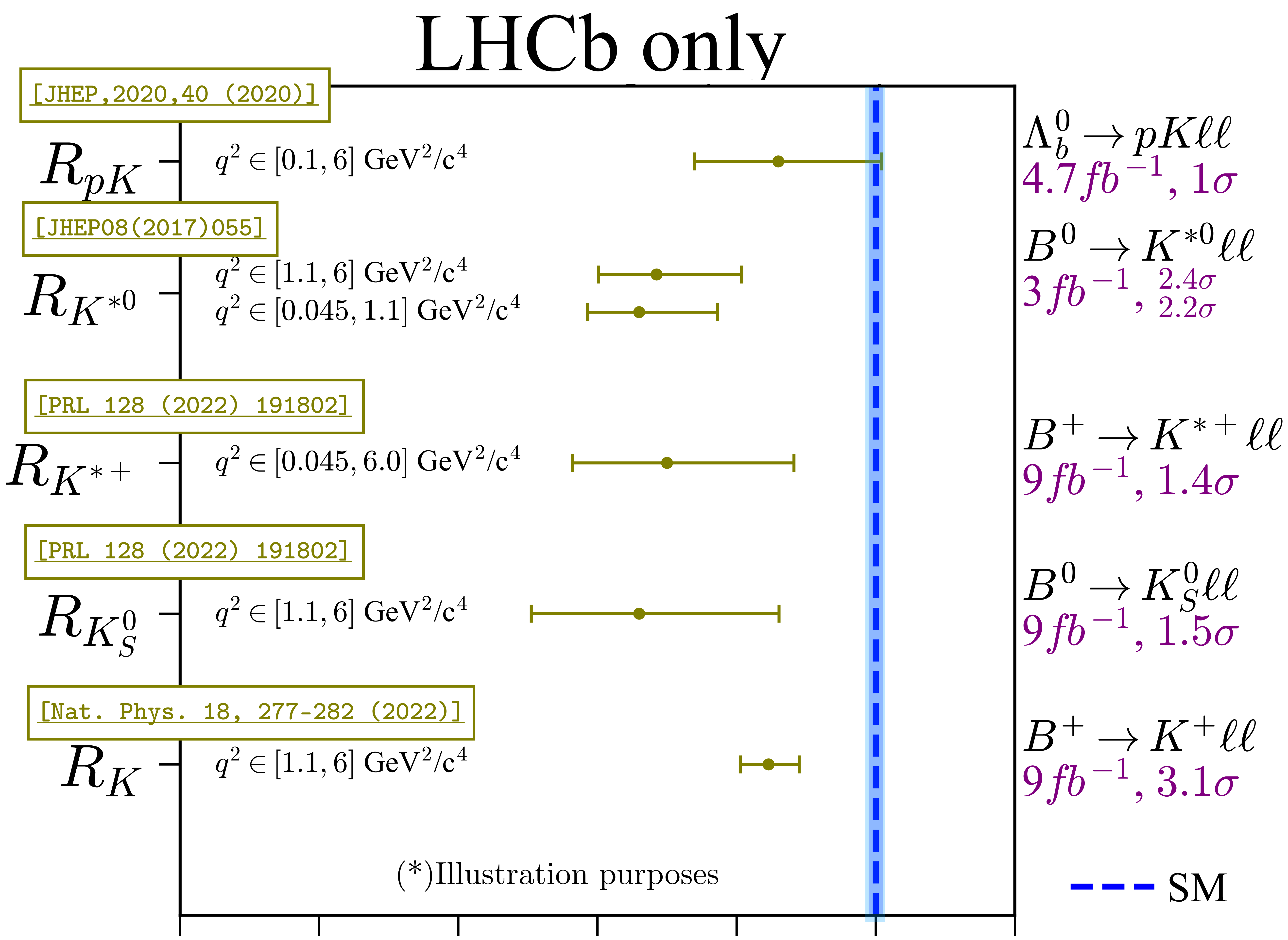

$$R_X = \frac{\mathcal{B}(b \to s\mu^+\mu^-)}{\mathcal{B}(b \to se^+e^-)}$$

(*) Measurements from Belle not shown (larger statistical uncertainties)

Lepton Flavour Universality (LFU) tests in $b \to s\ell^+\ell^-$ (today)

- *Now:* agreement to SM driven by latest LHCb measurement arXiv:2212.09153 arXiv:2212.09152
  - Re-analysis of R_K $q^2 \in [1.1,6]\, GeV^2/c^4$
  - New R_K $q^2 \in [0.1,1.1]\, GeV^2/c^4$
  - $3 \to 9\,\text{fb}^{-1}$ update of $R_{K^{*0}}$
- Main updates on analysis
  - *Selection revised*
  - *Simultaneous approach to measurement*
  - *Inclusion of additional backgrounds from mis-identification of electrons*
  - *Orthogonal choices for fit, efficiencies and selection where possible to previous analyses*

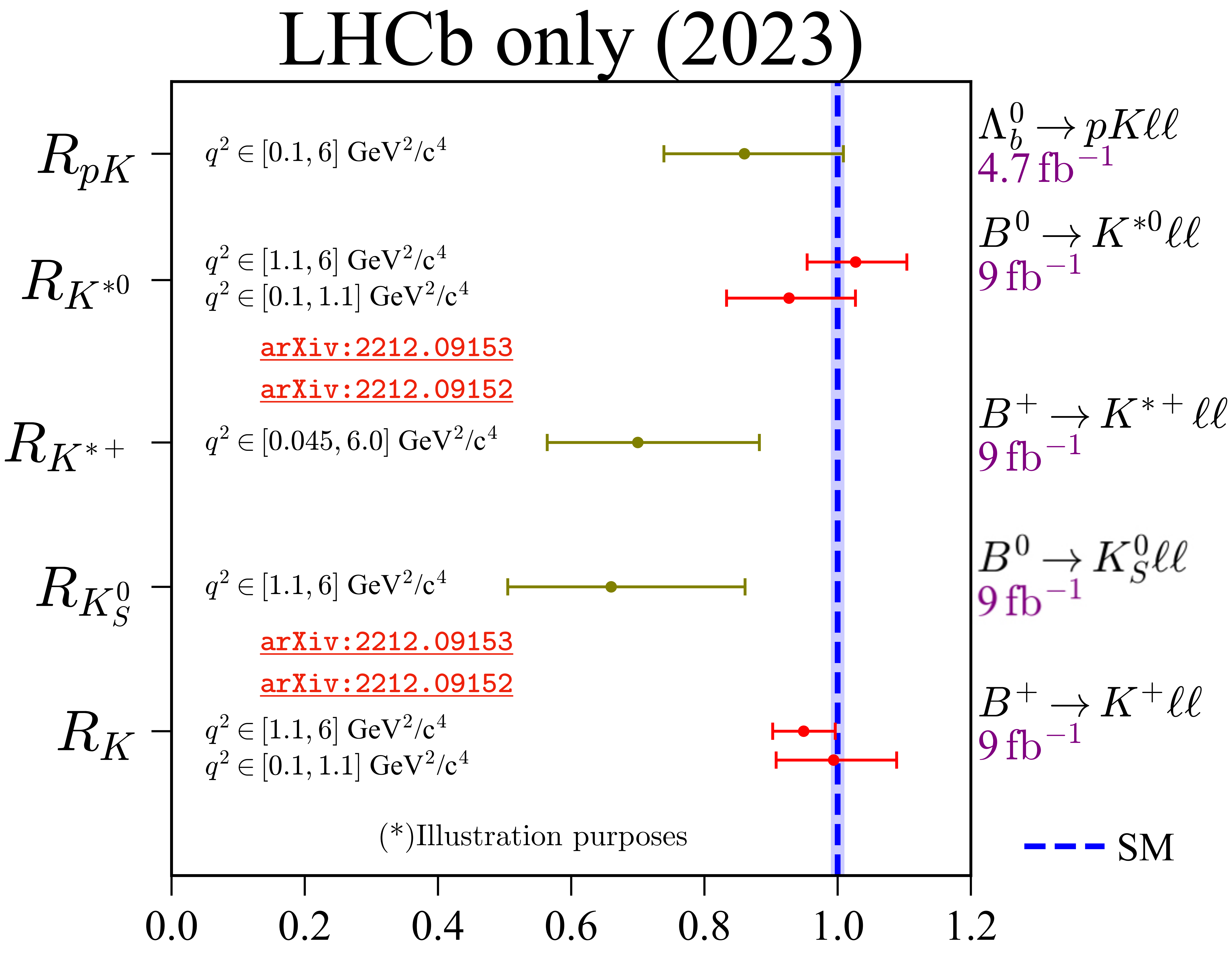

$$R_X = \frac{\mathcal{B}(b \to s\mu^+\mu^-)}{\mathcal{B}(b \to se^+e^-)}$$

(*) Measurements from Belle not shown (larger statistical uncertainties)

Challenges in LFU tests: electrons and energy losses

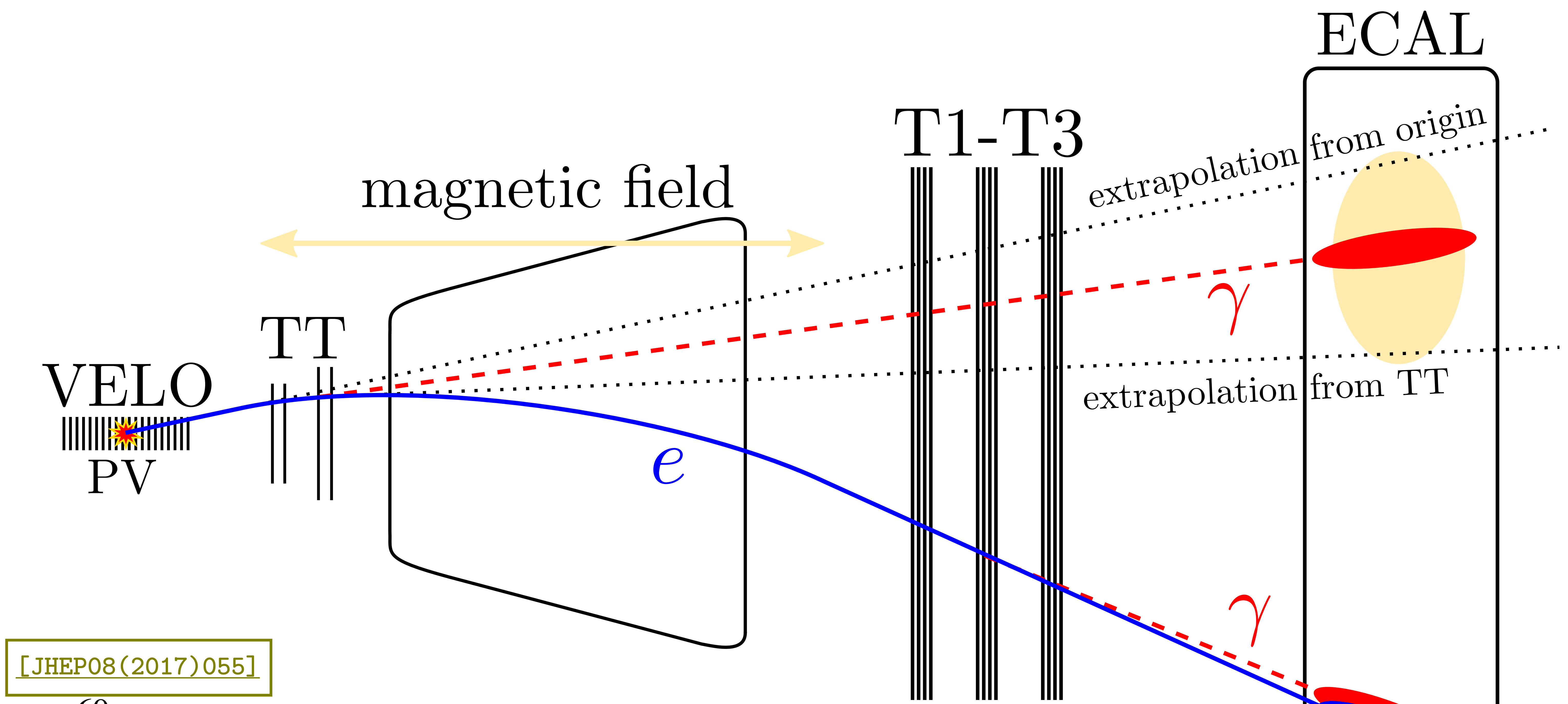

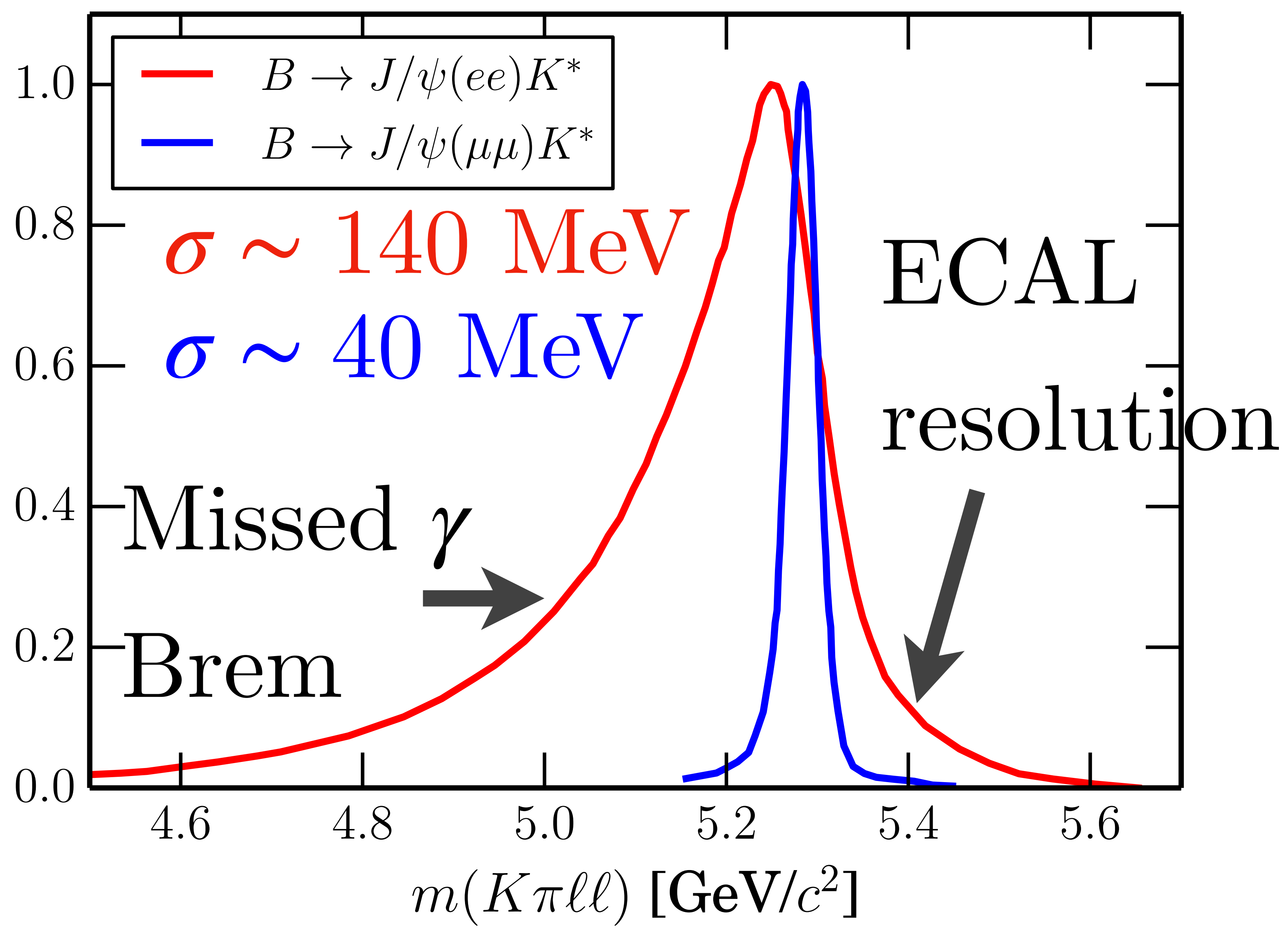

[JHEP08(2017)055]

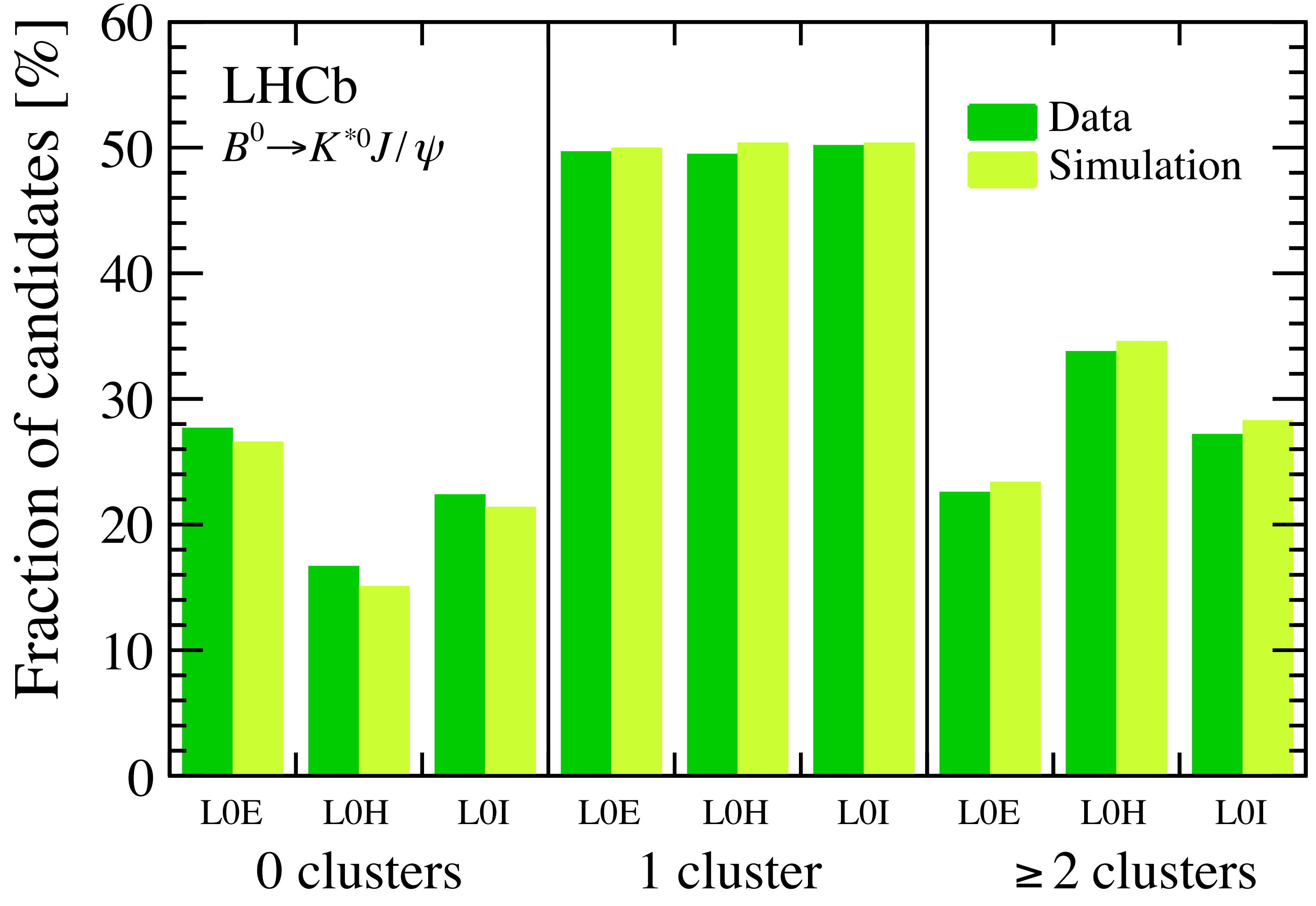

$\simeq$

- Brem recovery is O(50%) efficient
- Well described in simulation

Wider fit range than muons

- more background,
- more sensitive to peaking structures
- lineshapes are brem-dependent

Latest lepton flavour universality test in $b \to s\ell^+\ell^-$ at LHCb

- **Full LHCb dataset ($9\,\mathrm{fb}^{-1}$), simultaneous measurement of** R_K & R_{K^*}

$$R_{K,K^*}(q_a^2, q_b^2) = \frac{\displaystyle\int_{q_a^2}^{q_b^2} \frac{\mathrm{d}\Gamma(B^{(+,0)} \to K^{(+,*0)}\mu^+\mu^-)}{\mathrm{d}q^2}\mathrm{d}q^2}{\displaystyle\int_{q_a^2}^{q_b^2} \frac{\mathrm{d}\Gamma(B^{(+,0)} \to K^{(+,*0)}e^+e^-)}{\mathrm{d}q^2}\mathrm{d}q^2}$$

- q^2 **ranges:**
  - low-q^2 : $q^2 \in [0.1,1.1]\,\mathrm{GeV}^2/c^4$
  - central-q^2 : $q^2 \in [1.1,6.0]\,\mathrm{GeV}^2/c^4$
- **For** R_{K^*}

K^{*0} : $m(K^+\pi^-) \in [792,992]\,\mathrm{MeV/c}^2$

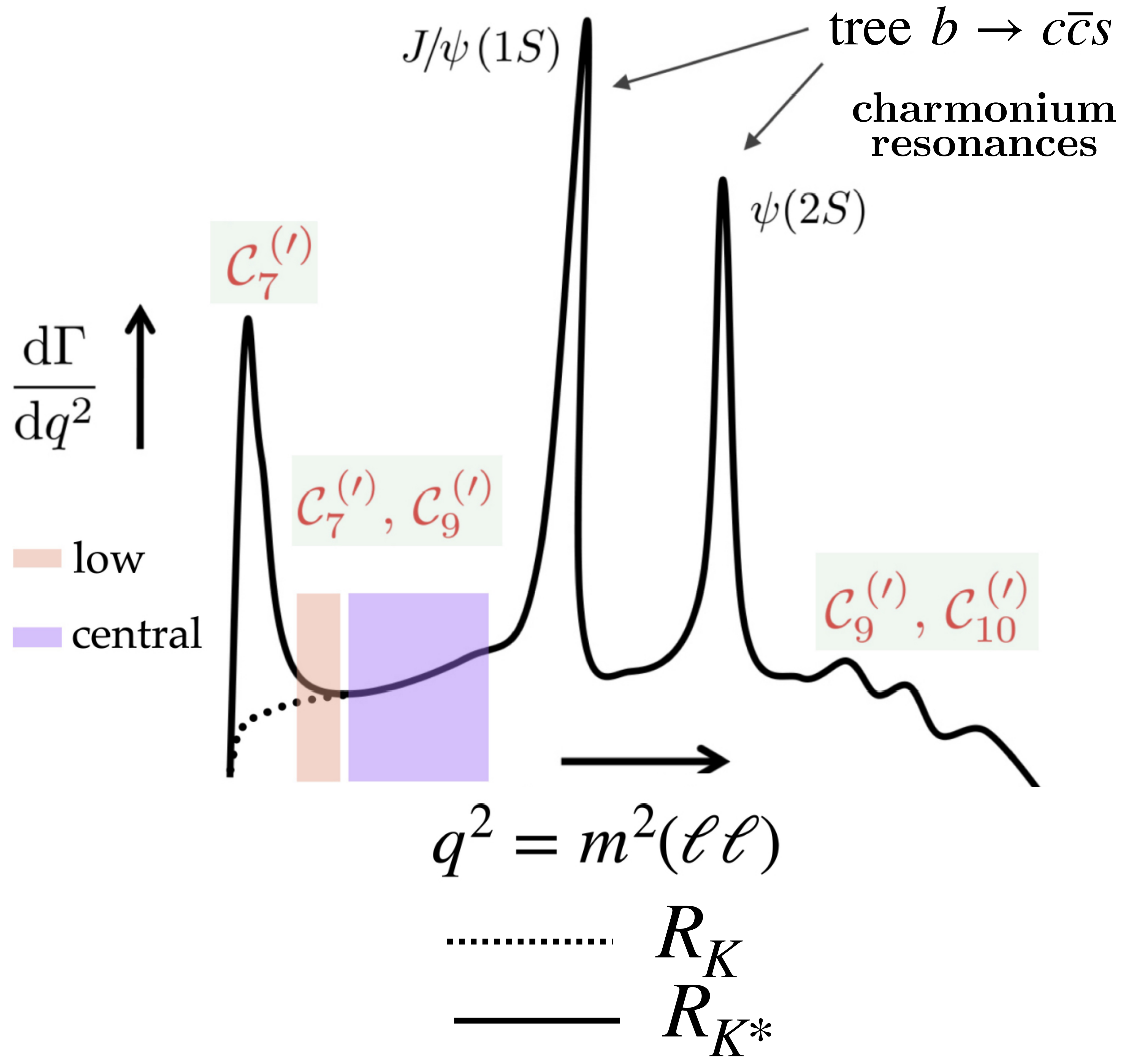

arXiv:2212.09153
arXiv:2212.09152

LFU test strategy

Measured to be 1 Phys. Lett. B731, 227 (2014)

$$R_{K,K^*}(q_a^2, q_b^2) = \frac{\displaystyle\int_{q_a^2}^{q_b^2} \frac{\mathrm{d}\Gamma(B^{(+,0)} \to K^{(+,*0)}\mu^+\mu^-)}{\mathrm{d}q^2}\mathrm{d}q^2}{\displaystyle\int_{q_a^2}^{q_b^2} \frac{\mathrm{d}\Gamma(B^{(+,0)} \to K^{(+,*0)}e^+e^-)}{\mathrm{d}q^2}\mathrm{d}q^2} \times \frac{\Gamma(J/\psi \to e^+e^-)}{\Gamma(J/\psi \to \mu^+\mu^-)}$$

$$R_{(K,K^*)} = \frac{\frac{\mathcal{N}}{\varepsilon}(B^{(+,0)} \to K^{(+,*0)}\mu^+\mu^-)}{\frac{\mathcal{N}}{\varepsilon}(B^{(+,0)} \to K^{(+,*0)}e^+e^-)} \times \overset{r_{J/\psi}^{-1} = 1}{\overleftrightarrow{\frac{\frac{\mathcal{N}}{\varepsilon}(B^{(+,0)} \to K^{(+,*0)}J/\psi(e^+e^-))}{\frac{\mathcal{N}}{\varepsilon}(B^{(+,0)} \to K^{(+,*0)}J/\psi(\mu^+\mu^-))}}}$$

- **$\mathcal{N}$ from mass fits, ε evaluated from data-driven corrected simulation**
- Use resonant-J/ψ mode as normalisation to cancel out most of ε systematics in e/μ differences. Resonant-J/ψ mode also used for ε calibration

LFU test strategy

Measured to be 1 PDG2022 **Measured to be 1** Phys. Lett. B731, 227 (2014)

$$\boxed{R_{\psi(2S)}} = \frac{\Gamma(\psi(2S)\to\mu^+\mu^-)}{\Gamma(\psi(2S)\to e^+e^-)} \times \frac{\Gamma(J/\psi\to e^+e^-)}{\Gamma(J/\psi\to\mu^+\mu^-)}$$

$$\boxed{R^{(K,K^*)}_{\psi(2S)}} = \frac{\frac{\mathcal{N}}{\varepsilon}(B^{(+,0)}\to K^{(+,*0)}\psi(2S)(\mu^+\mu^-))}{\frac{\mathcal{N}}{\varepsilon}(B^{(+,0)}\to K^{(+,*0)}\psi(2S)(e^+e^-))} \times \overbrace{\frac{\frac{\mathcal{N}}{\varepsilon}(B^{(+,0)}\to K^{(+,*0)}J/\psi(e^+e^-))}{\frac{\mathcal{N}}{\varepsilon}(B^{(+,0)}\to K^{(+,*0)}J/\psi(\mu^+\mu^-))}}^{r^{-1}_{J/\psi}=1}$$

- $\mathcal{N}$ **from mass fits,** ε **evaluated from data-driven corrected simulation**
- Use resonant-J/ψ mode as normalisation to cancel out most of ε systematics in e/μ differences. Resonant-J/ψ mode also used for ε calibration
- **Cross-check** goodness of calibration testing $r^{K,K^*}_{J/\psi} = 1$
- **Cross-check** goodness of method testing $\boxed{R^{K,K^*}_{\psi(2S)} = 1}$

Efficiency ratios and double ratios

A rather complex chain of corrections to control efficiencies differences on electrons and muons

- On *single-ratios*, the calibration of efficiencies moves $r_{J/\psi}$ by 25%

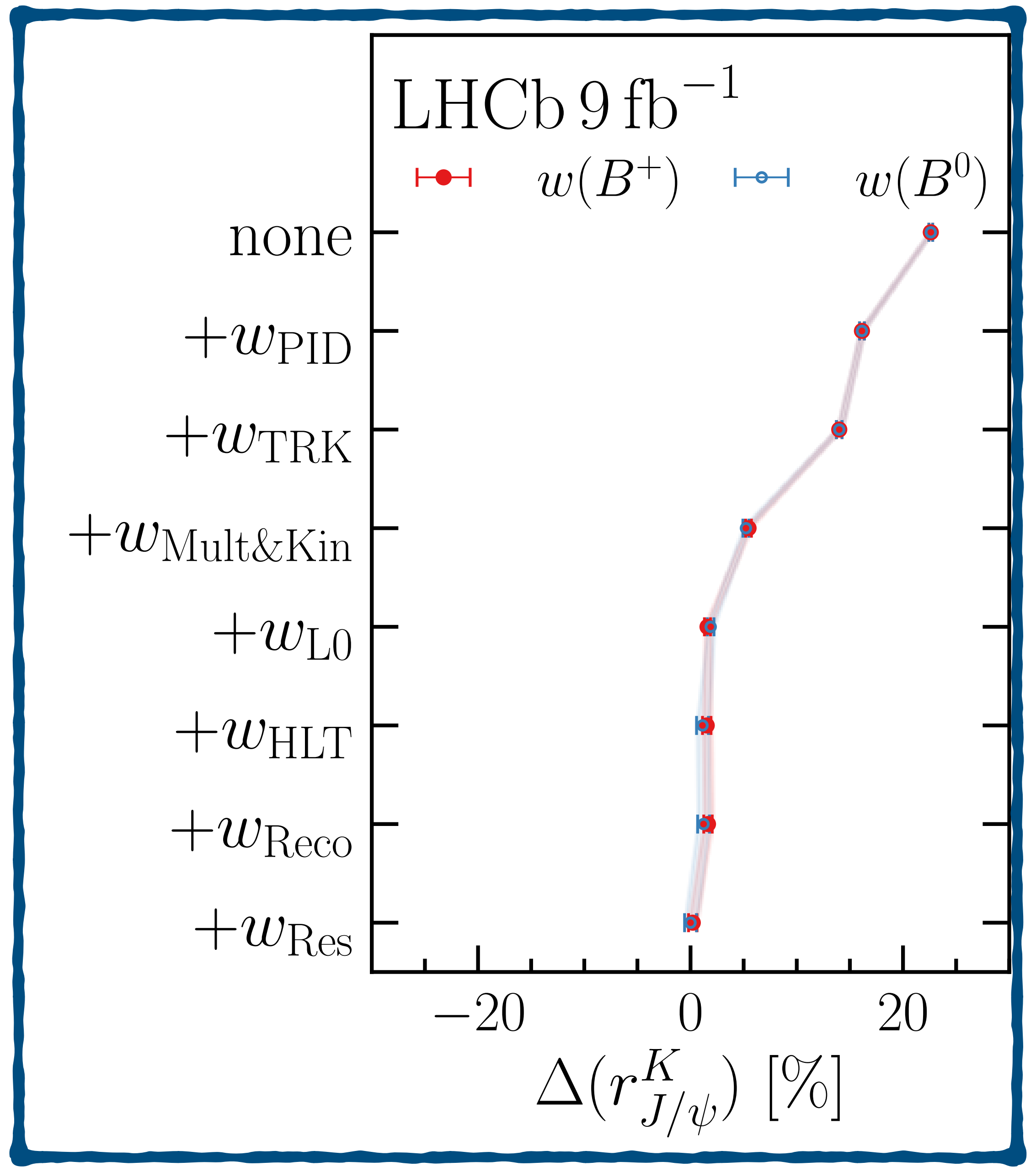

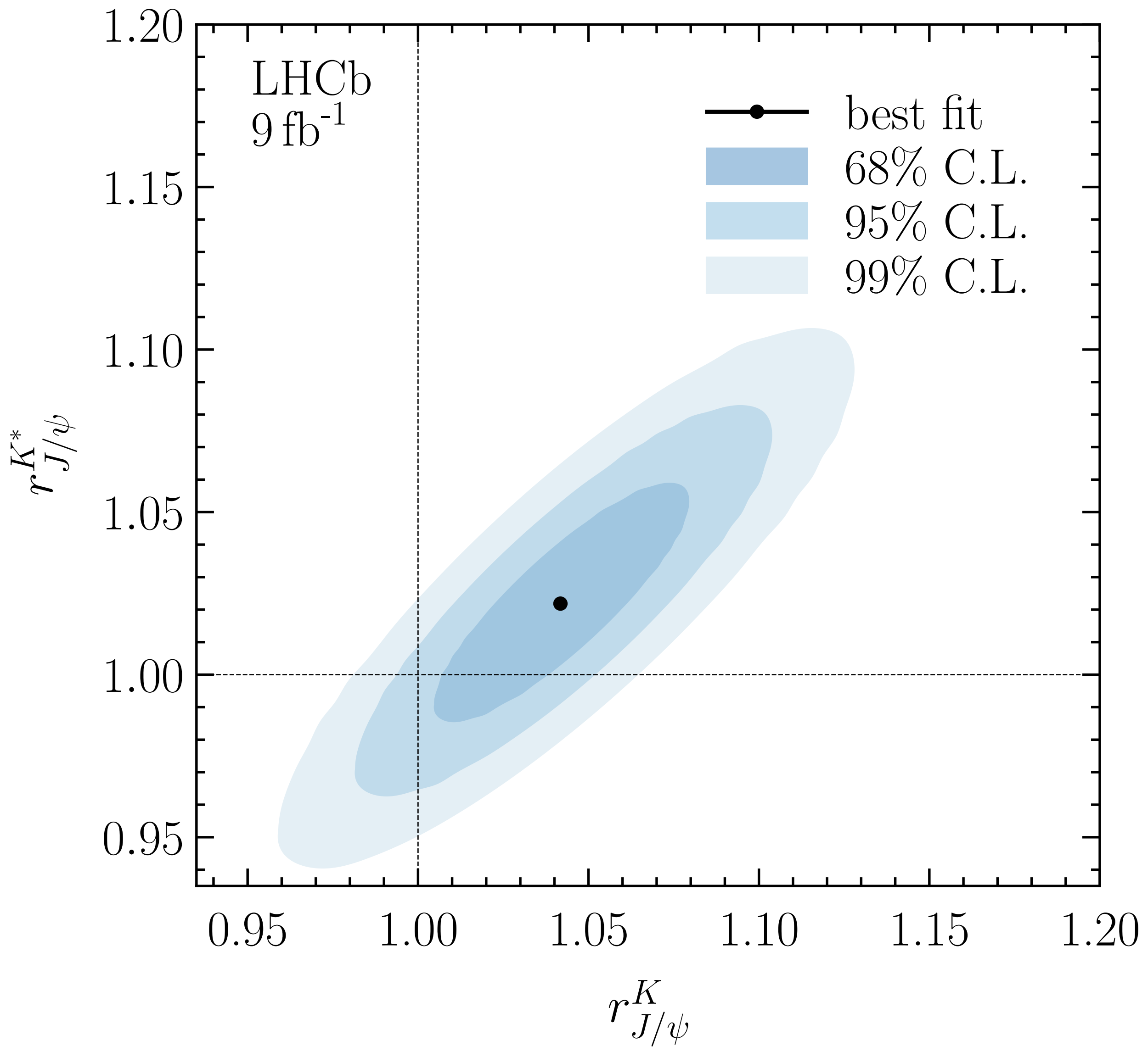

Efficiency ratios and double ratios

A rather complex chain of corrections to control efficiencies differences on electrons and muons

- On *single-ratios*, the calibration of efficiencies moves $r_{J/\psi}$ by 25%
- On all *double ratios*, the effect of corrections to simulation is moving the result by at most 5 %
- **ε well under control**

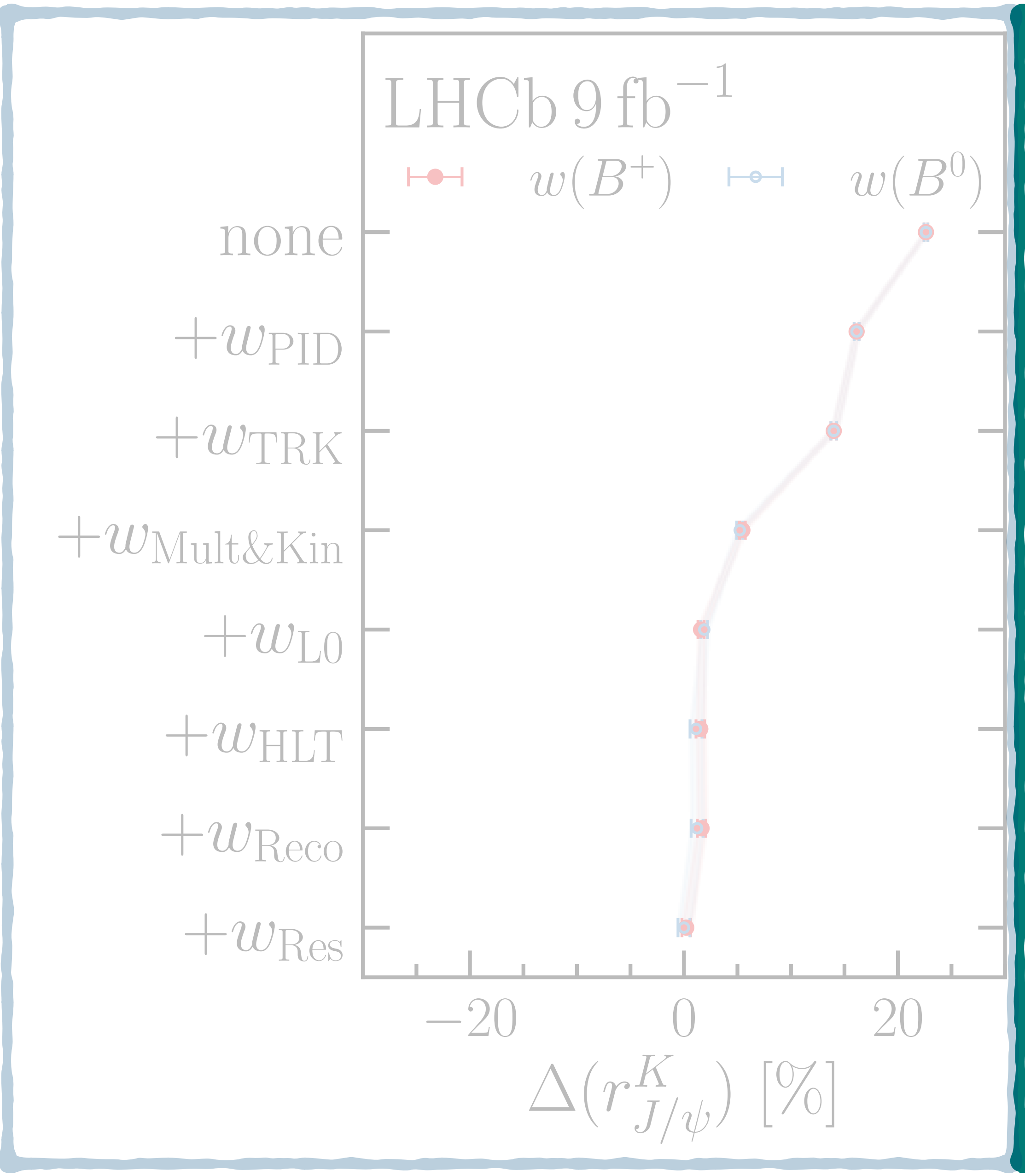

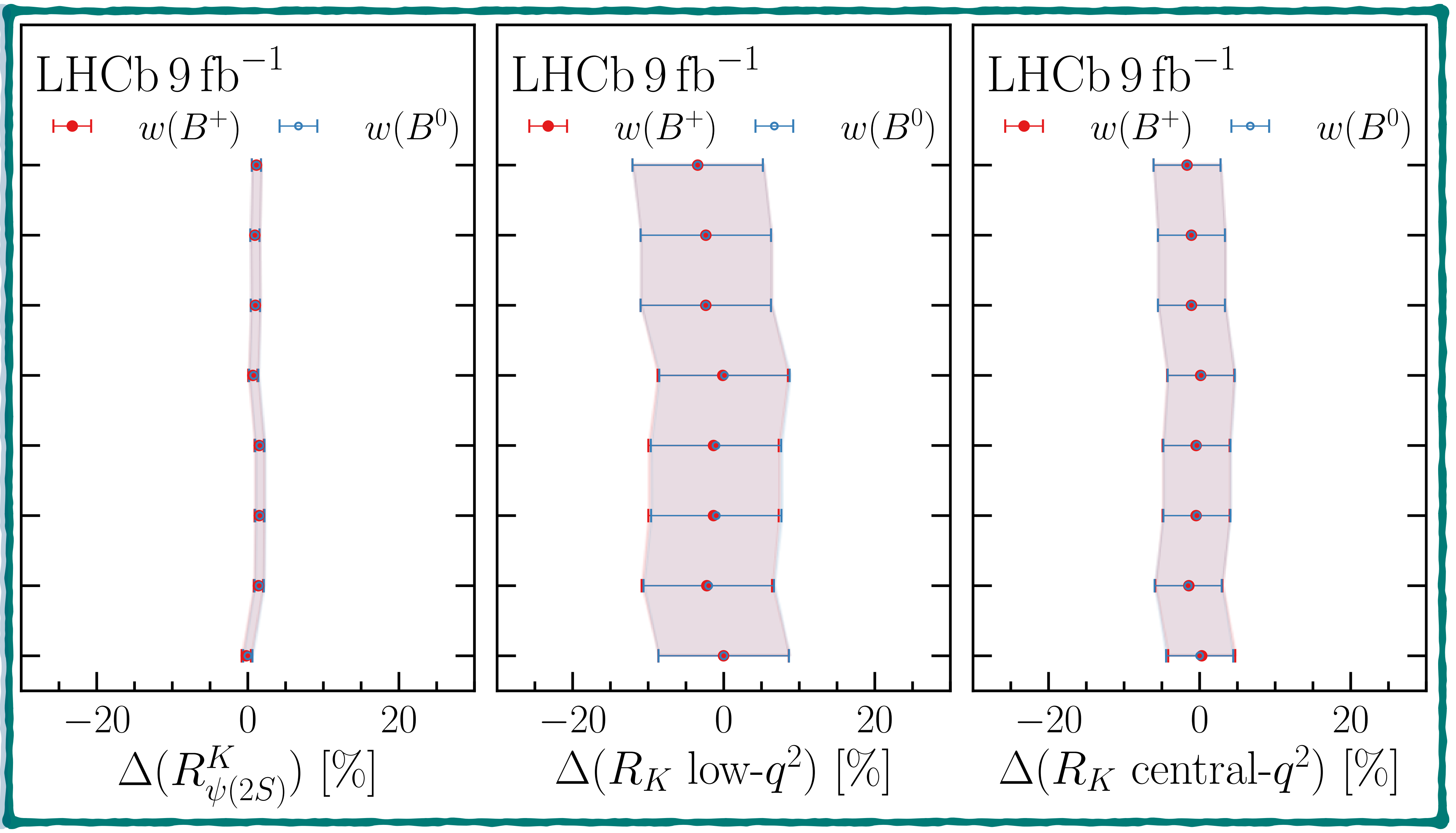

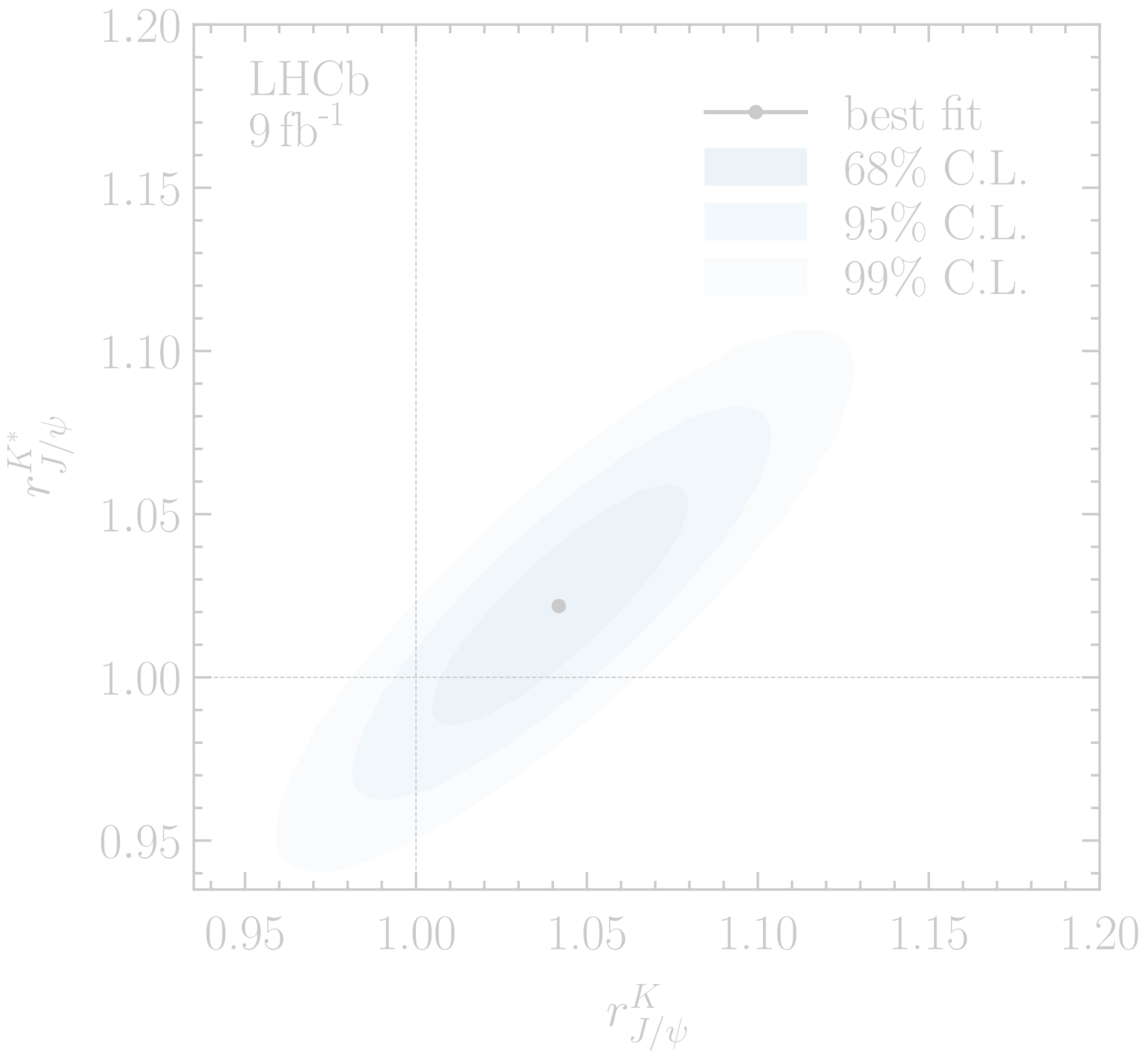

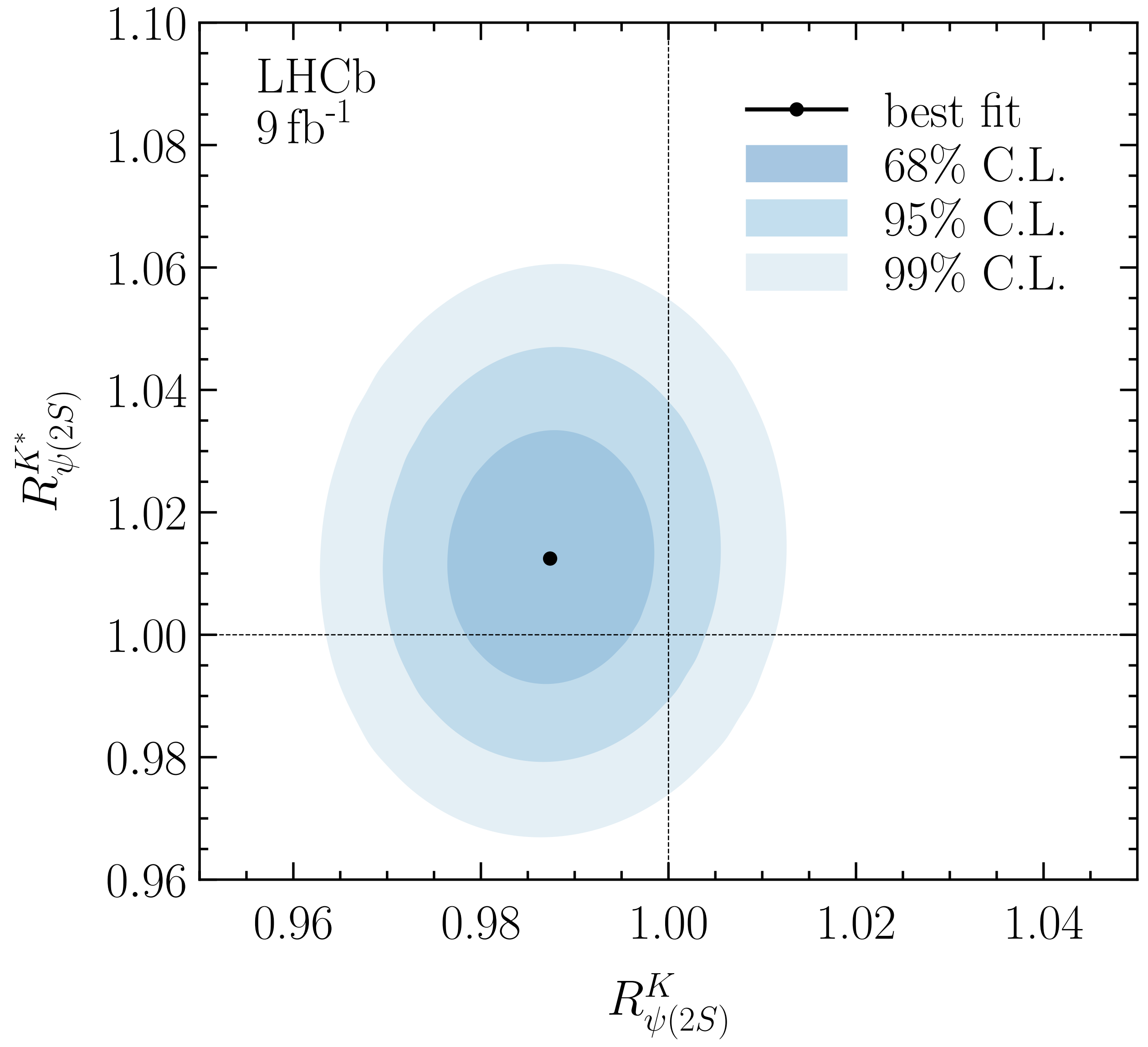

Simultaneous determination of $R_{K,K^{*0}}$

[JHEP08(2017)055]

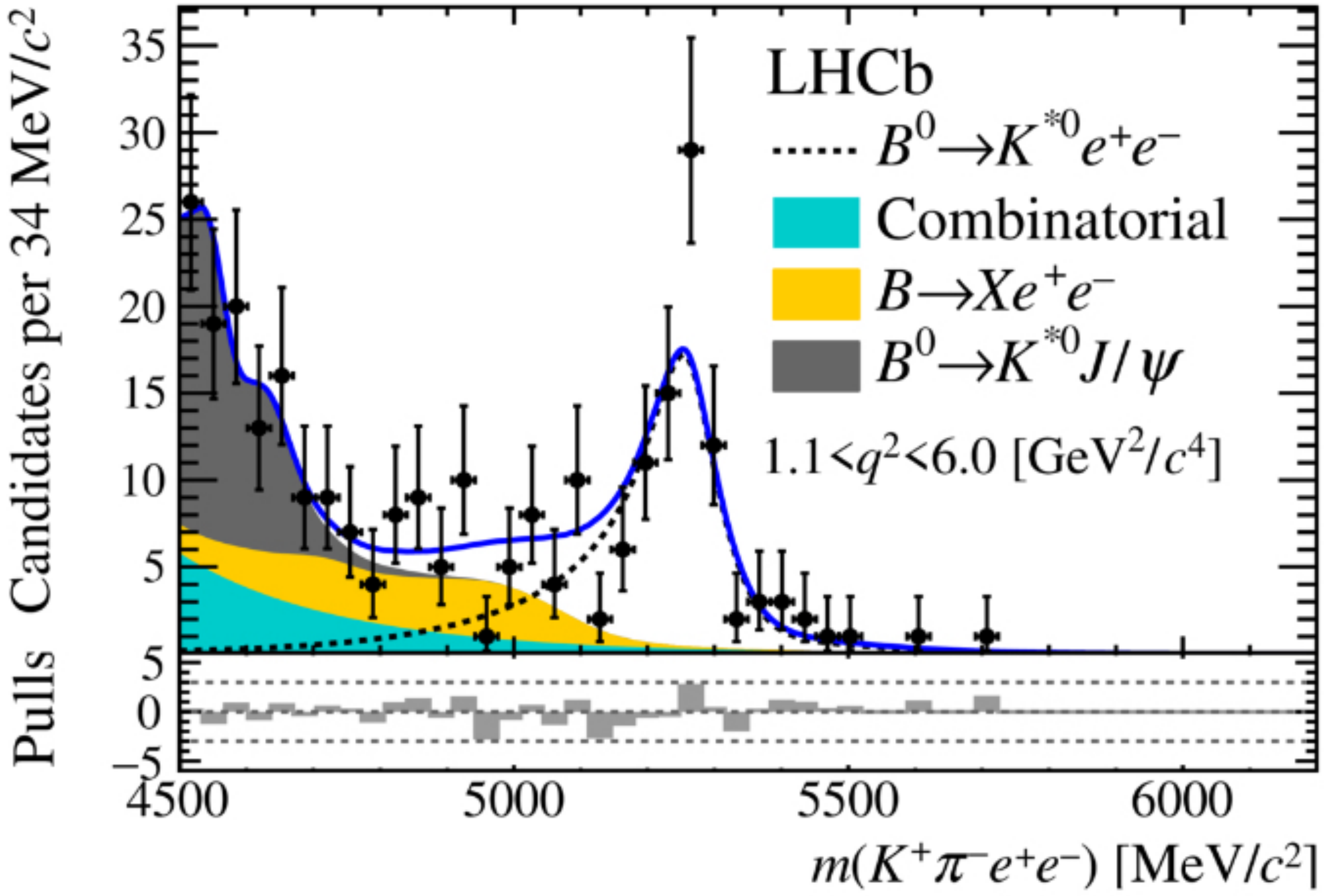

cross-feed

background

[Nat. Phys. 18, 277-282 (2022)]

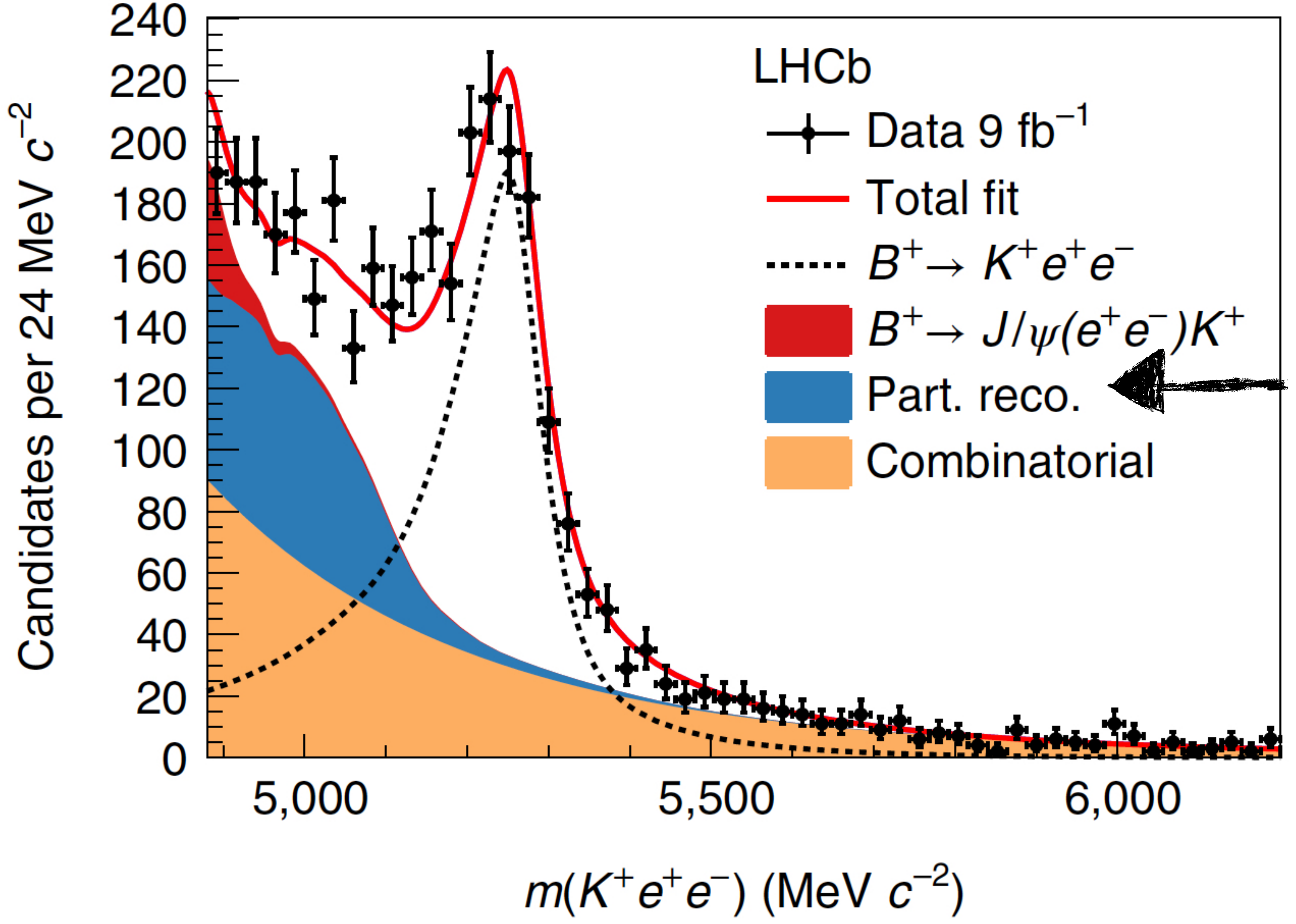

Was

free

- $R_{K,K^{*0}}$ determined from a simultaneous fit to muon/electron decay modes in the two q² bins of interest:
  - Improve per-event sensitivity constraining partially reconstructed backgrounds in $K^+e^+e^-$ from $K^{*0}e^+e^-$ signal
  - Coherent efficiency and systematics treatment

Scan results in electron PID w/o treatment of misID bkg

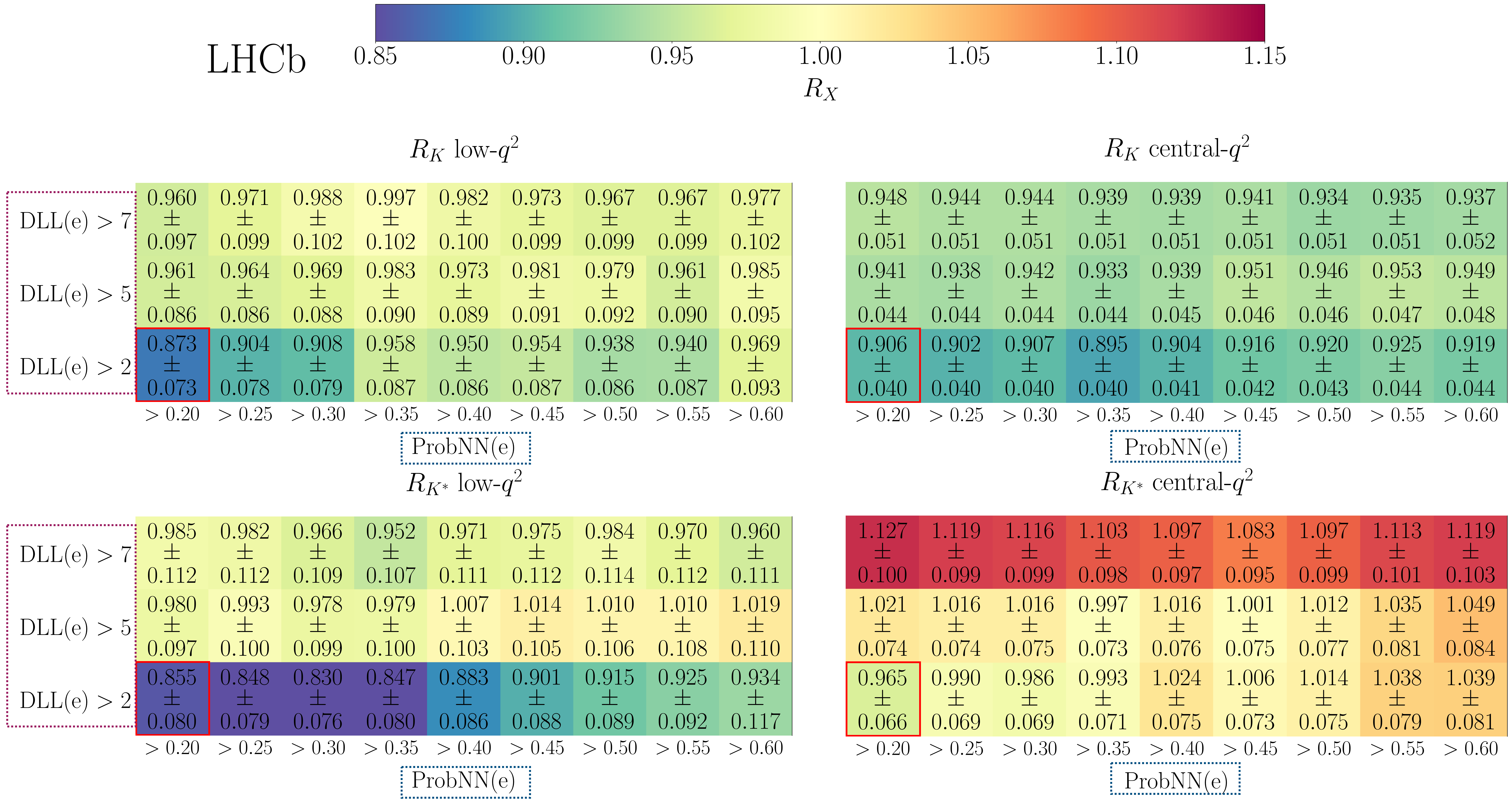

R_K low-q^2

	> 0.20	> 0.25	> 0.30	> 0.35	> 0.40	> 0.45	> 0.50	> 0.55	> 0.60
DLL(e) > 7	0.960 ± 0.097	0.971 ± 0.099	0.988 ± 0.102	0.997 ± 0.102	0.982 ± 0.100	0.973 ± 0.099	0.967 ± 0.099	0.967 ± 0.099	0.977 ± 0.102
DLL(e) > 5	0.961 ± 0.086	0.964 ± 0.086	0.969 ± 0.088	0.983 ± 0.090	0.973 ± 0.089	0.981 ± 0.091	0.979 ± 0.092	0.961 ± 0.090	0.985 ± 0.095
DLL(e) > 2	0.873 ± 0.073	0.904 ± 0.078	0.908 ± 0.079	0.958 ± 0.087	0.950 ± 0.086	0.954 ± 0.087	0.938 ± 0.086	0.940 ± 0.087	0.969 ± 0.093

ProbNN(e)

R_K central-q^2

	> 0.20	> 0.25	> 0.30	> 0.35	> 0.40	> 0.45	> 0.50	> 0.55	> 0.60
DLL(e) > 7	0.948 ± 0.051	0.944 ± 0.051	0.944 ± 0.051	0.939 ± 0.051	0.939 ± 0.051	0.941 ± 0.051	0.934 ± 0.051	0.935 ± 0.051	0.937 ± 0.052
DLL(e) > 5	0.941 ± 0.044	0.938 ± 0.044	0.942 ± 0.044	0.933 ± 0.044	0.939 ± 0.045	0.951 ± 0.046	0.946 ± 0.046	0.953 ± 0.047	0.949 ± 0.048
DLL(e) > 2	0.906 ± 0.040	0.902 ± 0.040	0.907 ± 0.040	0.895 ± 0.040	0.904 ± 0.041	0.916 ± 0.042	0.920 ± 0.043	0.925 ± 0.044	0.919 ± 0.044

ProbNN(e)

R_{K^*} low-q^2

	> 0.20	> 0.25	> 0.30	> 0.35	> 0.40	> 0.45	> 0.50	> 0.55	> 0.60
DLL(e) > 7	0.985 ± 0.112	0.982 ± 0.112	0.966 ± 0.109	0.952 ± 0.107	0.971 ± 0.111	0.975 ± 0.112	0.984 ± 0.114	0.970 ± 0.112	0.960 ± 0.111
DLL(e) > 5	0.980 ± 0.097	0.993 ± 0.100	0.978 ± 0.099	0.979 ± 0.100	1.007 ± 0.103	1.014 ± 0.105	1.010 ± 0.106	1.010 ± 0.108	1.019 ± 0.110
DLL(e) > 2	0.855 ± 0.080	0.848 ± 0.079	0.830 ± 0.076	0.847 ± 0.080	0.883 ± 0.086	0.901 ± 0.088	0.915 ± 0.089	0.925 ± 0.092	0.934 ± 0.117

ProbNN(e)

R_{K^*} central-q^2

	> 0.20	> 0.25	> 0.30	> 0.35	> 0.40	> 0.45	> 0.50	> 0.55	> 0.60
DLL(e) > 7	1.127 ± 0.100	1.119 ± 0.099	1.116 ± 0.099	1.103 ± 0.098	1.097 ± 0.097	1.083 ± 0.095	1.097 ± 0.099	1.113 ± 0.101	1.119 ± 0.103
DLL(e) > 5	1.021 ± 0.074	1.016 ± 0.074	1.016 ± 0.075	0.997 ± 0.073	1.016 ± 0.076	1.001 ± 0.075	1.012 ± 0.077	1.035 ± 0.081	1.049 ± 0.084
DLL(e) > 2	0.965 ± 0.066	0.990 ± 0.069	0.986 ± 0.069	0.993 ± 0.071	1.024 ± 0.075	1.006 ± 0.073	1.014 ± 0.075	1.038 ± 0.079	1.039 ± 0.081

ProbNN(e)

DLL(e): ***combination of sub-detectors delta-log-likelihood for π/e***

ProbNN(e): ***neural-net based e-ID score***

Tightening selection in electron PID without specific treatment of electron misidentified backgrounds exhibited a coherent pattern

Pass-Fail method to estimate mis-identified backgrounds

FailPass (FP) **PassFail (PF)** **FailFail (FF)**

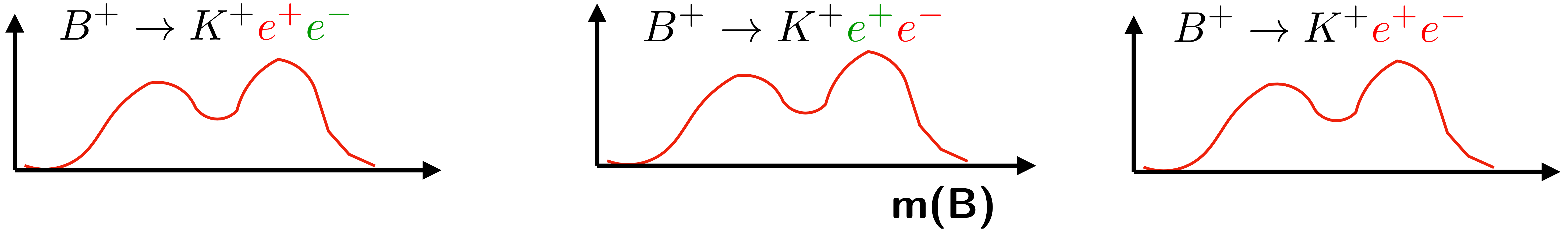

Transfer Function (From π/K calibration data samples)

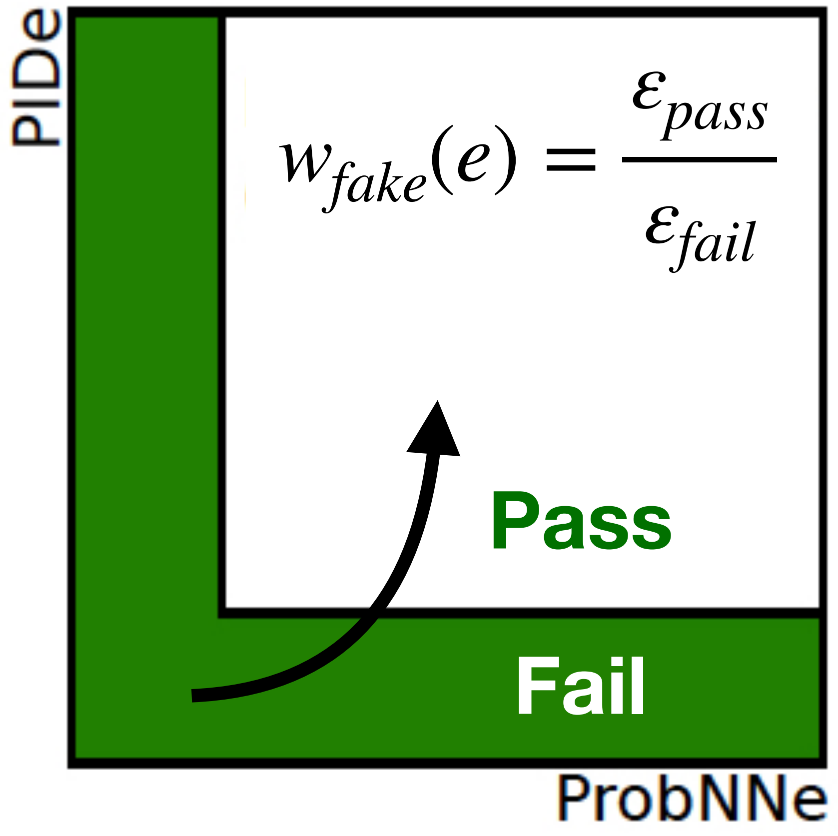

$$w_{fake}(e) = \frac{\varepsilon_{pass}}{\varepsilon_{fail}}$$

- Transfer from fail to pass region evaluated in bins of p_T and η in $D^{*+} \to D^0(K^+\pi^-)\pi^+$ data

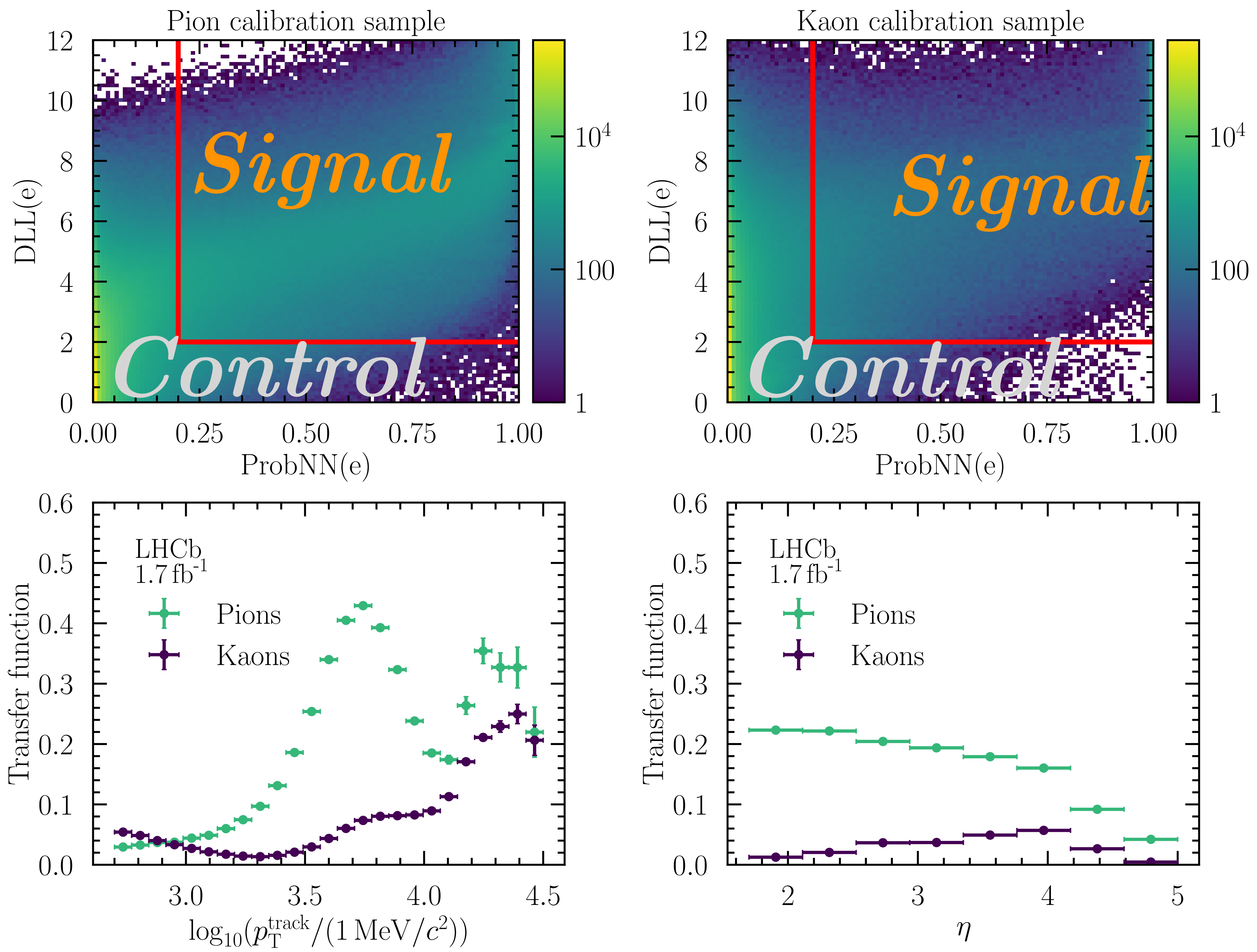

PassPass

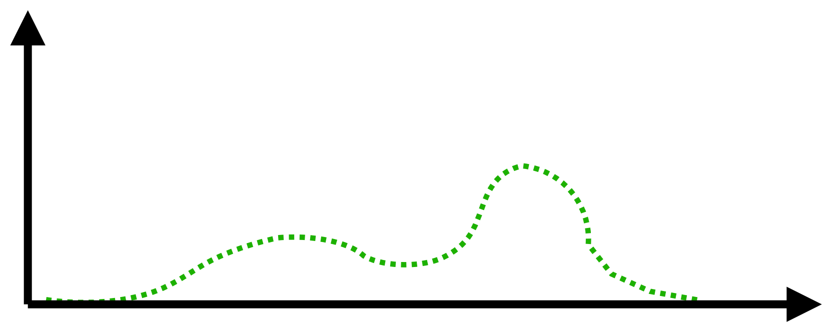

m(B)

Shape + Prediction

$$\begin{aligned} N(FP)+N(PF)-N(FF) &= N(B^+\to K^+e^+h^-)\\ &+N(B^+\to K^+h^+e^-)\\ &+N(B^+\to K^+h^+h'^-) \end{aligned}$$

Pass-Fail method to estimate mis-identified backgrounds

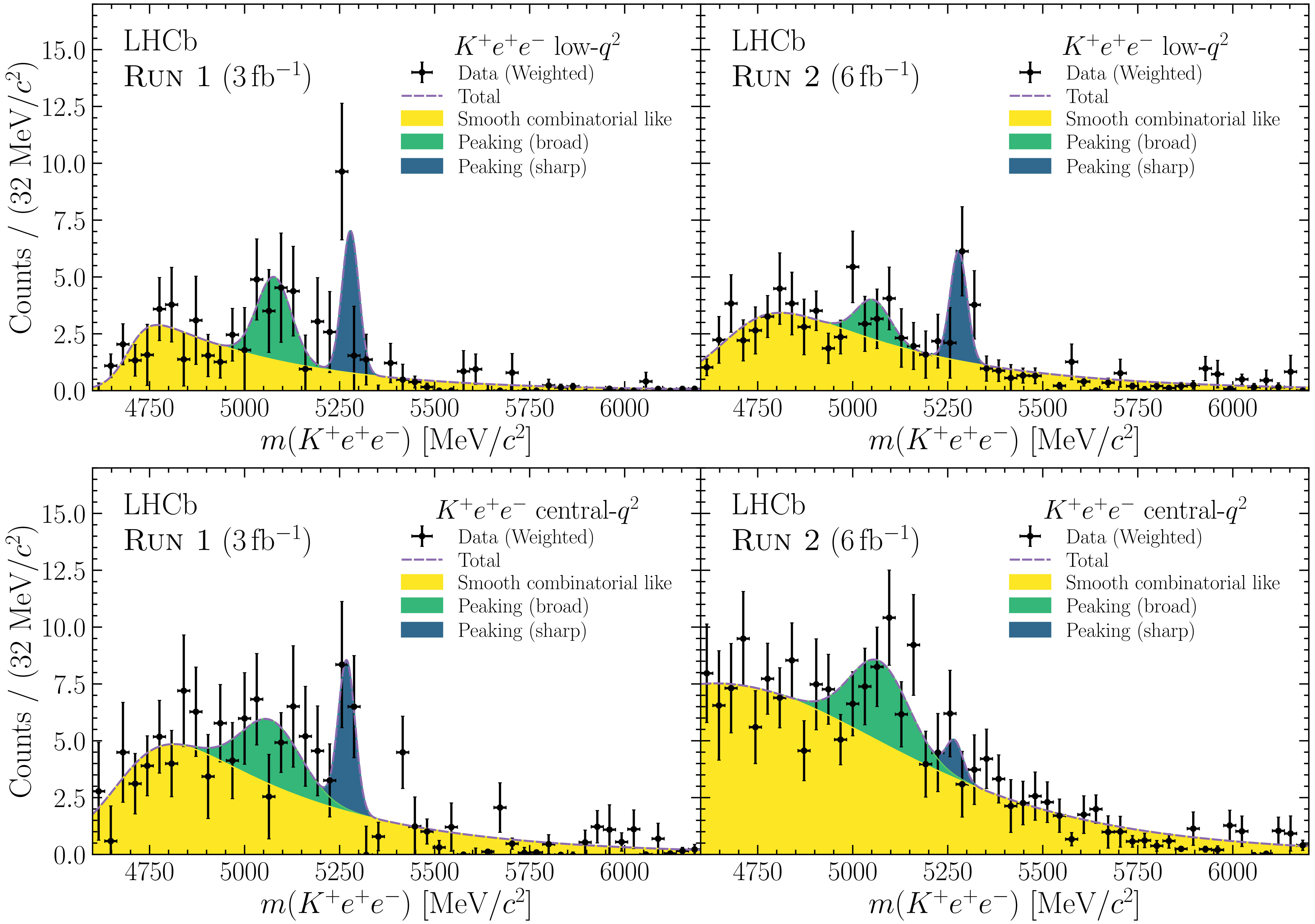

PassPass

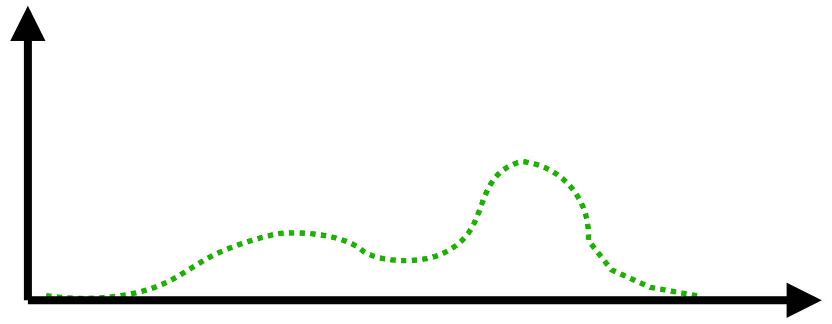

m(B)

Shape + **Prediction**

$$N(FP) + N(PF) - N(FF) = N(B^+ \to K^+e^+h^-) + N(B^+ \to K^+h^+e^-) + N(B^+ \to K^+h^+h'^-)$$

Mass fit to rare mode electrons: simultaneous fit $R_{K,K^{*0}}$

low-q^2 central-q^2 resonant-J/ψ

What we learnt from this latest measurement? [with R_K central q^2 re-analysis]

[Nat. Phys. 18, 277-282 (2022)]

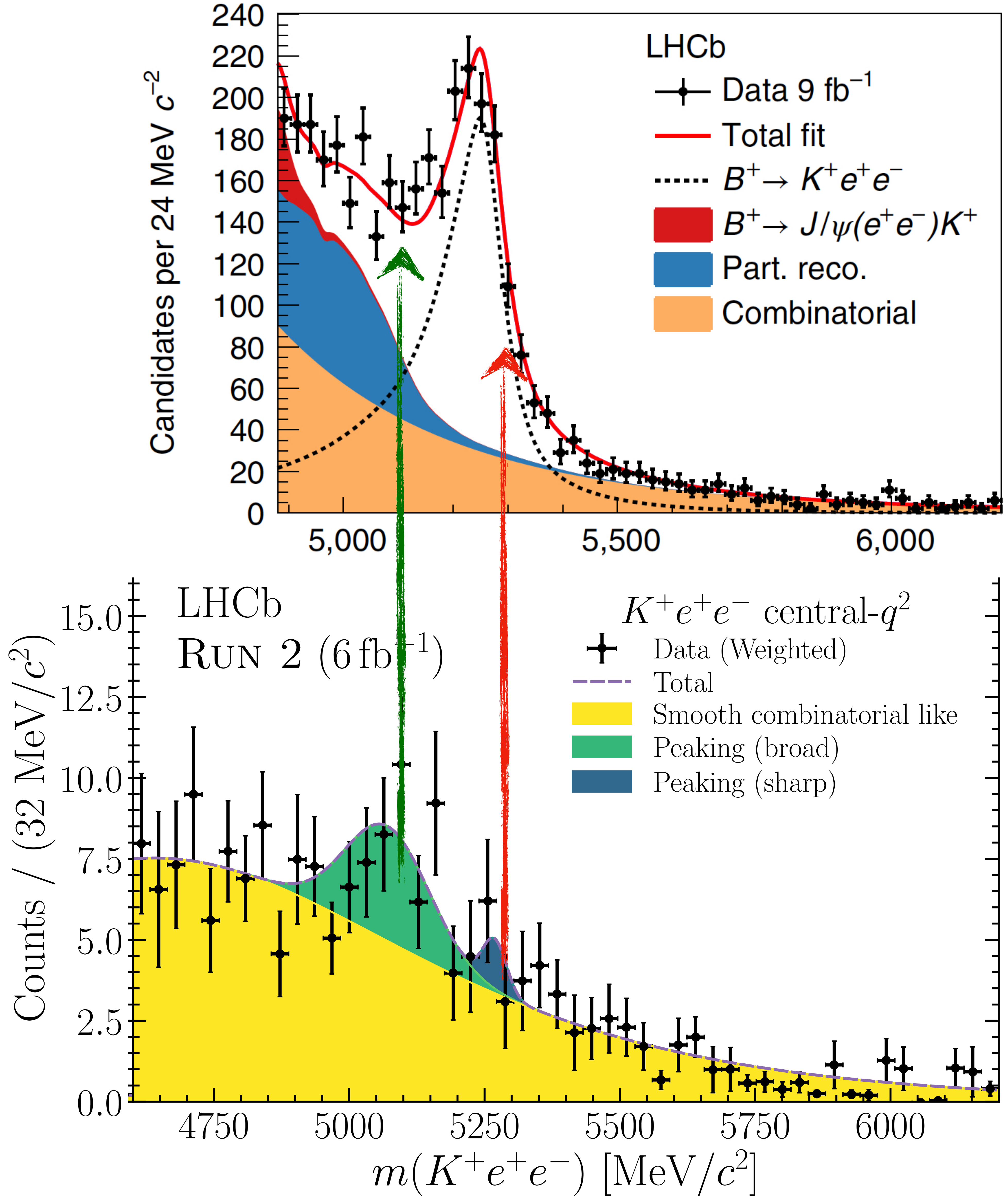

- ✦ Different PID cut used ➡ Allowed σ_{stat} : ±0.033
- ✦ Shift due to contamination at looser working point : **+0.064**
- ✦ Shift due to not inclusion of background in mass fit: **+0.038**

Adds linearly

Combination of small residual broad-peaking and combinatorial-like background on the "signal-shoulder" plus small peaking background in signal peaking region able to mimic perfectly the signal.

Effects driven by hadron misidentified as electrons.

Conclusion

- **SM very robust and describes results with excellent precision**
- **Tensions and *flavour anomalies* ($b \to s\ell\ell$)**
  - $d\mathcal{B}/dq^2$ in $b \to s\mu\mu$ decays , **1-3 σ**
  - Angular $b \to s\mu\mu$ **2-3 σ**
  - LFU tests (R_{K,K^*}) : **previously at 3σ, now** compatible with SM **at 0.2 σ**
  - $\mathcal{B}(B_{(s)} \to \mu^+\mu^-)$ compatible with SM, $\sigma_{stat} \sim 14\,\%$
  - Other anomalies ($b \to c\ell\nu$): see talk by Rizwaan

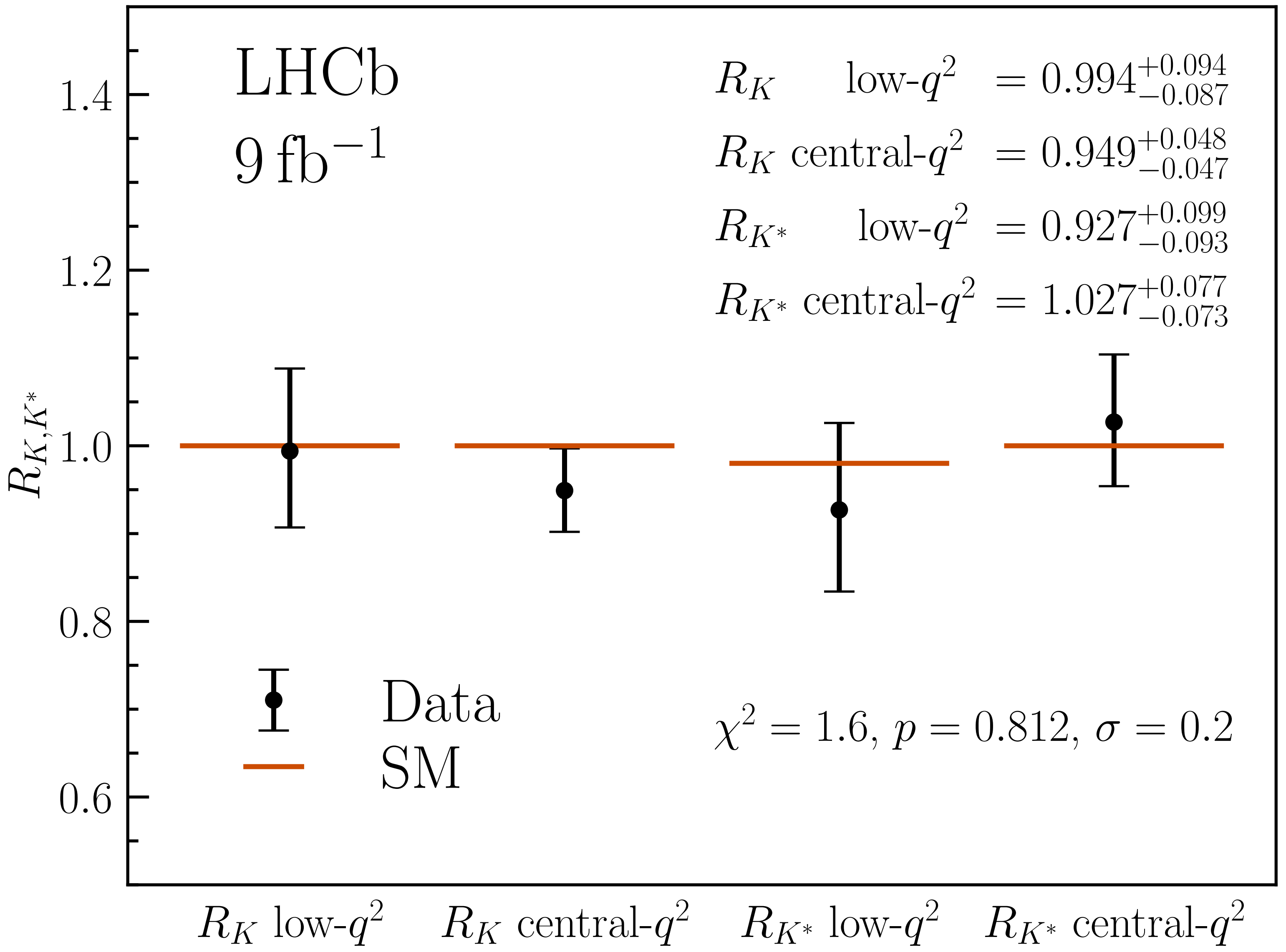

- **Improvements will come from theory/experimental synergy**
  - Improve σ_{th}, update measurements with Run1/2 using improved methods
  - Addition of complementary observables and decay modes, improve existing analysis techniques
- **LHCb Run3 just started**: boost the reach to unprecedented level with a *brand new detector*.
  - Expect from 2024, 3 x more stat in less than 2.5 years of data taking.

Backup

Run3 has just started, more stat coming soon

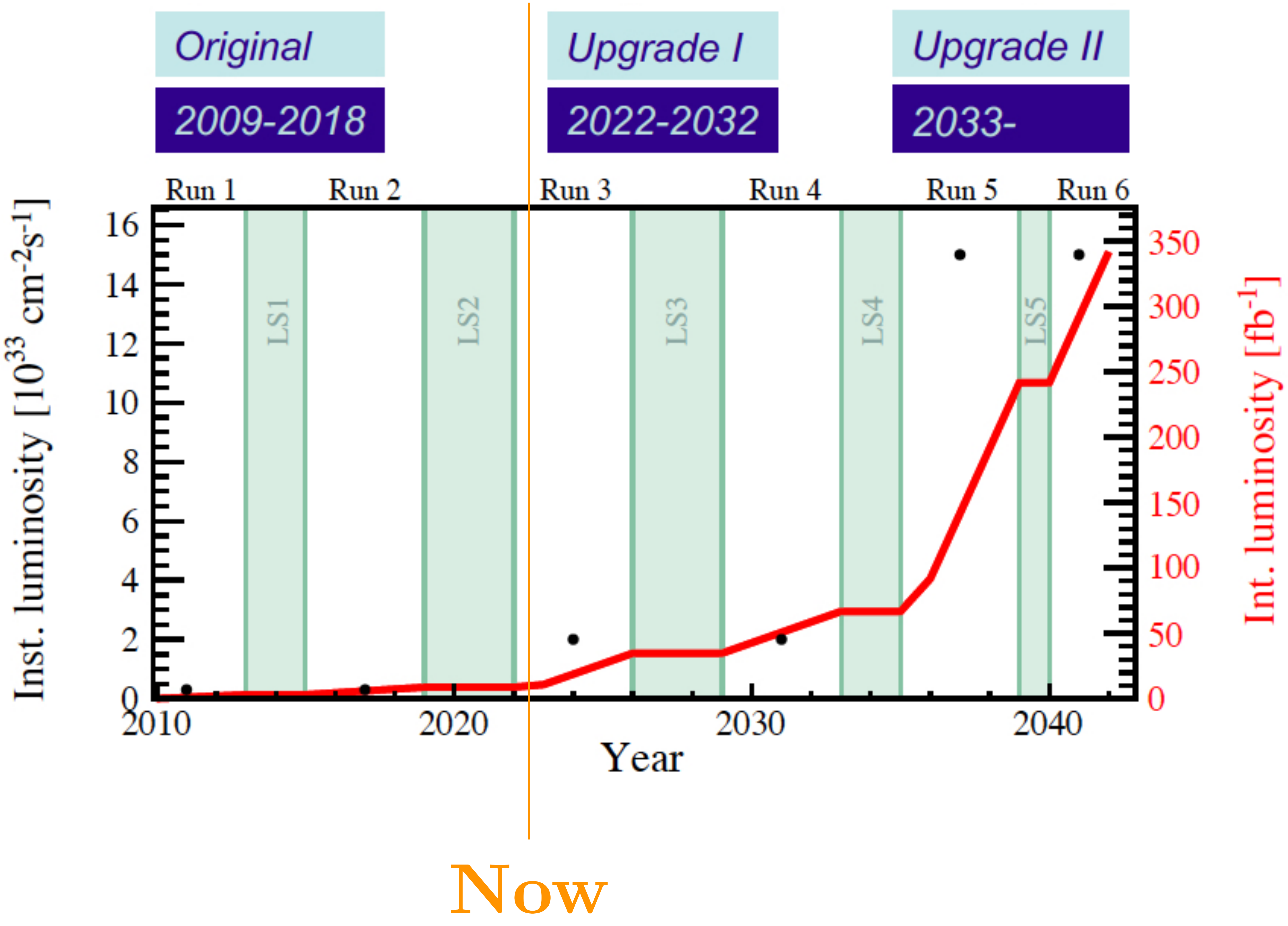

Run3: more stat coming soon, exploit available luminosity

- LHC pp collisions at $\sqrt{s} = 14\,\text{TeV}$, $25\,\text{ns}$ bunch spacing → 40 MHz collision rate.
- LHCb aims at boosting the physics output increasing the instantaneous luminosity and the signal rate.

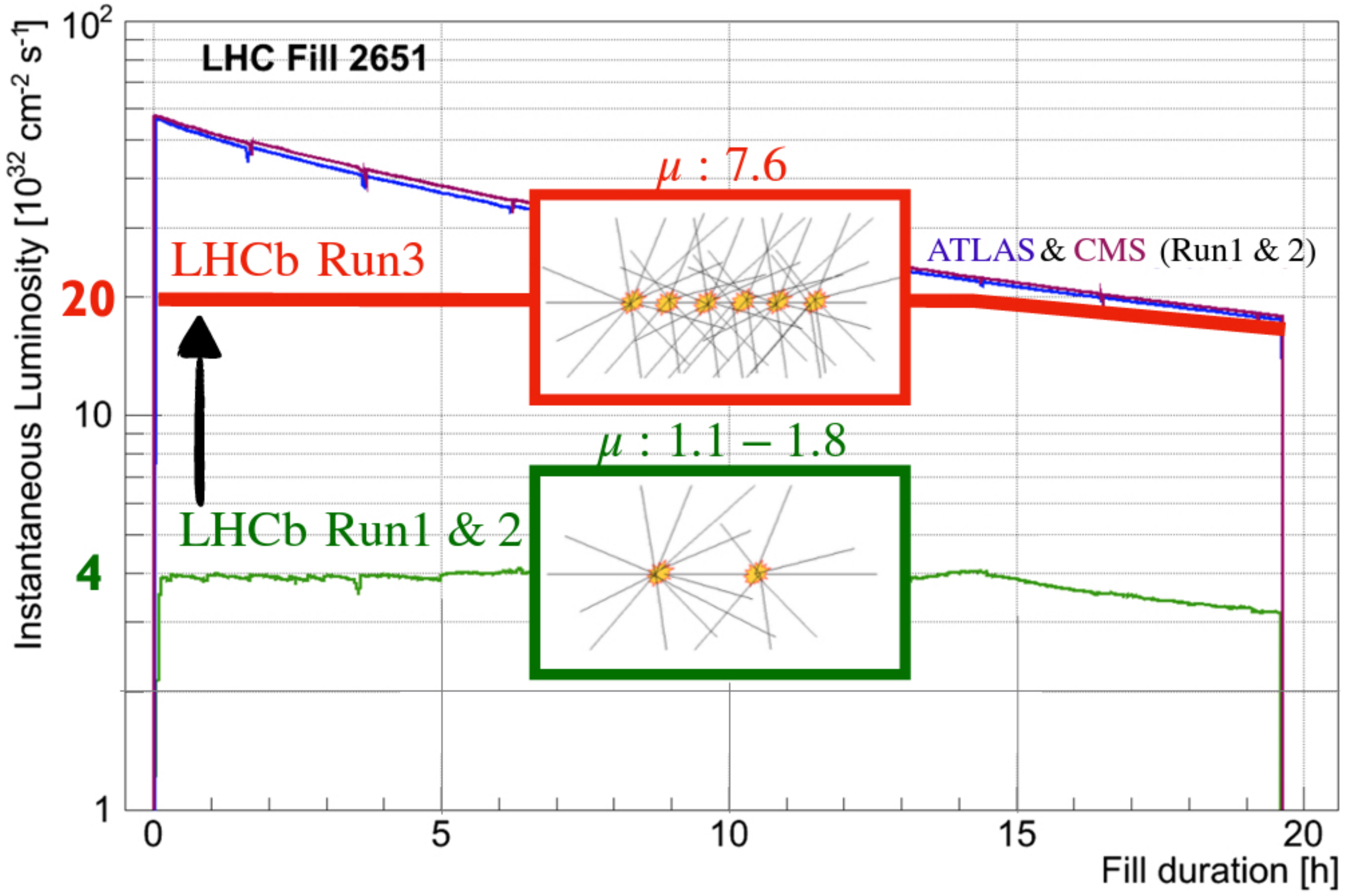

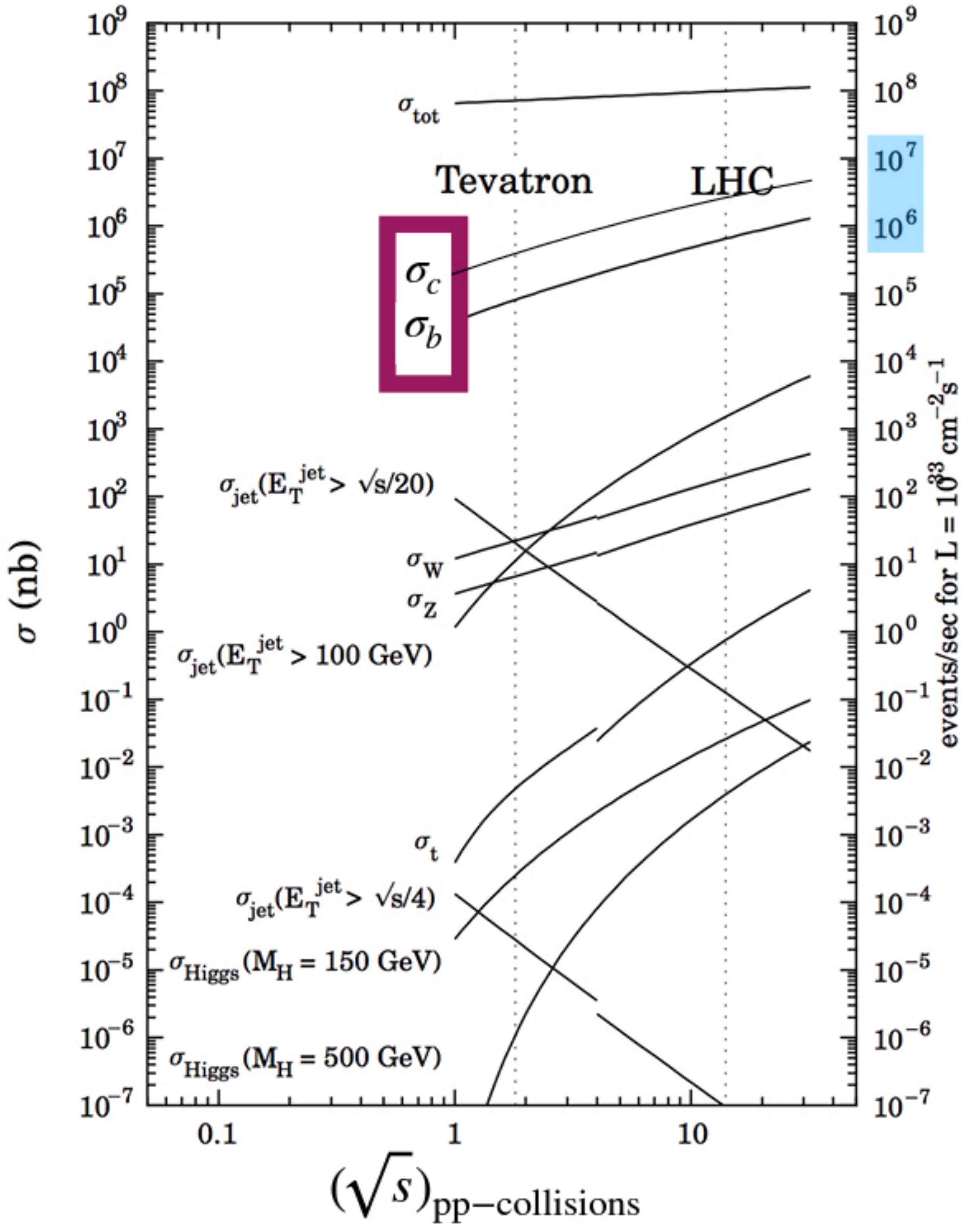

MHz signal rate

For $\mu \sim 7.6$

- 0.02 b hadron/event
- 0.2 c hadron/event
- 2 light-long-lived/event

$^{(*)}$accounting for $\epsilon_{acc}^{LHCb} \times \epsilon_{recoble}^{>=2-daughters}$

- More PVs, more tracks, more signal
- Almost all events will have a b or c hadron in Run 3

LHCb-PUB-2014-027

Run3: more stat coming soon, real time analysis

- **Run3 data taking has started, what to expect at LHCb with electron/muon reconstruction?**

If one would keep a 1MHz readout limit and HW triggers (L0)

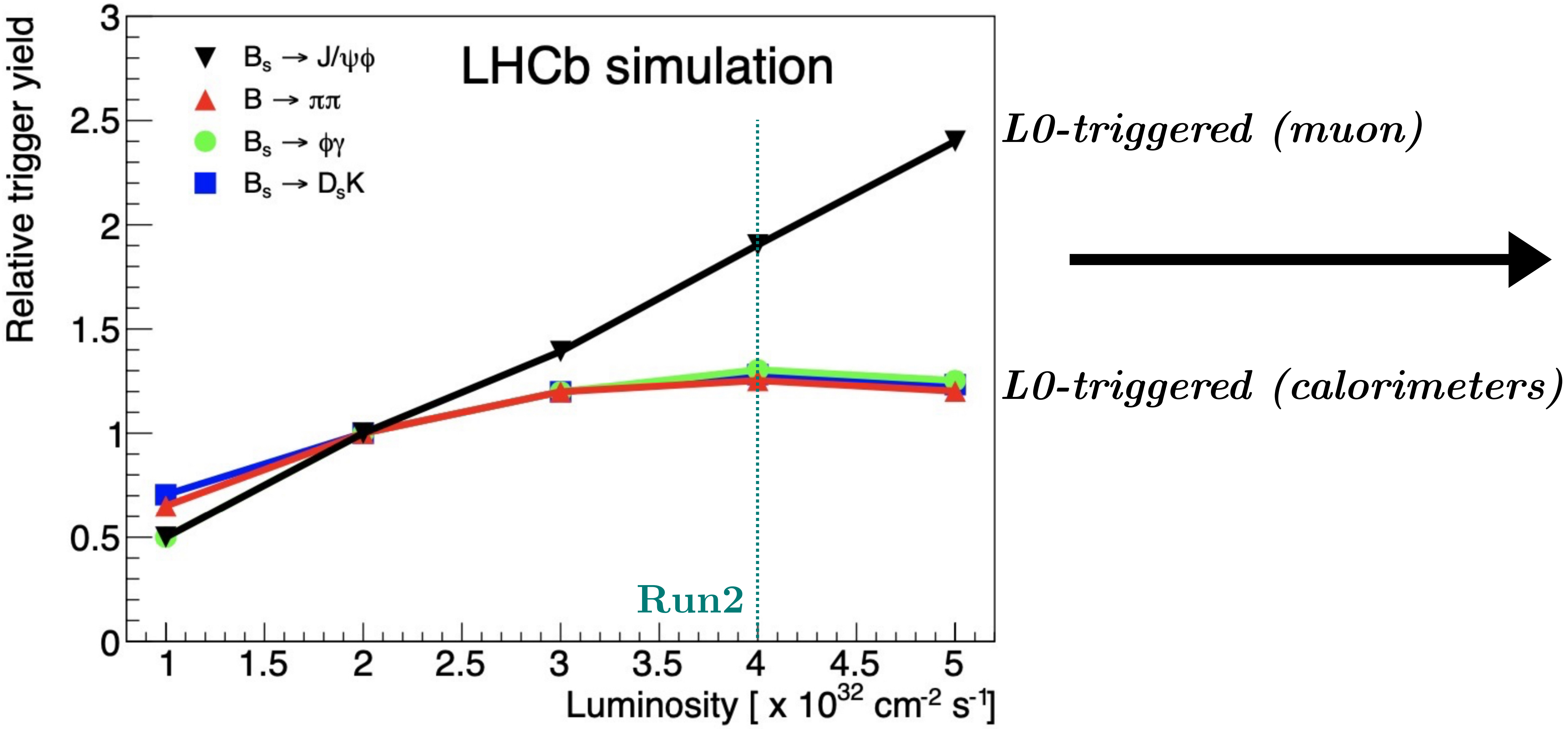

Fully removed hardware level trigger

Event reconstruction in real time at 40MHz

input rate with $\mathscr{L} = 20 \times 10^{32}\mathrm{cm}^{-2}s^{-1}$

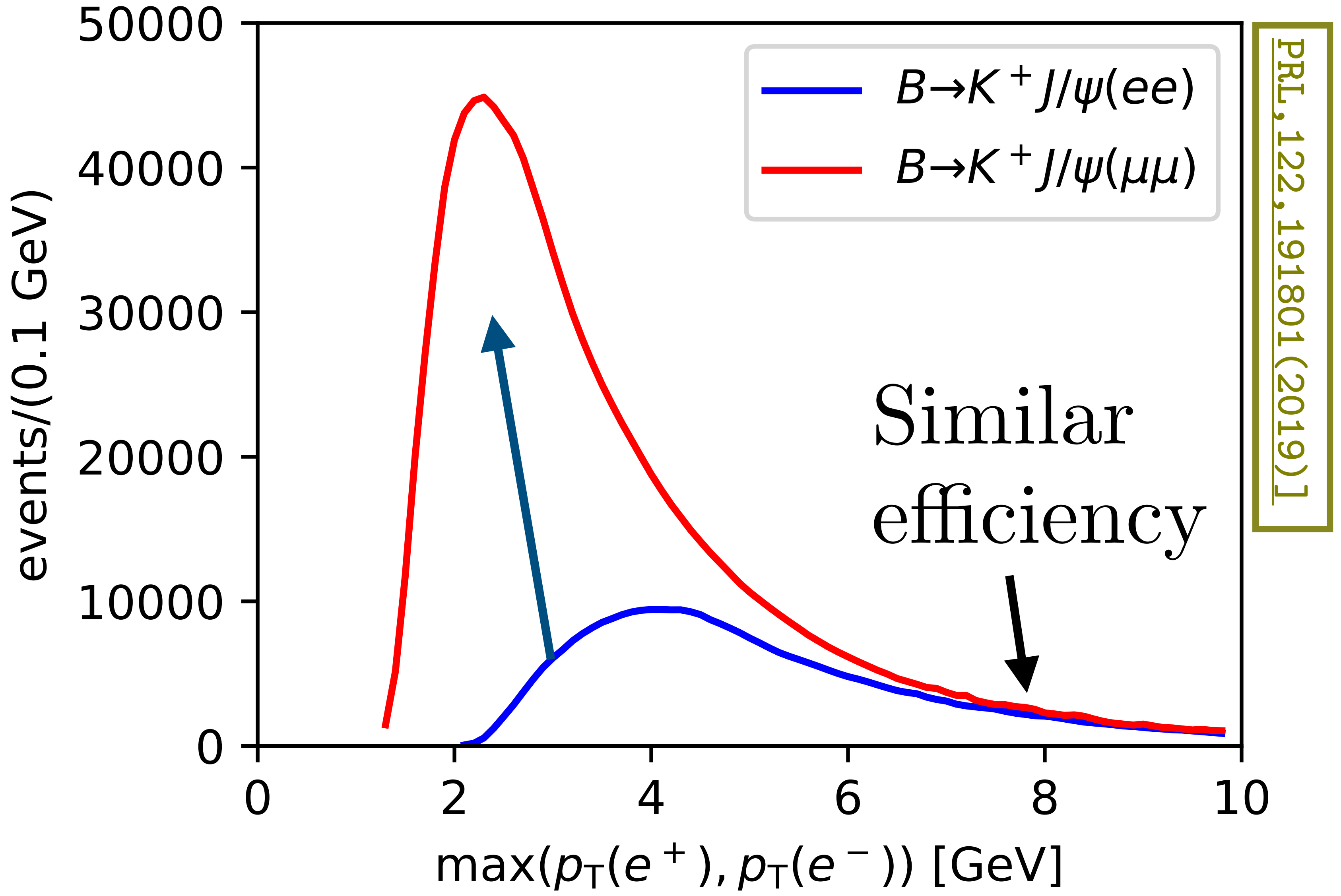

[PRL, 122, 191801 (2019)]

- Electrons vs Muon reconstruction efficiencies boosted thanks to $\varepsilon_{tracking}$ replacing ε_{L0} effect!
- PID electron performances in the harsher occupancy environment from calorimeter will be known soon once detector commissioning is finalised
  - Note : electron and calorimeter reconstruction algorithms heavily improved compared to Run1/2

Prospects: Run3 has just started

- **Run 1 (2011-2012)**:

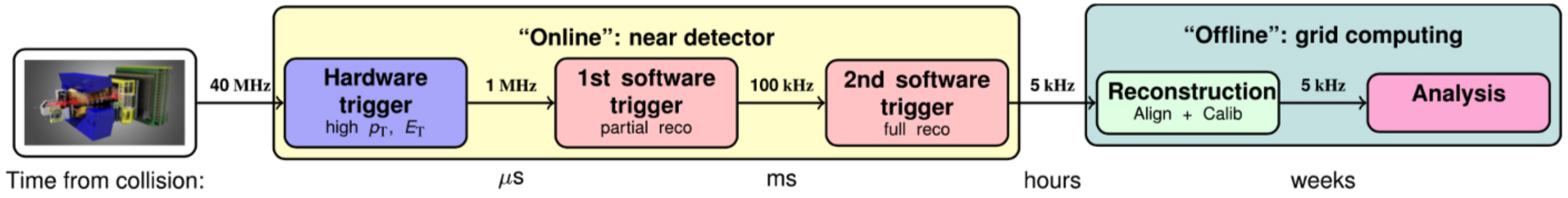

Time from collision:

40 MHz → **Hardware trigger** high p_T, E_T → 1 MHz → **1st software trigger** partial reco → 100 kHz → **2nd software trigger** full reco → 5 kHz → **Reconstruction** Align + Calib → 5 kHz → **Analysis**

"Online": near detector

"Offline": grid computing

μs ms hours weeks

- **Run 2 (2015-2018)**:

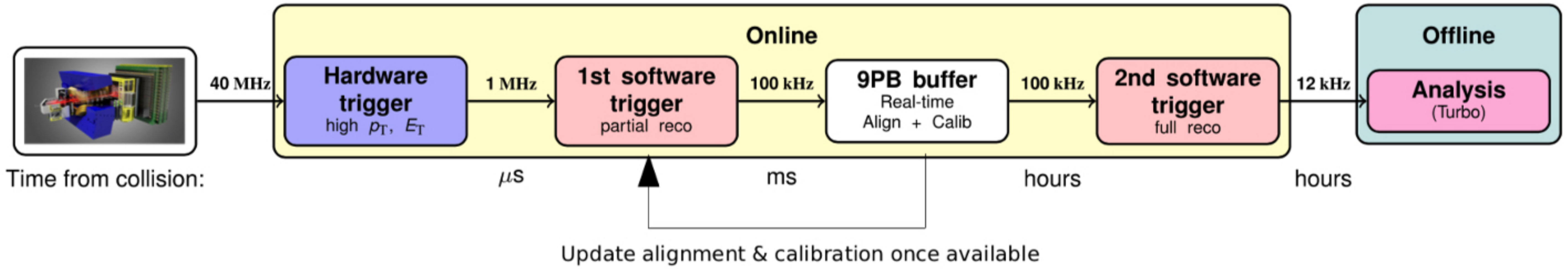

Time from collision:

40 MHz → **Hardware trigger** high p_T, E_T → 1 MHz → **1st software trigger** partial reco → 100 kHz → **9PB buffer** Real-time Align + Calib → 100 kHz → **2nd software trigger** full reco → 12 kHz → **Analysis** (Turbo)

Online

Offline

μs ms hours hours

Update alignment & calibration once available

- **Run 3 (2021-2025++)**:

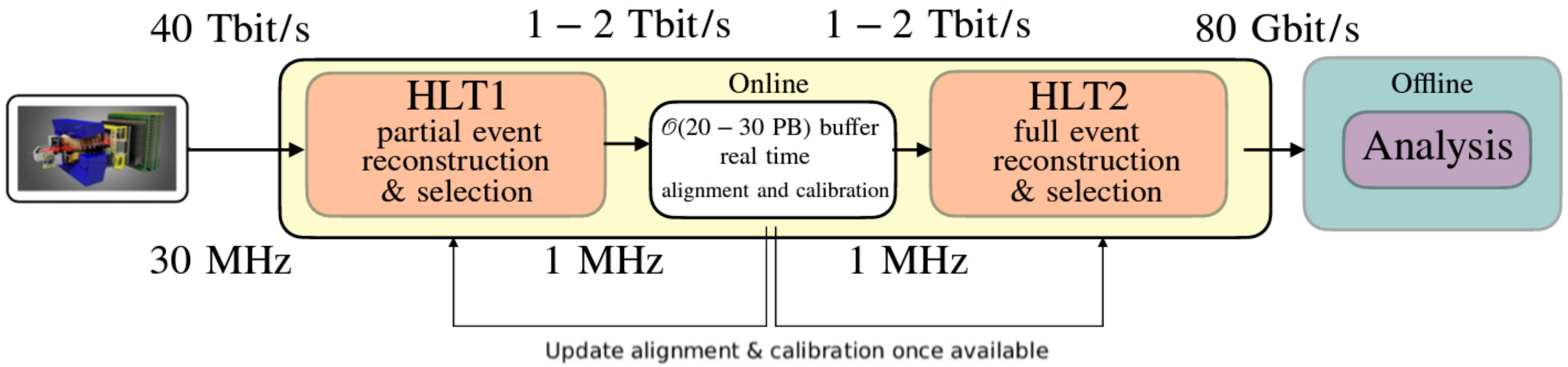

40 Tbit/s 1 – 2 Tbit/s 1 – 2 Tbit/s 80 Gbit/s

Online

HLT1 partial event reconstruction & selection

$\mathcal{O}(20-30$ PB$)$ buffer real time alignment and calibration

HLT2 full event reconstruction & selection

Offline

Analysis

30 MHz 1 MHz 1 MHz

Update alignment & calibration once available

- Hardware trigger: 40→ 1 MHz read-out limit in **Run1,2** based on Muon and Calorimeter signatures
- HLT1(partial) and HLT2(full) event reconstruction split in **Run2**
- **Buffer** data to disk to perform real time alignment and calibration
- Offline quality reconstruction and selection in the online system
- **Run3** : remove Hardware trigger in favour of a fully software based one.
- Event reconstruction at collision rate
- Full detector read-out at 40 MHz

LFU tests in $b \to s\ell\ell$

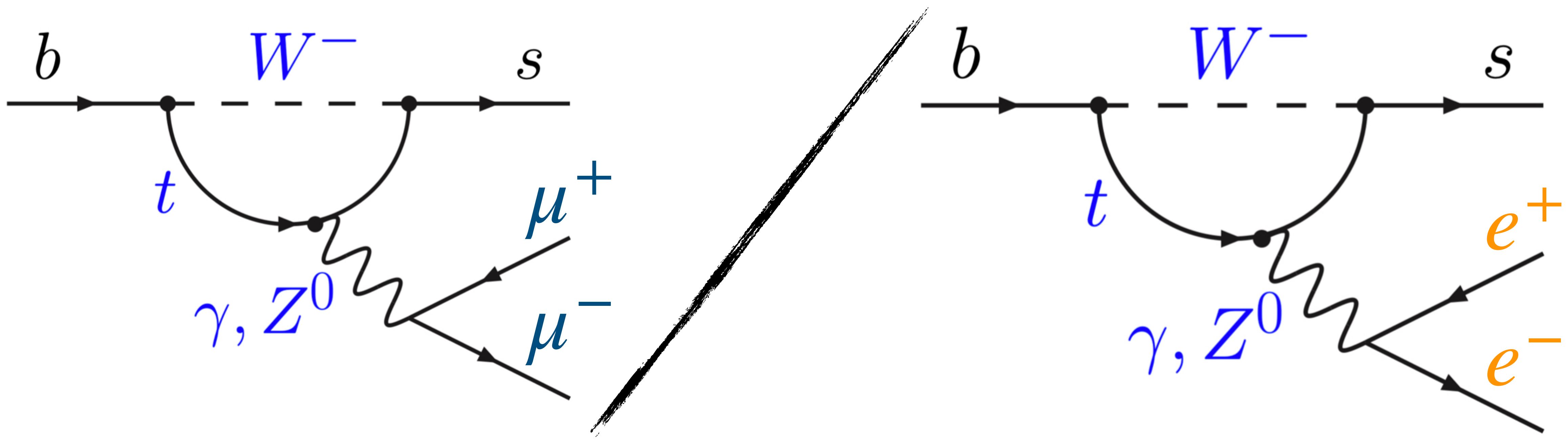

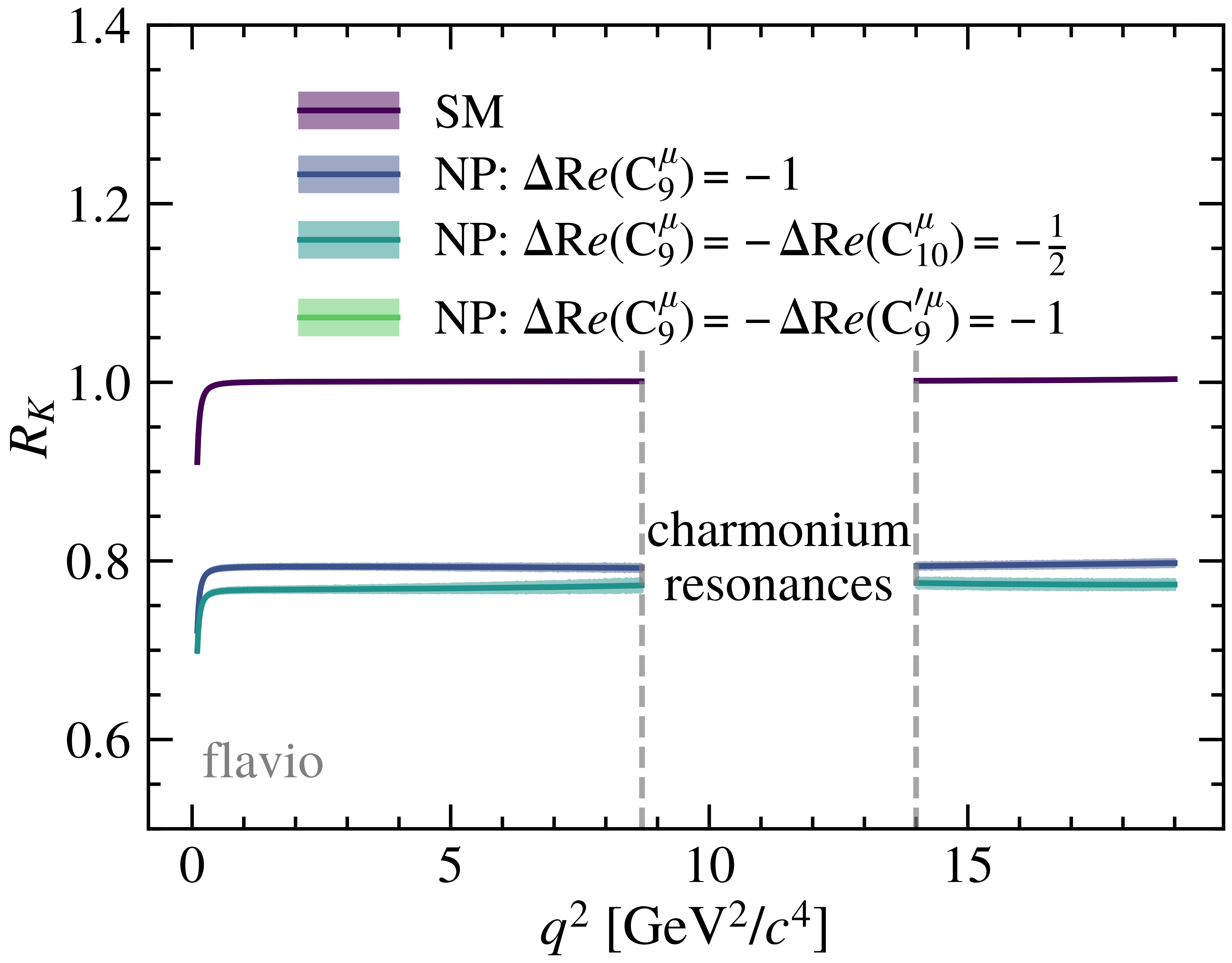

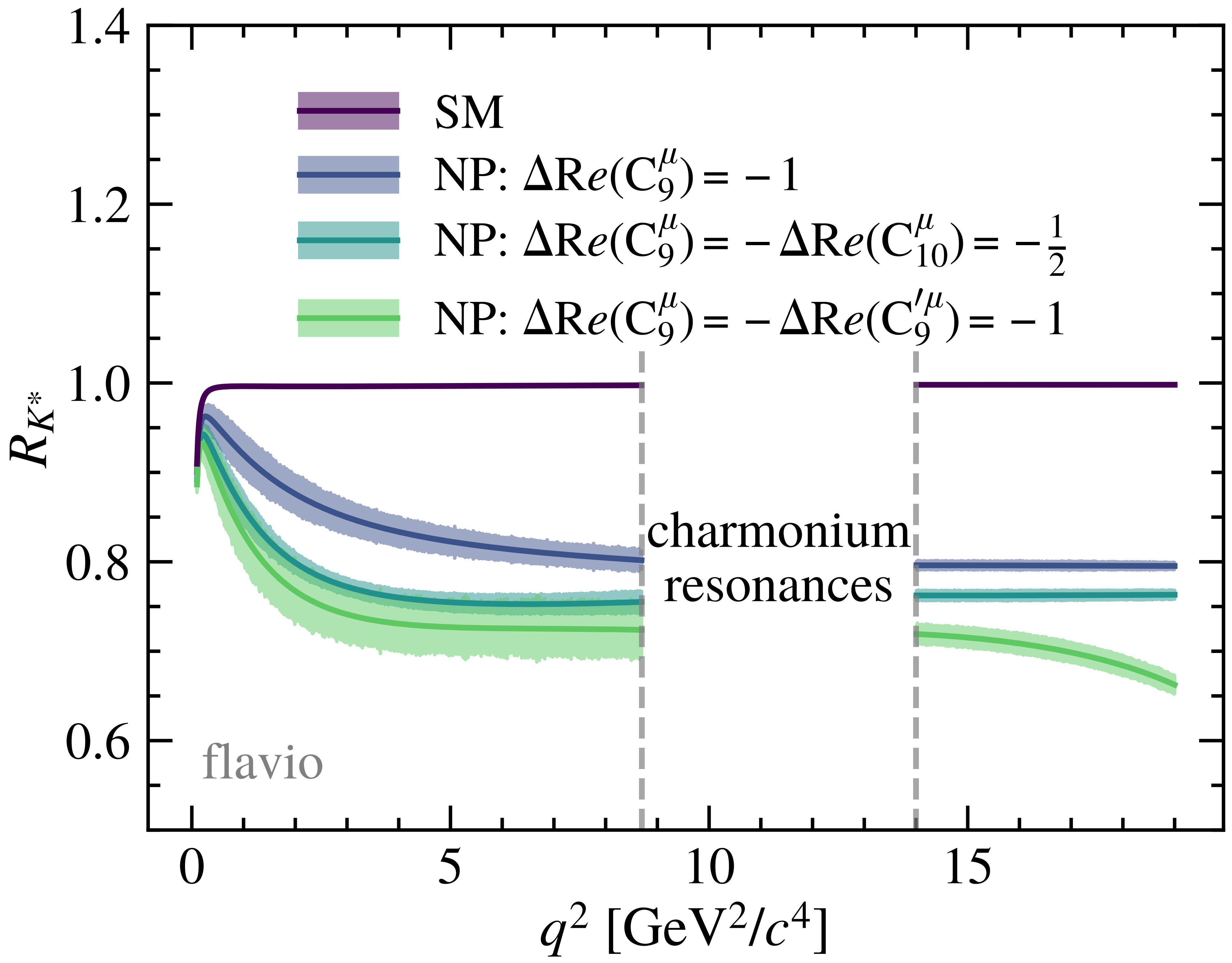

LFU results

$$
\text{low-}q^2 \begin{cases} R_K & = 0.994 \ {}^{+0.090}_{-0.082} \ (\text{stat}) \ {}^{+0.027}_{-0.029} \ (\text{syst}), \\ R_{K^*} & = 0.927 \ {}^{+0.093}_{-0.087} \ (\text{stat}) \ {}^{+0.034}_{-0.033} \ (\text{syst}) \end{cases}
$$

$$
\text{central-}q^2 \begin{cases} R_K & = 0.949 \ {}^{+0.042}_{-0.041} \ (\text{stat}) \ {}^{+0.023}_{-0.023} \ (\text{syst}), \\ R_{K^*} & = 1.027 \ {}^{+0.072}_{-0.068} \ (\text{stat}) \ {}^{+0.027}_{-0.027} \ (\text{syst}). \end{cases}
$$

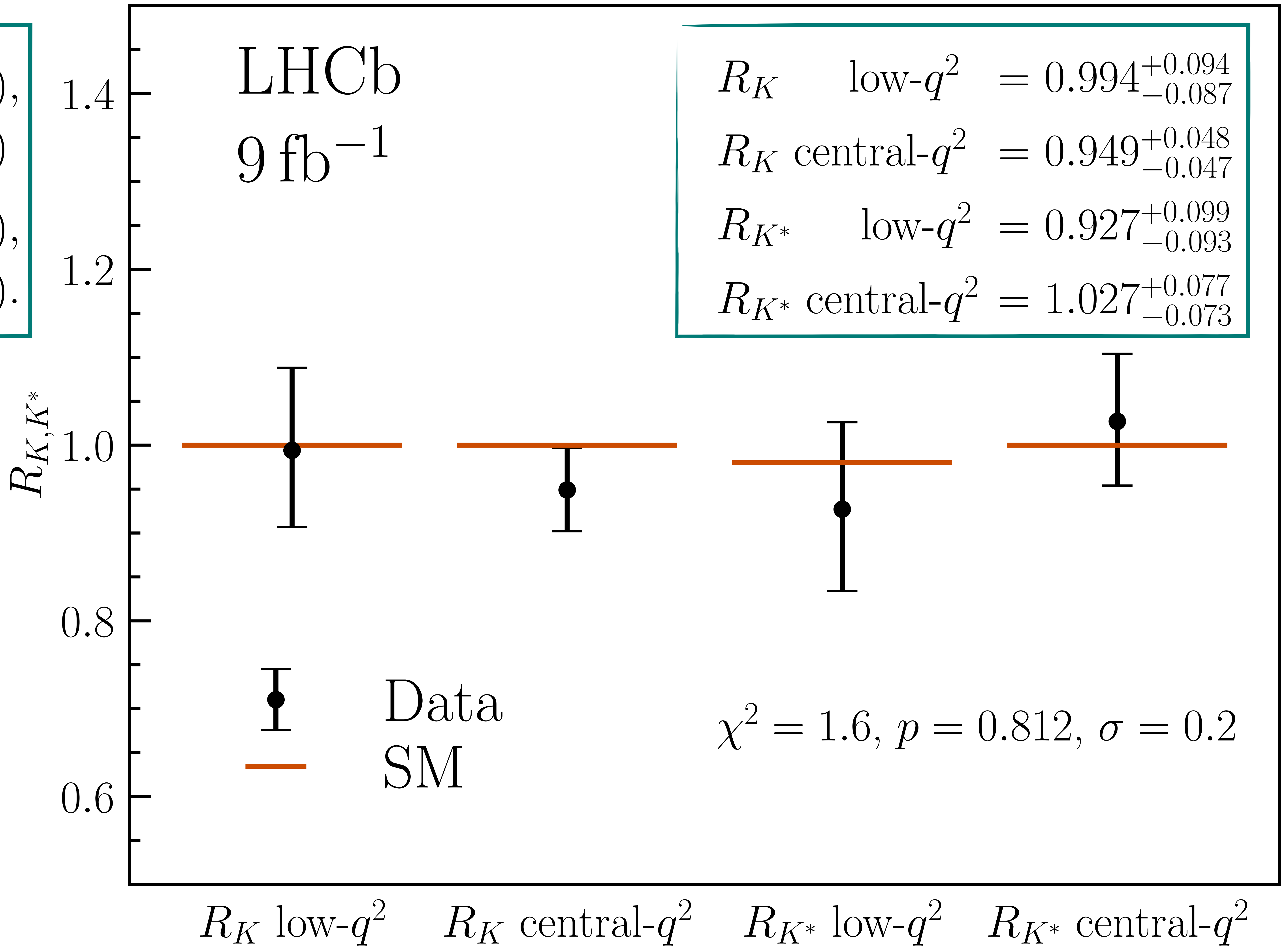

- Most precise and accurate LFU test in $b \to s\ell\ell$ transition
- Compatible with SM with a simple χ^2 test on 4 measurement at 0.2 σ

Net effect for LFU tests: muon vs electron modes

Narrow B signal window

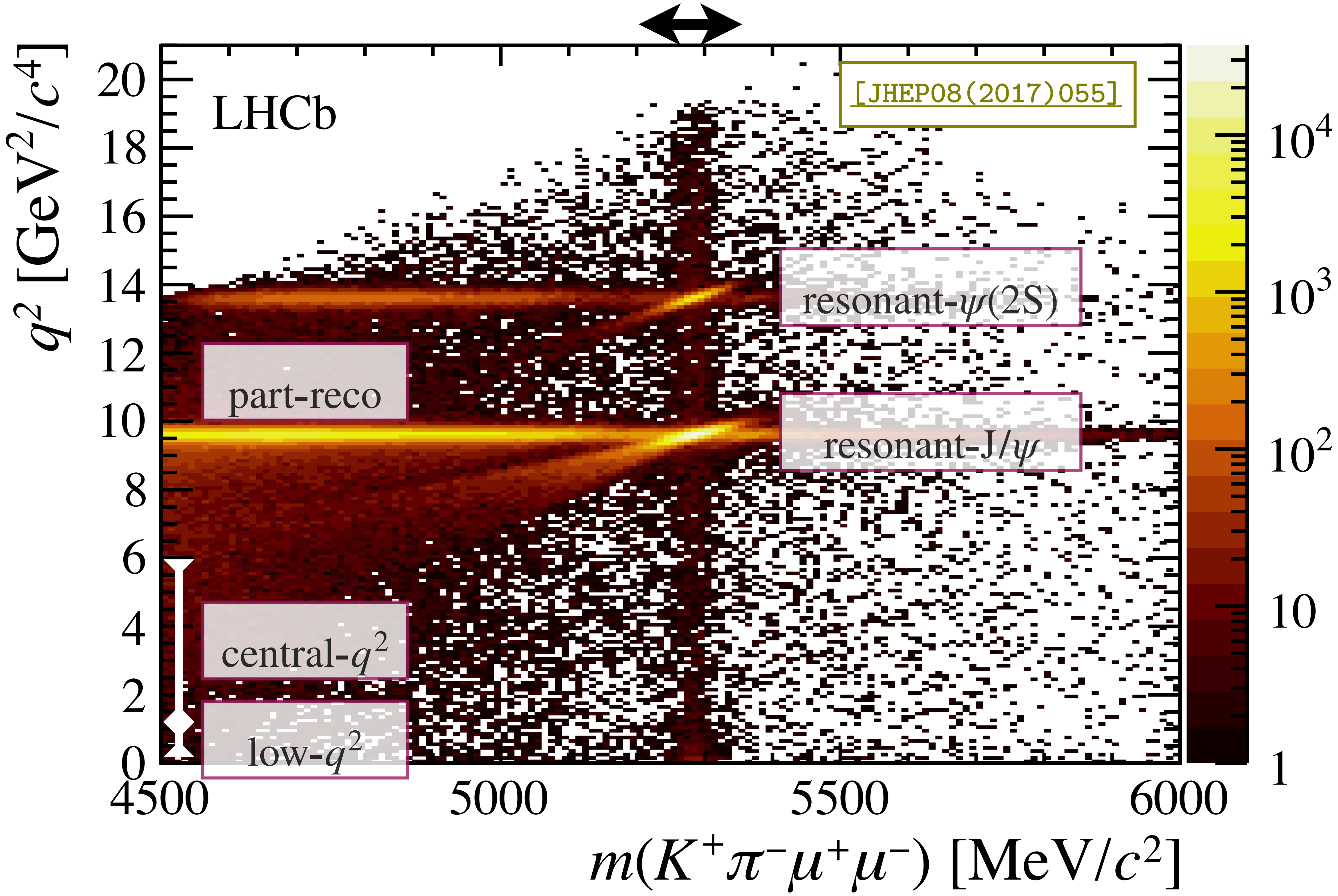

Wide B signal

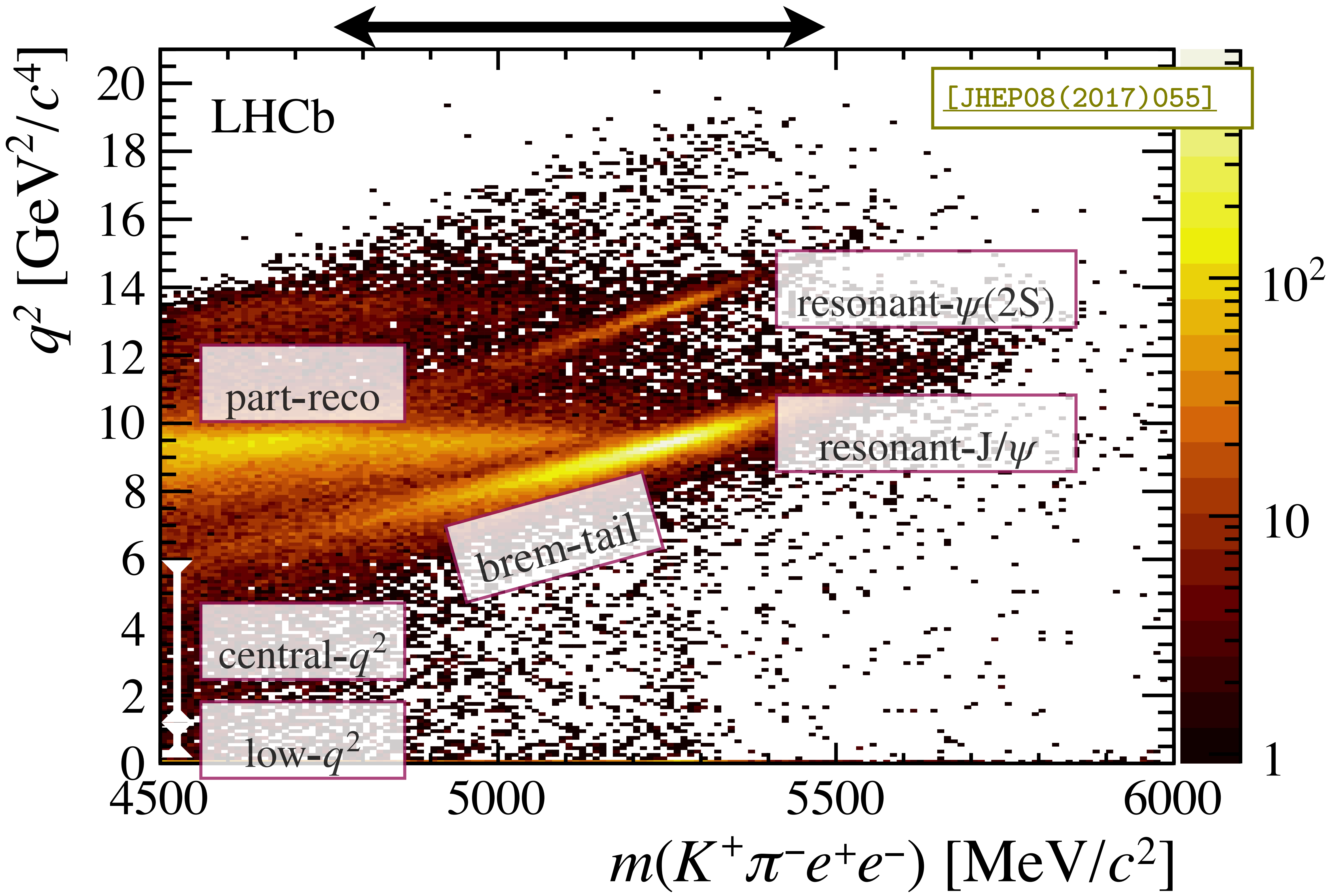

- Muons in final states benefit from excellent σ_p/p at LHCb and negligible energy losses
- Electrons in final states suffer from brem-losses and poorer σ_E/E from calorimeters compared to tracking
  - Mass fit and yield determination exposed to the interplay/modelling of backgrounds

- ***Electron mode yields ~ 1/3 Muon mode yields at LHCb in Run I/II due to hardware trigger***

R_X systematics

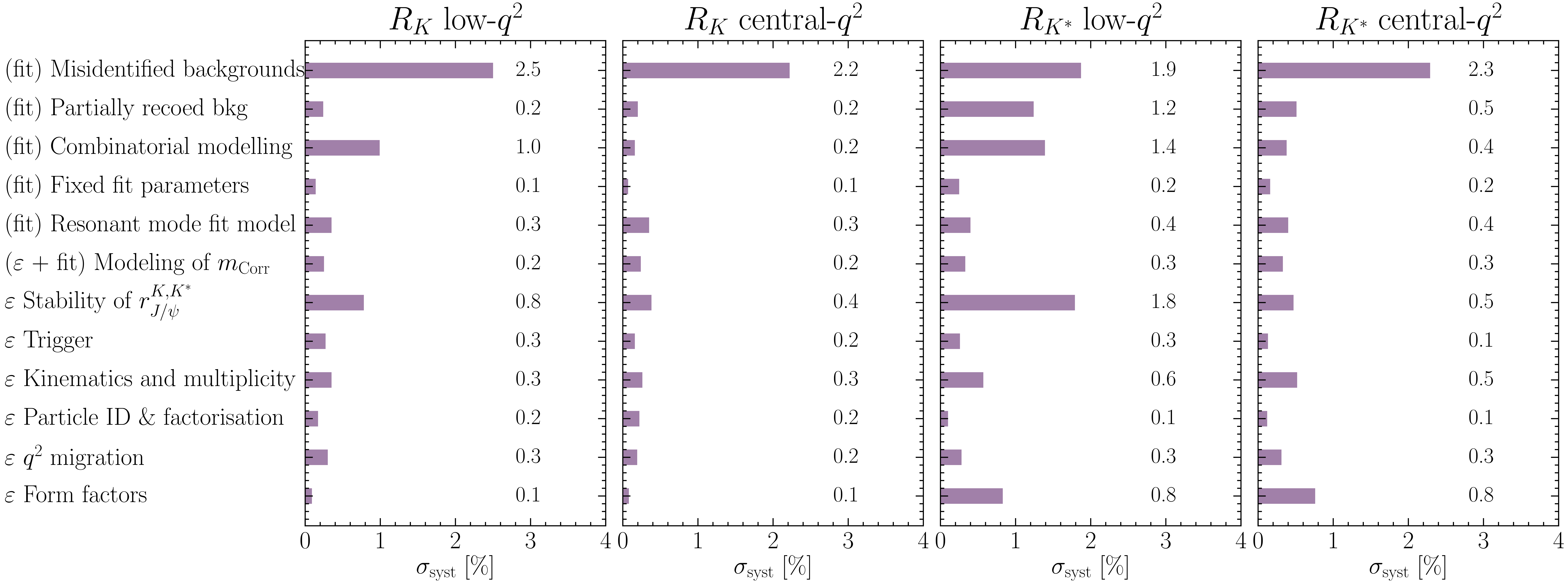

	R_K low-q^2	R_K central-q^2	R_{K^*} low-q^2	R_{K^*} central-q^2
(fit) Misidentified backgrounds	2.5	2.2	1.9	2.3
(fit) Partially recoed bkg	0.2	0.2	1.2	0.5
(fit) Combinatorial modelling	1.0	0.2	1.4	0.4
(fit) Fixed fit parameters	0.1	0.1	0.2	0.2
(fit) Resonant mode fit model	0.3	0.3	0.4	0.4
(ε + fit) Modeling of m_{Corr}	0.2	0.2	0.3	0.3
ε Stability of $r_{J/\psi}^{K,K^*}$	0.8	0.4	1.8	0.5
ε Trigger	0.3	0.2	0.3	0.1
ε Kinematics and multiplicity	0.3	0.3	0.6	0.5
ε Particle ID & factorisation	0.2	0.2	0.1	0.1
ε q^2 migration	0.3	0.2	0.3	0.3
ε Form factors	0.1	0.1	0.8	0.8

- Dominant systematic from misidentified backgrounds estimation from data driven method
- Measurement still statistically dominated

Simultaneous measurement: cross-feed $R_{K^{*0}}$ & R_K

[Nat. Phys. 18, 277-282 (2022)]

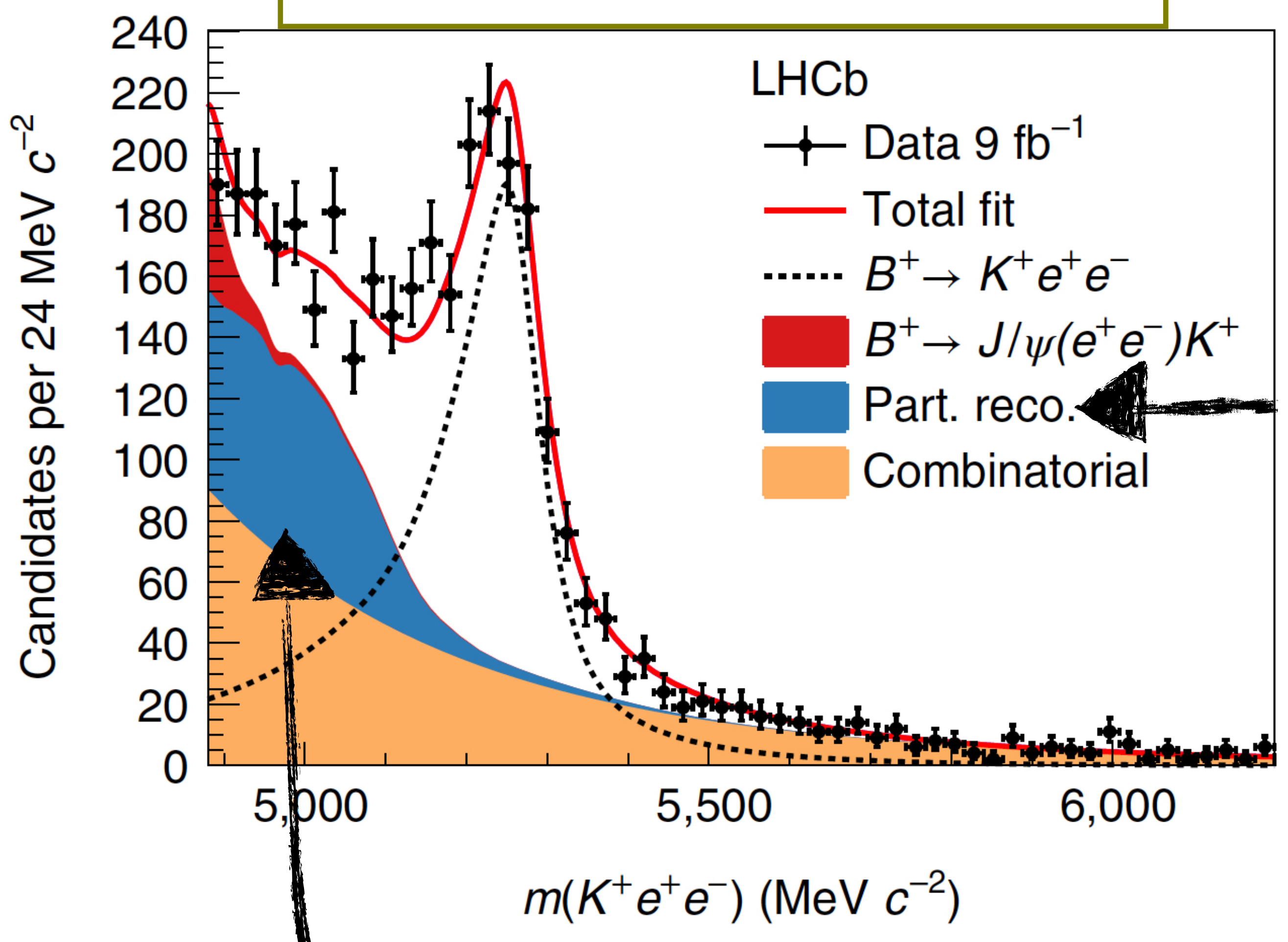

Was free

Improve per-event sensitivity constraining it from K^* mode

[JHEP08(2017)055]

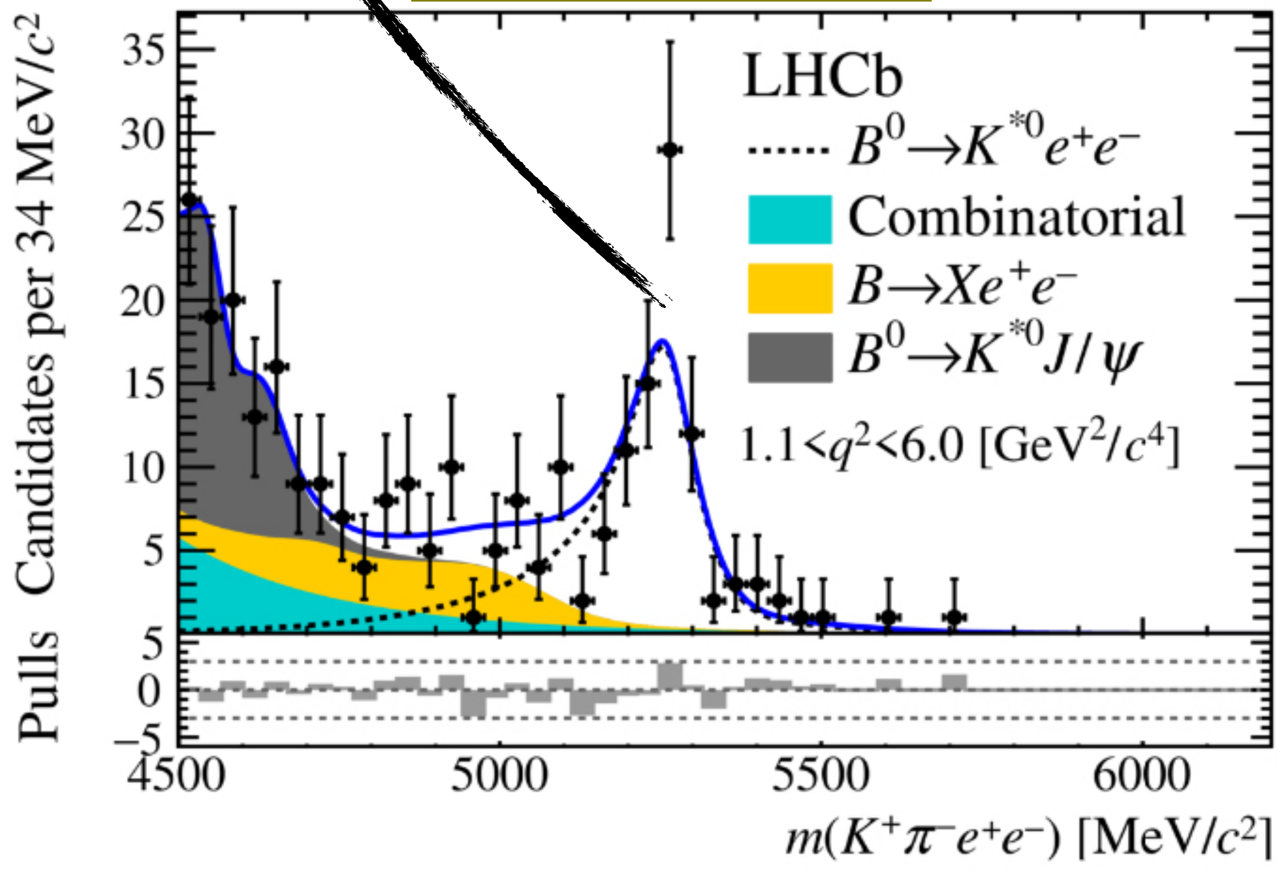

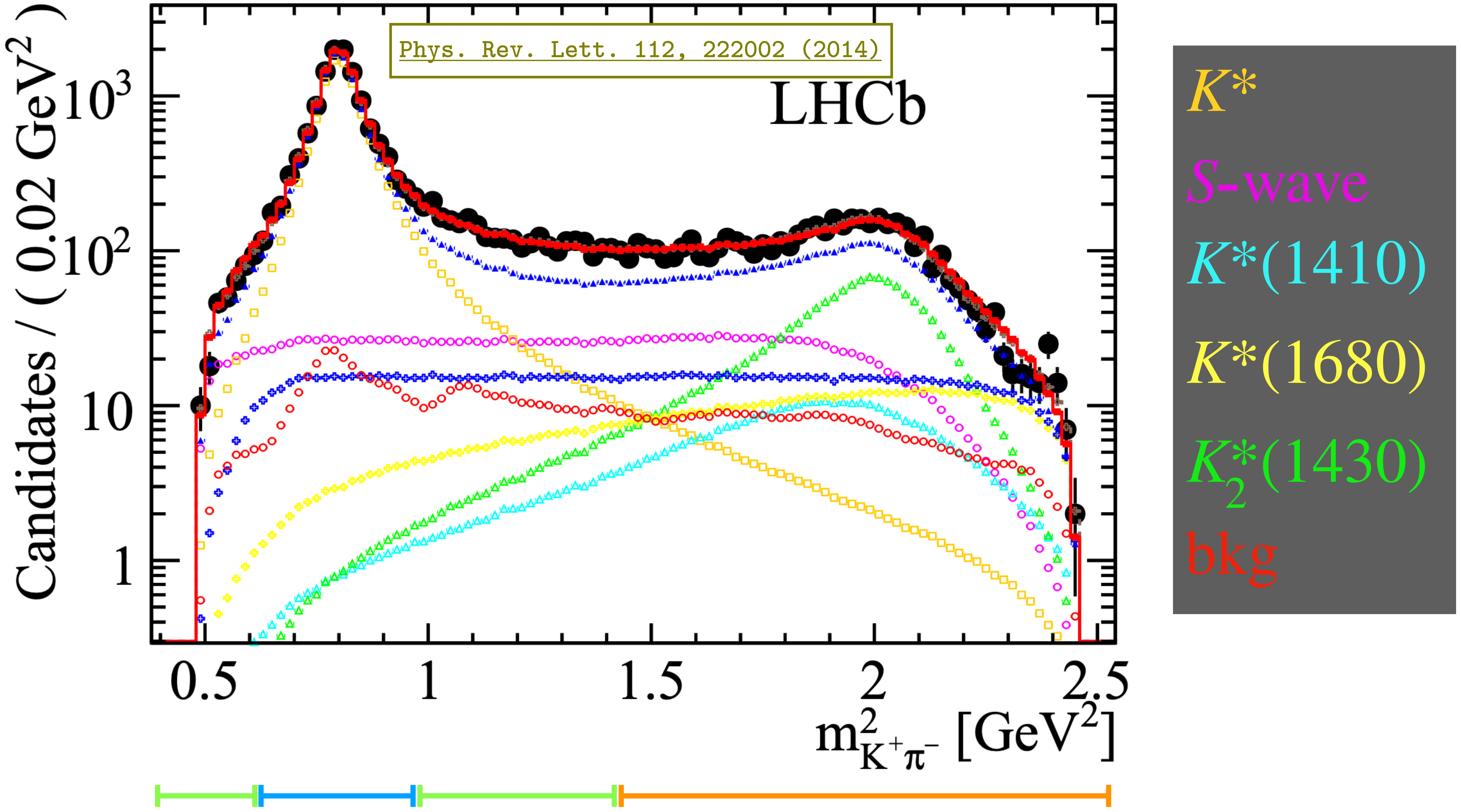

Phys. Rev. Lett. 112, 222002 (2014)

- Directly from $K^{*0}e^+e^-$
- Use F_S measurement in JHEP 11 (2016) 047 JHEP 04 (2017) 142 and Breit-Wigner tails
- Extrapolation factors / full amplitude from K^*J/ψ Phys. Rev. Lett. 112, 222002 (2014)

$K^+\cancel{\pi^0}$ accounting for isospin factors and ε corrections

Pass-Fail method to estimate mis-identified backgrounds

FailPass (FP)

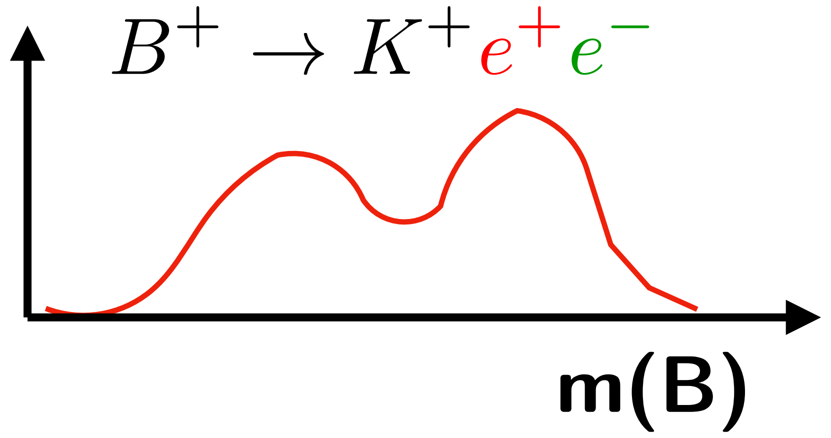

PassFail (PF)

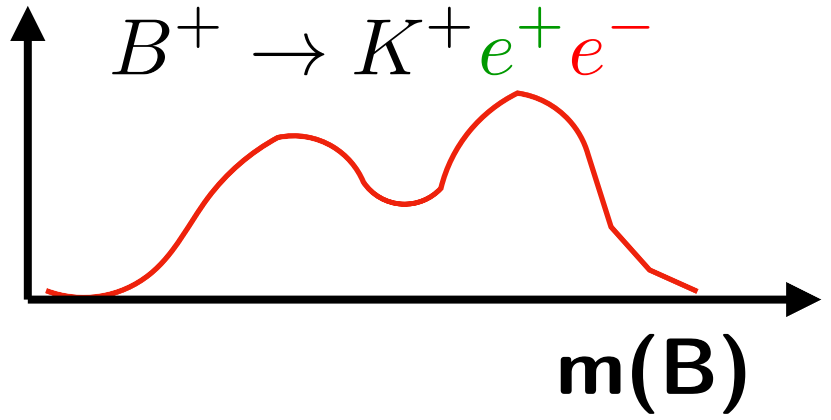

FailFail (FF)

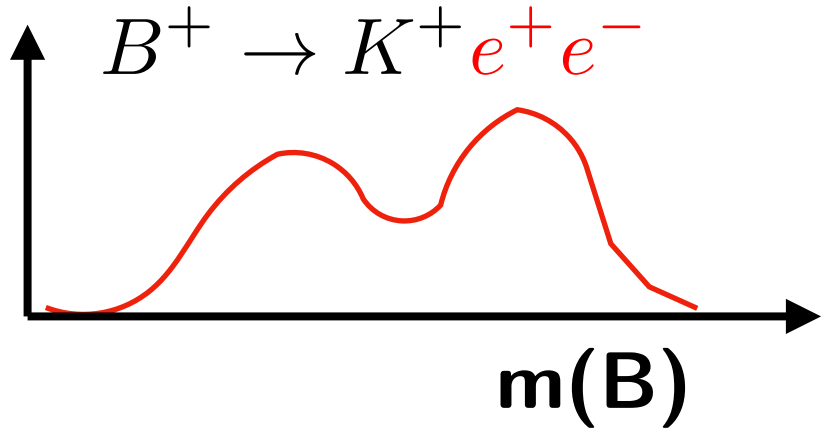

- Data with inverted PID cuts is enhanced in misID content

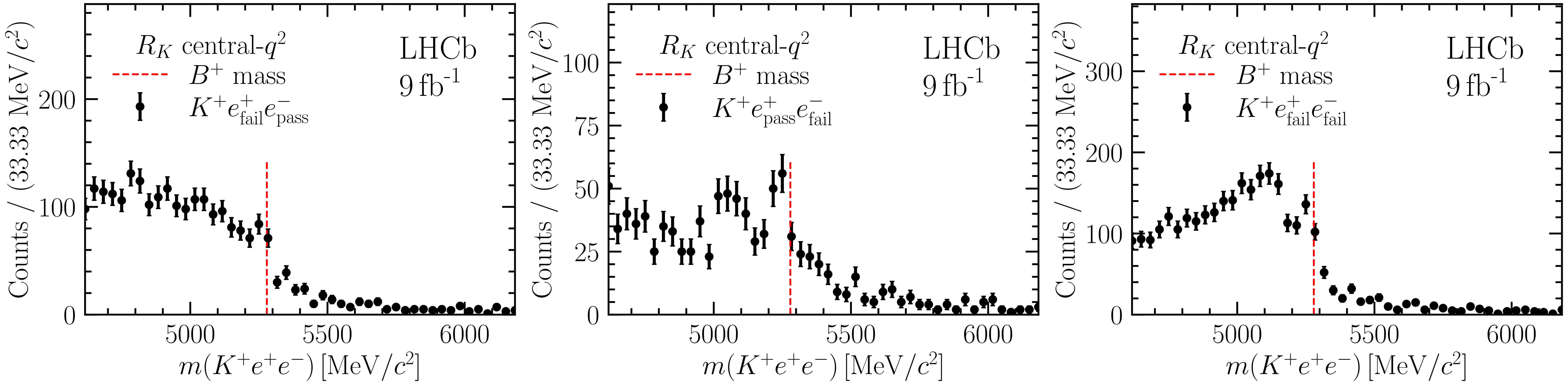

Inverted cuts and still use electron ID hypothesis

$$N(PF) : N(B^+ \to K^+e^+h^-) + N(B^+ \to K^+h^+h'^-) + N(B^+ \to K^+e^+e^-) + N(B^+ \to K^+J/\psi(\to e^+e^-))$$

$$N(FP) : N(B^+ \to K^+e^-h^+) + N(B^+ \to K^+h^+h'^-) + N(B^+ \to K^+e^+e^-) + N(B^+ \to K^+J/\psi(\to e^+e^-))$$

$$N(FF) : N(B^+ \to K^+h^+h'^-)$$

Residual double mis-id

Residual signal contribution - subtract using simulation

The LHCb Detector from 2011-2018 [Run1,Run2]

- Lower luminosity than ATLAS/CMS for $\langle\mu\rangle \simeq 1$, $\mathscr{L}^{\text{LHCb}}_{inst} \simeq 3.5 \times 10^{32}\ \text{cm}^{-2}\text{s}^{-1}$, $\int_{2011}^{2018} \mathscr{L} = 9\text{fb}^{-1}$
- Large $\sigma_{pp\to b\bar{b}}$ at LHC
- Acceptance in forward region of pp collisions $(2 < \eta < 5)$
  - Excellent displaced vertex identification
  - Low-p_{T} triggers (few GeV)
- Dipole magnet with very precise tracking detectors $\sigma_p/p \sim 0.5 - 1\,\%$
  - Particle ID with calorimeters, muon system and cherenkov detectors (RICH)

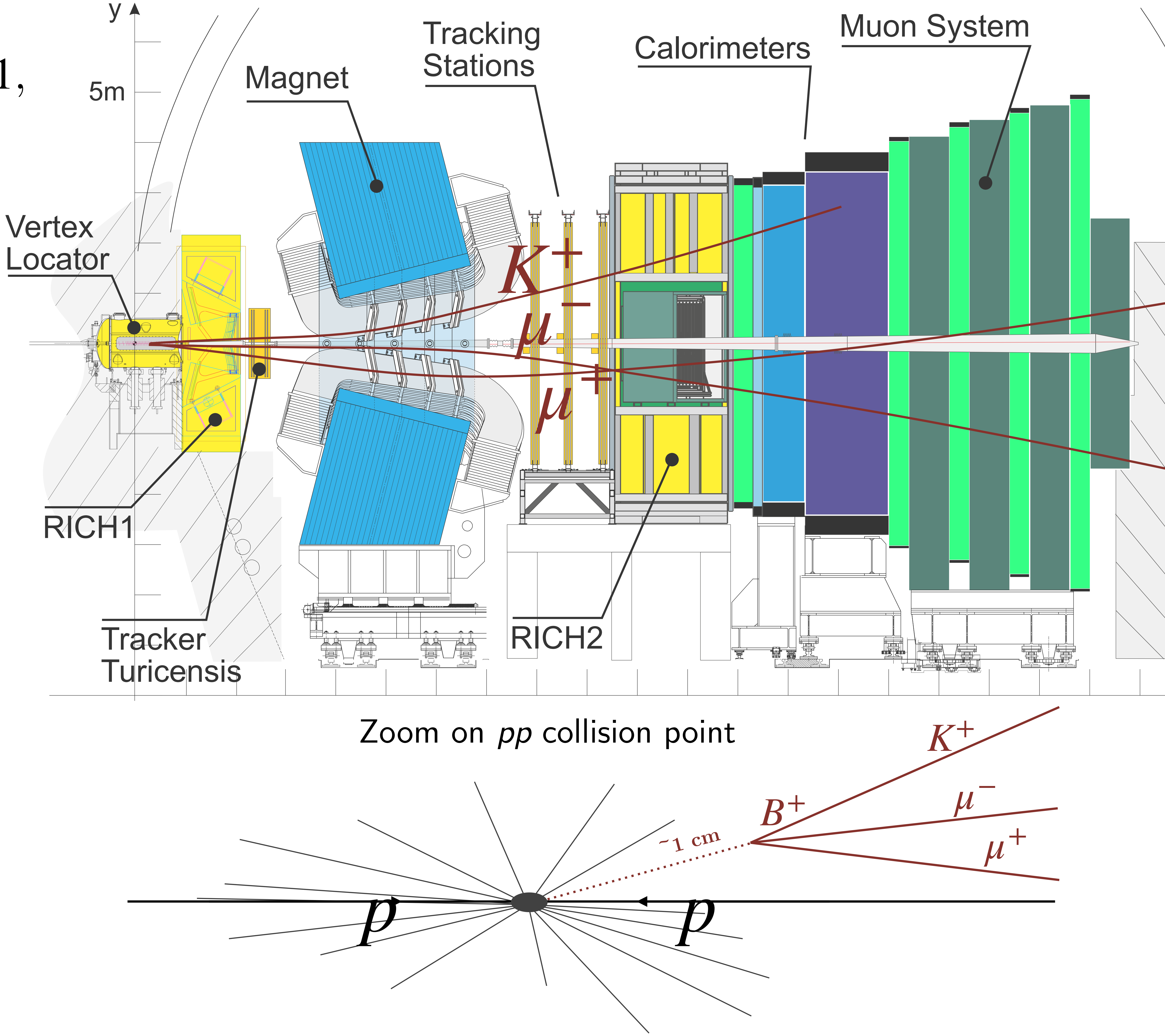

Overall picture from theory side on predictions

	parametric uncertainties	form factors	non-local matrix elements
$\mathcal{B}(B \to M\ell\ell)$	✗	✗	✗
angular observables	✓	✗	✗
$\overline{\mathcal{B}}(B_s \to \ell\ell)$	**CKM** ✗	✓	**Not-applicable** ✓ (N/A)
LFU observables	✓	✓	✓

$b \to s\ell^+\ell^-$ observables and interpretation

- **How to interpret $b \to s\ell\ell$ analyses results in terms of NP?**

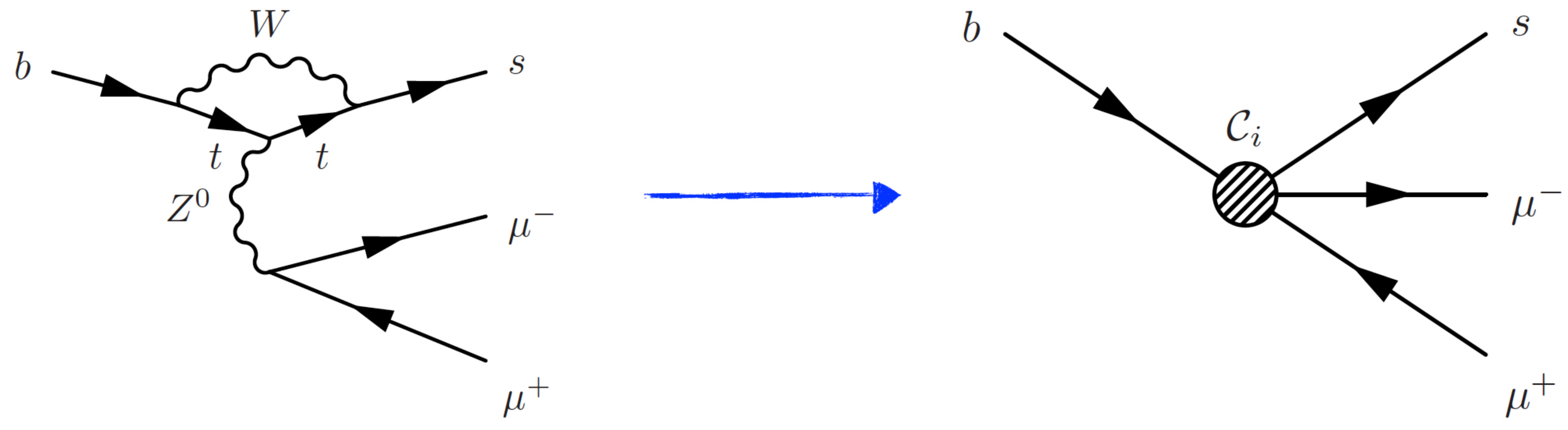

hadronic matrix elements

Local

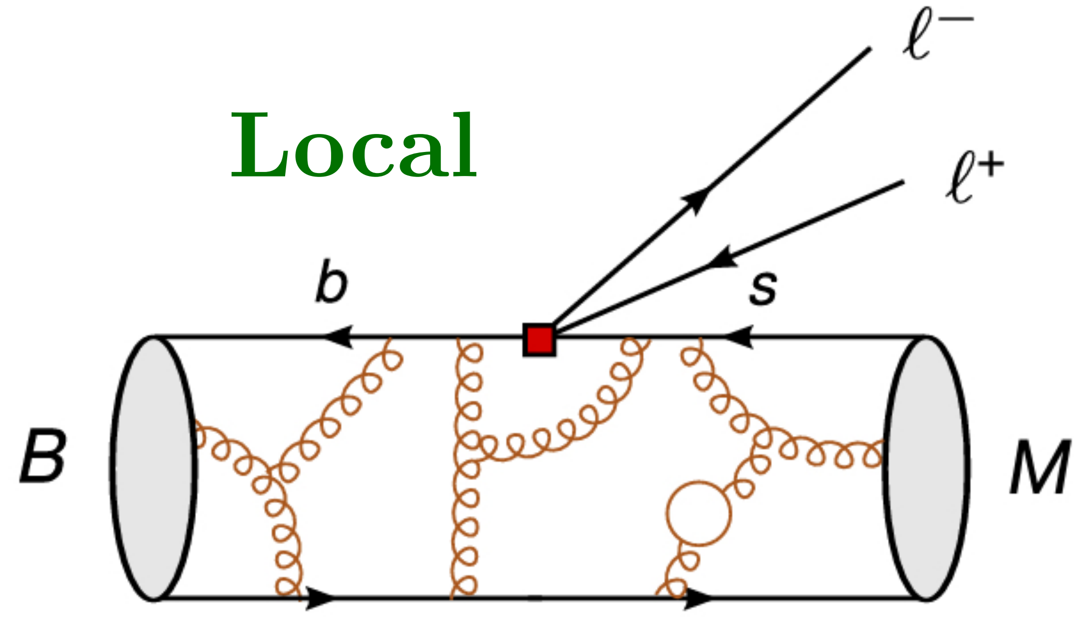

Non-local (e.g. charm-loops)

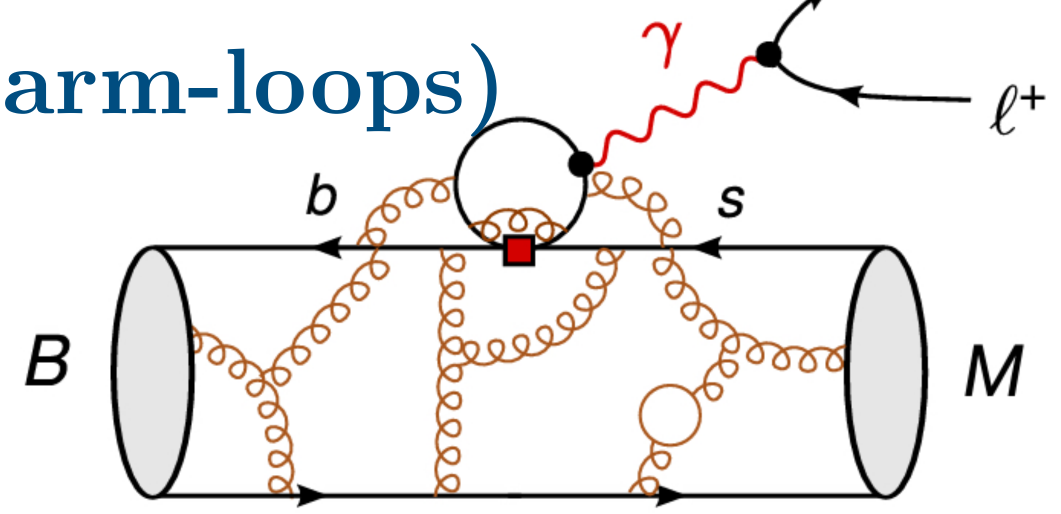

Depending on the observable, the SM predictions is more or less accurate

Theoretical uncertainties in SM predictions on $b \to s\ell\ell$ observables

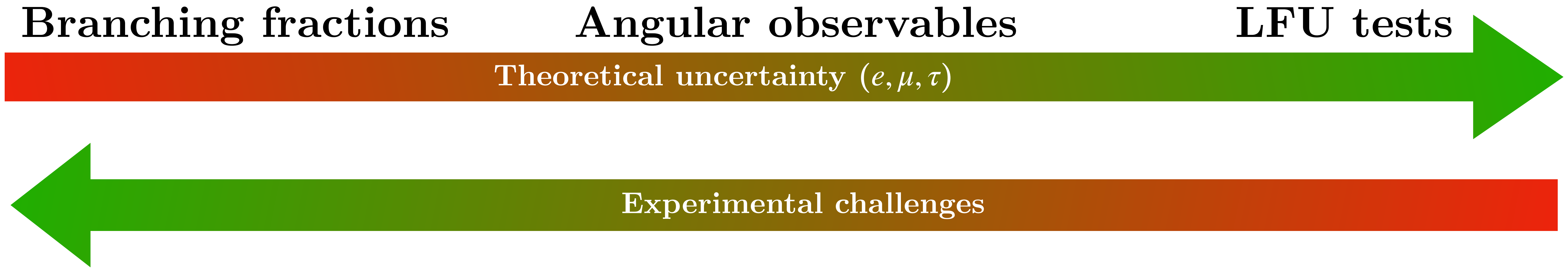

Branching fractions **Angular observables** **LFU tests**

Theoretical uncertainty (e, μ, τ)

Experimental challenges

LHCb and leptons

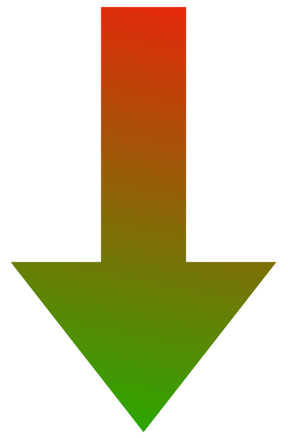

$\ell = \tau$
$\ell = e$
$\ell = \mu$

Radiative $b \to s\gamma$ transition

Left handed $C_7 = C_7^{\mathrm{SM}} + C_7^{\mathrm{NP}}$

- $\mathscr{B}(B \to X_s\gamma) \propto C_7^2 + C_7'^2$ **(inclusive)**
  - [1] ✦ 5% precise prediction
  - [2] ✦ 5% precise from *B*-factories
  - ✦ **Very hard at LHCb**
- $\mathrm{Im}(C_7)$ **measured with** A_{CP}
  - [2] ✦ $B \to K_S\pi^0\gamma$ at *B*-factories
  - [3] ✦ Tagged time-dep. analysis of $B_s \to \phi\gamma$ at LHCb

Right handed $C_7' = C_7'^{\mathrm{NP}}$

- [2] Mixing-induced CPV in $B \to K_S\pi^0\gamma$ at B-factories
- [3] $\Delta\Gamma_s$ induced rate asymmetry in $B_s \to \phi\gamma$ at LHCb
- [4] Angular analysis of $\Lambda_b \to \Lambda\gamma$ at LHCb
- [5] Transverse asymmetries in $B^0 \to K^* e^+ e^-$ at LHCb

Most sensitive

[1] M. Misiak et al JHEP 06(2020)175

[2] HFLAV average of BaBar and Belle

[3] LHCb PRL 123 (2019) 081802

[4] LHCb PRD 105 (2022) L051104

[5] LHCb JHEP 12 (2020) 081

$b \to s\gamma$ in $B^0 \to K^{*0}ee$

Right handed $C_7' = C_7'^{\mathrm{NP}}$

- **Transverse asymmetries in $B^0 \to K^{*}e^{+}e^{-}$ at LHCb**

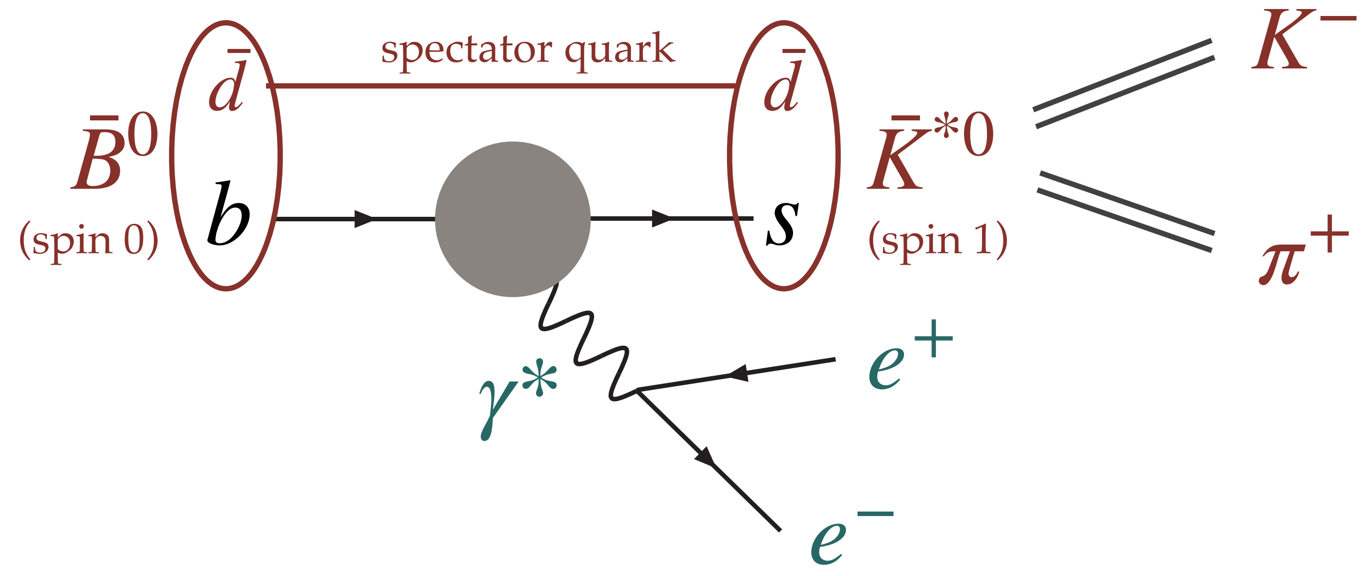

- **Use $\gamma^* \to ee$ to measure photon polarisation**

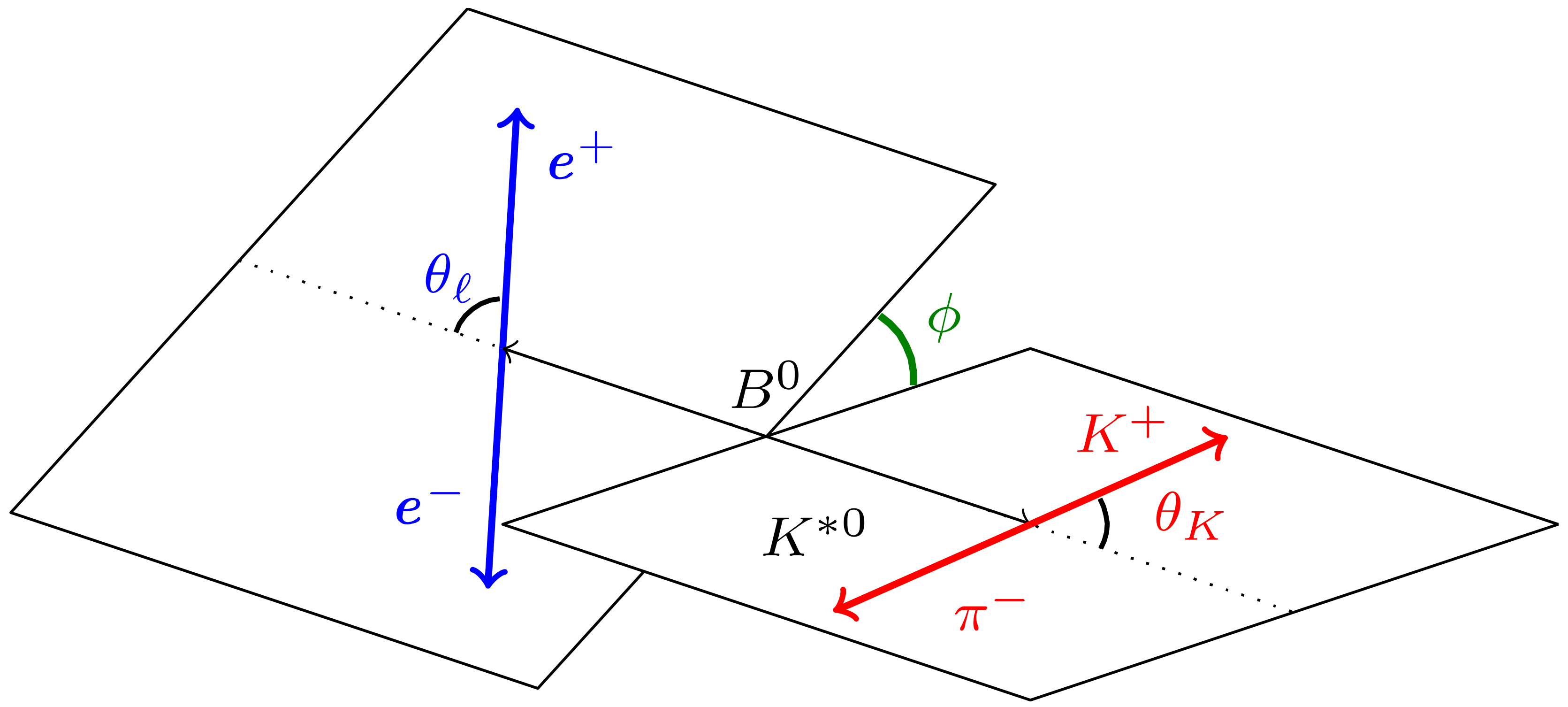

- **$\mathcal{O}(500)$ events despite $\mathscr{B} \sim 10^{-7}$**

[JHEP 12 (2020) 081]

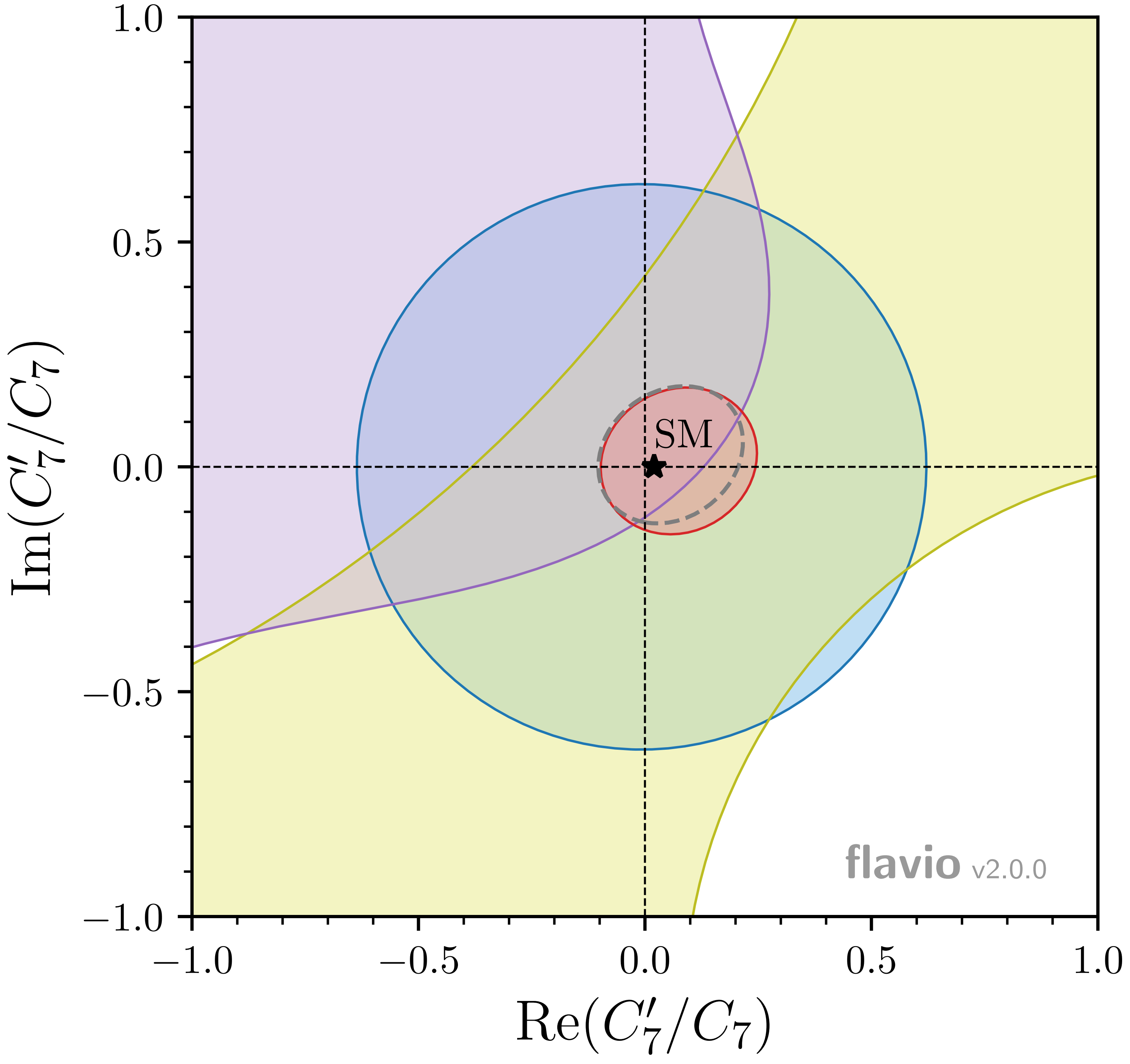

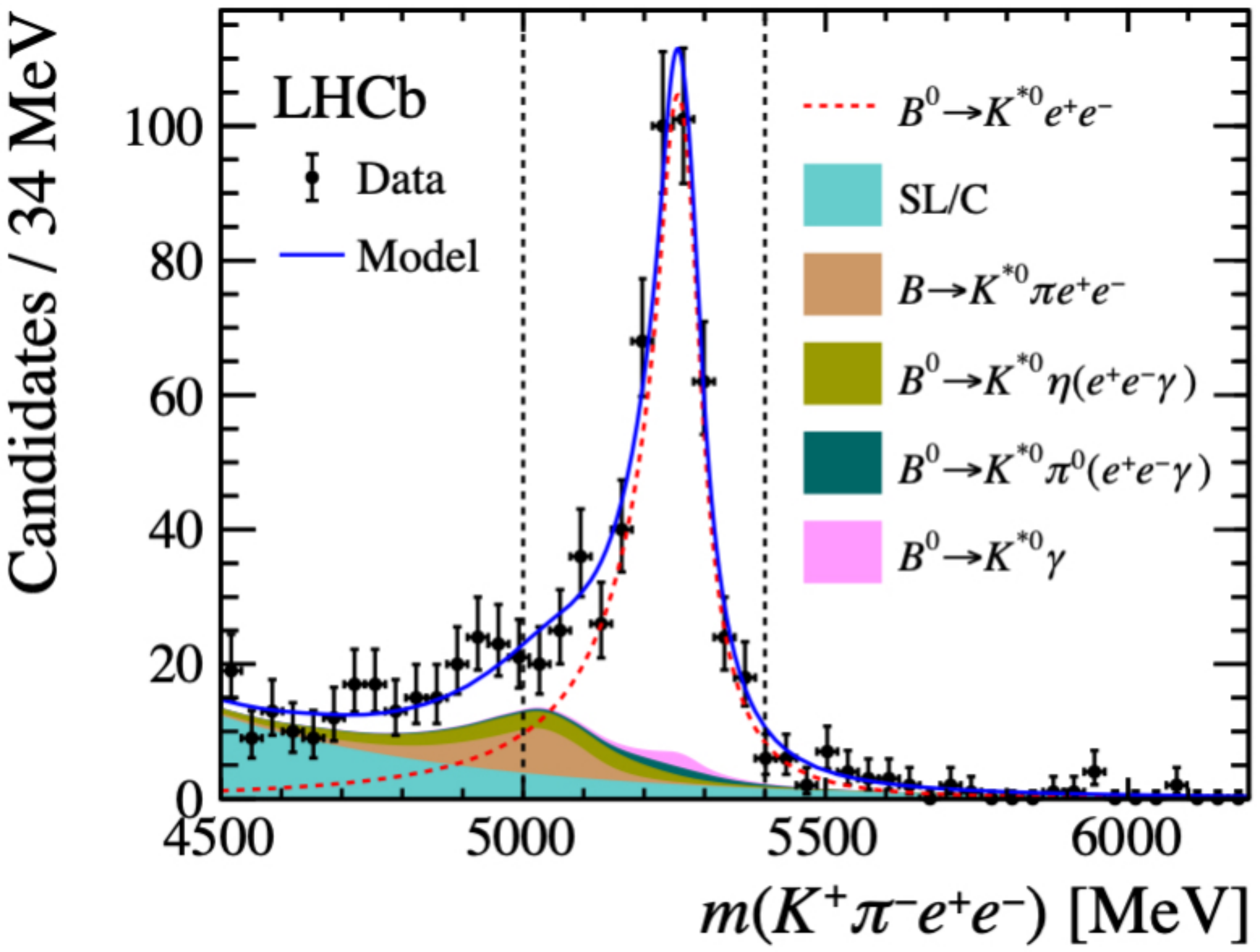

Place strong constraints on possible NP models

Theory of $B \to M\ell\ell$

$$\mathcal{M}(B \to M\ell\ell) = \langle M\ell\ell|\mathcal{H}_{\text{eff}}|B\rangle = \mathcal{N}\Big[\,(\mathcal{A}_V^\mu + \mathcal{H}^\mu)\;\bar{u}_\ell\gamma_\mu v_\ell$$

$$+\,\mathcal{A}_A^\mu\;\bar{u}_\ell\gamma_\mu\gamma_5 v_\ell$$

$$+\,\mathcal{A}_S\;\bar{u}_\ell v_\ell$$

$$+\,\mathcal{A}_P\;\bar{u}_\ell\gamma_5 v_\ell\Big]$$

Local:

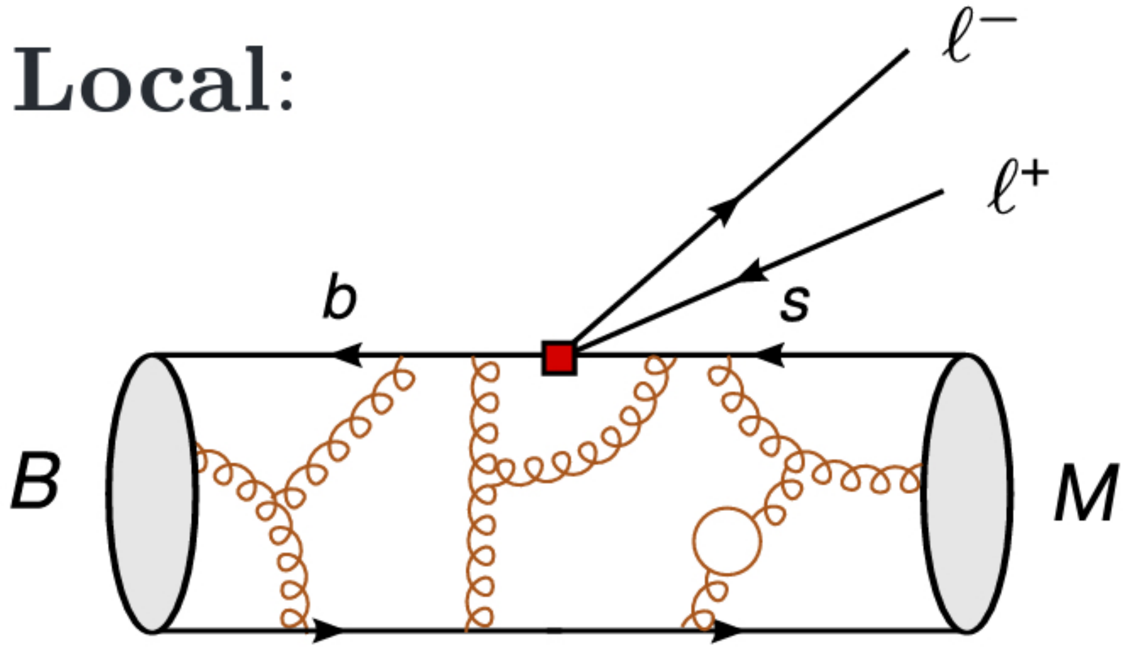

Non-Local:

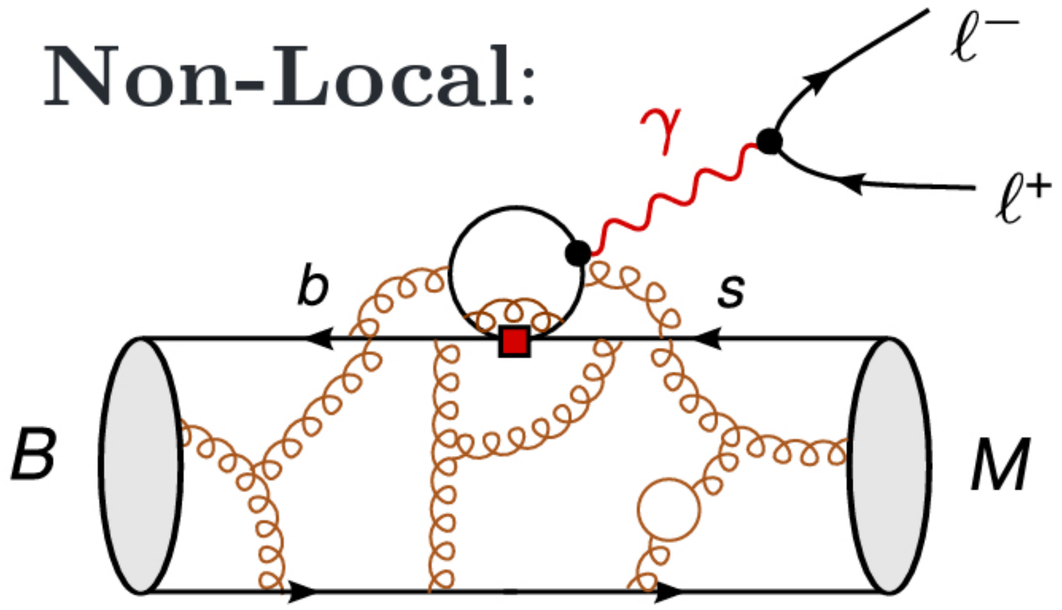

$$\mathcal{A}_V^\mu = -\frac{2im_b}{q^2}\,\mathcal{C}_7\langle M|\bar{s}\,\sigma^{\mu\nu}q_\nu\,P_R\,b|B\rangle$$

$$+\,\mathcal{C}_9\langle M|\bar{s}\,\gamma^\mu\,P_L\,b|B\rangle$$

$$+\,(P_L \leftrightarrow P_R, \mathcal{C}_i \to \mathcal{C}_i')$$

$$\mathcal{A}_A^\mu = \mathcal{C}_{10}\langle M|\bar{s}\,\gamma^\mu\,P_L\,b|B\rangle$$

$$+\,(P_L \leftrightarrow P_R, \mathcal{C}_i \to \mathcal{C}_i')$$

$$\mathcal{A}_{S,P} = \mathcal{C}_{S,P}\langle M|\bar{s}\,P_R\,b|B\rangle$$

$$+\,(P_L \leftrightarrow P_R, \mathcal{C}_i \to \mathcal{C}_i')$$

$$\mathcal{H}^\mu = \frac{-16i\pi^2}{q^2}\sum_{i=1,\ldots,6,8}\mathcal{C}_i\int dx^4 e^{iq\cdot x}\langle M|T\{j^\mu_{\text{em}}(x), O_i(0)\}|B\rangle$$

$$j^\mu_{\text{em}} = \sum_q Q_q\,\bar{q}\gamma^\mu q$$

Wilson coefficients $C_i = C_i^{SM} + C_i^{NP}$

Perturbative, short-distance physics (q^2 independent), well-known in SM, parameterise heavy NP

Local / Non-local hadronic matrix elements

Non-perturbative, long-distance physics (q^2 dependent), **main source of uncertainty**

Matrix elements - non perturbative/long-distance

Local

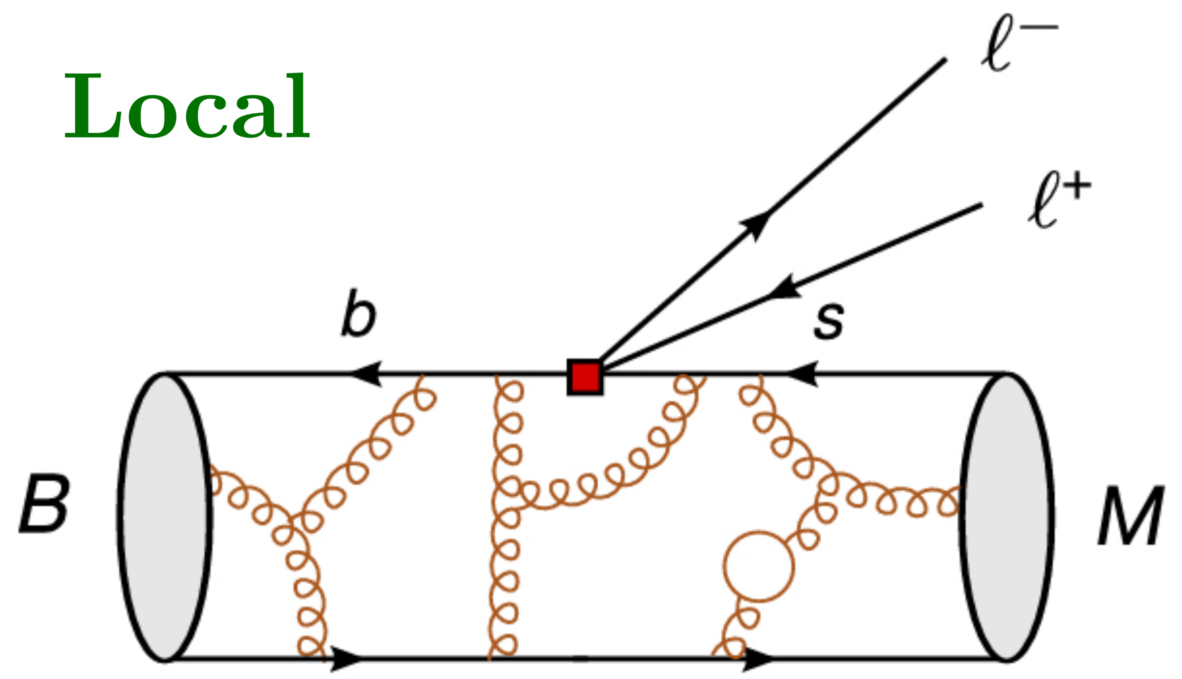

$$\mathcal{M}(B \to M\ell\ell) = \langle M\ell\ell|\mathcal{H}_{\text{eff}}|B\rangle = \mathcal{N}\Big[\left(\mathcal{A}_V^\mu + \mathcal{H}^\mu\right)\bar{u}_\ell\gamma_\mu v_\ell + \mathcal{A}_A^\mu\,\bar{u}_\ell\gamma_\mu\gamma_5 v_\ell + \mathcal{A}_S\,\bar{u}_\ell v_\ell + \mathcal{A}_P\,\bar{u}_\ell\gamma_5 v_\ell\Big]$$

$$\begin{aligned}\mathcal{A}_V^\mu &= -\frac{2im_b}{q^2}\,\mathcal{C}_7\langle M|\bar{s}\,\sigma^{\mu\nu}q_\nu\,P_R\,b|B\rangle + \mathcal{C}_9\langle M|\bar{s}\,\gamma^\mu\,P_L\,b|B\rangle \\ \mathcal{A}_A^\mu &= \mathcal{C}_{10}\langle M|\bar{s}\,\gamma^\mu\,P_L\,b|B\rangle \qquad + (P_L \leftrightarrow P_R, \mathcal{C}_i \to \mathcal{C}_i') \\ \mathcal{A}_{S,P} &= \mathcal{C}_{S,P}\langle M|\bar{s}\,P_R\,b|B\rangle\end{aligned}$$

$\langle M|(\ldots)|B\rangle$ parameterised by 3(7) form factors for spin 0(1) final state

@high q^2 LQCD

[0] HPQCD,arXiv:1306.2384,2207.12468
[1] Fermilab,MILC,arXiv:1509.06235
[2] Horgan,Liu,Meinel,Wingate,arXiv:1310.3722,arXiv:1501.00367

@low q^2 Continuum methods (LCSR)

[0] Ball,Zwicky,arXiv:hep-ph/0406232
[1] Khodjamirian,Mannel,Pivovarov,Wang,arXiv:1006.4945
[2] Bharucha,Straub,Zwicky,arXiv:1503.05534
[3] Gubernari,Kokulu,vanDyk,arXiv:1811.00983

@low+high q^2 Combined fit continuum + LQCD/LQCD

[0] Altmannshofer,Straub,arXiv:1411.3161
[1] Bharucha,Straub,Zwicky,arXiv:1503.05534
[2] Gubernari,Kokulu,vanDyk,arXiv:1811.

Non-local

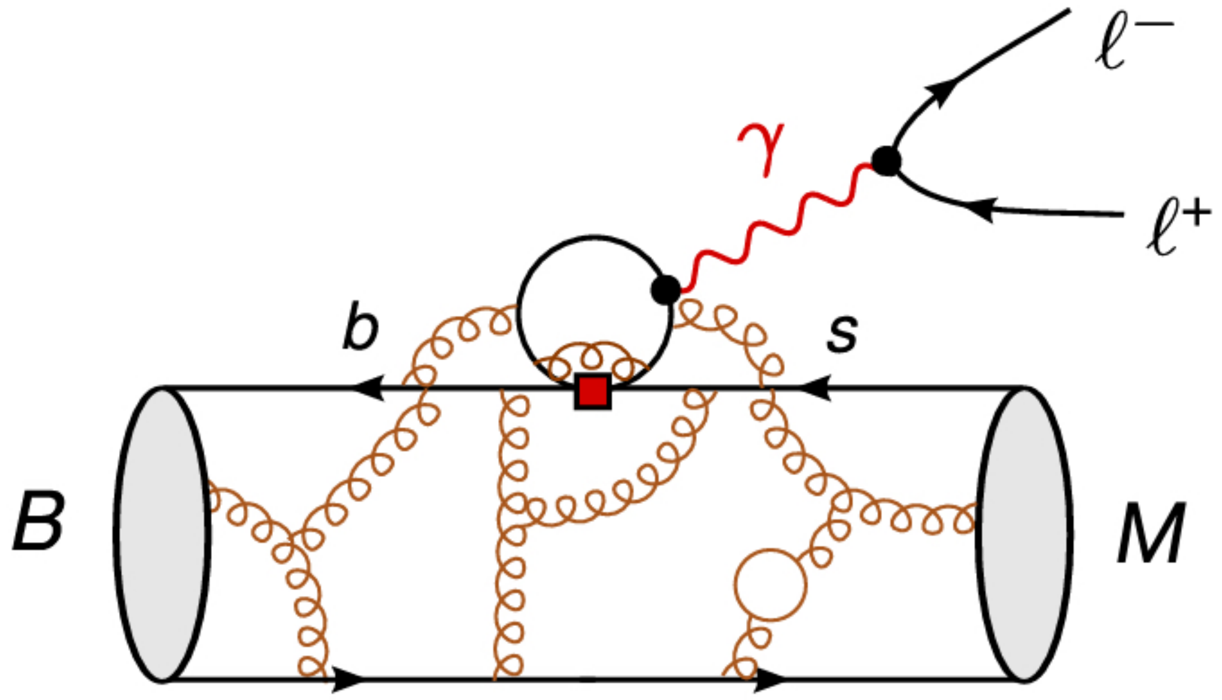

Form factors determined with Continuum methods (low q^2, Light-cone sum rules)

$$\mathcal{H}^\mu = \frac{-16i\pi^2}{q^2}\sum_{i=1,\ldots,6,8}\mathcal{C}_i\int dx^4 e^{iq\cdot x}\langle M|T\{j^\mu_{\text{em}}(x), O_i(0)\}|B\rangle\,, \qquad j^\mu_{\text{em}} = \sum_q Q_q\,\bar{q}\gamma^\mu q$$

Theoreticians wish-list

- Explicit numerical experimental likelihoods, e.g. to avoid digitisation of $B_{s,d} \to \mu\mu$ contour plots
- Measurements of other LFU observables, like e.g. R_ϕ or $Q_{4,5}/D_{P'_{4,5}}$
- $B \to K^* e^+ e^-$ angular analysis
- CP asymmetries to constrain imaginary parts of Wilson coefficients
- **Experimental updates** and **new measurements**, not only from **LHCb** but also from **ATLAS** and **CMS**, and eventually from **Belle II**

Purely leptonic channels ($B^0_{(s)} \to \mu\mu$) at LHCb

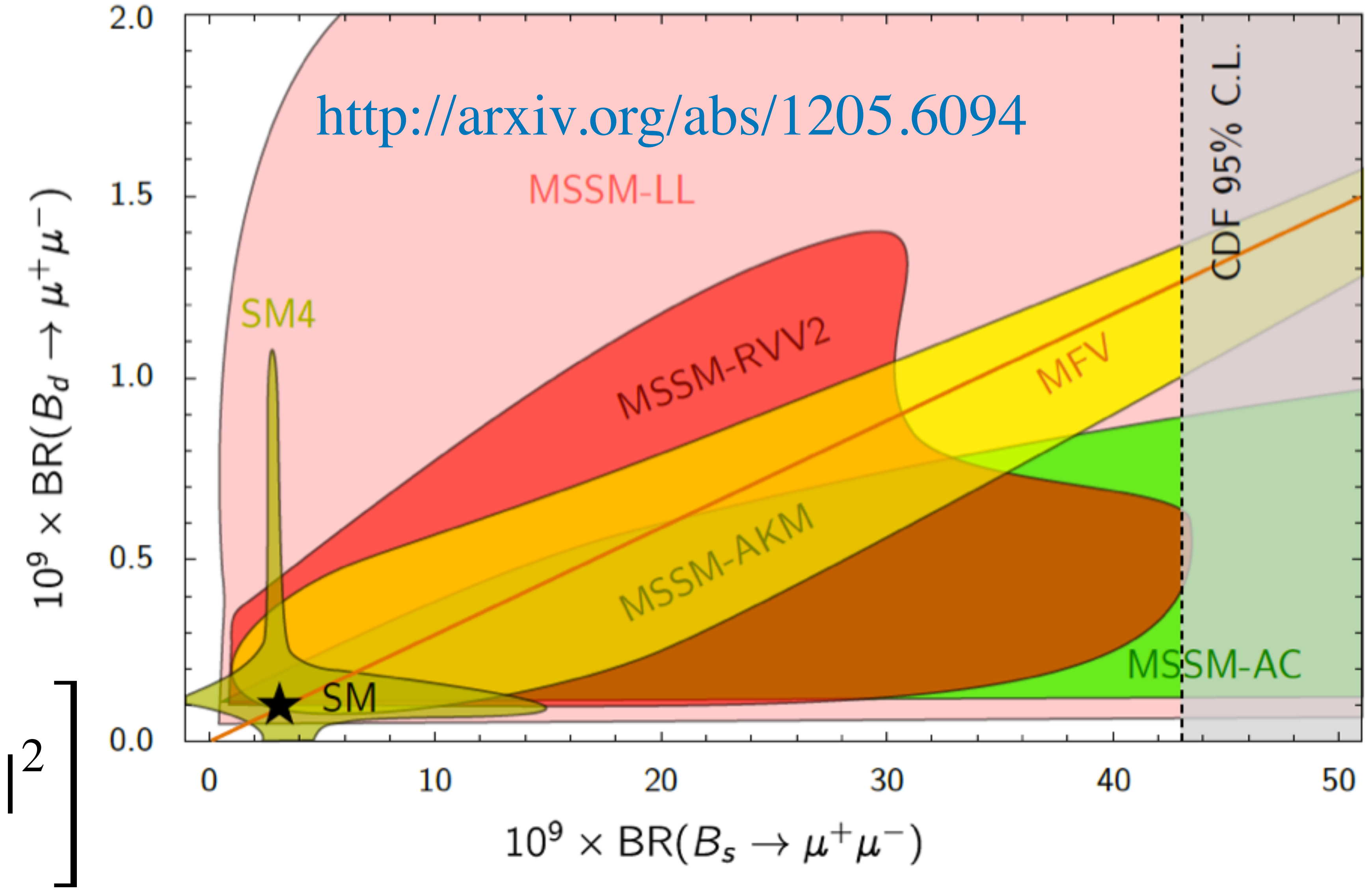

- $B^0_{(s)} \to \mu^+\mu^-$ **is a golden channel for LHCb**:
  - CKM suppressed, loop suppressed and helicity suppressed
  - Powerful probe of models with new enhanced (pseudo) scalar interaction, e.g SUSY at high $\tan(\beta)$ ($\mathcal{B} \propto \tan(\beta)^6/m_A^4$)

$$\mathcal{B} = \frac{G_F^2\alpha^2}{64\pi^3} f_{B_s}^2 m_{B_s}^3 |V_{tb}V_{tq}|^2 \tau_{B_s}\sqrt{1-\frac{4m_\mu^2}{m_{B_s}^2}}\left[(1-\frac{4m_\mu^2}{M_B^2})|C_S - C_S^{'}|^2 + |(C_P - C_P^{'}) + \frac{2m_\mu}{M_B}(C_{10} - C_{10}^{'})|^2\right]$$

$\mathcal{B} \propto \text{const} \times$

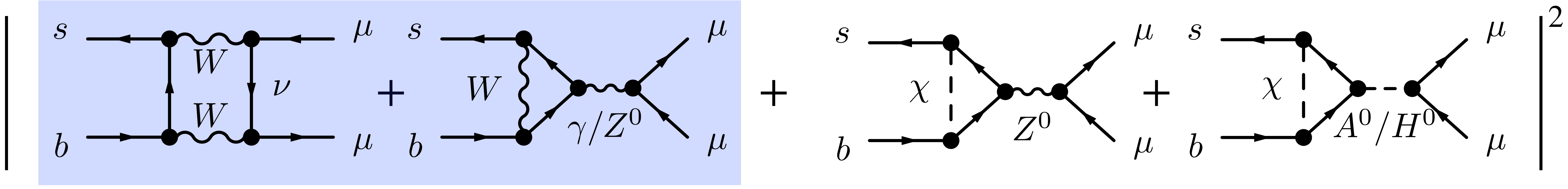

SM **NP**

- Branching fraction predicted precisely in the SM:
- $\mathcal{B}(B^0_s \to \mu^+\mu^-)_{SM} = (3.66 \pm 0.14) \times 10^{-9}$
- $\mathcal{B}(B^0 \to \mu^+\mu^-)_{SM} = (1.03 \pm 0.05) \times 10^{-10}$

Main uncertainties from CKM element

Decay constant f_{B_s} from Lattice QCD

Purely leptonic channels ($B^0_{(s)} \to \mu\mu$) at LHCb

- Main background due to combinatorics of two μ's.

- Signal/Background separation obtained through $m_{\mu\mu}$ and BDT trained on two body kinematics and topology

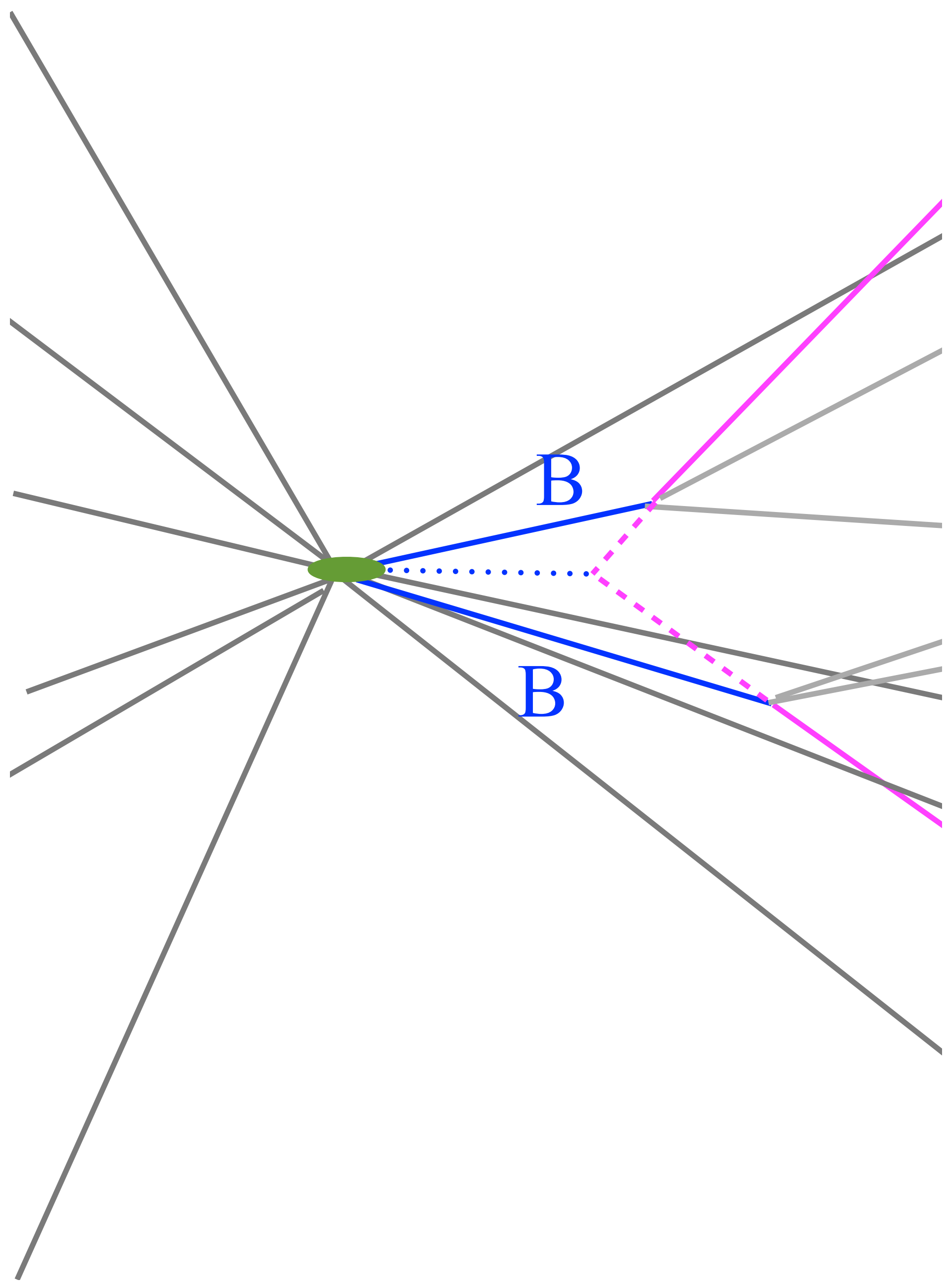

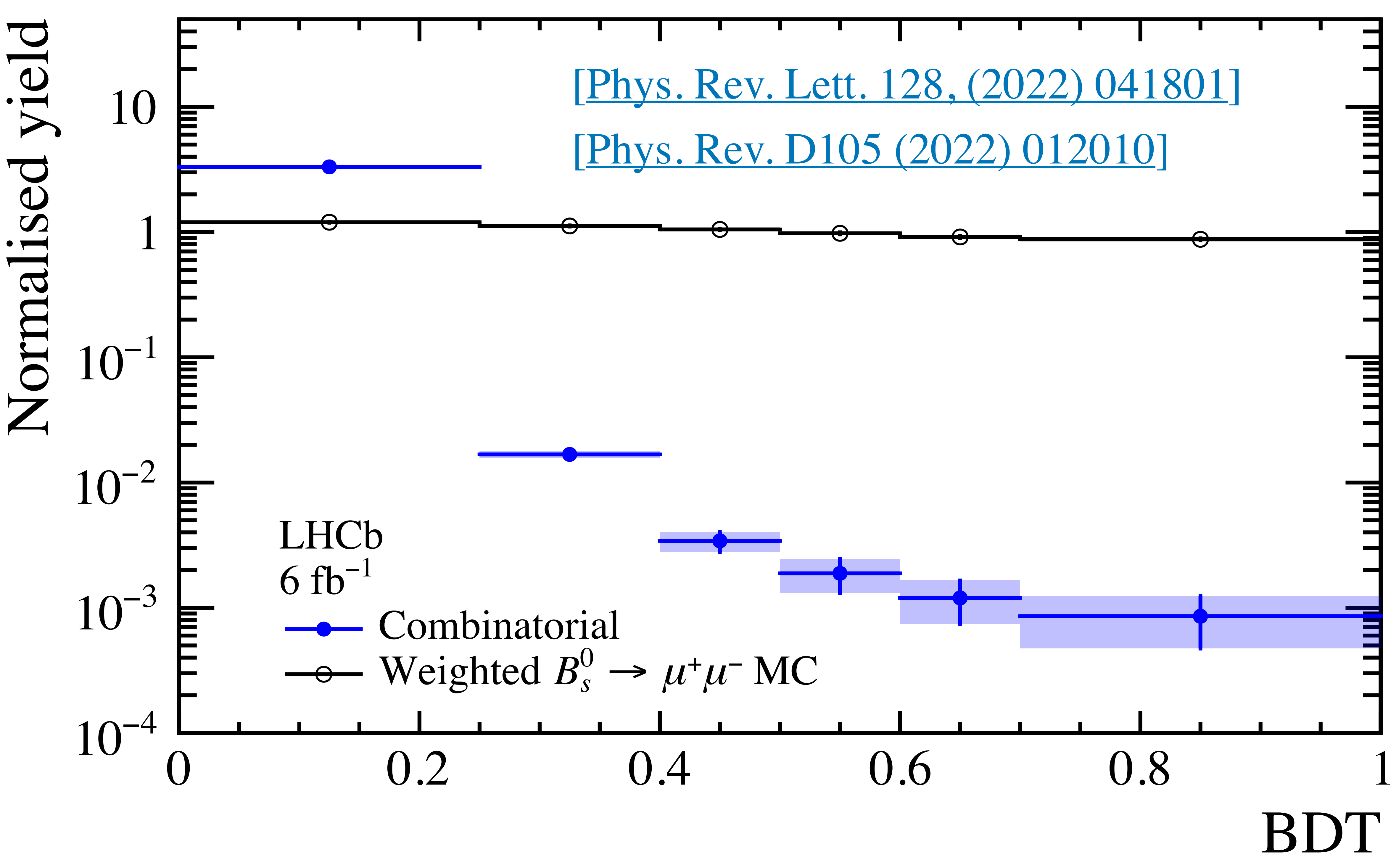

[Phys. Rev. Lett. 128, (2022) 041801]

[Phys. Rev. D105 (2022) 012010]

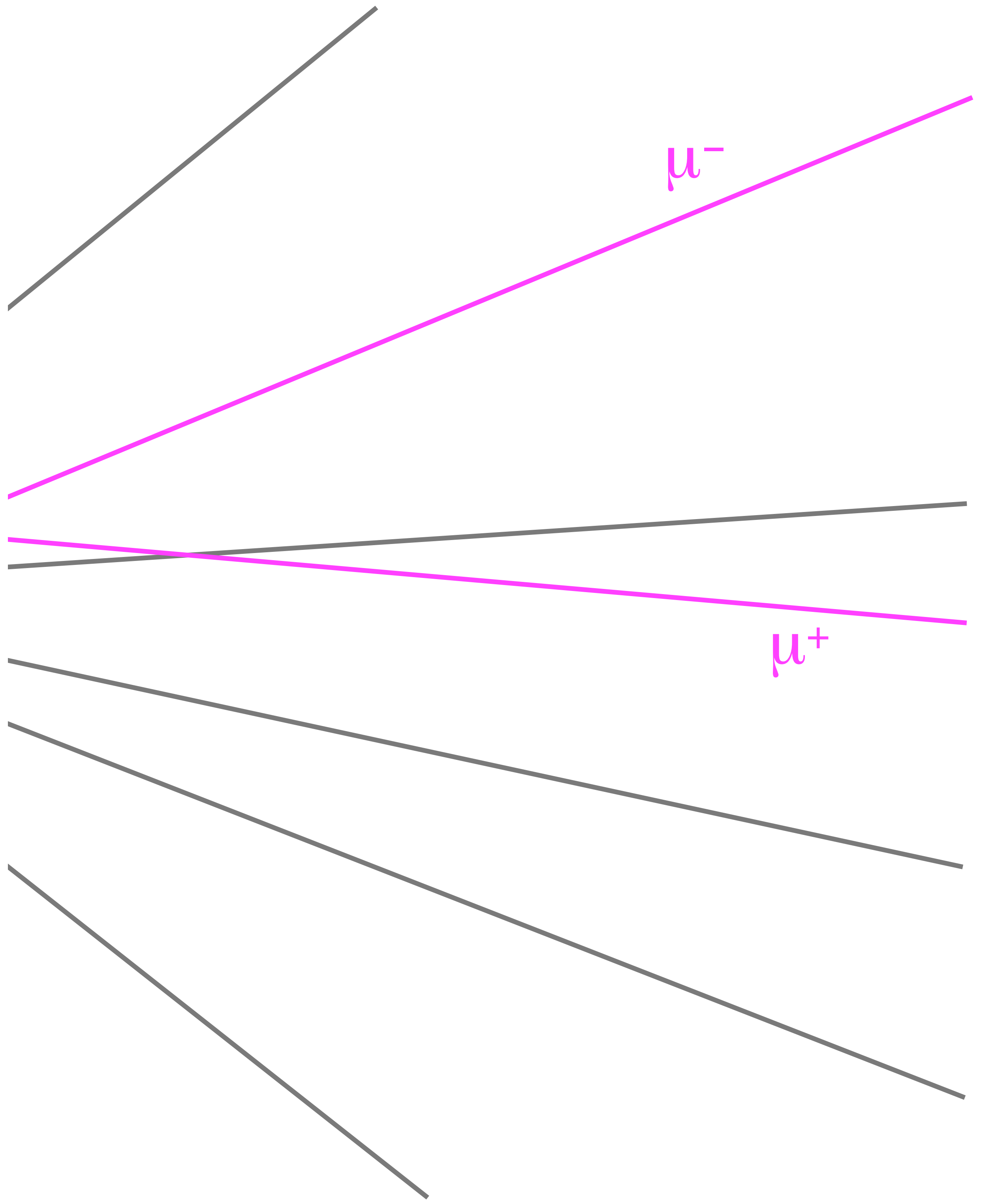

Purely leptonic channels ($B^0_{(s)} \to \mu\mu$) at LHCb peaking bkgs

- The most sensitive region is polluted by both combinatorial background and exclusive channels $B^0_{(s)} \to h^+h^{'-}$

Semileptonic decays

eventually with one hadron misidentified as muon:estimated with large samples of MC, and normalising to $B^\pm \to J/\psi K^\pm$

Combinatorial backgroun

from $b\bar{b} \to \mu^+\mu^- X$:
an exponential shape is used, the normalisation is a free parameter of the invariant mass fit

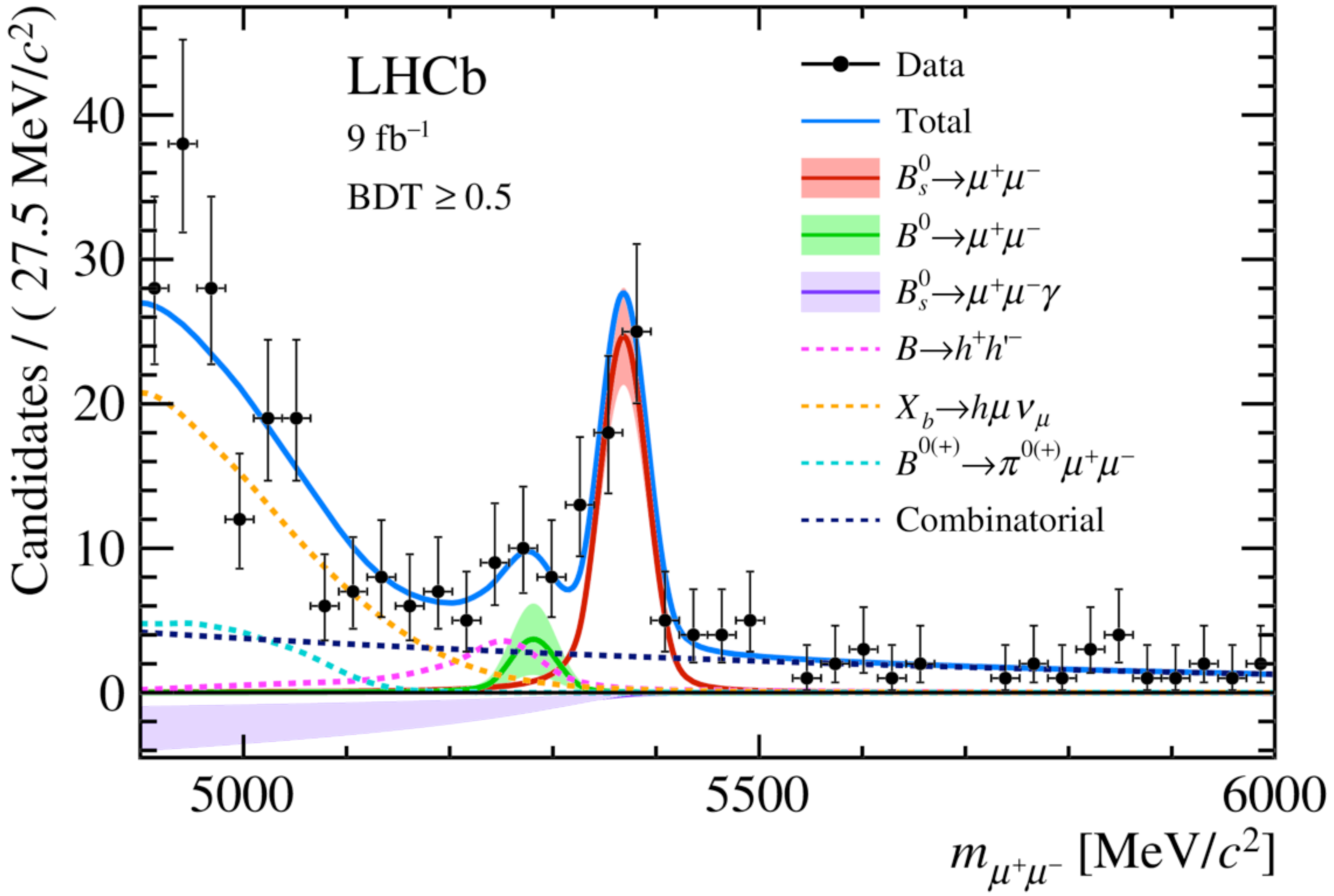

$B^0_{(s)} \to h^+h^{'-}$ decays (h=K,π)

both hadrons misidentified as muons (prob~2x10^{-5}): this background peaks in the B^0 signal region; it is estimated from not misidentified events, and using PID efficiencies from data

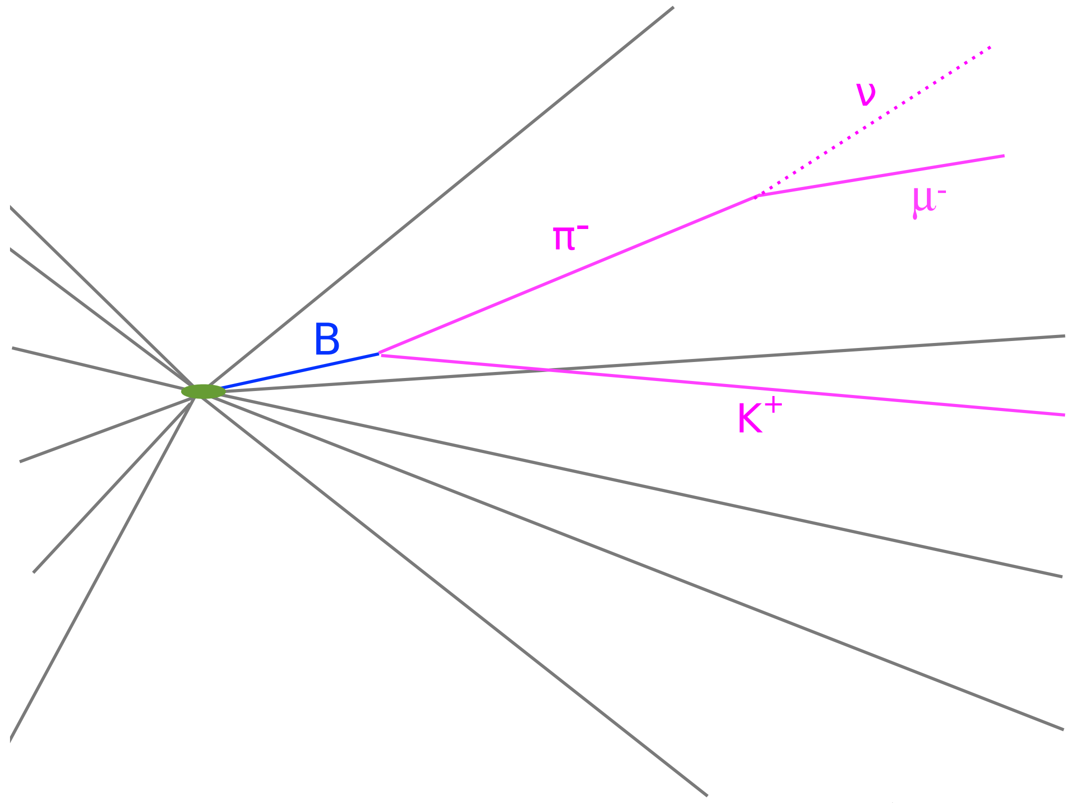

$\mathscr{B}(B \to hh') \sim 10^{-5}$

"LHCb is not a continuous tracker" ,

kink of track Identification not trivial

Status LHCb on angular analyses

Decay Mode	Status & Approach
$B^0 \rightarrow K^{*0}\mu^+\mu^-$	2011-2016, 8 (+2 wide) q^2 bins. CP-averaged observable only. CP-asymmetry only 2011-2012. **Tension with SM**
$B^+ \rightarrow K^{*+}\mu^+\mu^-$	2011-2018 CP-averaged observable only. **Local tension with SM as in K^{*0} mode**
$B^{0(+)} \rightarrow K^{0(+)}\mu^+\mu^-$	2011-2012, 17 bins in B+, 5 bins in B0 , Afb and Fh SM-like
$\Lambda_b \rightarrow \Lambda\mu\mu$	2011-2016: Moments analysis for 34 observables No CPV observed. Only high q^2. Consistent with SM.
$B_s^0 \rightarrow \phi\mu\mu$	2011-2018, 6 q^2 bins. Untagged B_s, SM-like

Cross-check resonant modes: mass fits

Partially reconstructed

$B_s \to J/\psi K^+ \cancel{pi}$

Mis-ID $B^+ \to J/\psi \pi^+_{\to K^+}$

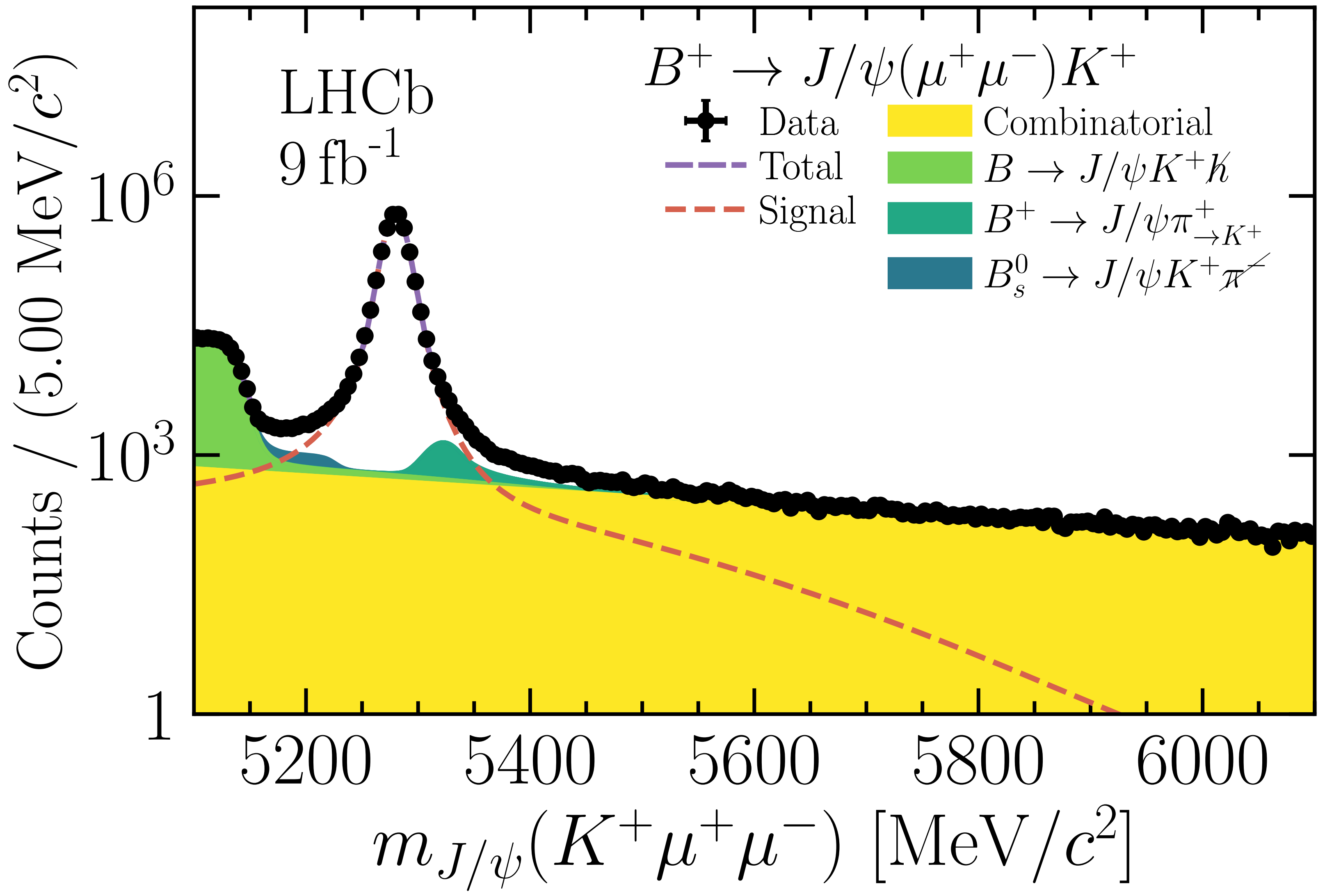

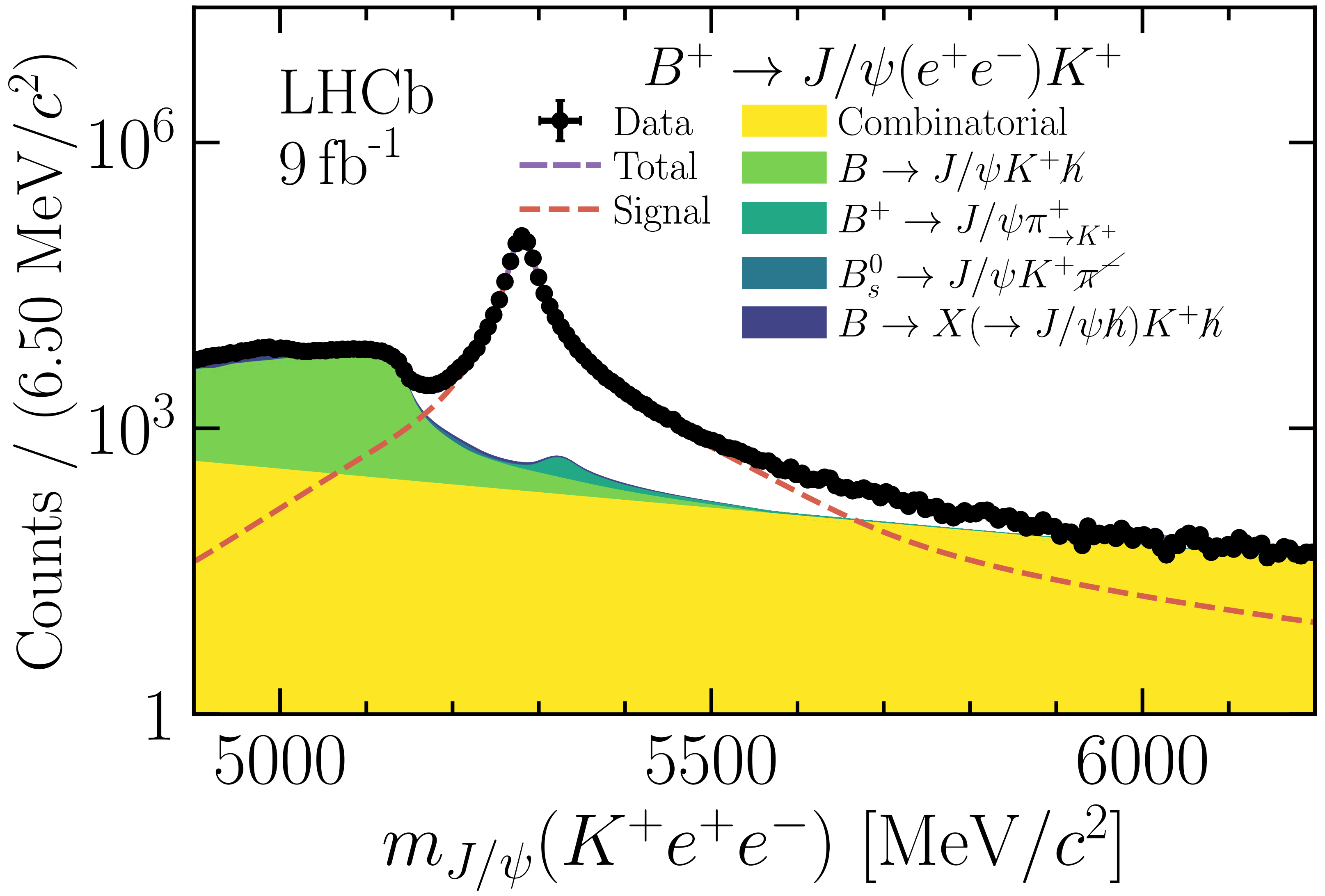

Partially reconstructed

$B_s \to J/\psi K^+ \cancel{pi}$

Mis-ID $B^+ \to J/\psi \pi^+_{\to K^+}$

Partially reconstructed (charmonia cascade)

Partially reconstructed

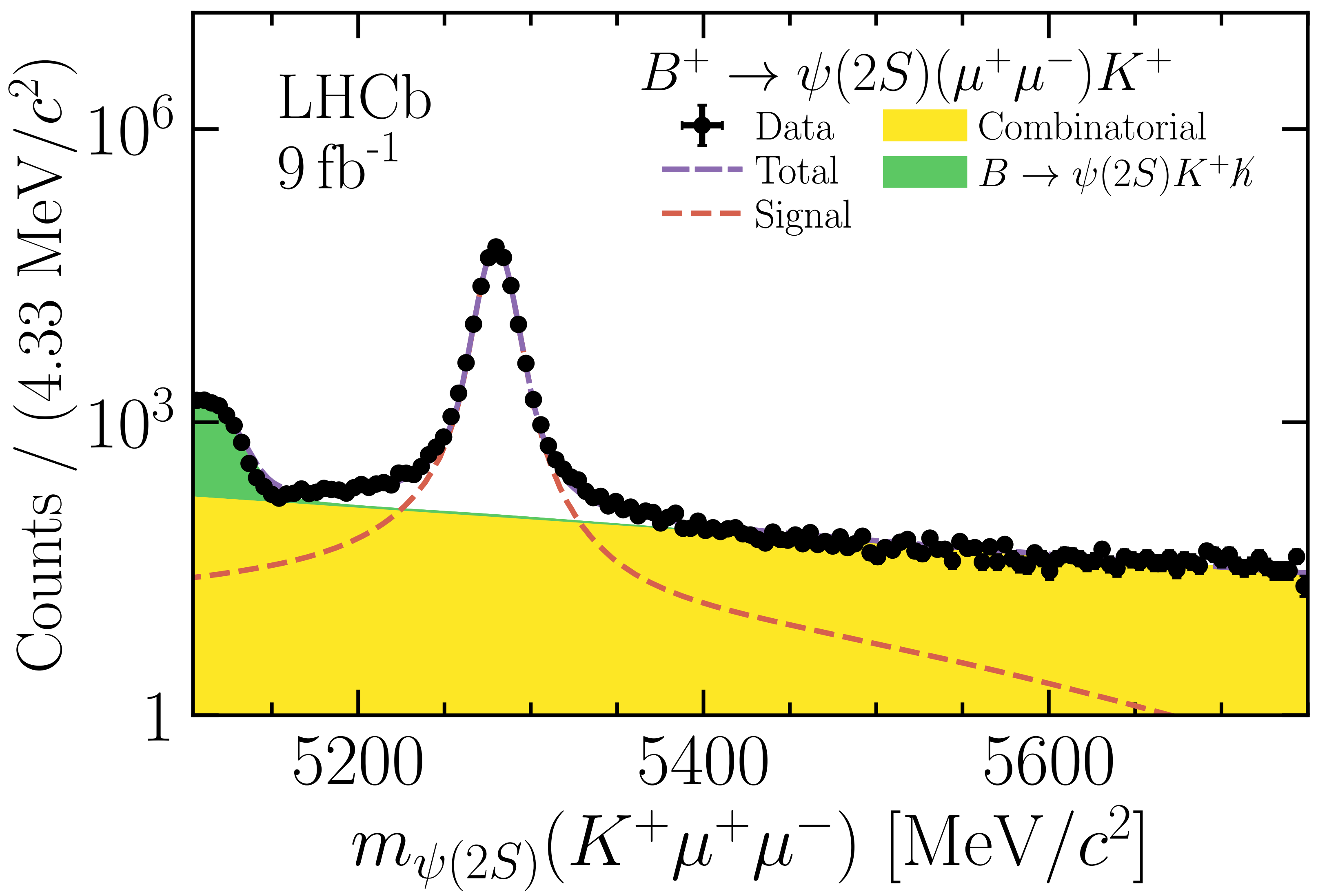

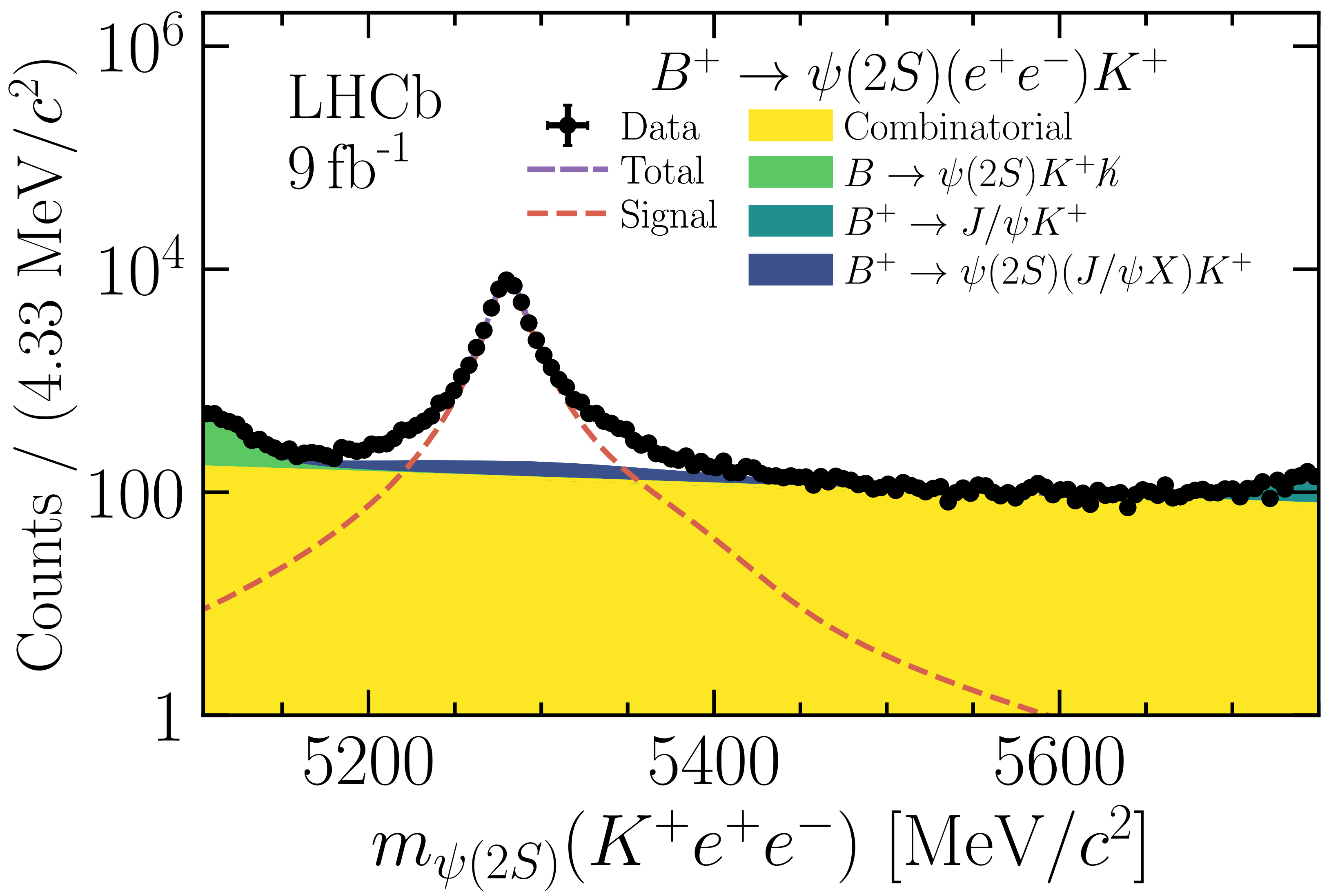

Partially reconstructed

Leaking $B^+ \to J/\psi K^+$

$B^+ \to (\psi(2S) \to J/\psi X)K^+$

Cross-check resonant modes: mass fits

Partially reconstructed

$B_s \to J/\psi K^{*0}$

Hadronic misID (Λ_b^0)

Hadronic misID (B_s^0)

Double misID $K \leftrightarrow \pi$

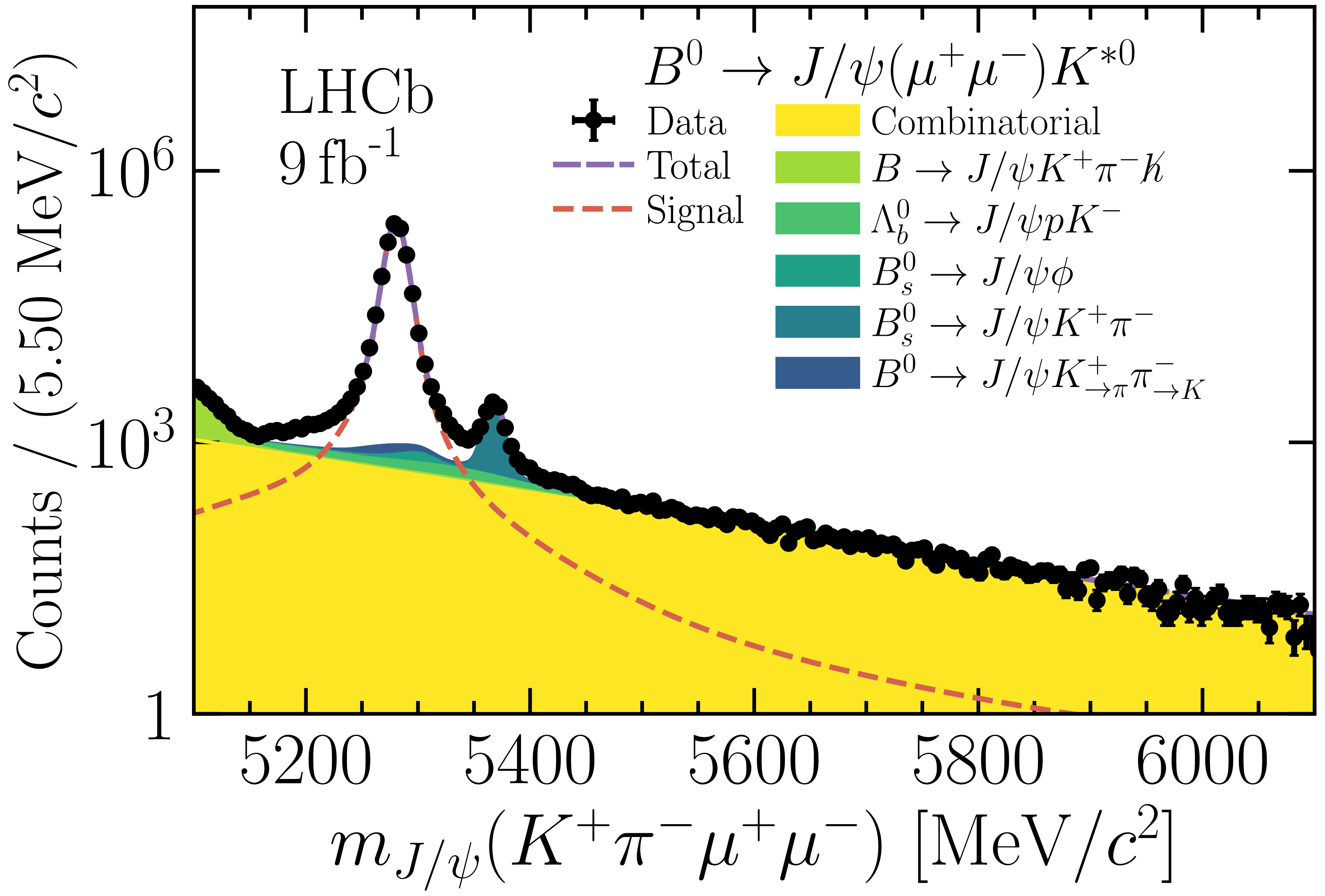

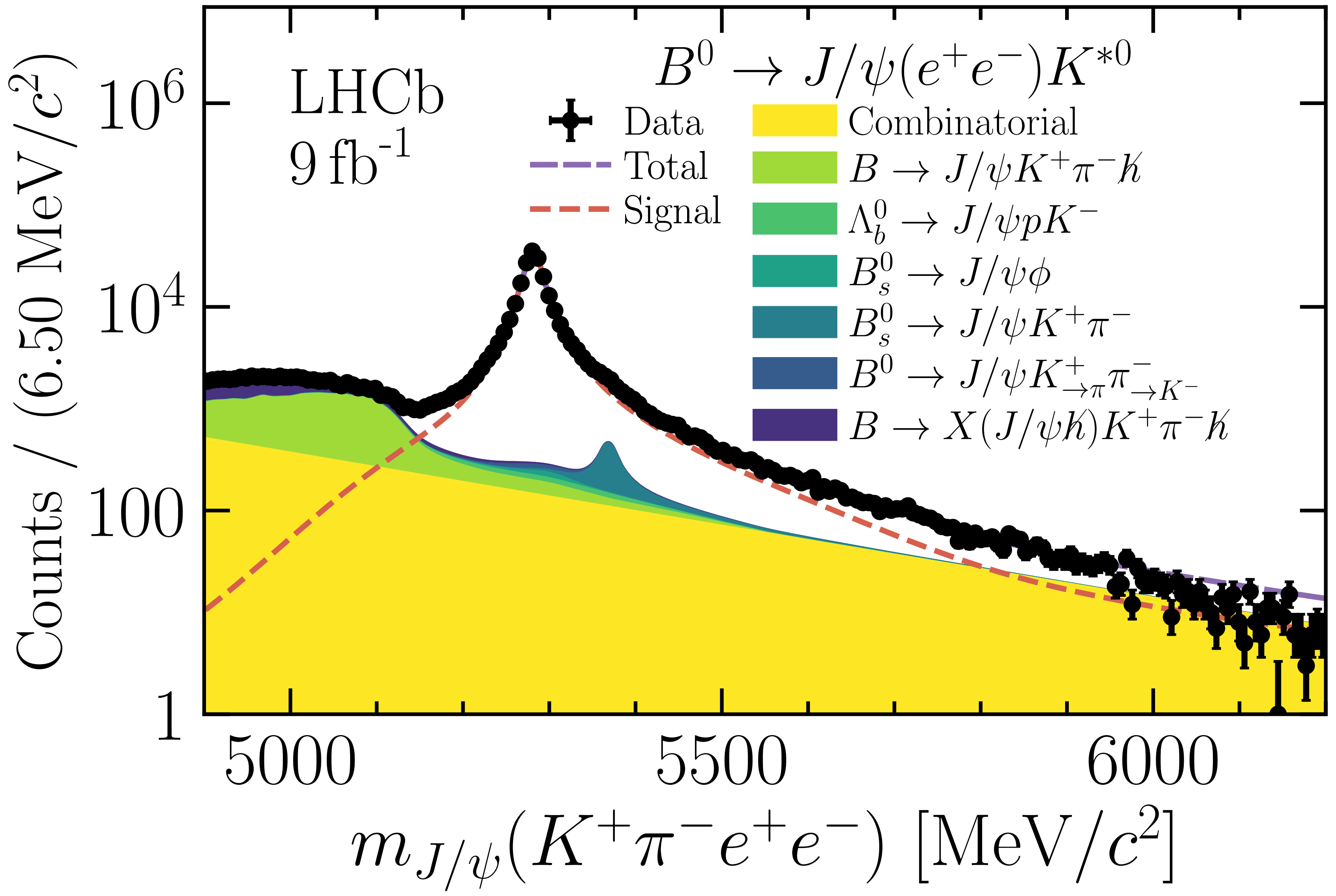

Partially reconstructed

$B_s \to J/\psi K^{*0}$

Hadronic misID (Λ_b^0)

Hadronic misID (B_s^0)

Double misID $K \leftrightarrow \pi$

Partially reconstructed (charmonia cascade)

Partially reconstructed

Hadronic misID (Λ_b^0)

$B_s \to \psi(2S)K^{*0}$

Double misID $K \leftrightarrow \pi$

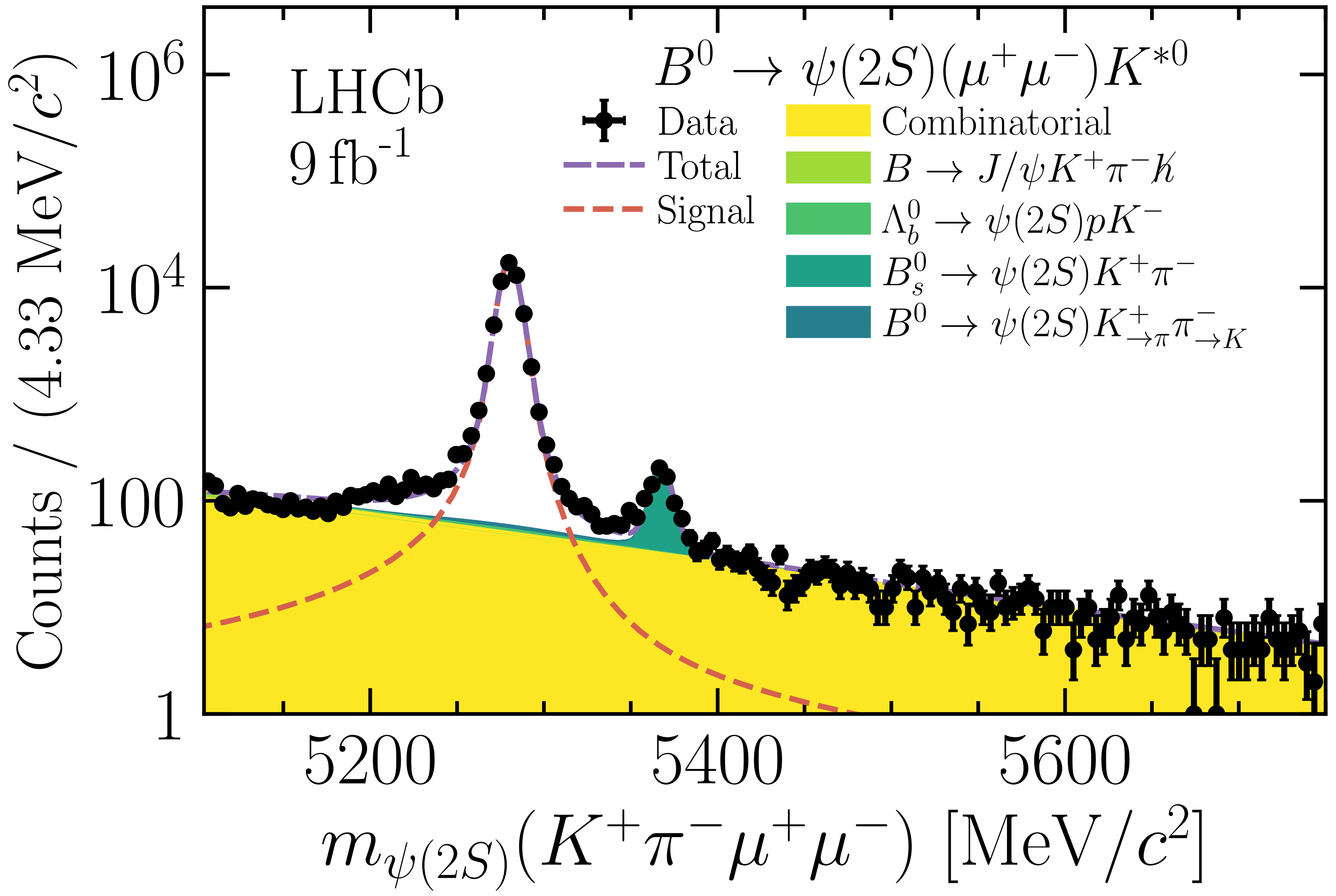

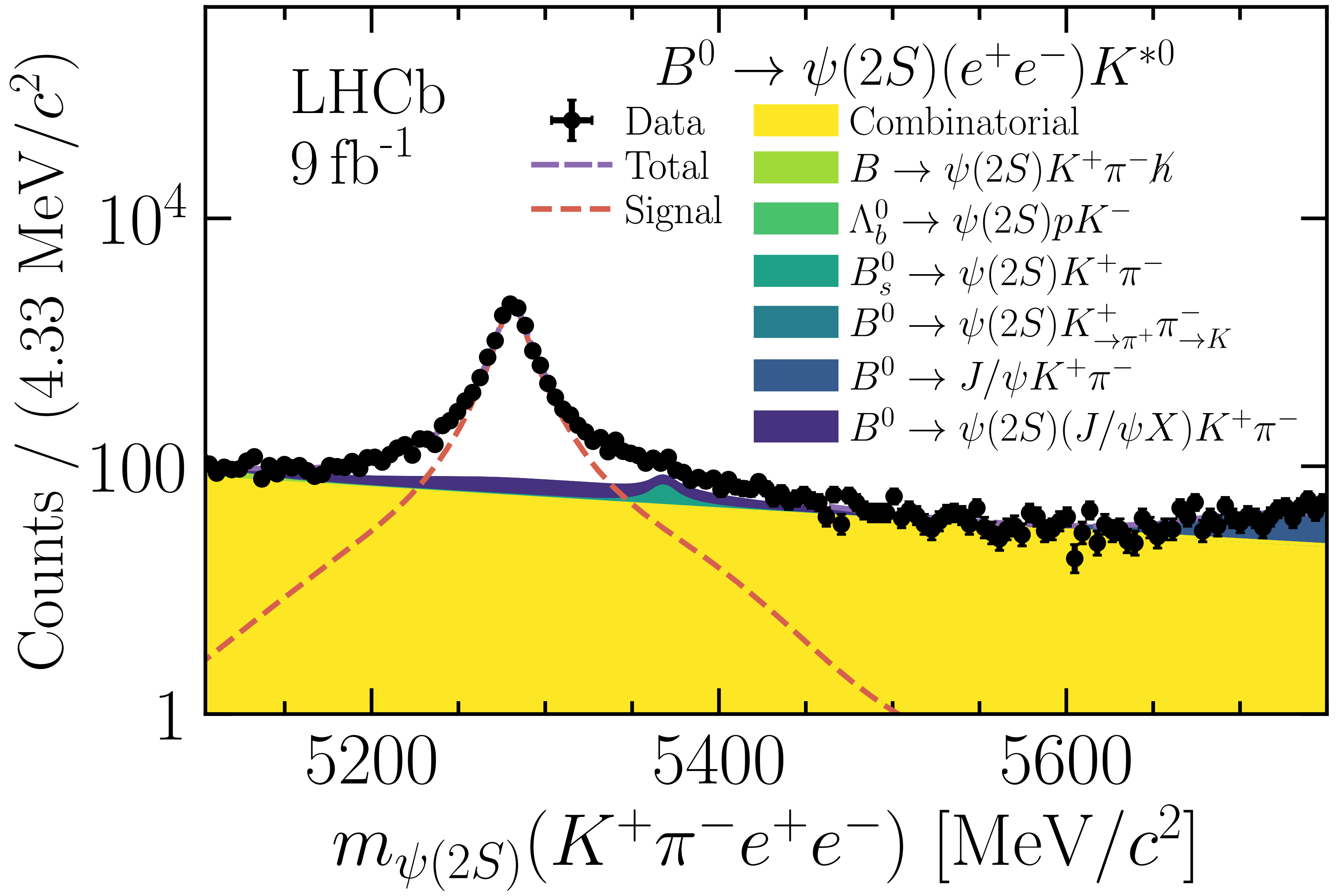

Partially reconstructed

$B_s \to \psi(2S)K^{*0}$

Hadronic misID (Λ_b^0)

Double misID $K \leftrightarrow \pi$

Leaking $B^+ \to J/\psi K^+$

$B^+ \to (\psi(2S) \to J/\psi X)K^+$

Mass fit to rare mode muons: simultaneous fit $R_{K,K^{*0}}$

low-q^2 | central-q^2 | resonant-J/ψ

Impact of hardware trigger in Run1/2

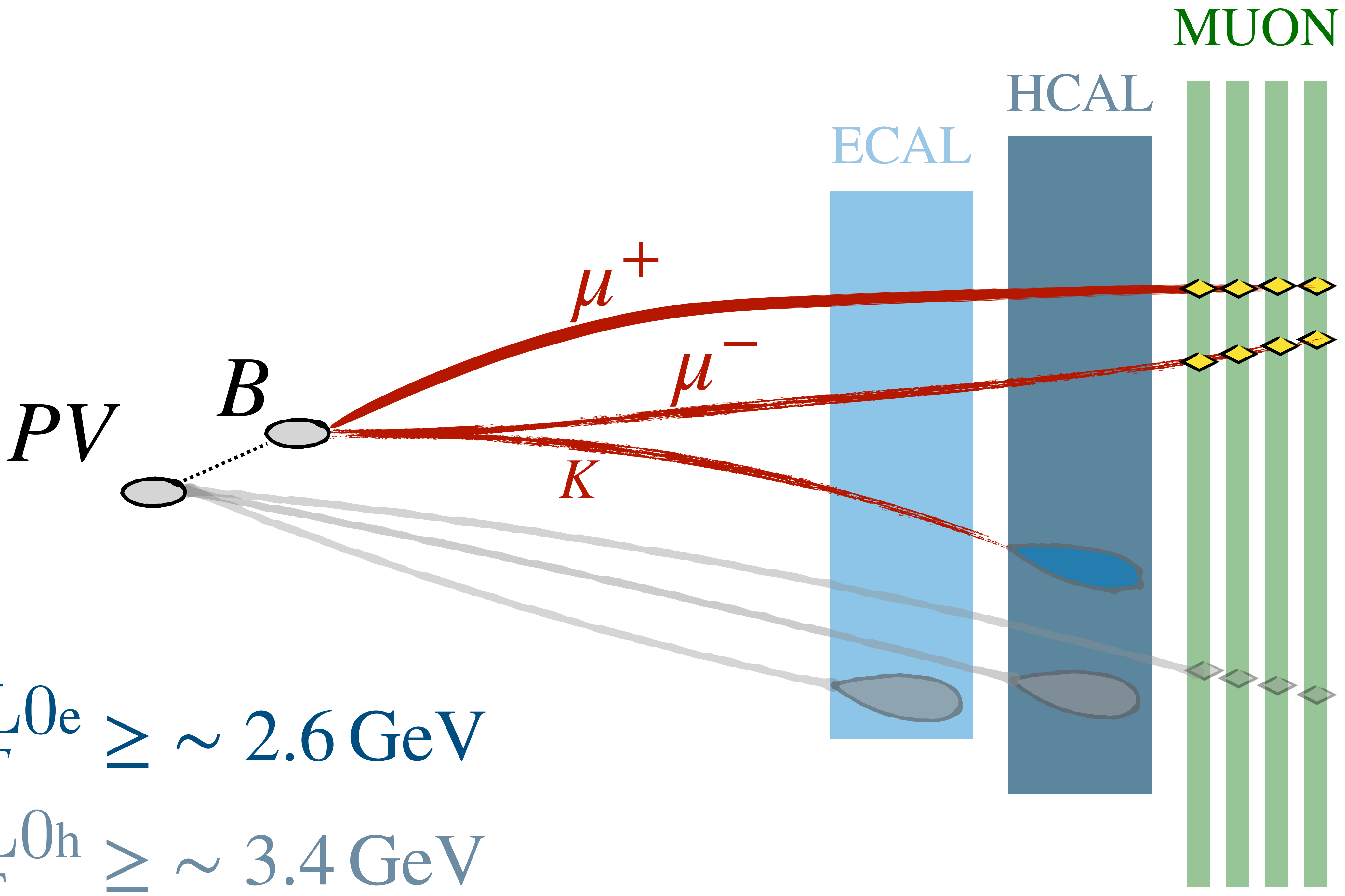

$E_T^{\mathrm{L0e}} \geq \sim 2.6\,\mathrm{GeV}$

$E_\mathrm{T}^{\mathrm{L0h}} \geq \sim 3.4\,\mathrm{GeV}$

$p_\mathrm{T}^{\mathrm{L0}\mu} \geq \sim 1.4\,\mathrm{GeV}$

Selection effect from L0e vs L0μ

$$\sim \frac{1}{3}$$

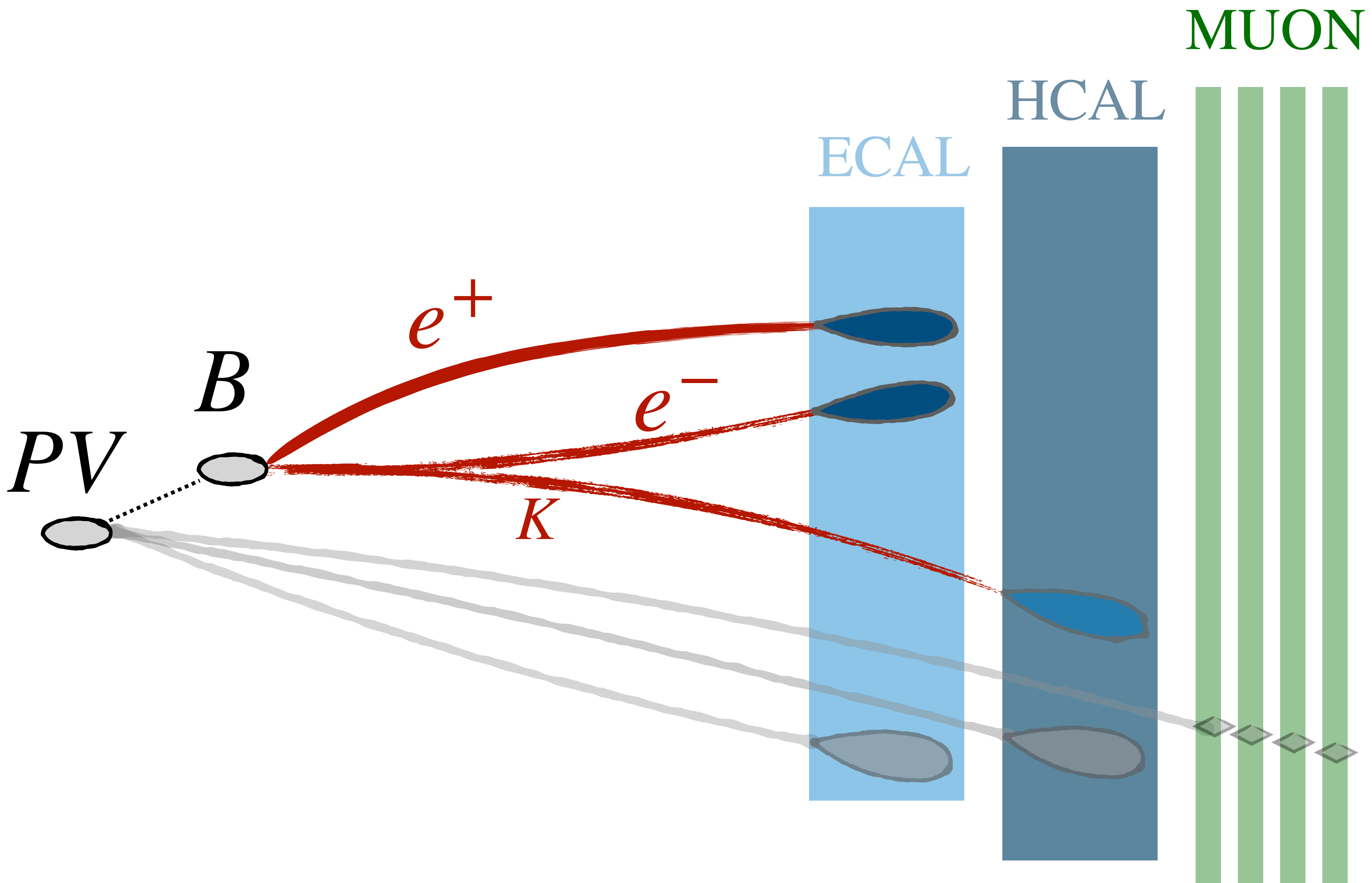

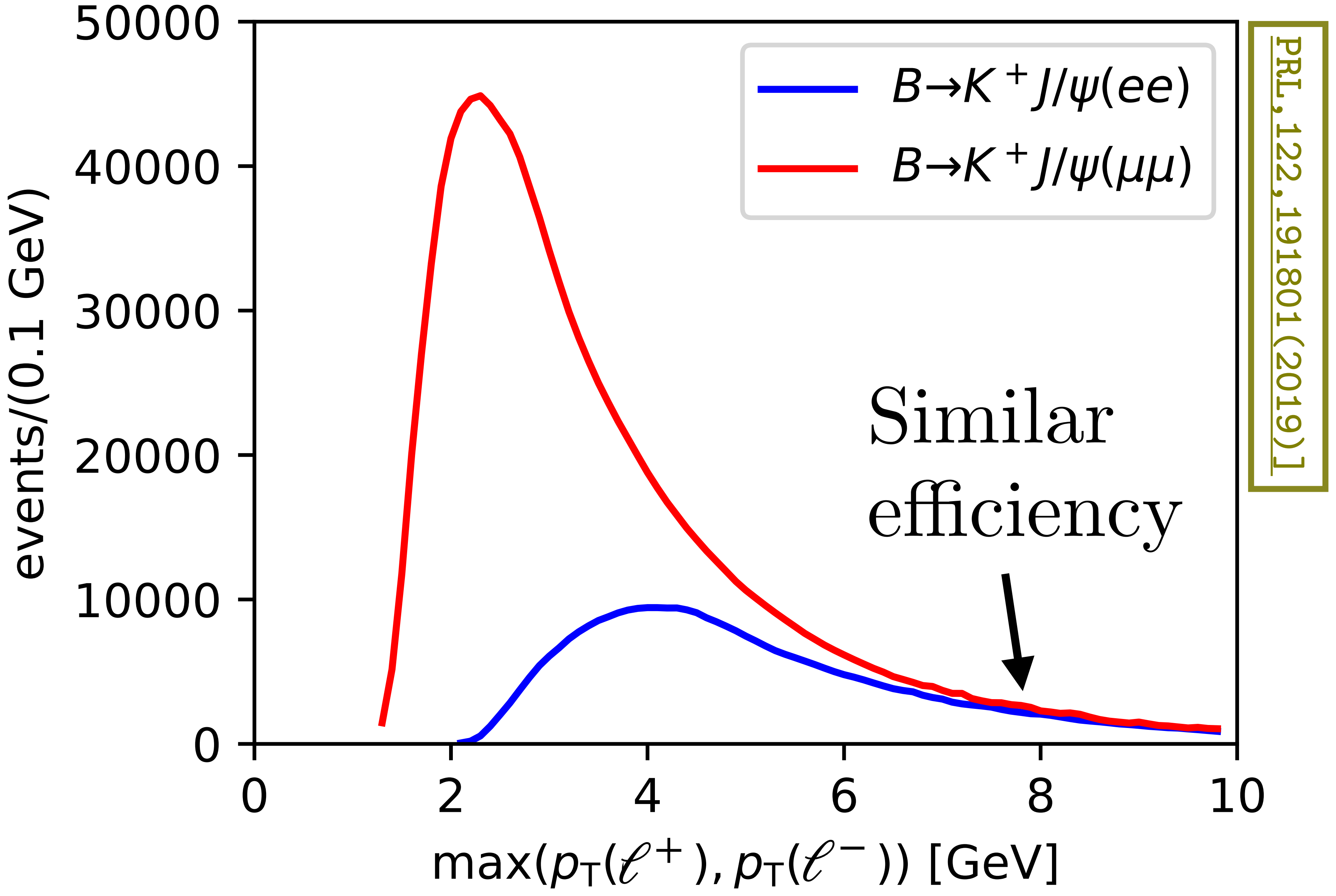

Similar efficiency

PRL, 122, 191801 (2019)]

Selection: hardware trigger choice in R_{K,K^*}

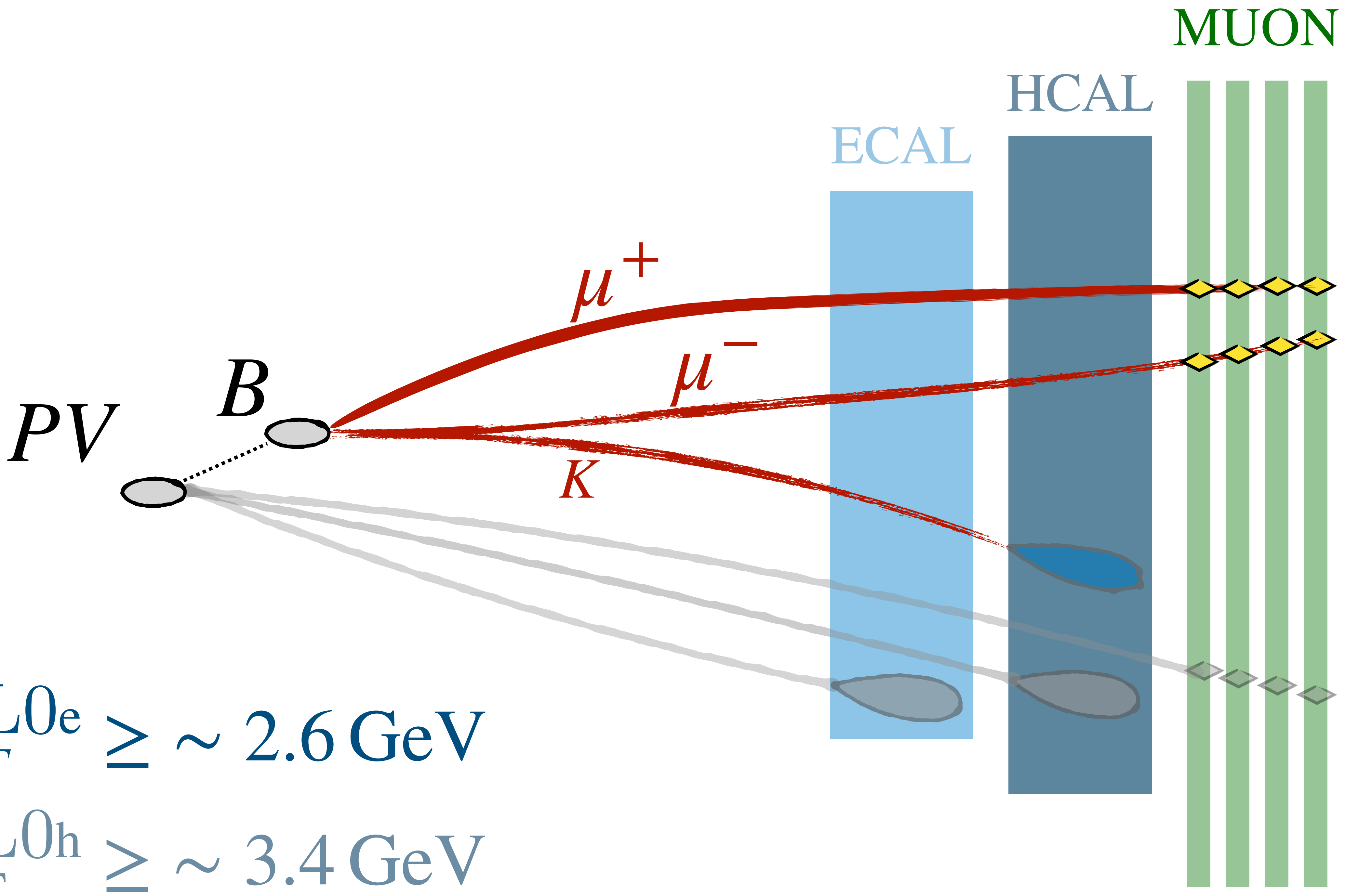

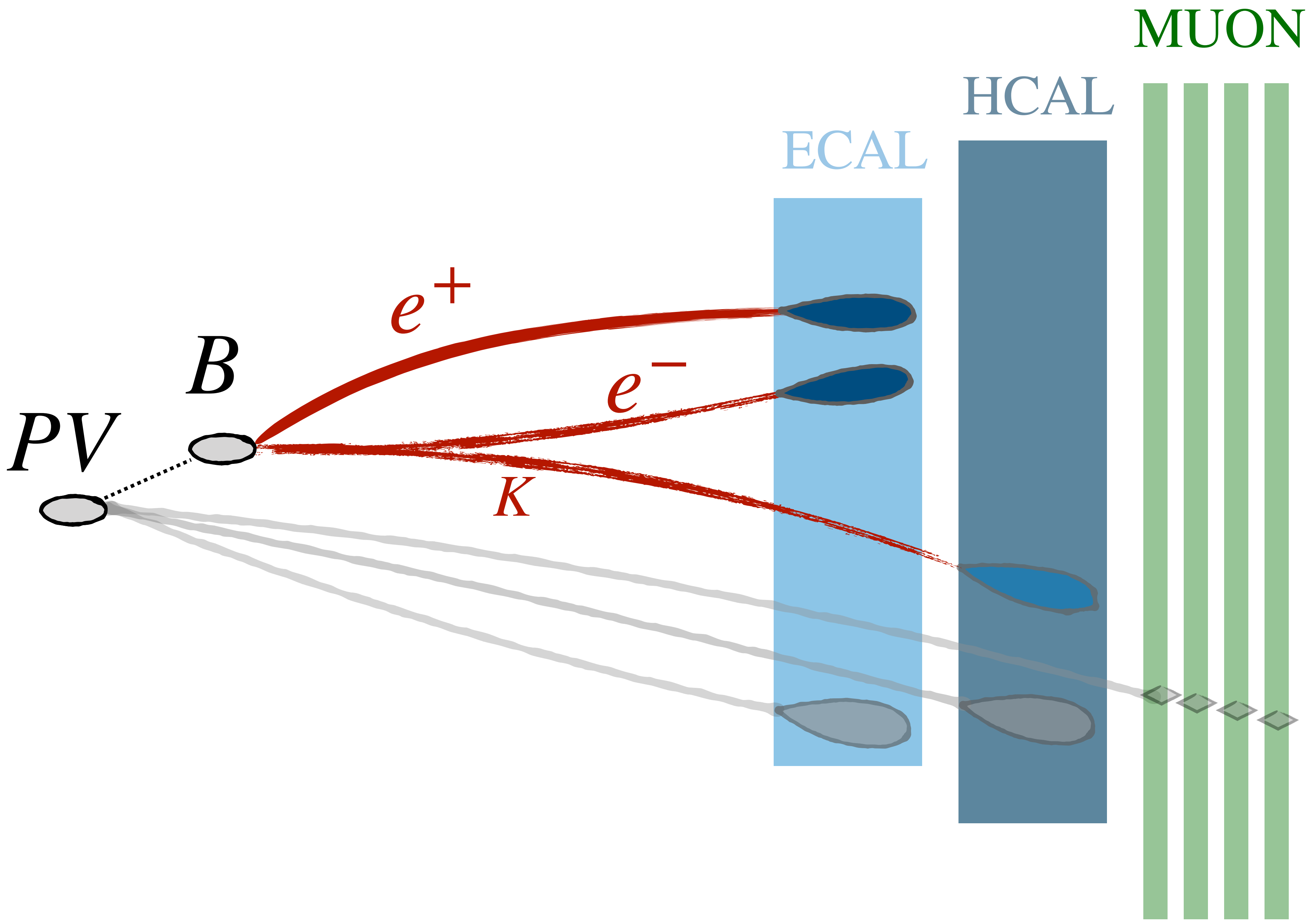

$E_T^{\mathrm{L0e}} \geq \sim 2.6\,\mathrm{GeV}$

$E_T^{\mathrm{L0h}} \geq \sim 3.4\,\mathrm{GeV}$

$p_T^{\mathrm{L0}\mu} \geq \sim 1.4\,\mathrm{GeV}$

Trigger-Independent-Signal (`TIS`)

- $\dfrac{\varepsilon(\mathrm{L0}\mu, \mathrm{h}, \mathrm{e})}{\varepsilon(\mathrm{L0}\mu, \mathrm{h}, \mathrm{e})}$ from underlying event

Trigger-On-Signal (`TOS`)

- $\dfrac{\varepsilon(\mathrm{L0}\mu)}{\varepsilon(\mathrm{L0e})}$ from tracks in B candidate

➡ R-ratio from $\left\langle \dfrac{\mathrm{TIS}}{\mathrm{TIS}}, \dfrac{\mathrm{L0}\mu}{\mathrm{L0e}} \right\rangle$

✦ Less $\varepsilon(e/\mu)$ differences to correct in `TIS`

✦ Previous R_{K,K^*} only L0μ in muon mode

Selection: multivariate classifiers

1. $B^{(+,0)} \to K^{(+,*0)}\mu^+\mu^-$ **and** $B^{(+,0)} \to K^{(+,*0)}e^+e^-$: suppress combinatorial with multivariate classifier using kinematic and vertex quality information.

2. $B^{(+,0)} \to K^{(+,*0)}e^+e^-$: dedicated classifier to fight partially reconstructed background, exploiting vertex and track isolation

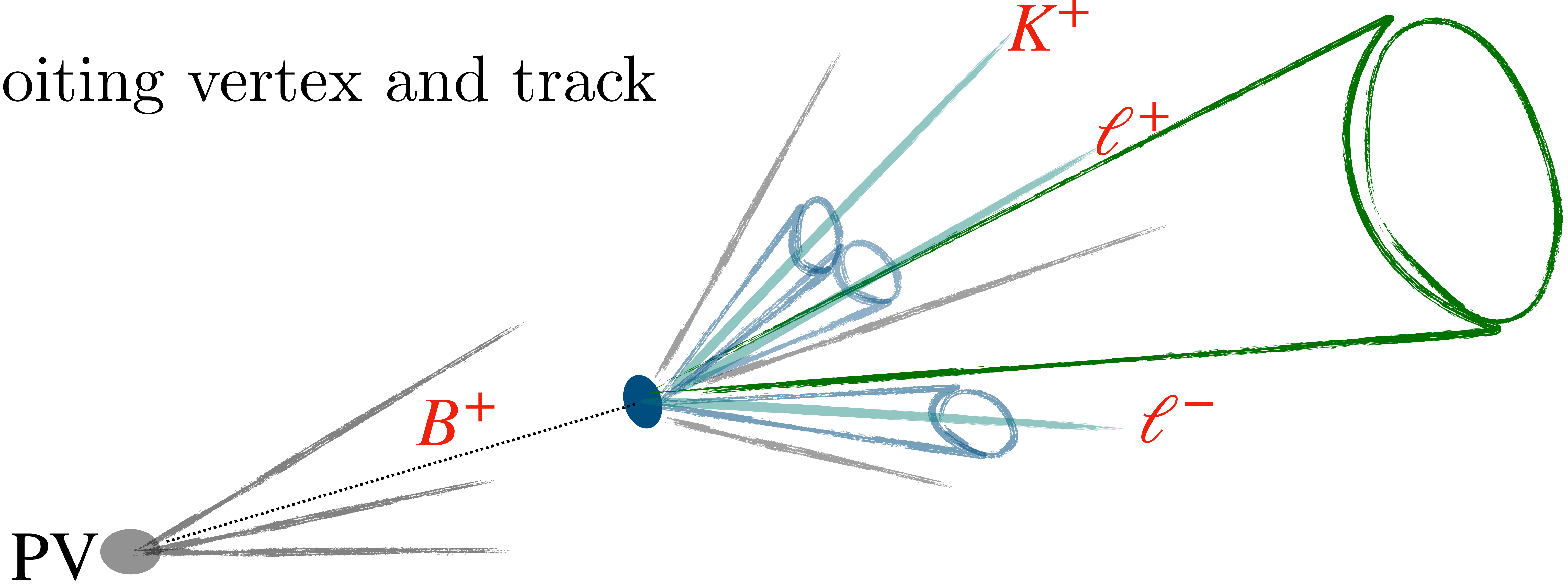

- **Optimisation of significance for each mode/q^2 regions and data taking period**

Calibration of simulation to determine ε

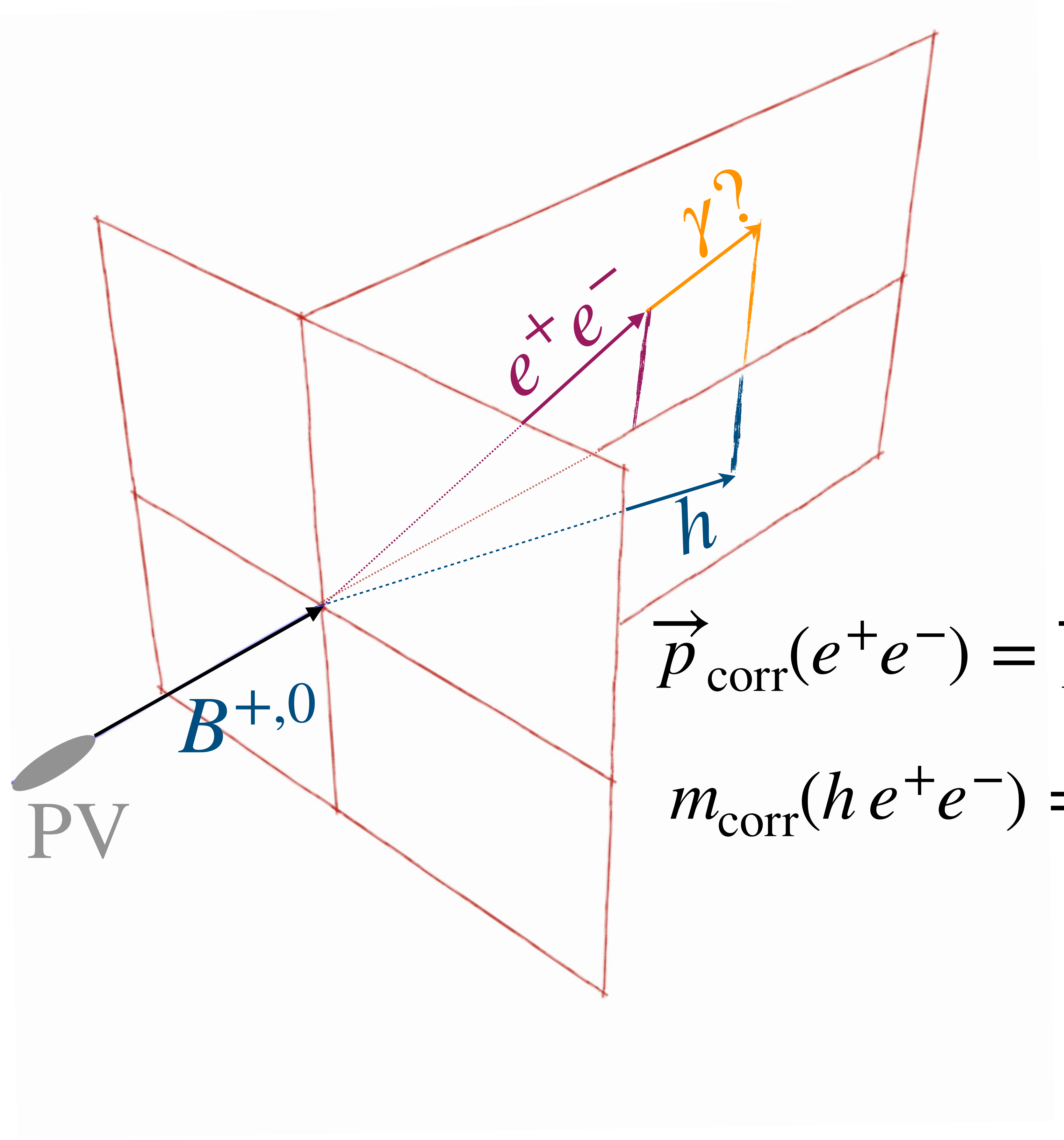

$$\vec{p}_{\text{corr}}(e^+e^-) = \vec{p}(e^+e^-) \cdot \frac{p_{\text{T}}(h)}{p_{\text{T}}(e^+e^-)}$$

$$m_{\text{corr}}(h\,e^+e^-) = |p_{\text{corr}}(e^+e^-) + p_h|$$

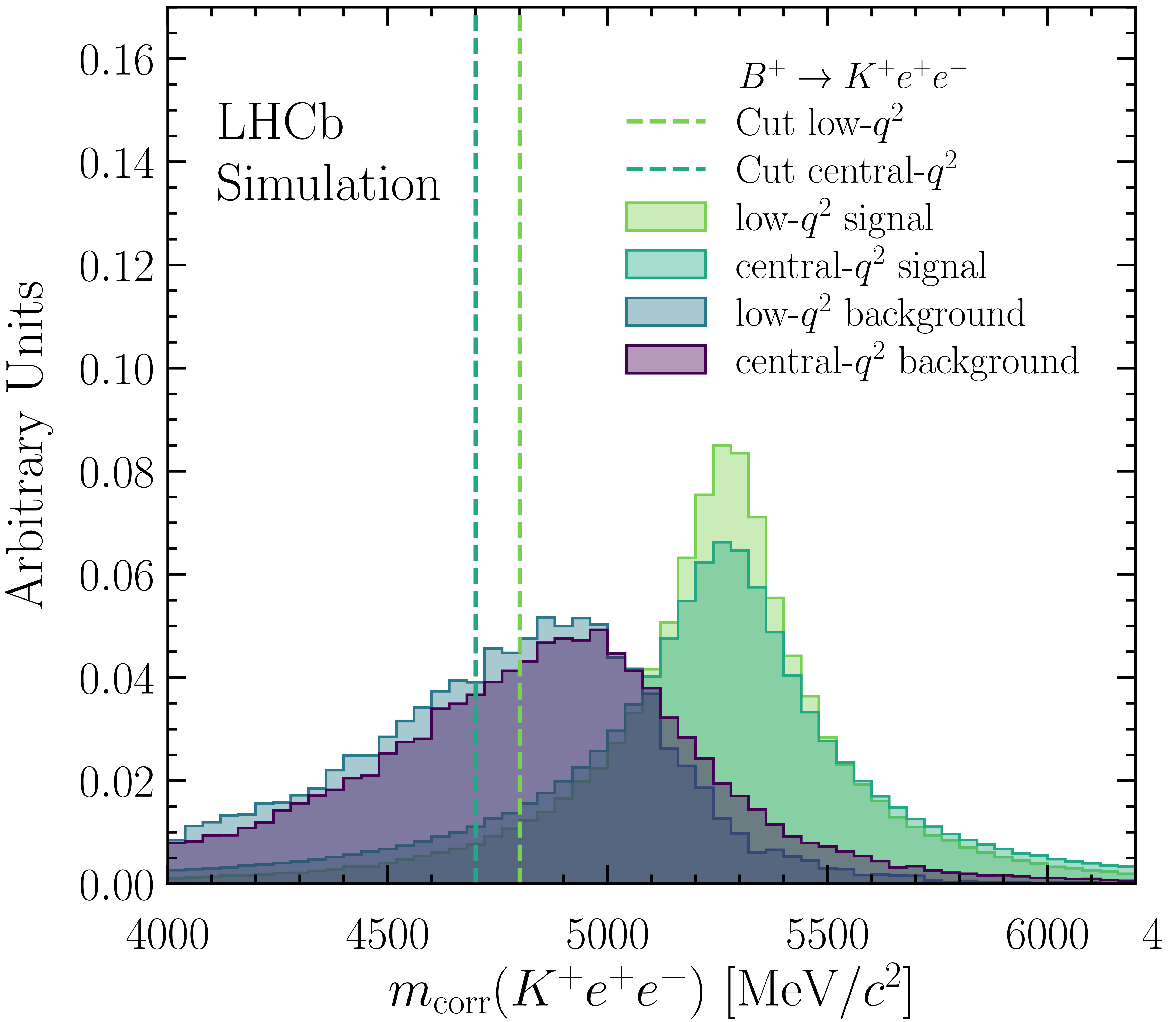

- **Small-correlation with combinatorial shape: modelled according to same-sign data $K^{+,*0}\ell^\pm\ell^\pm$**
- **After m_{corr} selection, no ≥ 2 missing hadron background expected in fit range.**

Selection: veto specific backgrounds B^+ mode

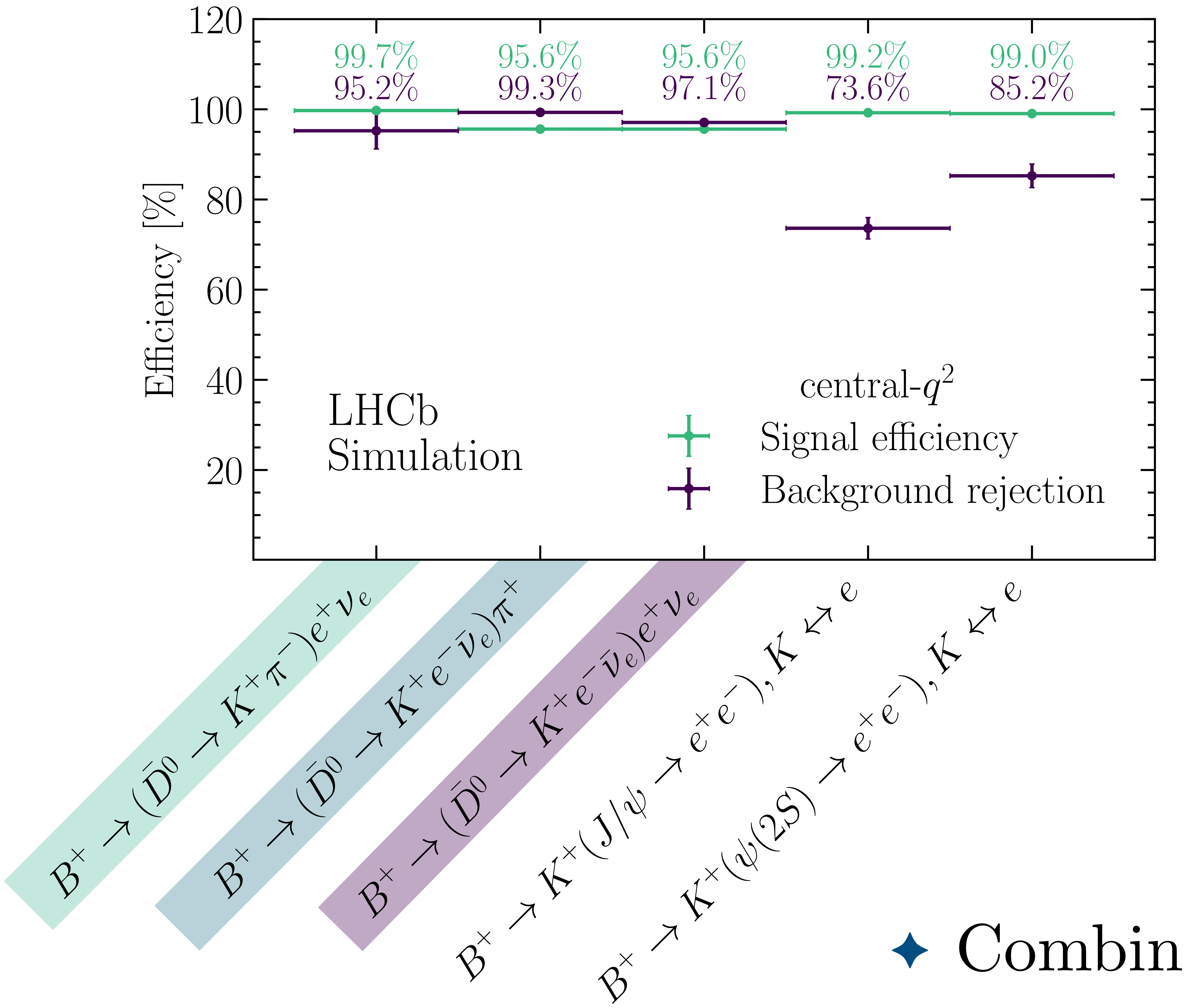

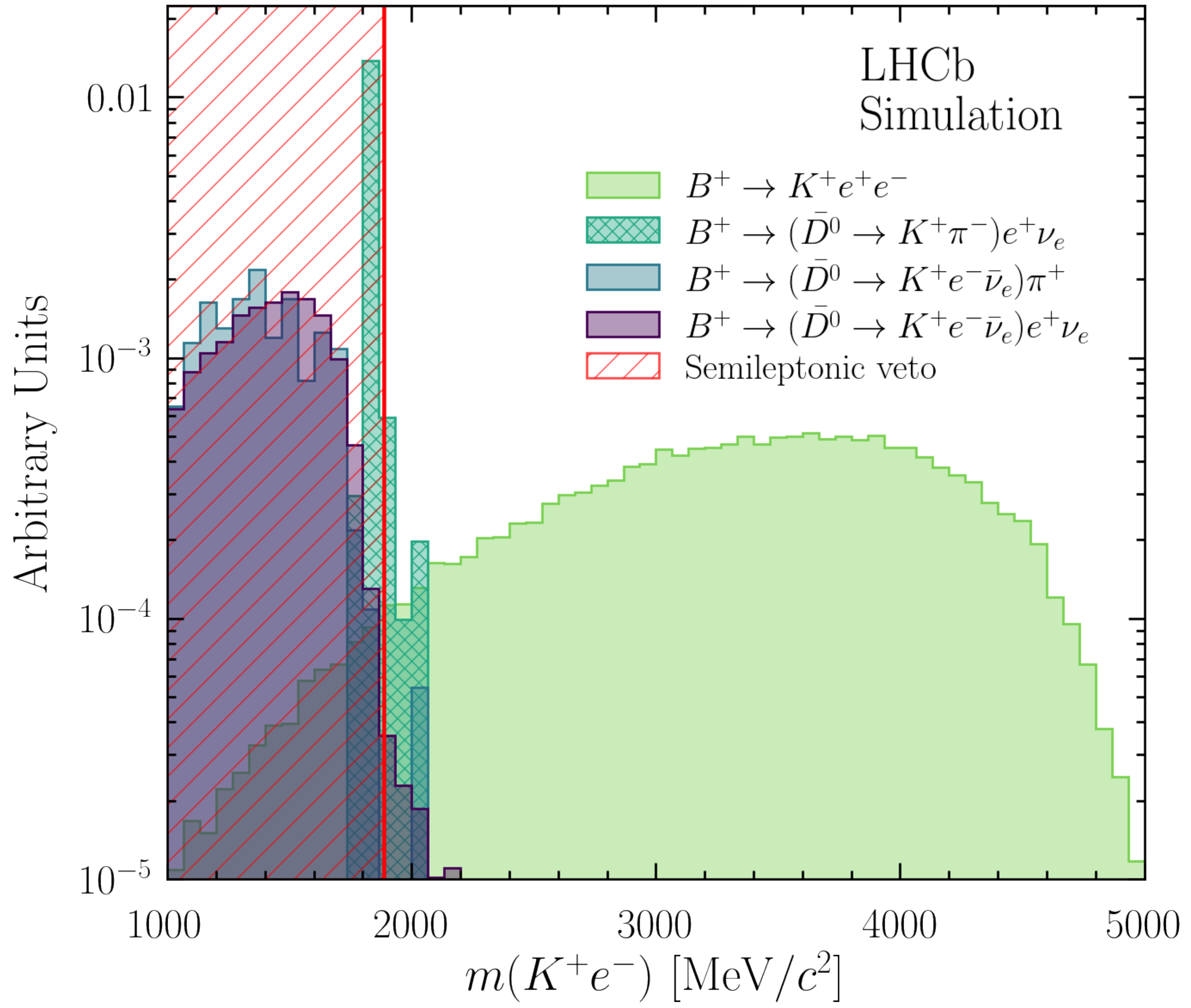

Semileptonic

Hadrons and leptons swaps

- Combination of efficient kinematic and particle identification criteria to remove background
- Specific vetoes under electron mis-ID hypothesis on $\overline{D}^0 \to K^+\pi^-_{\to e}$

Selection: veto specific backgrounds B^0 mode

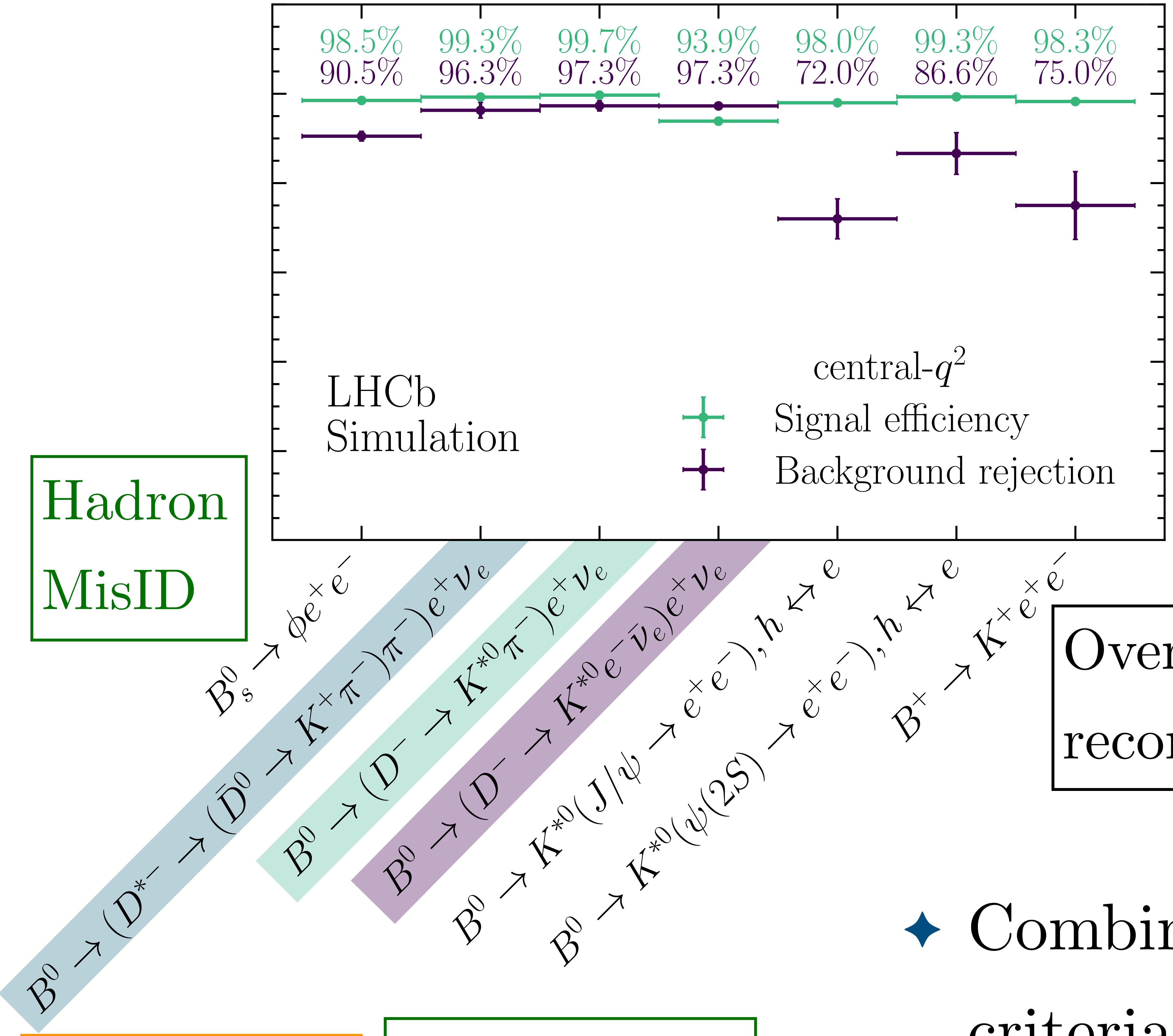

Hadron MisID

Over-reconstructed

Semileptonic

Hadrons and leptons swaps

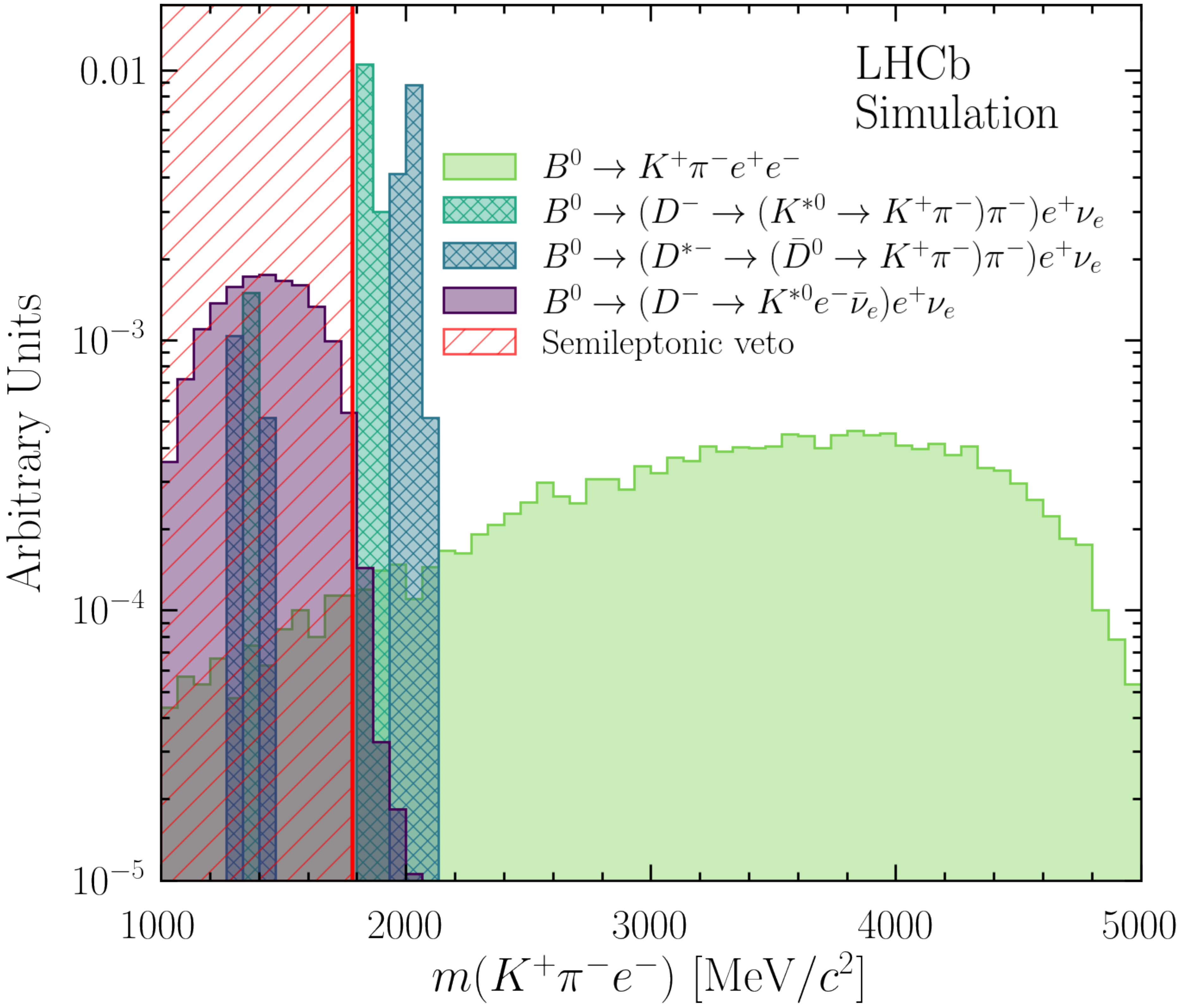

- ✦ Combination of efficient kinematic and particle identification criteria to remove background
- ✦ Specific vetoes under electron mis-ID hypothesis on $\overline{D}^0 \to K^+\pi^-_{\to e}$ and $D^- \to K^+\pi^-\pi^-_{\to e^-}$

Challenges in LFU tests: electrons and PID

From RICH I (upstream) and RICH II (downstream) detector

$m = \frac{p}{c\beta\gamma}$ from tracking

Ring Radius $\cos\theta_C = \frac{1}{n\beta}$

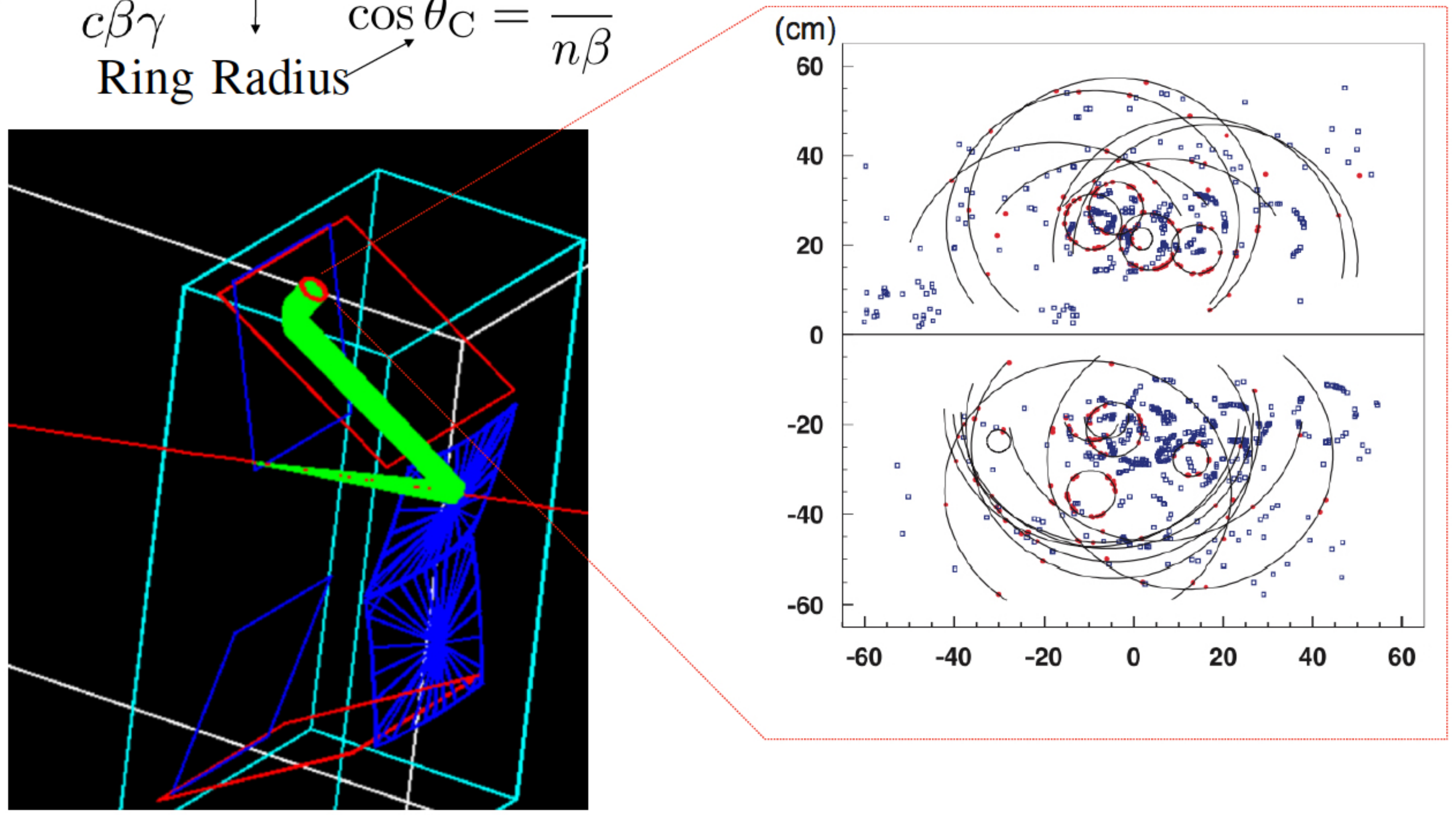

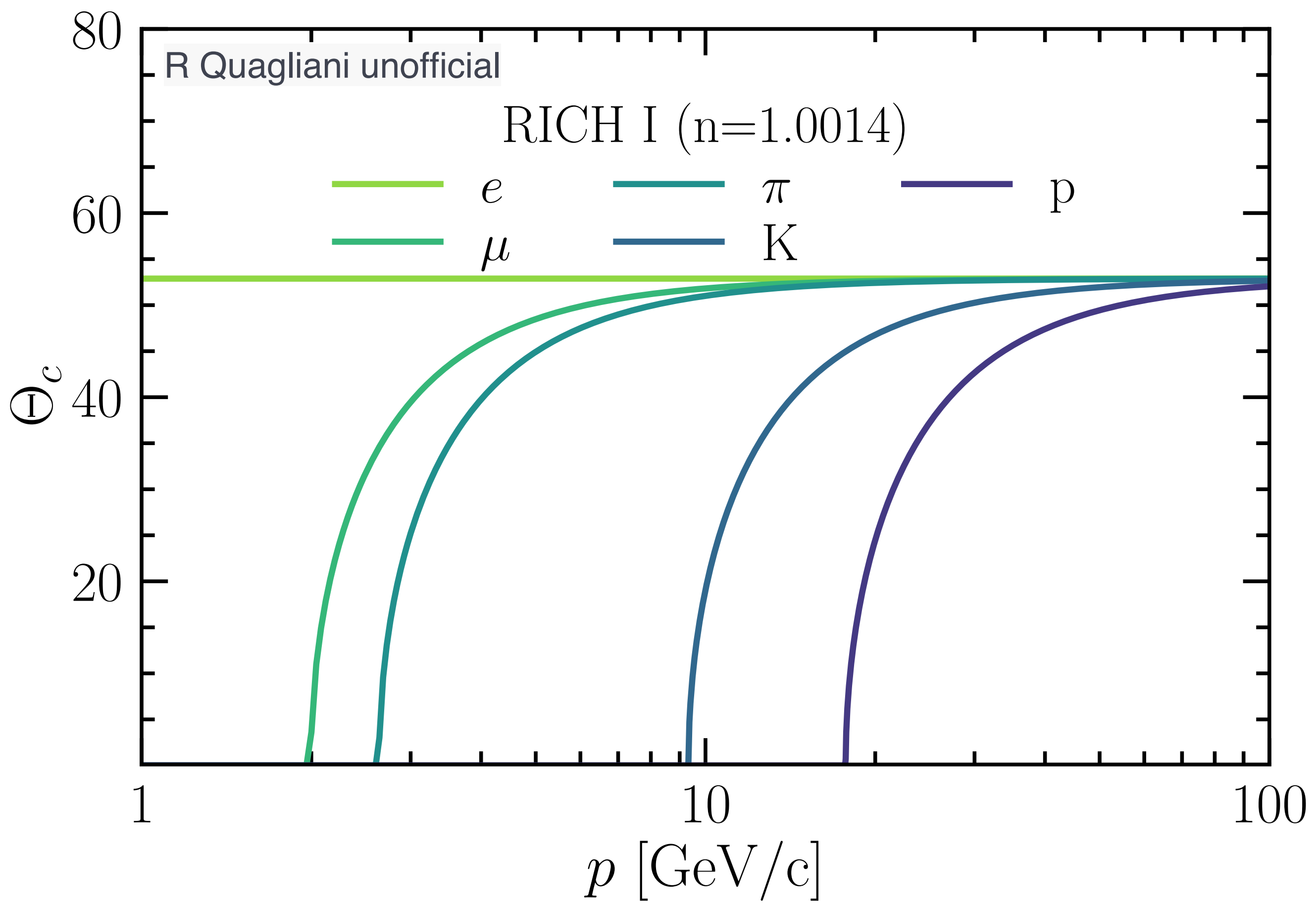

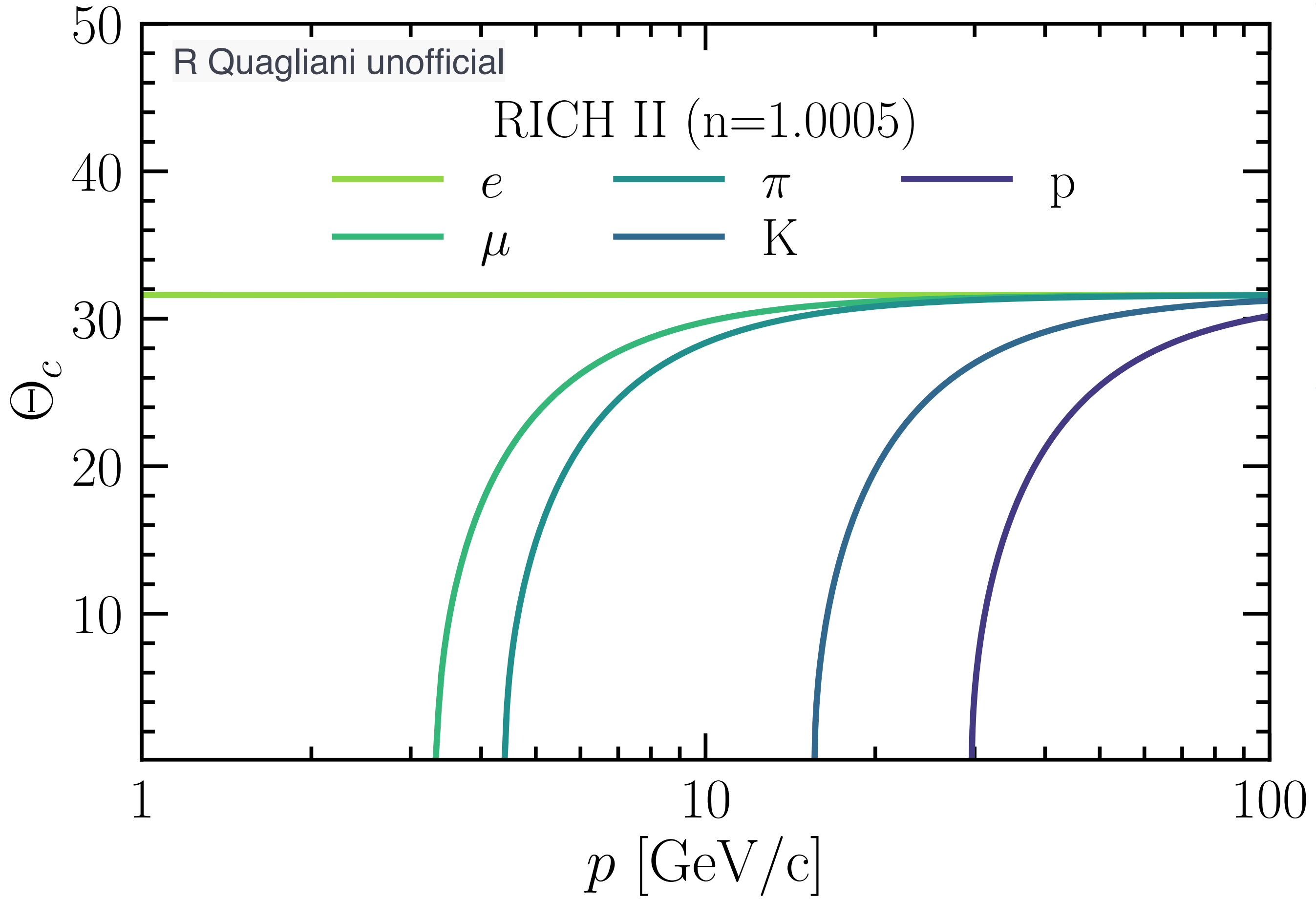

From ECAL

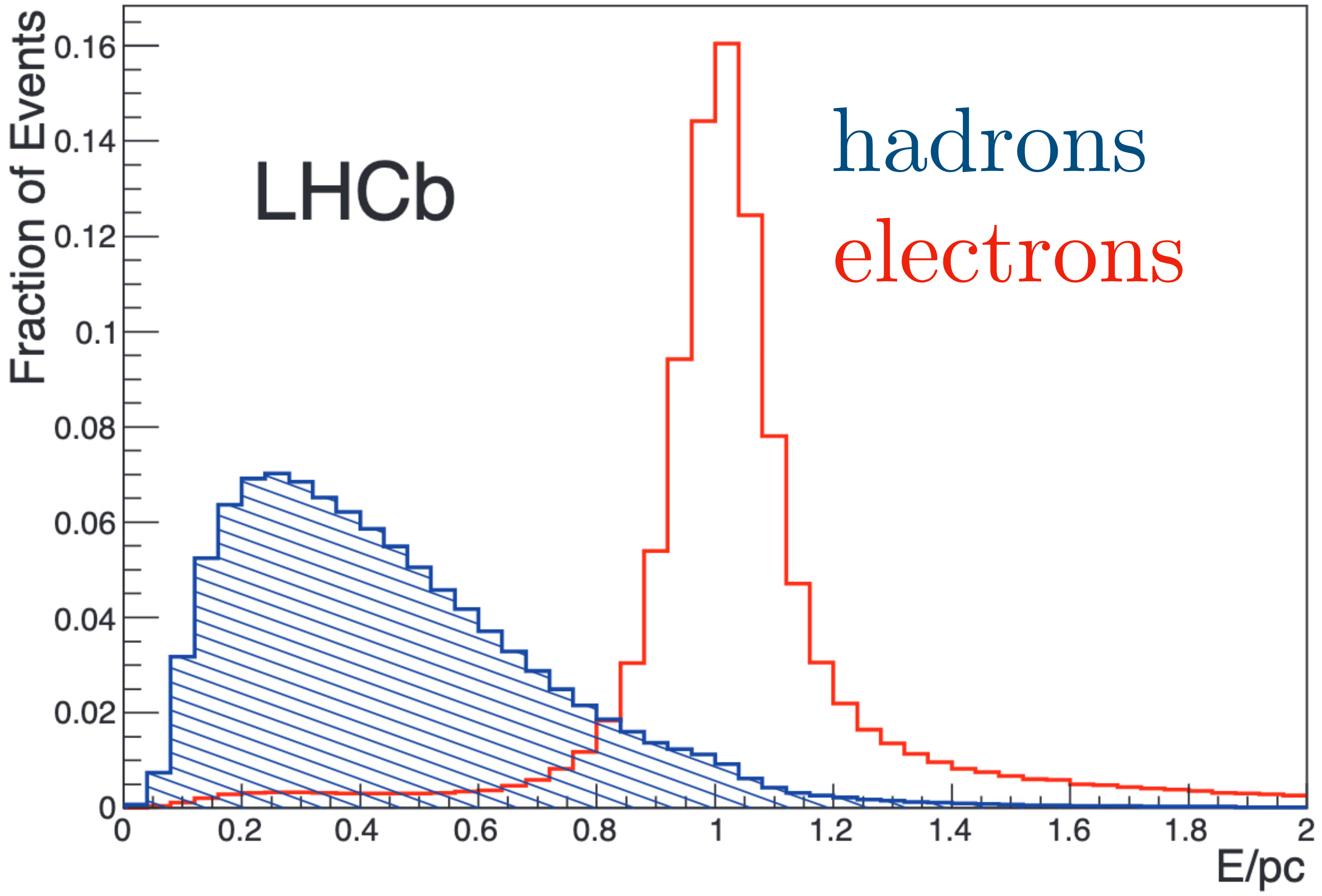

- $\text{DLL(e)} = \sum_{\text{ECAL,HCAL,RICH,MUON}} \Delta \log \mathscr{L}(e-\pi)$
- **ProbNNe**= Neural Net using tracking + PID of each detectors: e/h separation from simple sub-detectors greatly improved.

LFU tests: muons and PID

From RICH I (upstream) and RICH II (downstream) detector

$$m = \frac{p}{c\beta\gamma}$$

from tracking

Ring Radius

$$\cos\theta_C = \frac{1}{n\beta}$$

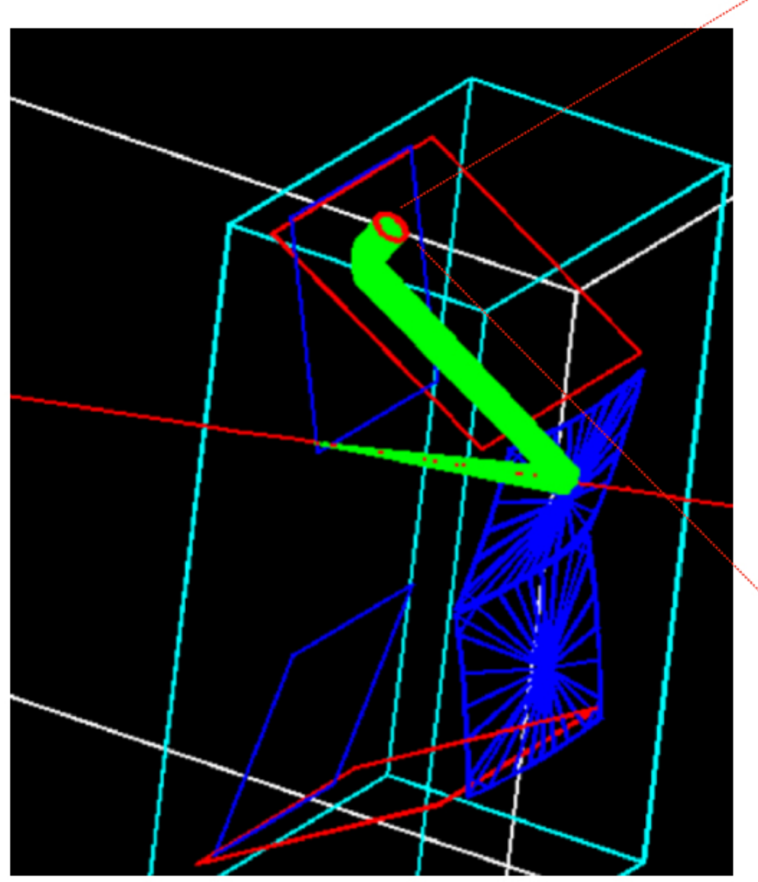

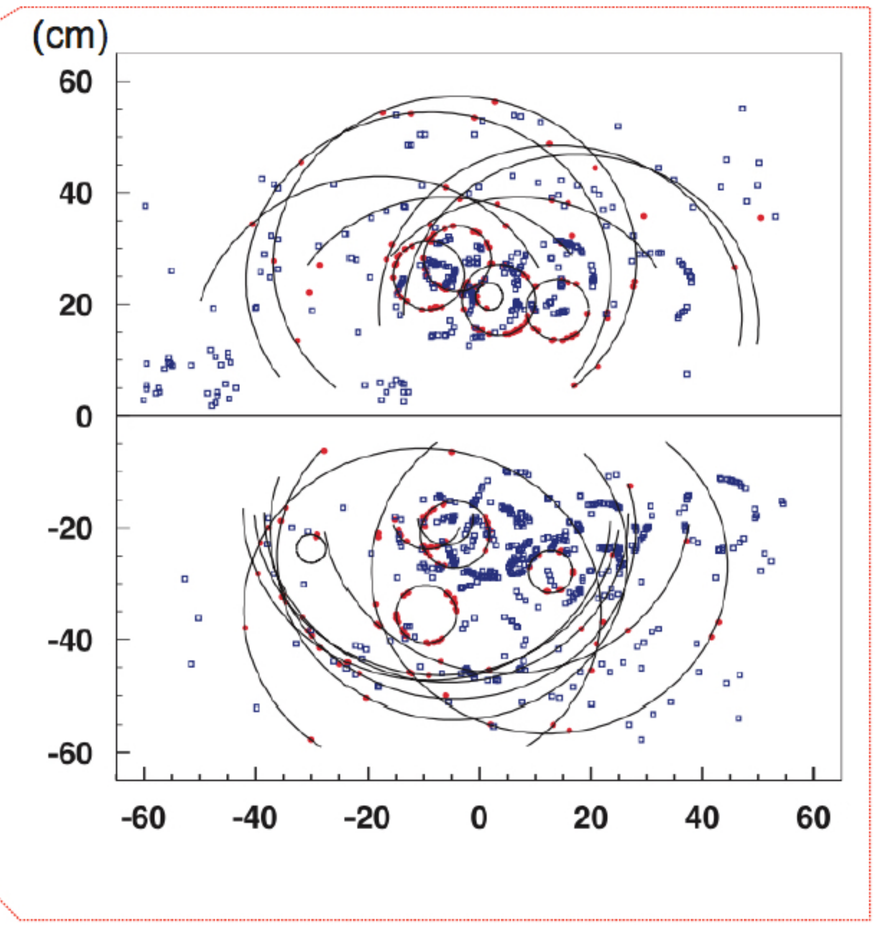

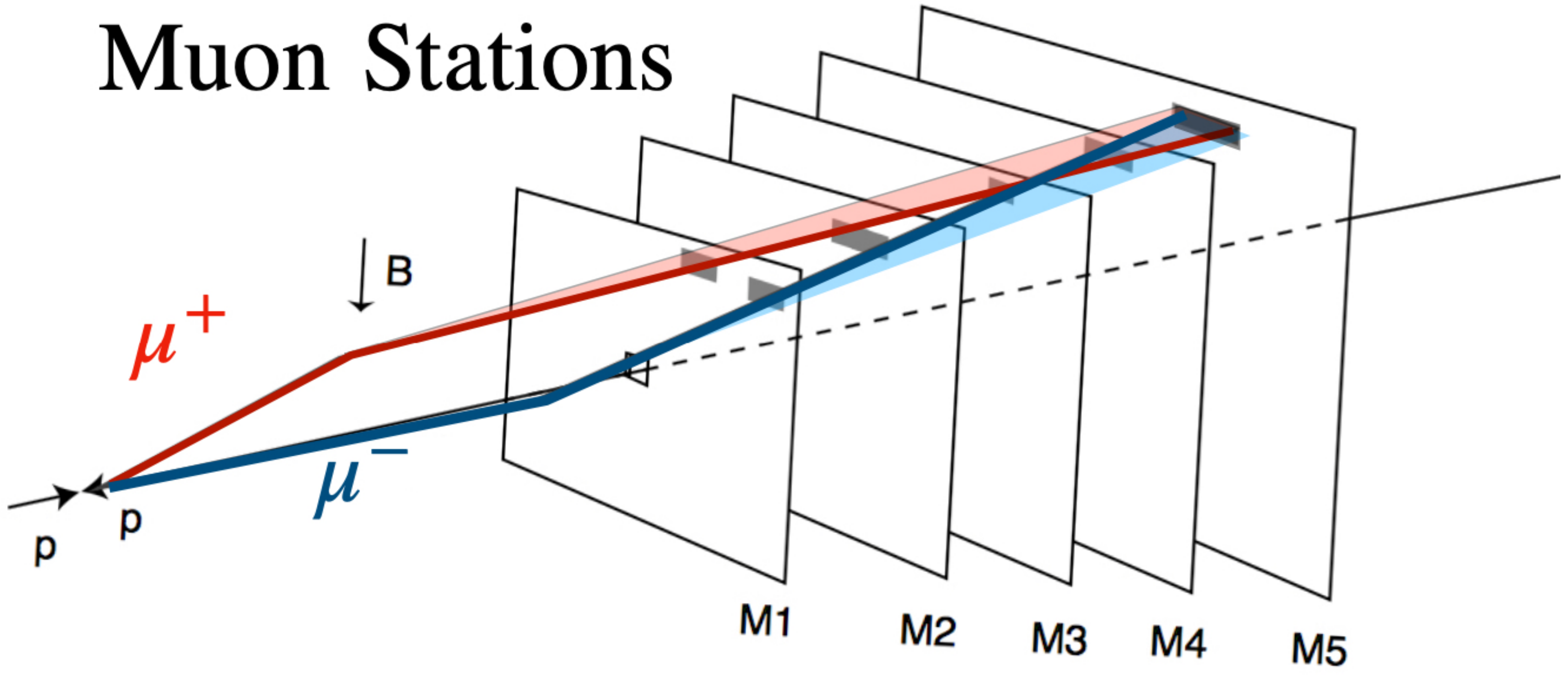

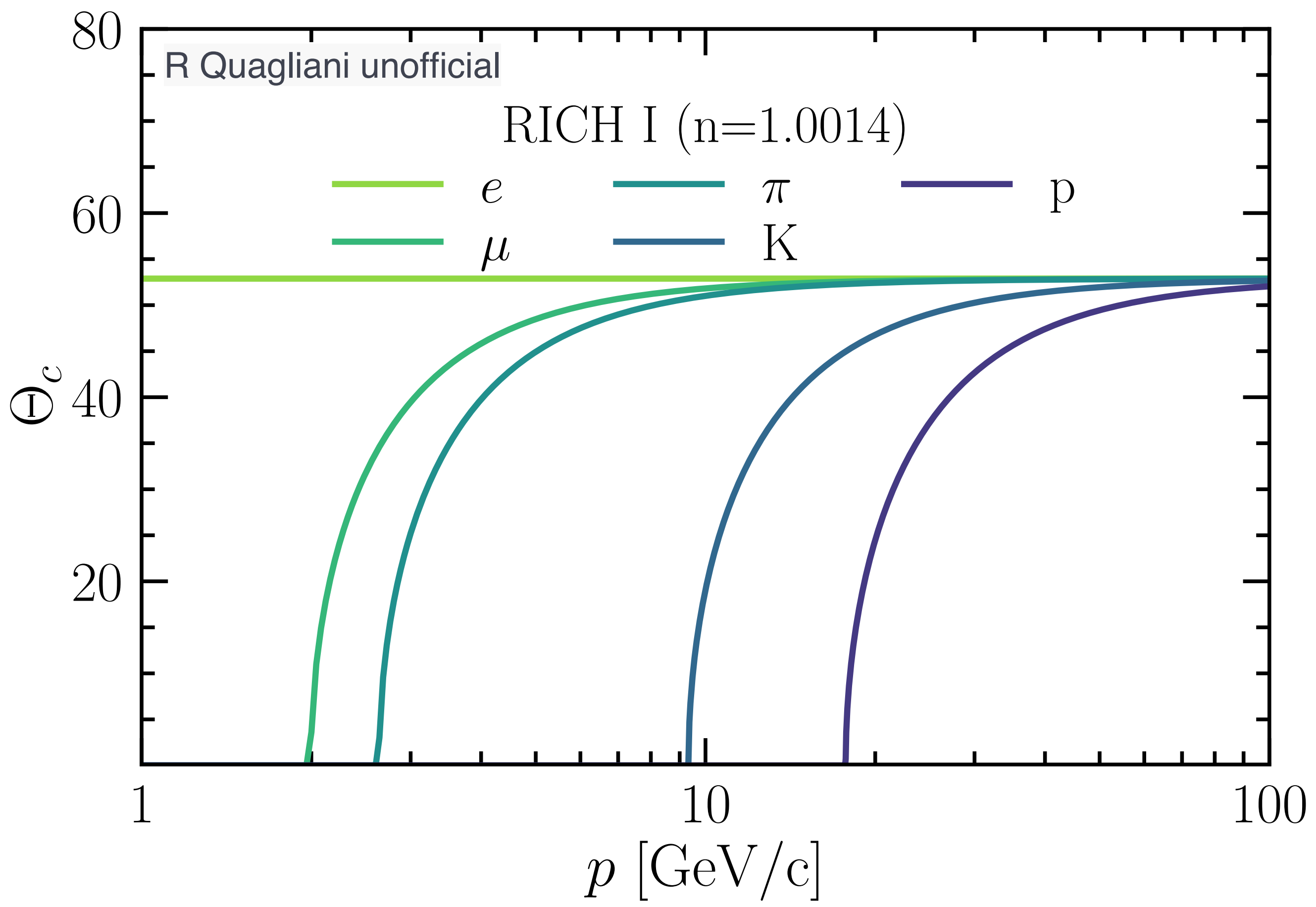

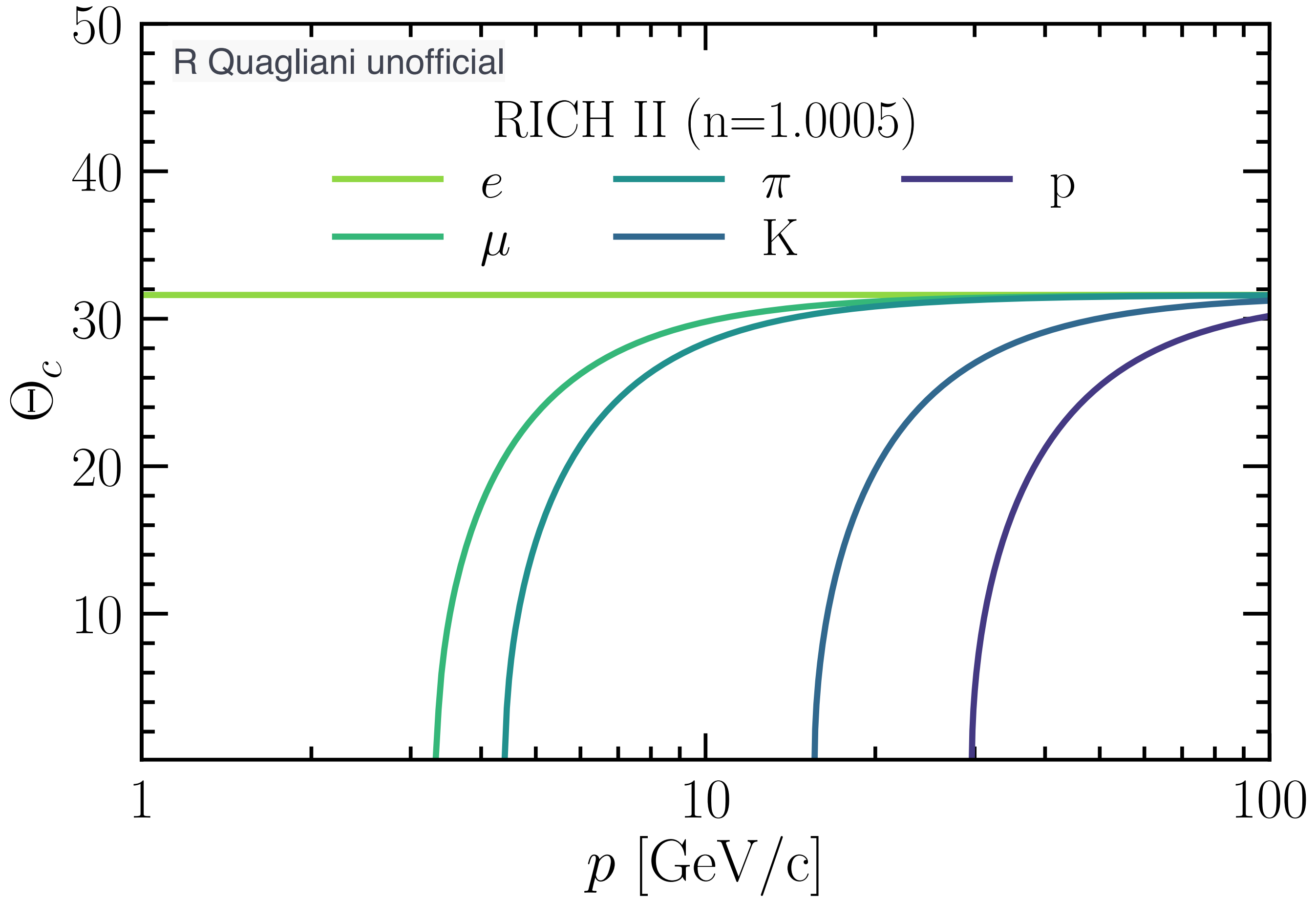

- Excellent **MuonID** and μ/h already with muon station coincidence
- Negligible brem losses at LHCb
- **Muon stations occupancy much lower than ECAL**

PID scan and coherent pattern observed, rule out an efficiency effect

- **Verify that the trend is not an “efficiency” calibration effect for electrons. How?**

Theoretical prediction of $r_{\gamma^*} = \dfrac{\mathcal{B}(B^0 \to K^{*0}e^+e^-)}{\mathcal{B}(B^0 \to K^{*0}\gamma)}$ *extremely clean the closer* q^2 *is to photon pole, even in presence of NP. Can be used as candle to validate* ε *on electron mode (M. Borsato).*

Strength of the check currently limited by external measurement of $\mathcal{B}(B^0 \to K^{*0}\gamma)_{Belle}$.

`CERN-THESIS-2022-122 (master thesis C.Lamettais)`

- Verified compatibility at different PID selection of
  $\mathcal{B}(B^0 \to K^{*0}e^+e^-)^{exp}_{q^2\in[0.0001,0.1]GeV^2/c^4} = r^{theory}_{\gamma^*} \times \mathcal{B}(B^0 \to K^{*0}\gamma)_{Belle}$
- Relative efficiency checks performed also with converted photons comparing variation of yields in data to predictions from corrected simulation
- Additional validation of $\varepsilon(q^2)$ dependency and double ratio approach

Going beyond to cross-check ε *double ratio approach at lower* q^2

- **On-going analysis of $R(\phi\pi)$ using $D_{(s)} \to \phi\pi$ with $\phi \to \ell\ell$ at LHCb**

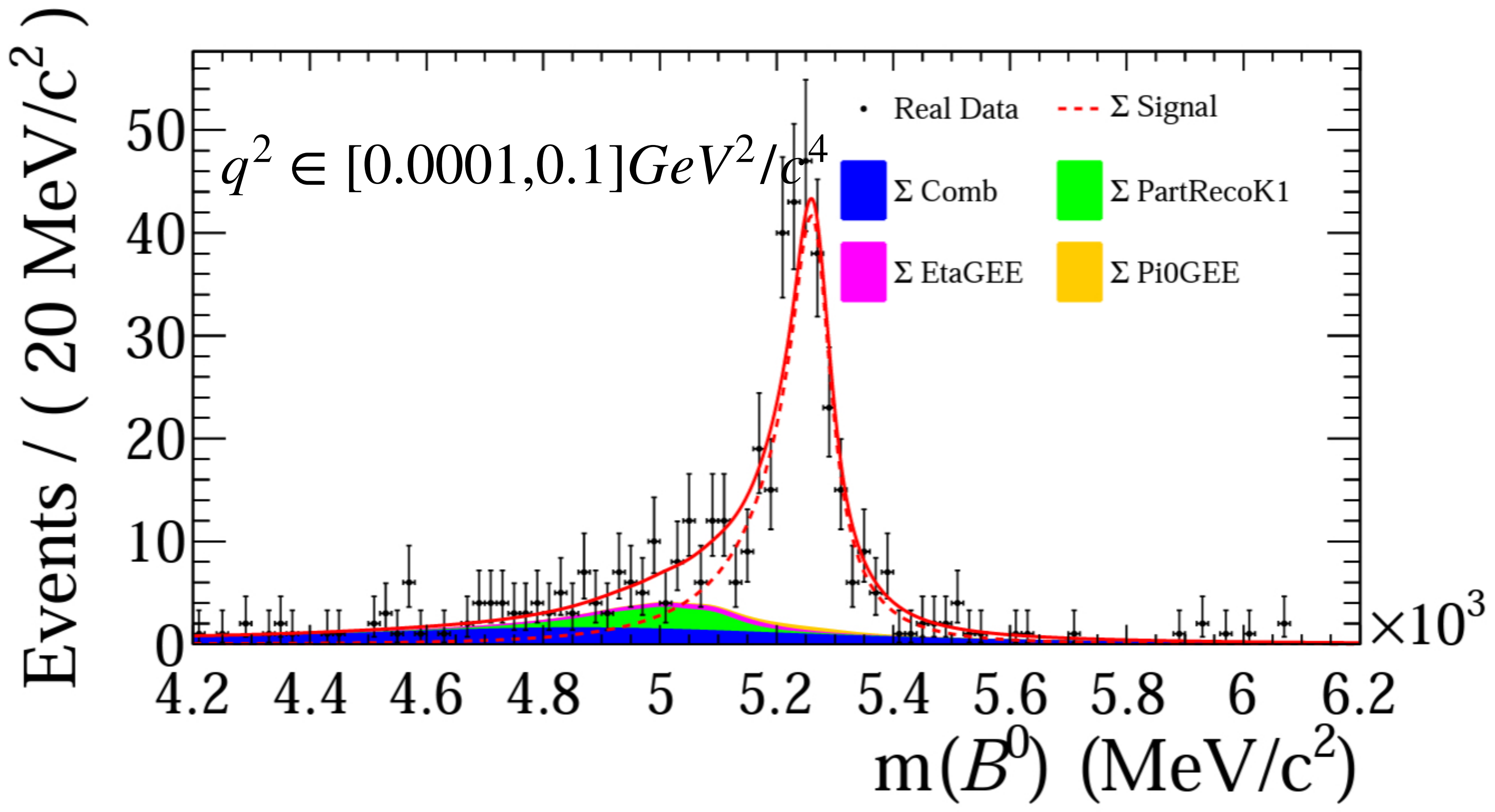

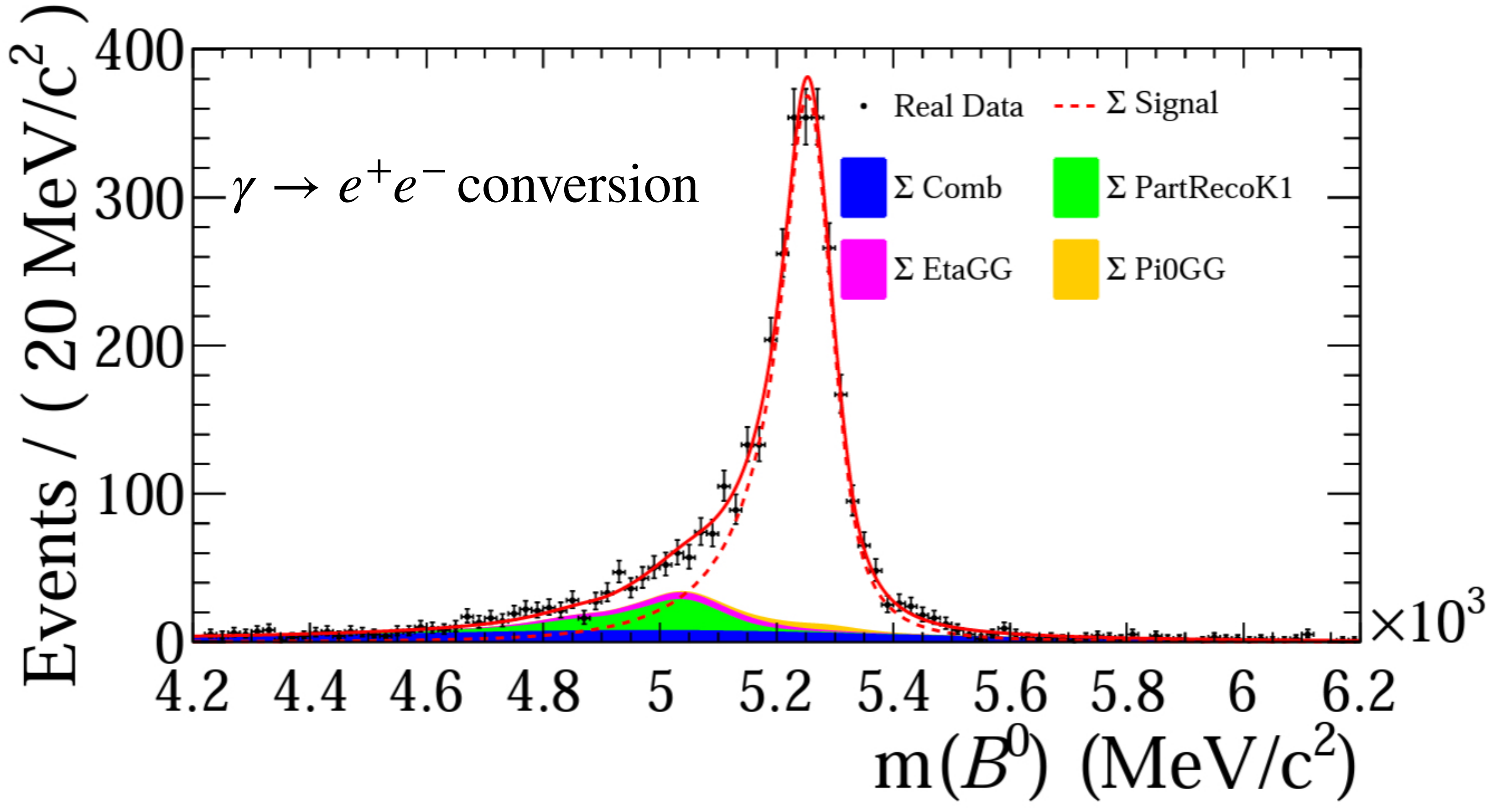

Results using misidentified background at different PID

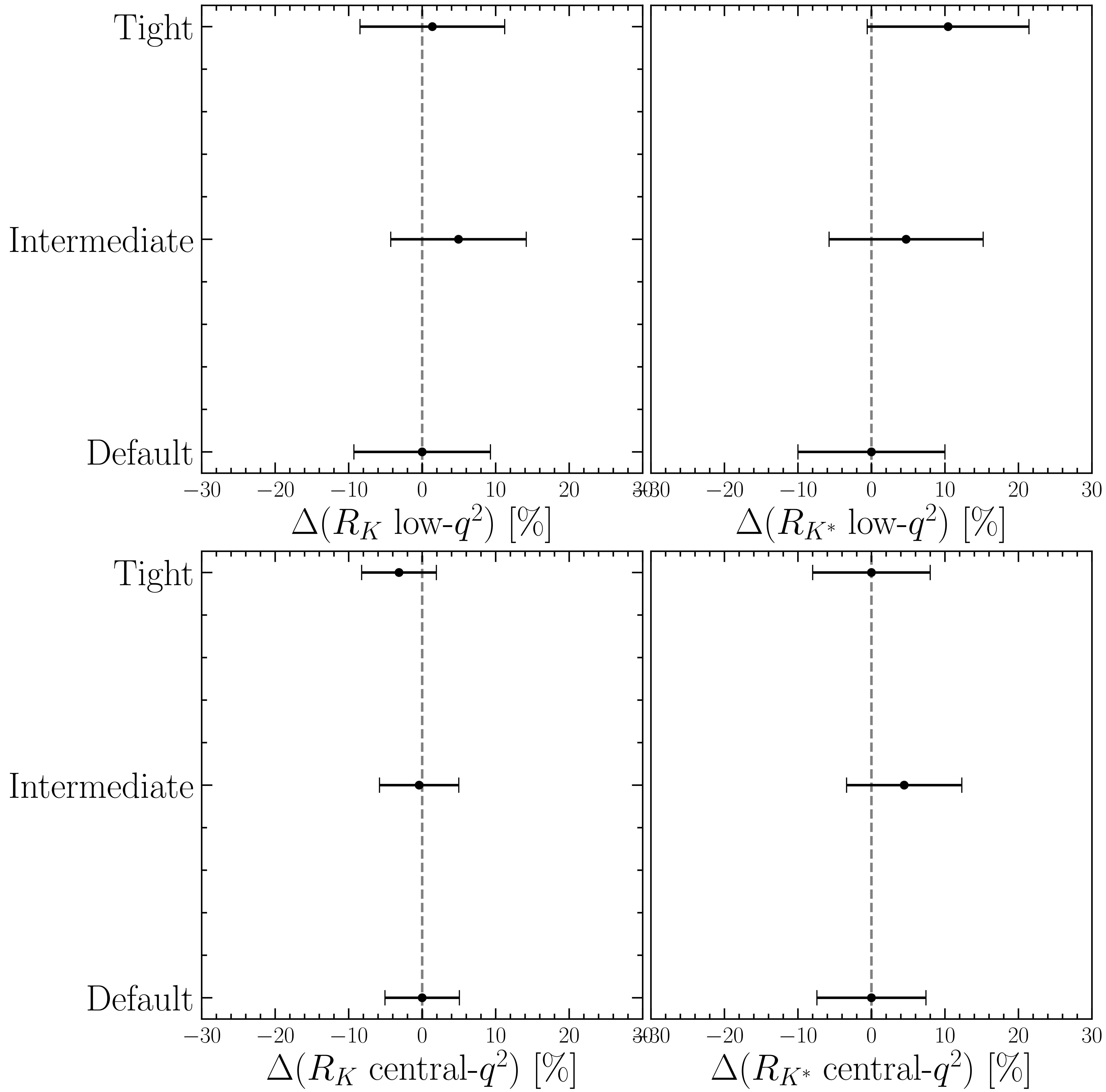

- *Tight*
  - 80% misID suppression
  - 50-60% signal loss
- *Intermediate*
  - 50% misID suppression
  - 20-30% signal loss

Misidentified background

included in fit model

at tighter working point

results are stable

Misidentified background in electron mode

- Simple backgrounds from double-misidentification can be isolated inverting PID criteria (close to nominal selection) after full selection (i.e $K^{+,*0}h^+h^-$) on electron mode

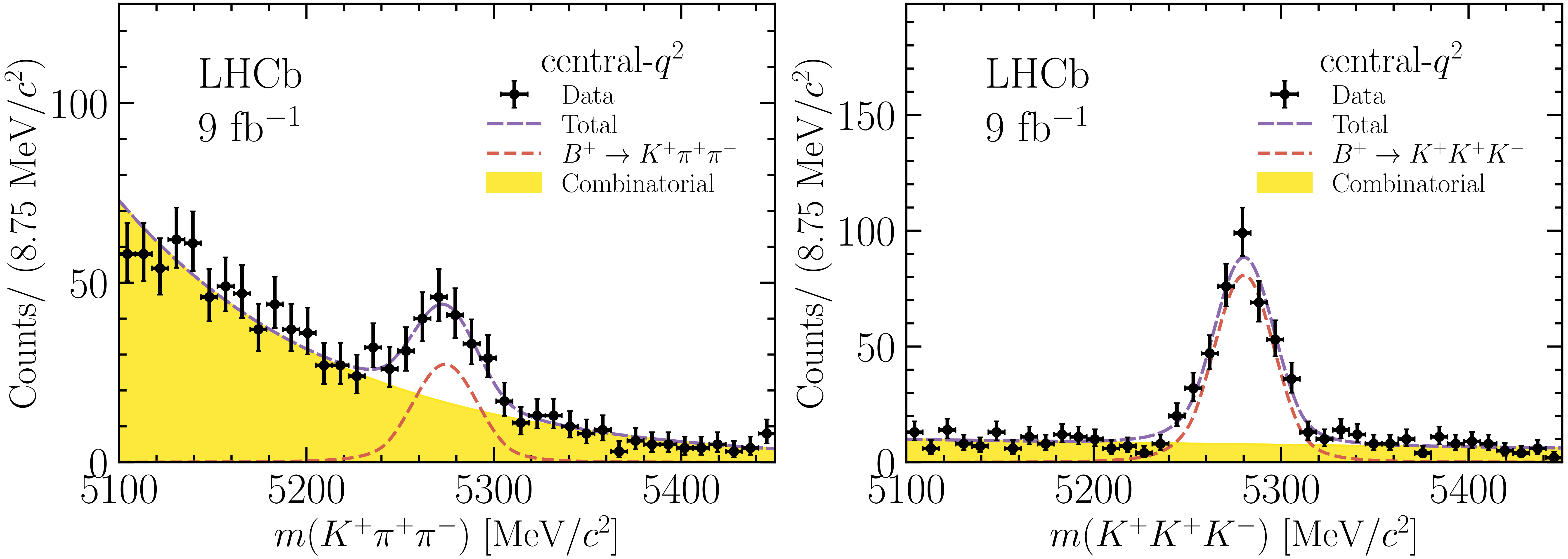

- Similar structures also for R_{K*}, however unknown Dalitz for $K^{*0}h^+h^-$
- Single misidentification background as well, often unknown decays.
- This motivated primarily the use of an inclusive data-driven treatment of misidentified background.

Misidentified background in electron mode

- Invert PID requirements on one or both e after full selection (*control region*)
- Subtract residual e^+e^- signal falling in the *control region*

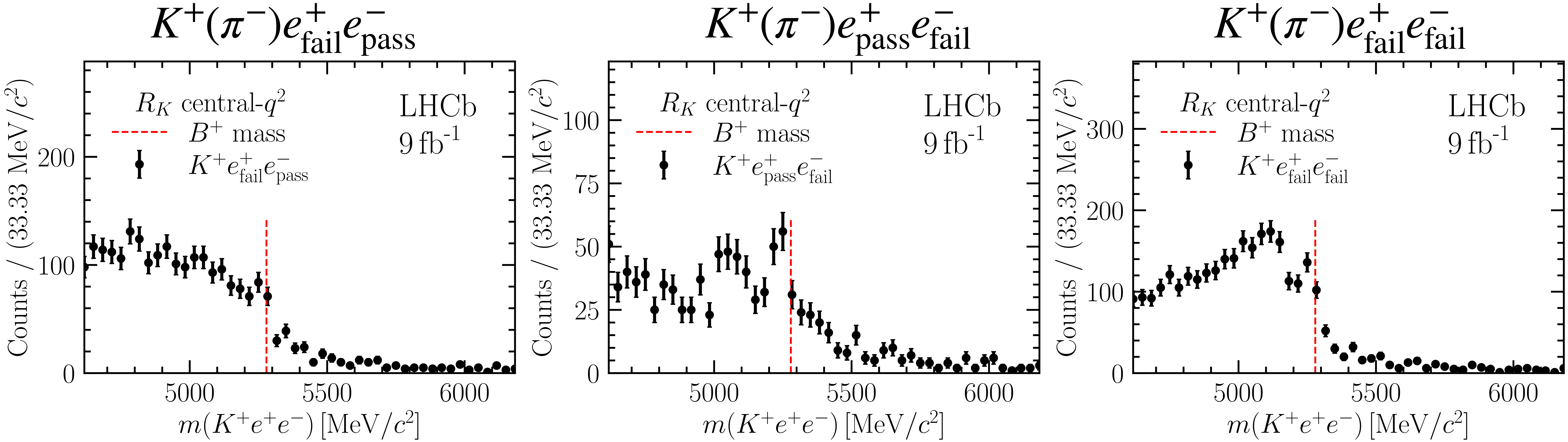

- Categorise pion- and kaon-like electrons in *control region* based on neural-net kaon ID classifier
- Per-event/per-track weights on e_{fail} to predict background shape and normalisation for e_{pass}

K^+K^- double mis-ID in ‘*control*’ region

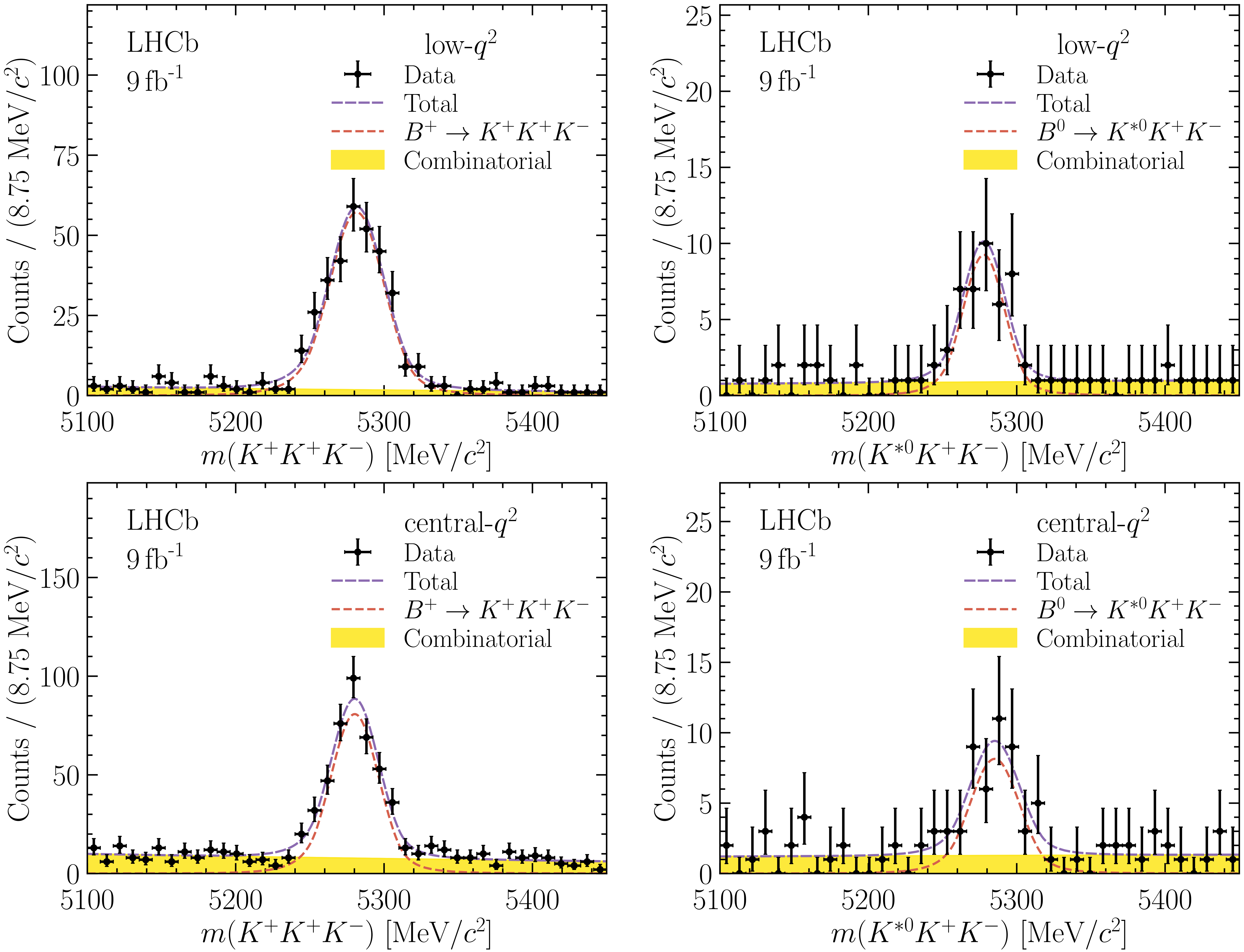

$\pi^+\pi^-$ double mis-ID in '*control*' region

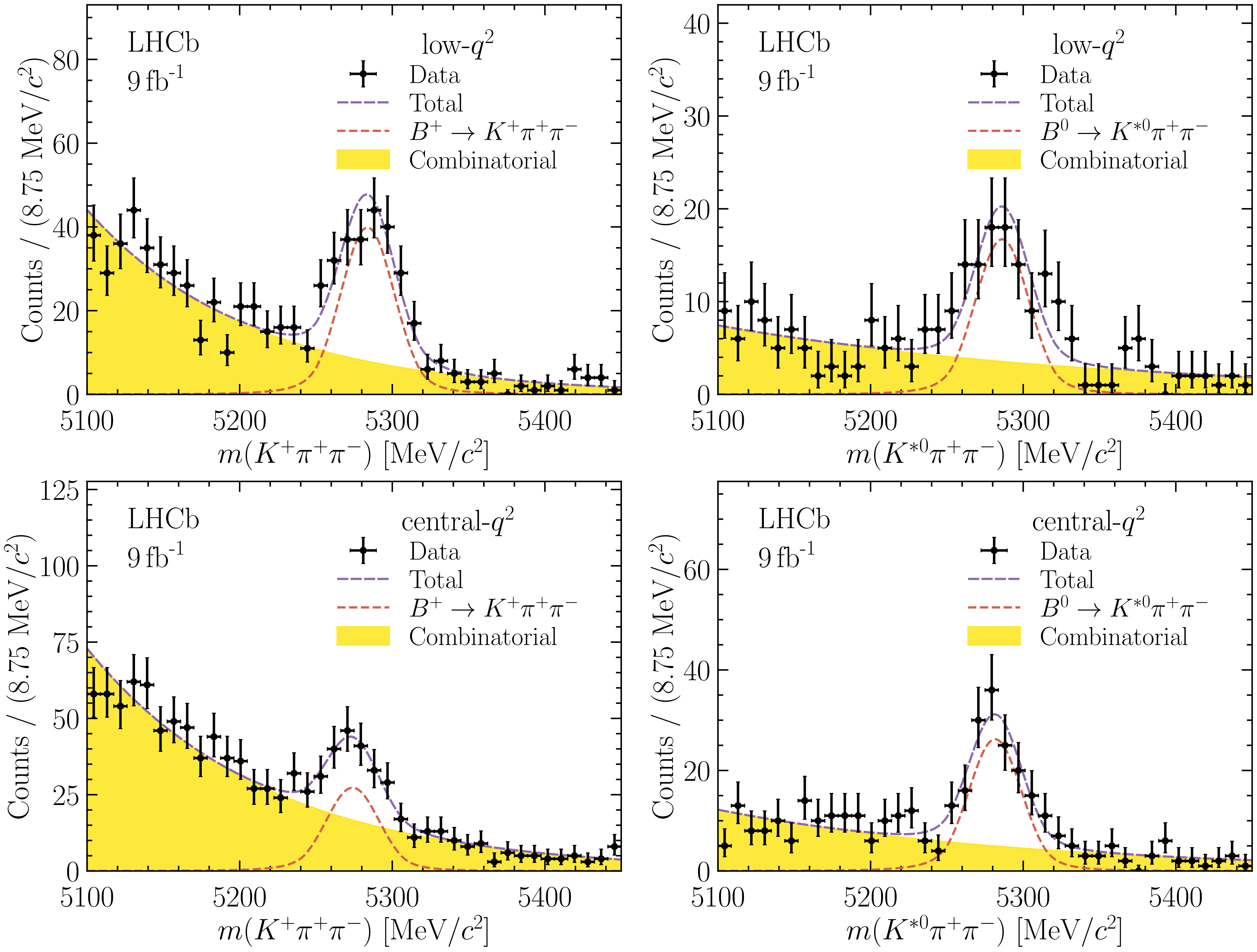

Choice of control region

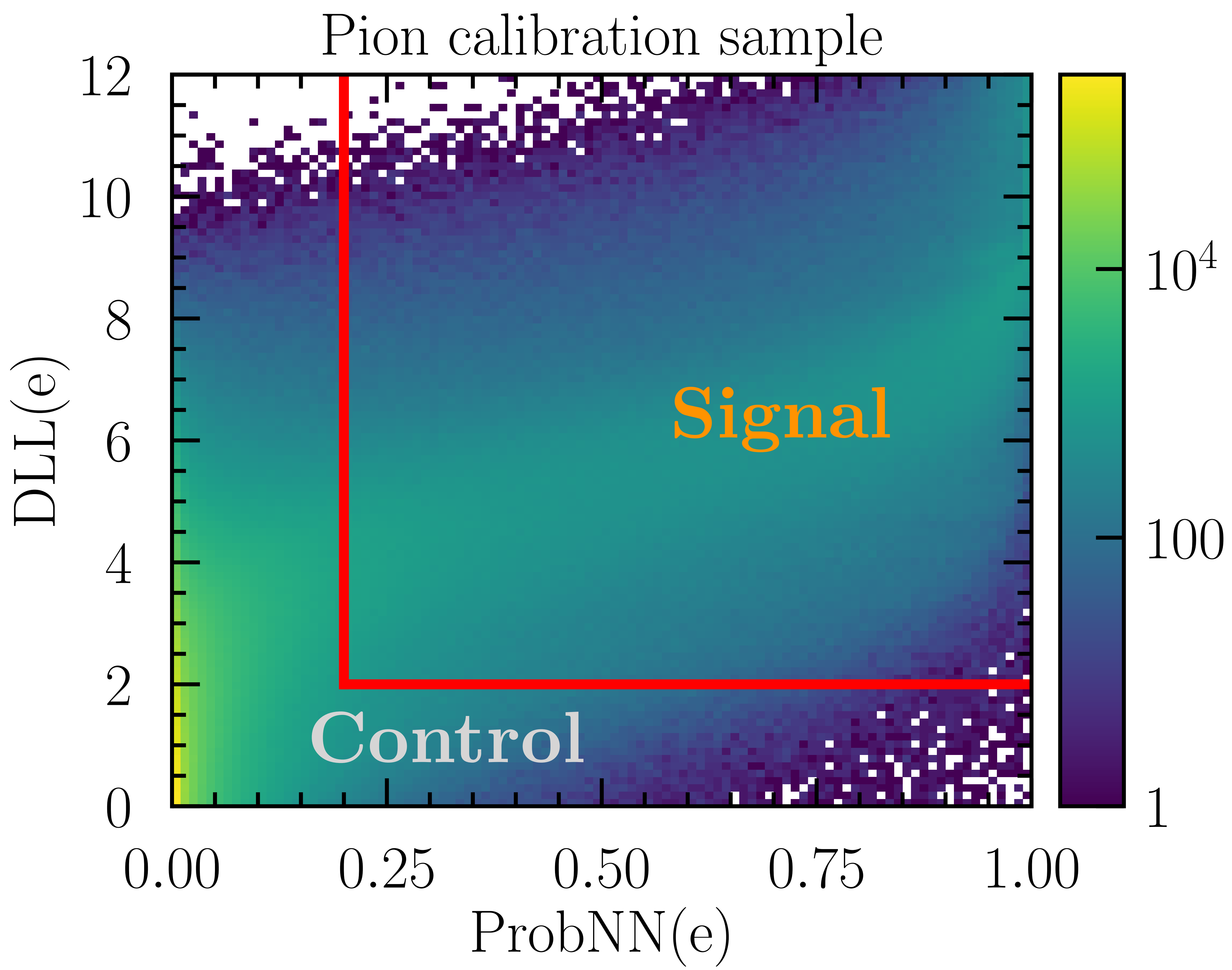

- Control region next to signal region
- Choose available region (`DLL(e) < 2 || ProbNNe < 0.2`) while `DLL(e)>0`.
- Other choices for a systematic uncertainty

Misidentified background in electron mode

- *Control region* **choice:**
  - not too far from signal, ensuring only pion/kaon misID is relevant
- $\frac{\text{pass}}{\text{fail}}$ (transfer function) from $D^{*-} \to \overline{D}^0(K^+\pi^-)\pi^-$ calibration data in p_T, η bins
  - $K/\pi \to e$: *"control"*→*"signal"*
- ***Validation:***
  - *Data*: use $\overline{D}^0(K^+\pi^-)$ in $K^+e^+e^-$ (no vetoes)
  - *Simulation*: $B^+ \to K^+K^+K^-$ and $B^+ \to K^+\pi^+\pi^-$
  - Prediction within 2% margin

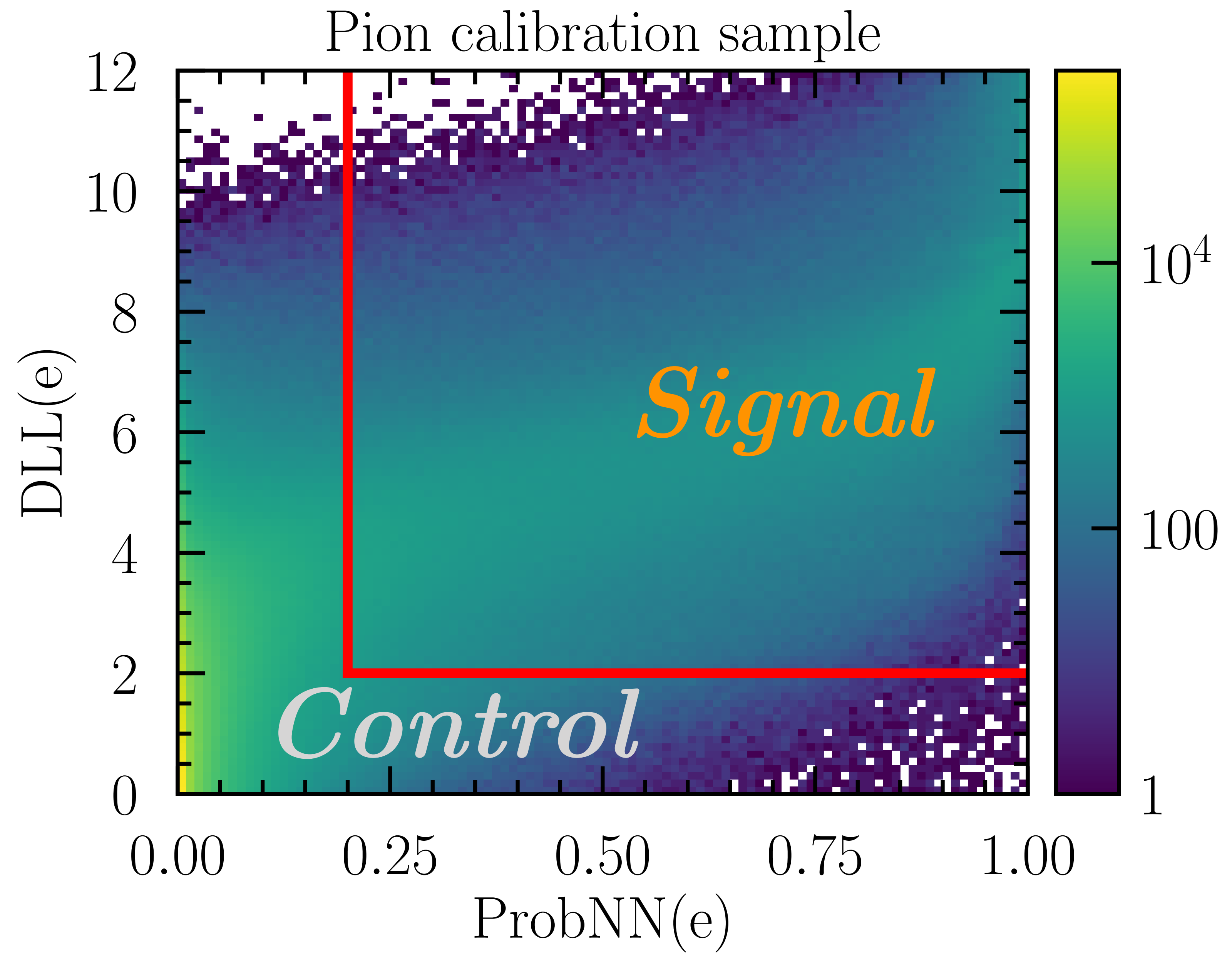
Pion calibration sample

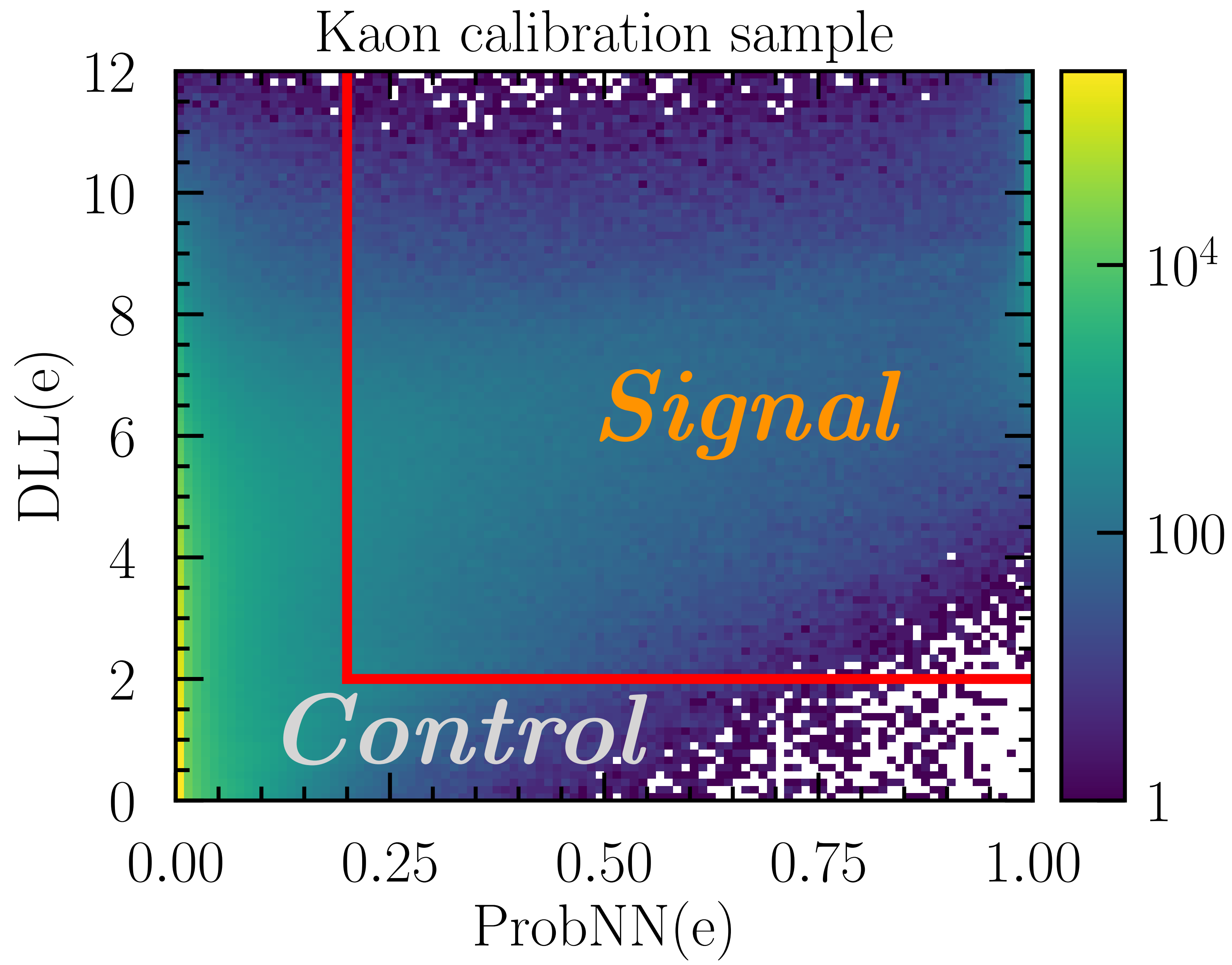
Kaon calibration sample

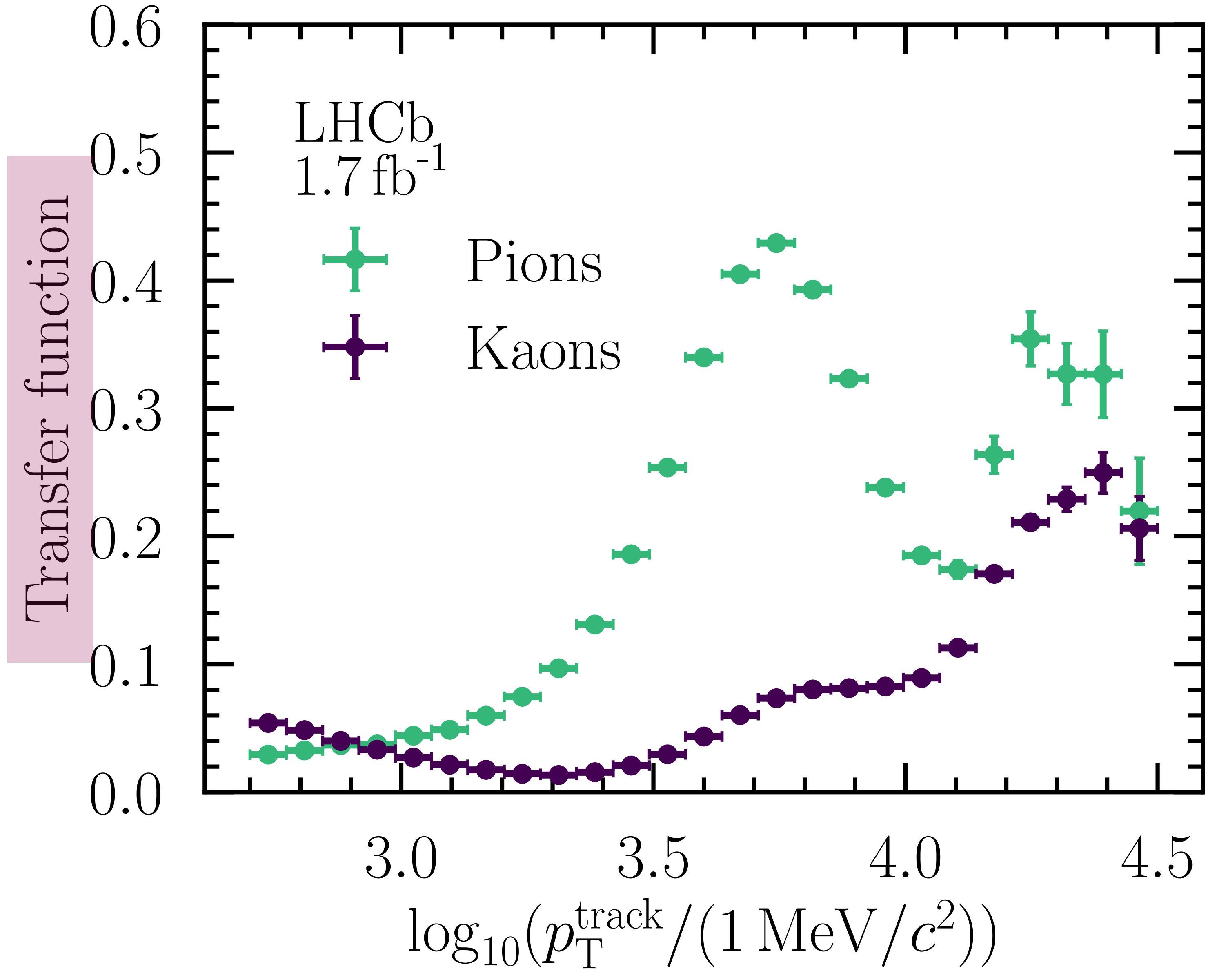

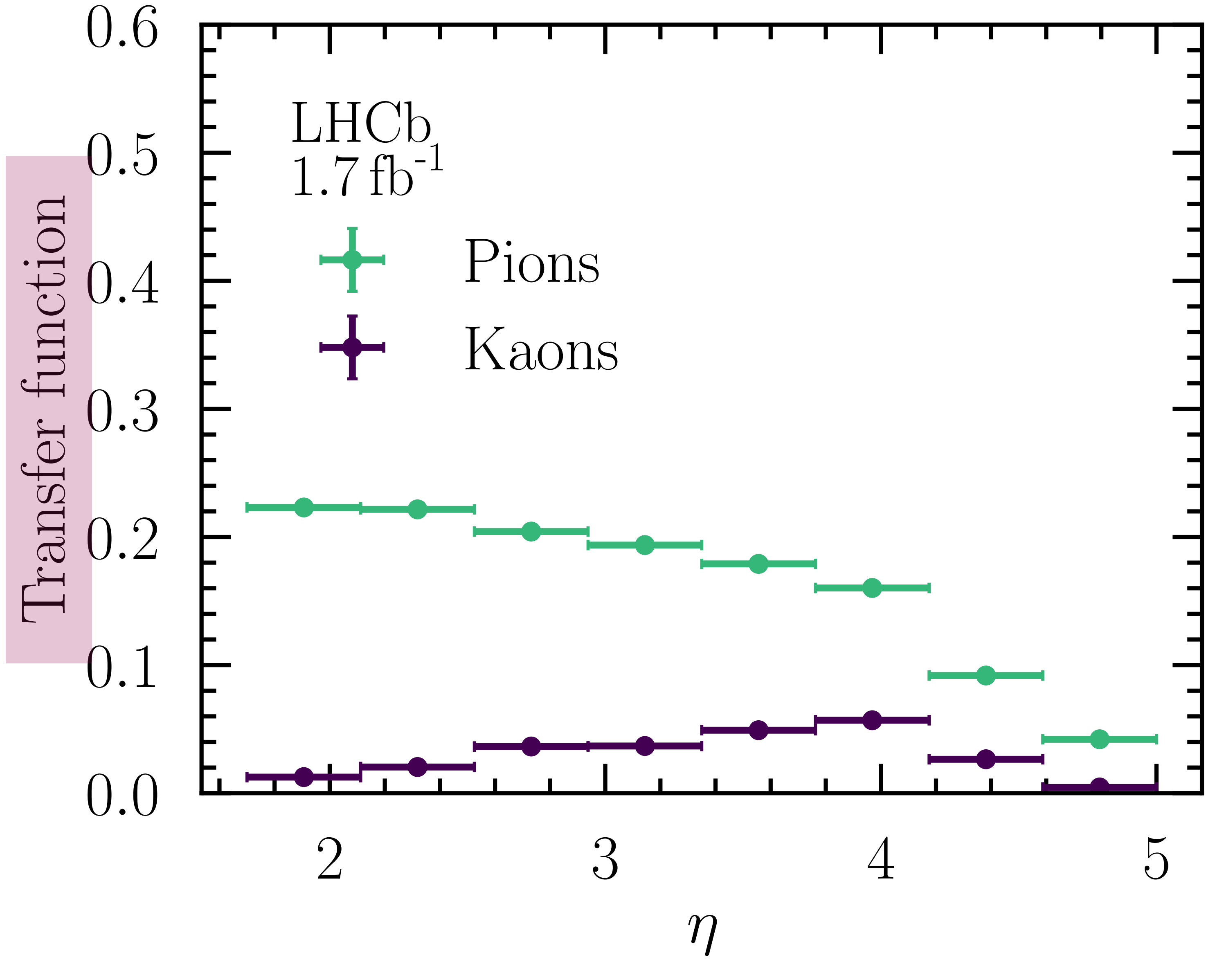

Misidentified background in electron mode

- ***Model them analytically***
  - Kernel density estimation for systematic
- ***Normalisation***
  - Gaussian constrained (stat. precision of prediction)
- ***Systematics***
  - Use alternative *"control"* regions
  - *Different kaon/pion ID tagging in control region*
  - *Trigger effects, binning transfer function*

NB: misidentified background not included in mass fit in previous analysis (see backup for comparison)

Predictions after per-track and per-event weighting (signal subtracted)

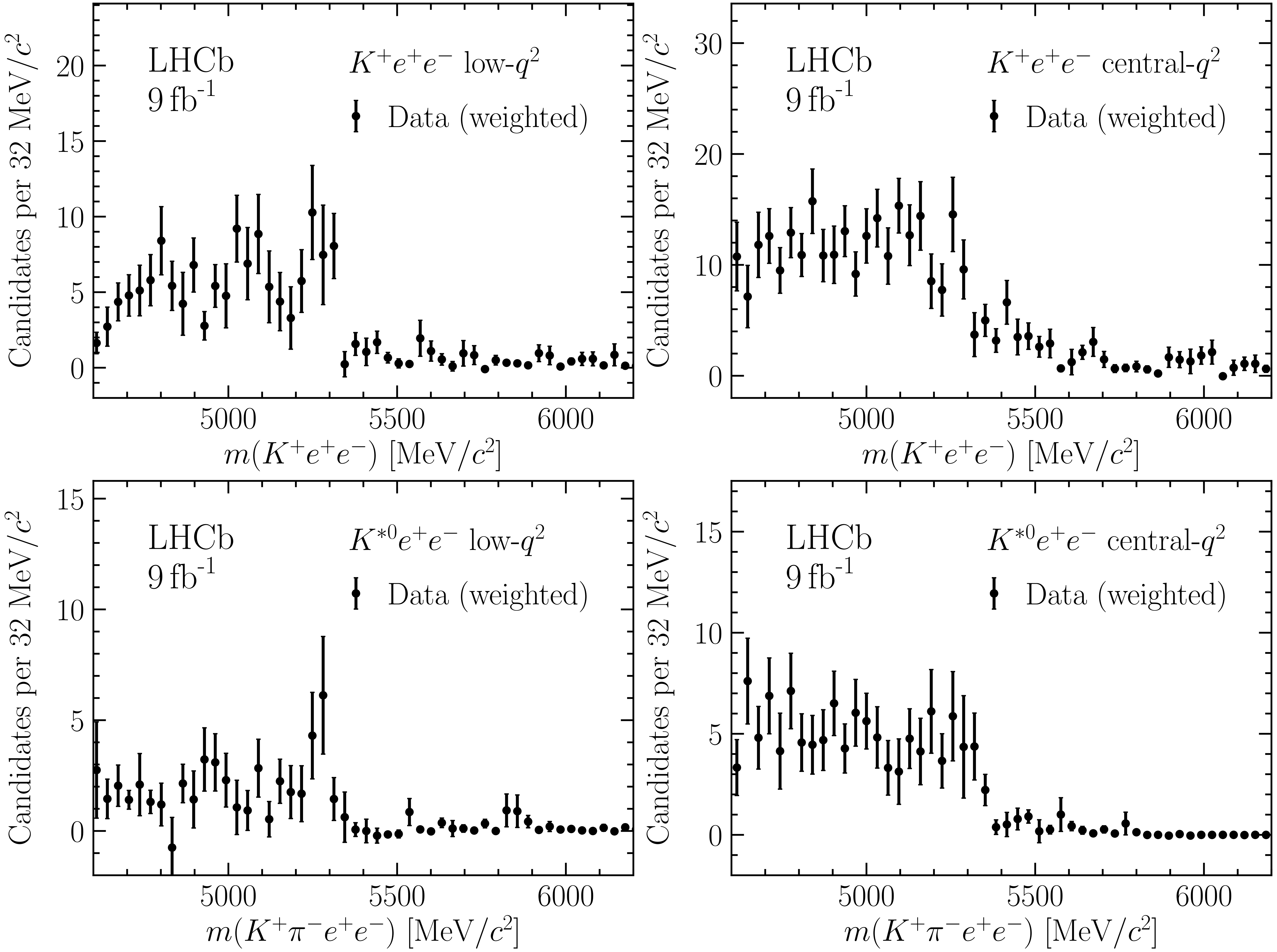

Data fully selected in "*control*" regions ($B^+ \to K^+e^+e^-$) [before weights]

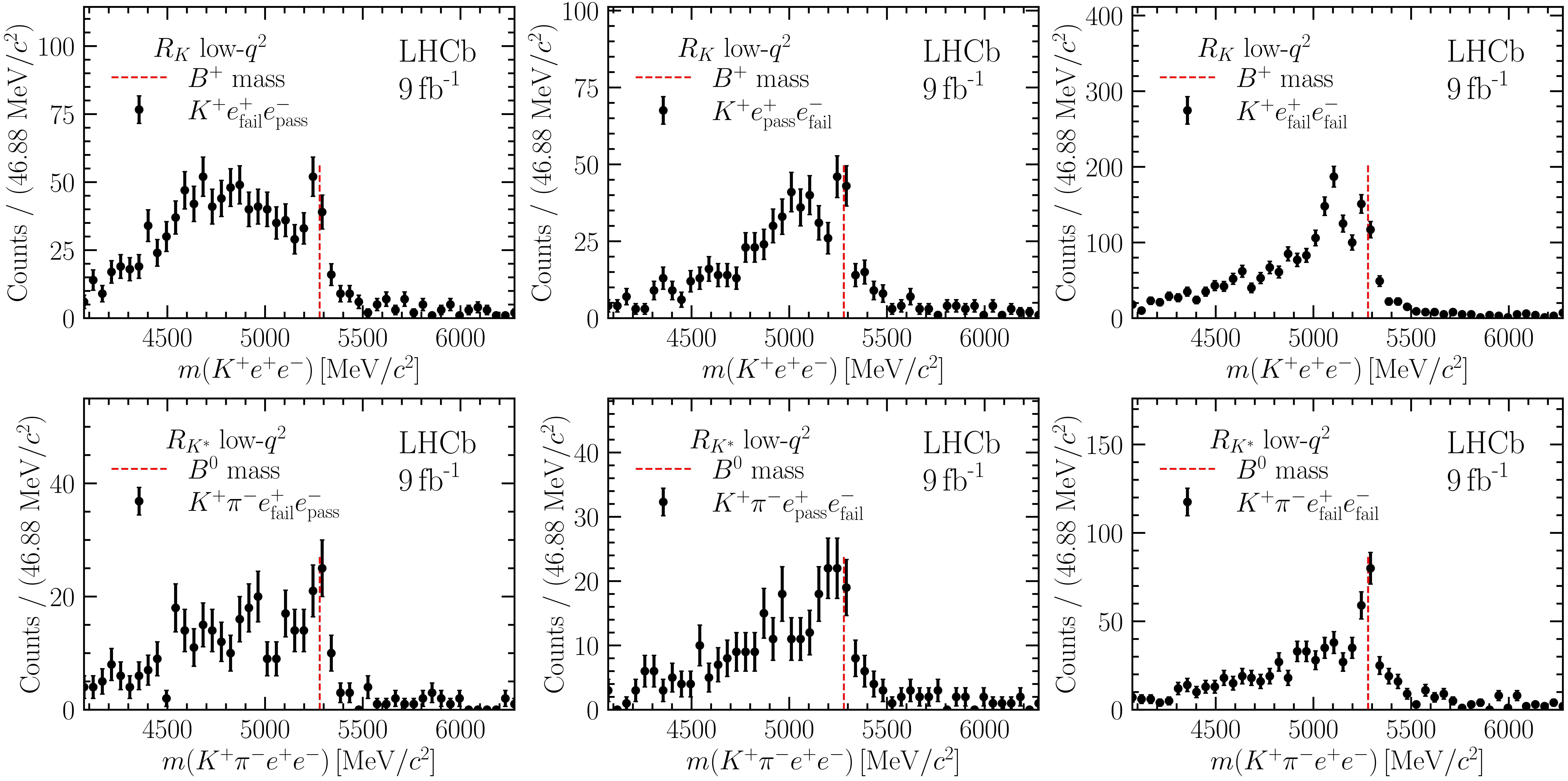

Data fully selected in "*control*" regions ($B^0 \to K^{*0}e^+e^-$) [before weights]

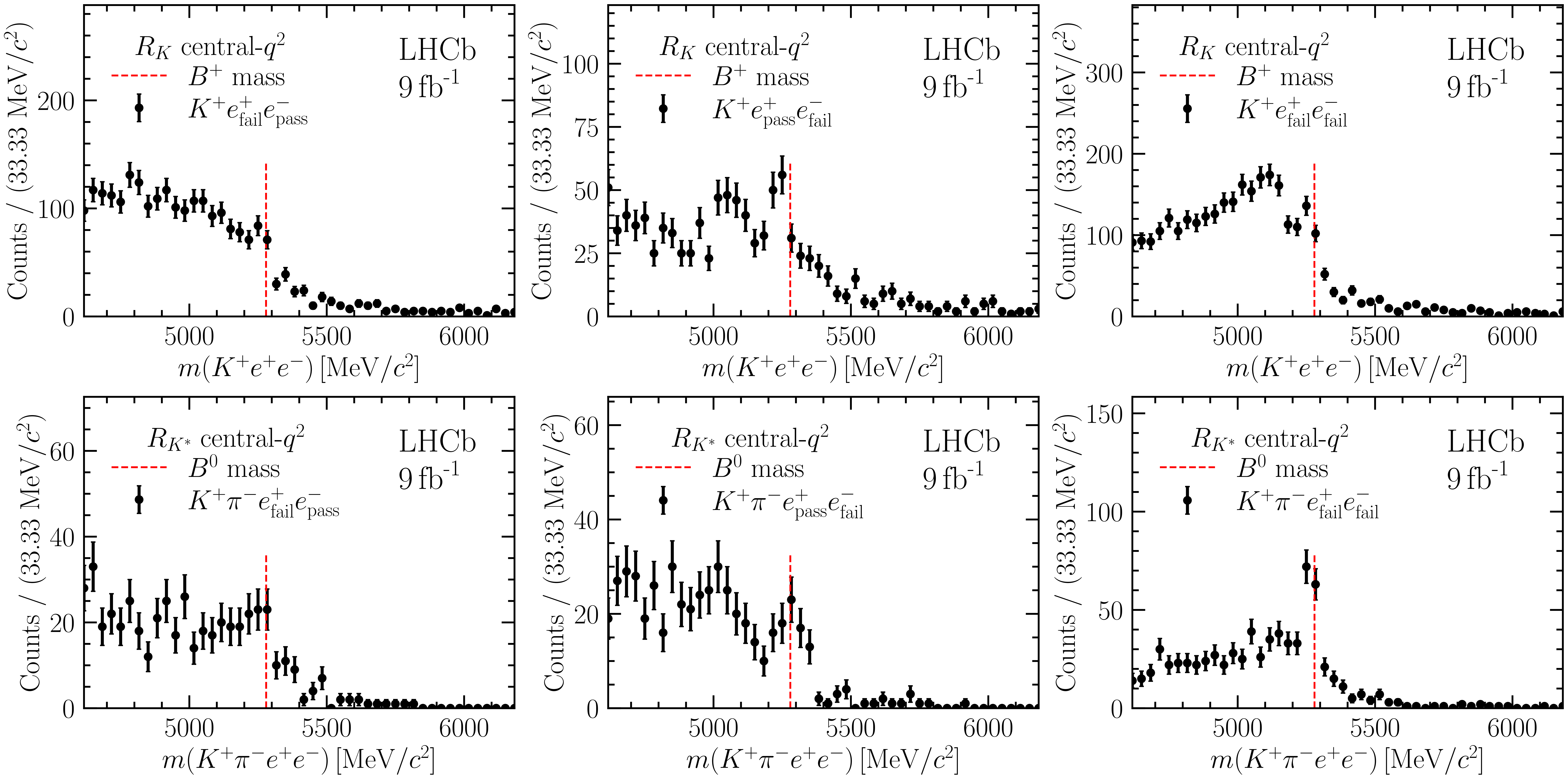

Misidentified background in electron mode (R_K)

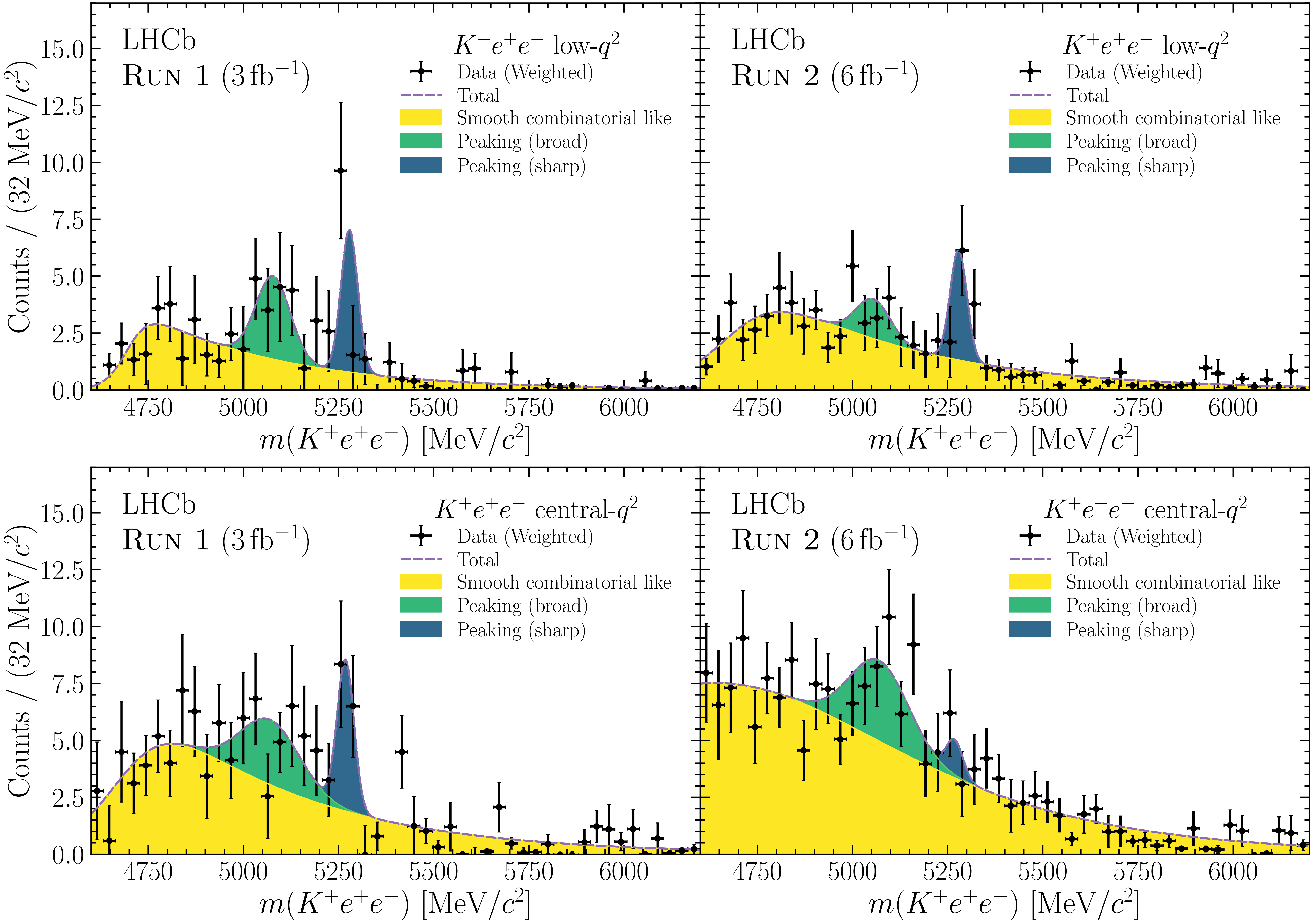

Mass fit to rare mode muons: simultaneous fit $R_{K,K^{*0}}$

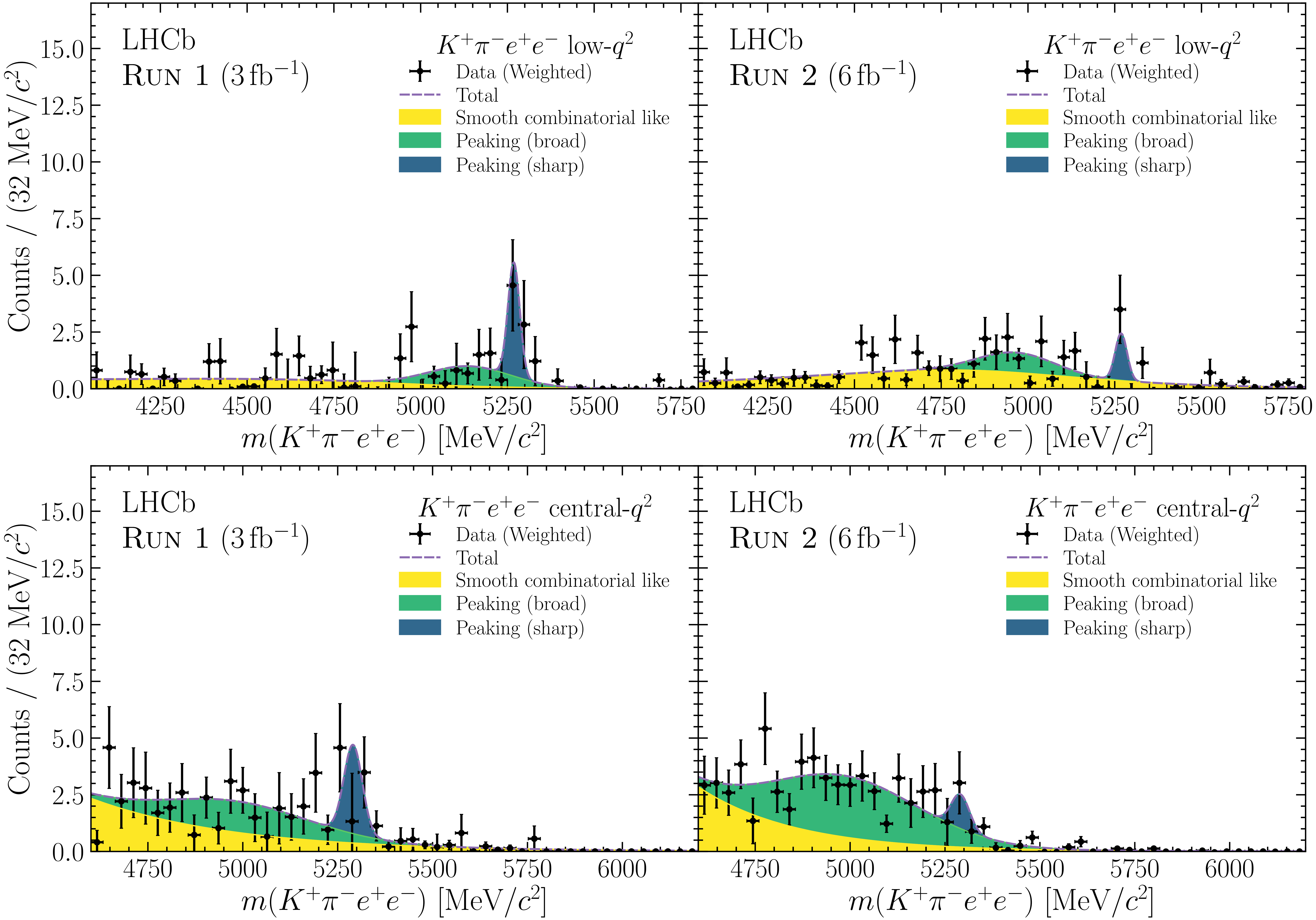

Can we go beyond the "inclusive" mis-ID treatment?

- **Need to achieve precise control of mis-identified backgrounds $H_b \to h_1 h_2 h_3 (h_4)$ for double mis-ID & $H_b \to h_1 h_2 (h_3) e X$ single mis-ID**
  - Mis-identification of electrons heavily depends on kinematics of final states (η, p_T) [RICH, CALO], requires 4-body charmless decay full amplitude analysis and branching ratios measurements which are not available to date $(B^0 \to K^+ \pi^- (\pi/K)^+ (\pi/K)^-)$
  - Also, need to ping down all the possible single misID backgrounds which would show up from single-electron misID contribution

Simplest peaking backgrounds in electron mode in "control" region (same in K^{*0} final states)

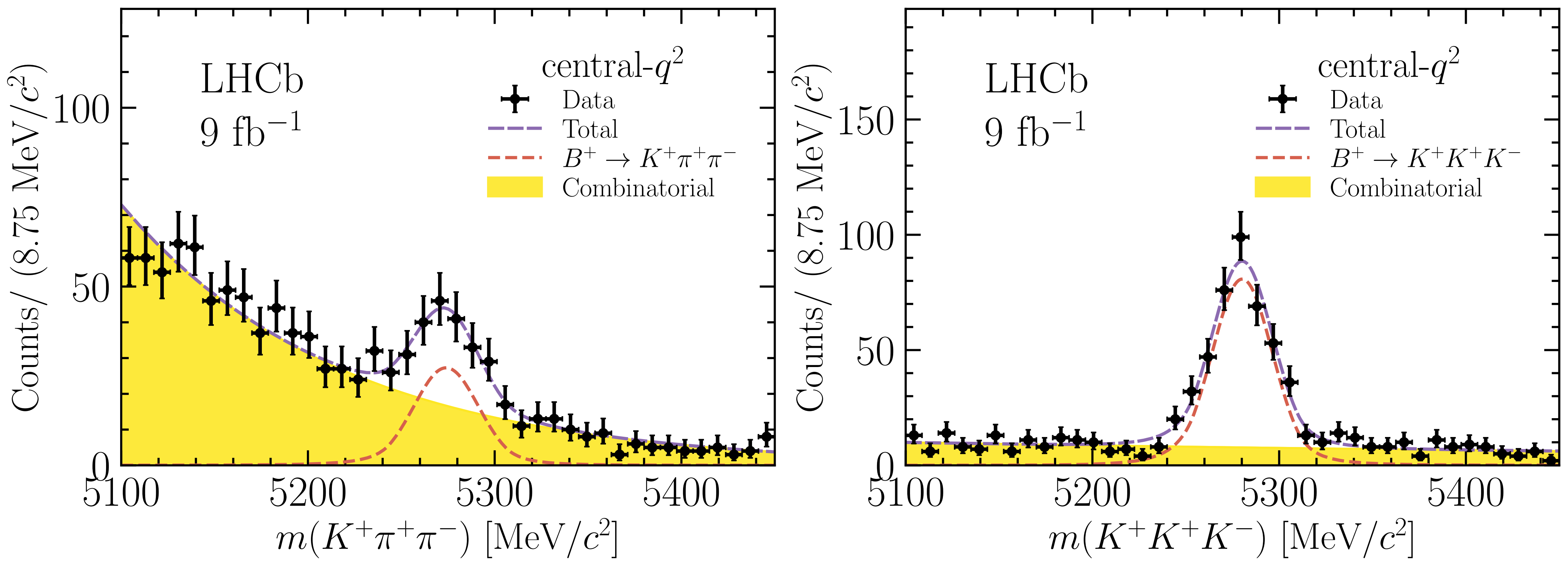

- **Use tighter PID requirements?**
  - It has a direct effect to signal yields and statistical precision we can reach
  - Still need to ensure backgrounds become negligible
- **Differentiate more the analysis need more statistics**
  - Split analysis in "with/without" brem added category, presence of recovered photon is more effective to reject mis-ID and combinatorial
  - Also, backgrounds/signal interplay can benefit from going beyond the 1D fit on invariant masses motivating LFU tests coupled to simultaneous angular analyses in muon/electron states